TOWARDS THE ENHANCEMENT OF BIPED LOCOMOTION AND CONTROL TECHNIQUES

A THESIS SUBMITTED TO
THE GRADUATE SCHOOL OF NATURAL AND APPLIED SCIENCES
OF
MIDDLE EAST TECHNICAL UNIVERSITY

BY

BAŞAK YÜKSEL

IN PARTIAL FULFILLMENT OF THE REQUIREMENTS
FOR
THE DEGREE OF DOCTOR OF PHILOSOPHY
IN
ELECTRICAL AND ELECTRONICS ENGINEERING

AUGUST 2008

Approval of the thesis:

TOWARDS THE ENHANCEMENT OF BIPED LOCOMOTION AND CONTROL TECHNIQUES

submitted by **BAŞAK YÜKSEL** in partial fulfillment of the requirements for the degree of **Doctor of Philosophy in Electrical and Electronics Engineering, Middle East Technical University** by,

Prof. Dr. Canan Özgen _____
Dean, Graduate School of **Natural and Applied Sciences**

Prof. Dr. İsmet Erkmen _____
Head of Department, **Electrical and Electronics Engineering**

Prof. Dr. Kemal Leblebicioğlu _____
Supervisor, **Electrical and Electronics Engineering Dept., METU**

Examining Committee Members

Prof. Dr. Uğur Halıcı _____
Electrical and Electronics Engineering Dept., METU

Prof. Dr. Kemal Leblebicioğlu _____
Electrical and Electronics Engineering Dept., METU

Prof. Dr. Kemal Özgören _____
Mechanical Engineering Dept., METU

Prof. Dr. Ömer Morgül _____
Electrical and Electronics Engineering Dept., Bilkent University

Assist. Prof. Dr. Cüneyt F. Bazlamaçcı _____
Electrical and Electronics Engineering Dept., METU

Date: 14.08.2008

I hereby declare that all information in this document has been obtained and presented in accordance with academic rules and ethical conduct. I also declare that, as required by these rules and conduct, I have fully cited and referenced all material and results that are not original to this work.

Name, Last Name: **Başak Yüksel**

Signature:

ABSTRACT

TOWARDS THE ENHANCEMENT OF BIPED LOCOMOTION AND CONTROL TECHNIQUES

Yüksel, Başak

Ph.D., Department of Electrical and Electronics Engineering

Supervisor: Prof. Dr. Kemal Leblebicioğlu

August 2008, 308 Pages

The omnipresent tendency to “live easy” is a sign of our need for automatization. To enable for such a “comfortable and safe” world, the automatic systems have to be developed that satisfies the necessities of life. Biologically inspired robots, especially the humanoids, are thus the key, and research in this area focuses on the improvement of such systems. Lately, it has been shown by high dexterity examples that the humanoid robots achieved to a mature level even if there are still open issues to be improved, especially in the control and stability of the bipeds. The purpose of this thesis is to study biped locomotion in different floor conditions, such as stairs and obstacles; to improve the research done in this area; to contribute to the development of autonomous biped robots, dynamic modeling, gait planning, supervisory and guidence control, stability analysis of biped robots; and to implement new control algorithms for biped locomotion, especially by using optimization and high level intelligent control techniques. The locomotion aimed to be realized results from complex, high-dimensional, nonlinear and dynamically related interactions between the robot and its environment. The mathematical modeling of the physical system is realized based on a 5-link 7 DOF biped robot model walking on a 3D planar surface and the dynamic simulation is performed using MATLAB. In terms of control, several different methods applied, comparison and the performance of each method are given. The 3D dynamic simulation software is developed, which allows the user to operate the biped systems within a 3D virtual environment.

Keywords: Biped Robot, Mathematical Modeling, Dynamic Simulation, Trajectory Planning, Controller Design

ÖZ

İKİ BACAKLI ROBOTUN YÜRÜME VE KONTROL TEKNİKLERİNİN ZENGİNLEŞTİRİLMESİ

Yüksel, Başak

Doktora, Elektrik-Elektronik Mühendisliği Bölümü

Tez Yöneticisi: Prof. Dr. Kemal Leblebicioğlu

Ağustos 2008, 308 sayfa

Otomatikleşme ihtiyacı, her zaman ve her yerde kendini gösteren "kolay yaşam" eğiliminin bir işaretidir. Hayattaki ihtiyaçları karşılayan otomatik sistemlerin geliştirilmesi, "rahat ve güvenli" bir dünyayı mümkün kılmak için gereklidir. Biyolojik açıdan esinlenilerek geliştirilen, özellikle iki bacaklı robotlar bu nedenle istenilendir ve bu alandaki çalışmalar bu tür sistemlerin geliştirilmesine odaklanmıştır. Son zamanlarda, çok yetenekli örneklerin geliştirilmesiyle, iki bacaklı robotların, özellikle robotun kontrolü ve dengesinin sağlanması konularında iyileştirilmesi gereken açık sorunlar olmasına rağmen, olgun bir seviyeye ulaştığı gösterilmiştir. Bu tezin amacı, iki bacaklı robotun merdiven ve engel gibi değişik zemin şartlarında yürümesini incelemek; bu alanda yapılan araştırmaları geliştirmek; otonom iki bacaklı robotların geliştirilmesine, dinamik modellemesine, yürüyüş planlamasına, denetleyici ve yol gösterici kontrolüne, dinamik denge ve stabilite analizine katkıda bulunmak; ve iki bacaklı robotun hareketi için, özellikle optimizasyon ve yüksek dereceli akıllı kontrol tekniklerini kullanarak, yeni kontrol algoritmaları gerçekleştirmektir. Gerçekleştirilecek olan hareket, robot ile çevresi arasındaki kompleks, yüksek dereceli, doğrusal olmayan ve dinamik bağlantılı etkileşim sonucudur. Fiziksel sistemin matematiksel modellemesi, 5 bağlantılı 7 erkinlik dereceli, 3 boyutlu yüzeyde yürüyen iki bacaklı robot modeline dayanmaktadır ve dinamik simülasyon MATLAB'da gerçekleştirilmiştir. Kontrol açısından değişik metodlar uygulanmış, her metodun karşılaştırması ve performansı verilmiştir. Kullanıcıya, iki bacaklı robotu 3 boyutlu sanal ortamda işletme imkanı sağlayan, 3 boyutlu dinamik simülasyon yazılımı geliştirilmiştir.

Anahtar Kelimeler: İki Bacaklı Robot, Matematiksel Modelleme, Dinamik Simülasyon, Yörünge Planlama, Kontro Birimi Tasarımı

To My Parents;
Zeliha and Arif YÜKSEL

Aileme;
Zeliha ve Arif YÜKSEL

ACKNOWLEDGEMENTS

This city, Ankara is magnificent... It became a home town to me for years. Mainly the significance comes from the METU life I have had in it. The spectrum of people I met is just wide.

I, first of all, would like to thank to my parents, Zeliha & Arif Yüksel; my siblings, Dildar & Mehmet Bilal; and Prof. Dr. Kemal Leblebicioğlu even if simply saying 'thanks' is not at all enough to appreciate their encourage and patience at every instant of these years.

Cheers to my 91-year-old granny, who is still planting flowers or feeding the chickens in a distant town by Gaziantep. It is not simple to express my deep admiration and sincere thanks to my neighbours Şakire Teyze and Abdullah Amca; to my uncle Mustafa and Hediye Yenge for making my life easier during these years.

I also would like to thank to Prof. Dr. Kemal Özgören and Prof. Dr. Uğur Halıcı for their academic support.

My academic research extended till to Singapore, my favorite country, la! And I very much enjoyed speaking Singlish… There, I have been given the gift of meeting many wonderful people. I especially want to thank Changjiu Zhou and ARICC members, my roommates and neigbours and especially to Karl Krummel, Barbara and Simone.

And then… IEEE life, IEEE friends… Thanks goes to Roland Saam from London for supporting me in the editorial work of IEEE Region 8 News, that I had fun in every second of working with him, also gorgeous thanks to IEEE Turkey Section Committee and especially the term of 2006-2009; Ozlem, Birsen, Ibrahim, Engin, Vakur, Cahit and Ferhan for easing my work as a Student Activities Coordinator. Thanks to Iztok for accompanying and hosting me during my IEEE visit to Slovenia, which also extended to Zagreb.

There are many life experiences I have learned as being engaged to Havelsan and I'm particularly grateful to Havelsan and Boeing colleagues for making the working hours efficient and fruitful.

And my friends, who know an enjoying life is all about! I can not name all but very special thanks to METU EE assistants Evren, Turker, Mehmet, Kagan; Ercan especially for organizing movie parties; Eda, Seckin, Oguz, Baran, Nazir, Evrim, Esra, Ozgul, Belgin; my dormitory and life-long friends Derya, Bengi, Melike, Yesim; Jim, Cem, Olcay, Gonul, Murat, Sezin, Lutfullah; my METU EE students for their respect and enthusiasm, special thanks to Esra, Can, Sukru; my sport friends Guler, Ilke, Lee, Magara, Sargun; Mustafa, Sema; "Korocanlar", the old and current members of Bach Korosu; especially to our correpetitor Umit and conductor Emel; and many many more.

And last kudo goes to Middle East Technical University and everybody in it, for simply being there and smiling!

TABLE OF CONTENTS

LIST OF TABLES

LIST OF FIGURES

LIST OF ABBREVIATIONS

3D	:	3 Dimensional
AIST	:	Advanced Industrial Science and Technology
ANFIS	:	Adaptive-Network-Based Fuzzy Inference System
ARICC	:	Advanced Robotic and Intelligent Control Centre
ASIMO	:	Advanced Step in Innovative Mobility
AUV	:	Autonomous Underwater Vehicle
CMAC	:	Cerebellar Model Arithmetic Computer
COG	:	Center of Gravity
COM	:	Center of Mass
CPG	:	Central Pattern Generator
CTC	:	Computed Torque Controller
DOF	:	Degrees of Freedom
DSP	:	Double Support Phase
GA	:	Genetic Algorithm
GARIC	:	Generalized Approximate Reasoning for Intelligent Control
HMCD	:	Human Motion Capture Data
HOAP	:	Humanoid for Open Architecture Platform
IFR	:	International Federation of Robotics
IP	:	Inverted Pendulum
IPM	:	Inverted Pendulum Model
ISO	:	International Standards Organization
JIRA	:	Japanese Industrial Robot Association
KAIST	:	Korea Advanced Institute of Science and Technology
LQ	:	Linear Quadratic
LQR	:	Linear Quadratic Regulator
MATLAB	:	Matrix Laboratory
METI	:	Ministry of Economy, Trade and Industry
MSTC	:	Manufacturing Science and Technology Center
NEDO	:	New Energy and Industrial Technology Development Organization
PID	:	Proportional-Integral-Derivative

QRIO	:	Quest for cuRIOsity
RCGA	:	Real Coded Genetic Algorithms
RIA	:	Robotics Institute of America
SQP	:	Sequential Quadratic Programming
SSP	:	Single Support Phase
TUBITAK	:	the Scientific and Technical Research Council of Turkey
UAV	:	Unmanned Aerial Vehicle
UNECE	:	United Nations Economic Commission for Europe
VMC	:	Virtual Model Control
ZMP	:	Zero Moment Point

CHAPTER 1

INTRODUCTION

1.1 Overview

Locomotion is the ability for active movement or travel of an organism from one position to another. In a biological sense, locomotion, a necessity for the body in order to continue living, is a patterned motor behavior of limbs or other body parts ensuring the movement. Without this ability, most of the organisms could not collect nutrient, flee from dangerous situations, or copulate.

In nature, the locomotion exists in many forms: walking, running, crawling, climbing, jumping, gliding, swimming, diving, flying (gliding, soaring, hovering…), hopping, burrowing, etc. The form of the locomotion depends on the morphological structure, dimensions and circumferences of the organisms. Over the uneven terrains, it is the fact that the most suitable, reliable and energy efficient means for locomotion is legs. It also provides advantages in terms of speed, acceleration, and most importantly, maneuverability.

Legged locomotion is the movement by the organism's external prolongation. The major aspects of legged locomotion are structure of the legs (Figure 1.1), number of the legs, the gait pattern and stance. The number of legs varies from locomotor to locomotor and also sometimes the animal may change the number of legs used during locomotion in different circumstances, such as switching from slow motion to fast.

In nature, a little number of legged organisms are bipedal, meaning two-legged (Latin bi = two + ped = foot) [1]. Human nature is of bipedal type and admits great variation, flexibility and subtle differences in gait, style, speed, and endurance [2]. Bipedalism is not unique to humans, though our particular form of it is. There are also other biped locomotors in the universe, such as bird, dinosaur, kangaroo, ostrich, giant pangolin, etc. Although most other mammalian bipeds hop or waddle, human strides. Homo sapiens are

the only mammal that is adapted exclusively to bipedal striding [3]. It is also very crucial to note that walking on two legs requires certain adjustments to body proportions. Most of the legged animals in nature are quadrupedal. The list of them includes dogs, cats, lions, etc. There are also more than four-legged animals such as hexapods (collembola, protura, diplura, etc.) and octopeds (spider, scorpion, tarantula, etc.). In the nature, the organisms with the biggest number of legs of 750 are the rare species Illacme plenipes [4].

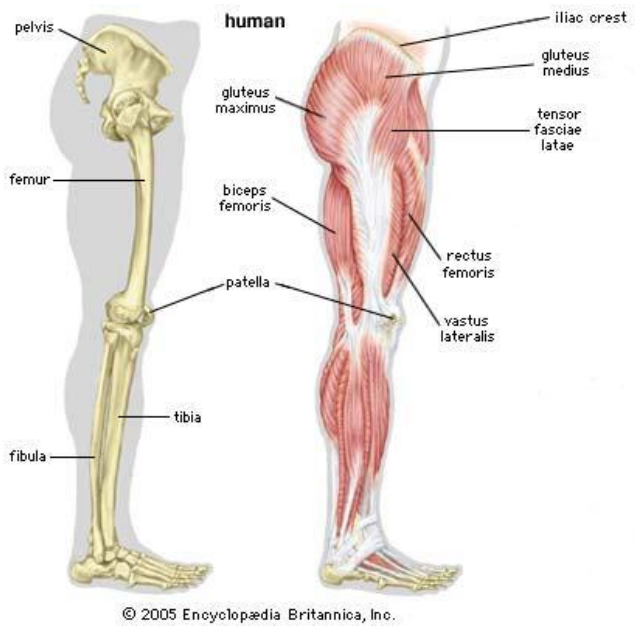

Figure 1.1 Skeletal and muscular structures of a human's leg

Human imitates the nature whenever necessary. Similarly, the idea of robotics was born from the dreams and necessity in improving the human life. The word “robot” has a Czech origin, meaning “forced labor” or “serf”, and was introduced by the Czech playwright Karel Čapek, in his play “R.U.R (Rossum’s Universal Robots)” (premiered in Prague, 1920) [5]. In his story “Runaround” (1942) and later in his book “I Robot” (1950), Isaac Asimov used the term “robotics” for the first time, referring to the use or study of robots. Furthermore, Issac Asimov's most important contribution to the robotic history is the creation of his famous Three Laws of Robotics [6]:

1. A robot may not injure a human being, or, through inaction, allow a human being to come to harm.

2. A robot must obey the orders given it by human beings except where such orders would conflict with the First Law.
3. A robot must protect its own existence as long as such protection does not conflict with the First or Second Law.

In our modern era, there are many definitions used for the term “robot”. The Japanese Industrial Robot Association (JIRA) uses a wider definition for robots and counts more machines as robots. On the other hand, the Robotics Institute of America (RIA) divides robots into four classes which covers less when compared to JIRA’s definition. In order to eliminate these variations in the definition and categorization of robots, it is worth to use the definition of “robot” given by the International Standards Organization (ISO) in the international standard ISO 8373 as:

“An automatically controlled, reprogrammable, multipurpose, manipulator programmable in three or more axes, which may be either fixed in place or mobile for use in industrial automation applications.”

The robotics area uses other fields of studies such as mechanical, electrical, electronics, and computer engineering [7]. It involves interdisciplinary subjects such as kinematics, dynamics, planning systems, control, sensing, programming languages and machine intelligence.

In the past, the researchers made a huge effort to construct mechanical autonomous vehicles that performs some predefined tasks. The very first example of such an autonomous robot goes back to 350 B.C. to a wooden self-propelled bird called “the Pigeon” which was built by the Greek scientist, philosopher, and major Pythagorean mathematician Archytas of Tarentum [8]. This bird was revolved by means of a jet of steam or compressed air and can be probably named as the one of the earliest studies of flight. More complete information about other devices is found in the writings of Hero of Alexandria (fl. 1st century AD), who described devices actuated by water, falling weights, and steam.

At the beginning of the robotics technology, the robots were imagined to be used for serving the people or alleviate their laborious works. In a general sense, the robots are developed in order to replace the human beings in realizing the tasks that are either not

possible to be done by the humans or not preferable. By using robots, some of the advantages obtained are performing several different tasks better and safer than the human labor; labor saving; working condition improvement; increasing flexibility, productivity and quality in realizing the tasks; etc. Although today, the technology to implement these wishes does not fully exist, day by day, the direction goes forward fast to realize these wishes.

Thring classifies the development stages of robotics in four generations [9]:

1. Senseless pick and place vehicles;
2. Simple sensory adaptability vehicles equipped with simple tactile contact, limit switches, proximity sensors, etc.;
3. Complex information processing vehicles such as vision, tactile force sensors, with highly intelligent software supports for the execution of high level commands; and
4. Vehicles which are believed to behave like human beings, i.e., working on its own objectives, and having a plan of campaign to achieve, or modify those objectives.

Robotics suppliers and researhcers are concerned with the design, construction, and operation of robots. To better understand the current robot industry, it is worth to look at the statistics world-wide. Based on the "World ROBOTICS 2007" prepared by United Nations Economic Commission for Europe (UNECE) and International Federation of Robotics (IFR), the sales (supply) of robots in the world market decreased by 11% to 112,203 units in 2006, compared to the year 2005 (Figure 1.2) [10]. On the contrary, the world total stock of operational industrial robots increased by 3% to minimum of 951,000 units (and a possible maximum of 1,200,000 units) in 2006, compared to the year 2005 (Figure 1.3). Also, a yearly estimation of industrial robots' supply at year-end in the world by main industries 2005 – 2006 is given in Figure 1.4.

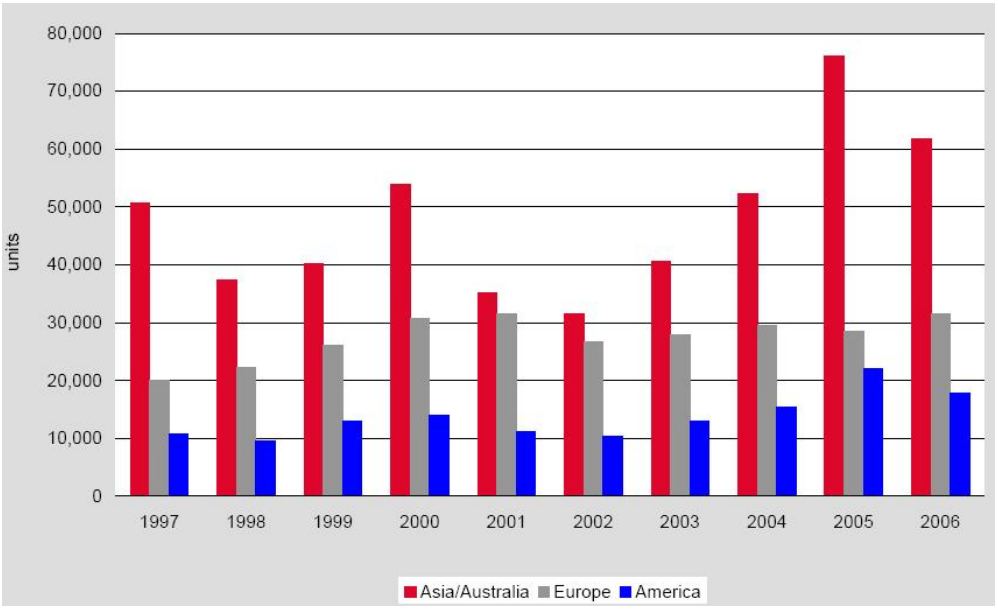

Figure 1.2 Estimated yearly sales of industrial robots [10]

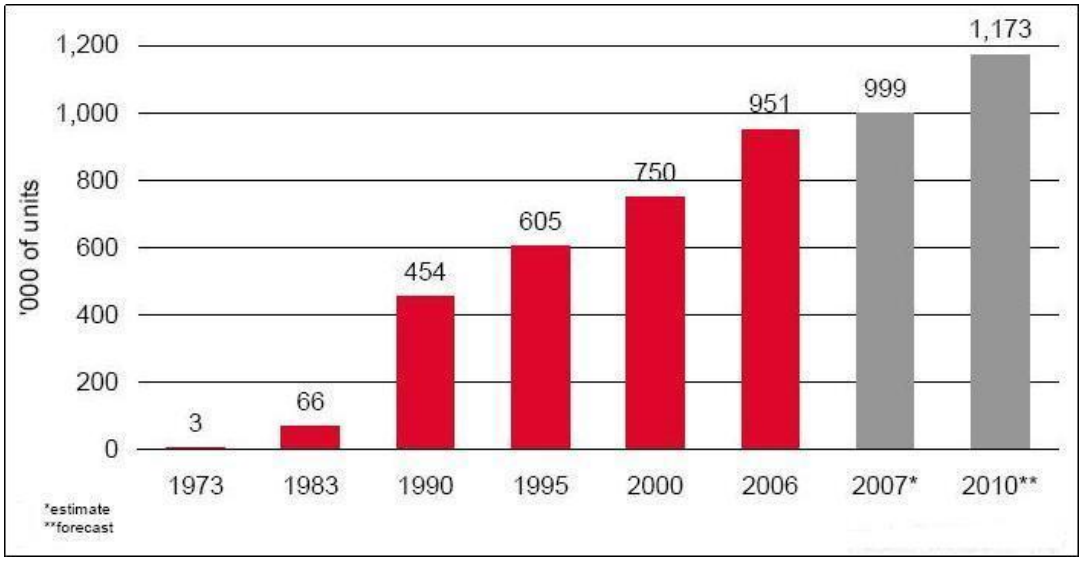

Figure 1.3 Estimated worldwide operational stock of industrial robots [10]

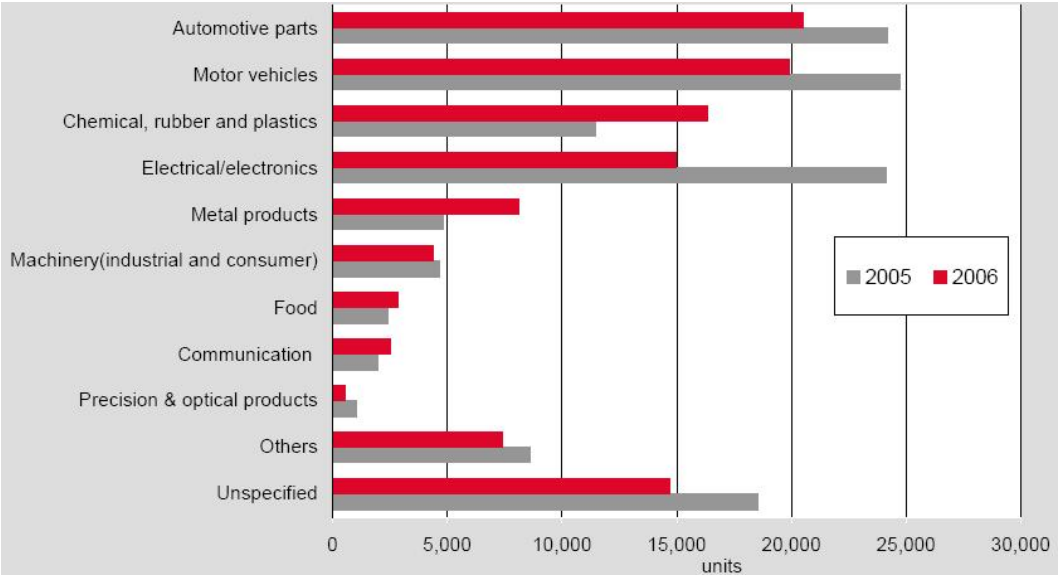

Figure 1.4 Estimated yearly supply of industrial robots at year-end in Total World by main industries 2005 – 2006 [10]

The forecast of robots in the world market for industrial robots is projected to increase from 112,200 units in 2006 to 123,100 in 2007 [10]. From 2008, it is expected to rise by a yearly average of 4.2% to 139,300 in 2010. In 2007, the worldwide supply of industrial robots is expected to increase by 10% as the details are given in Figure 1.5. So at the end of 2010, about 1.2 million industrial robots will do their job in the factories worldwide.

As a result of fast increase of the robot industry, the questions arise to be investigated carefully and shortly from ethical robotics point of view, such as [11]:

- Although farsighted and forewarning, could Asimov's three Laws become really the Ethics of Robots?
- Is it more important the ethics of robots or the ethics of robotic scientists?
- Is it right that robots could develop a "personality"?
- Is it right that robots could feel "emotions"?

Number of units

Country	Yearly installations				Operational stock at year-end			
	2005	2006	2007	2010	2005	2006	2007	2010
America	**21,986**	**17,910**	**21,400**	**24,400**	**143,634**	**154,680**	**167,100**	**209,000**
North America (Canada, Mexico, USA)	21,567	17,417	20,500	23,000	139,984	150,725	162,400	200,900
Central and South America	419	493	900	1,400	3,650	3,955	4,700	8,100
Asia/Australia	**76,047**	**61,748**	**66,000**	**75,000**	**481,652**	**479,027**	**500,500**	**579,900**
China	4,461	5,770	6,600	7,900	11,557	17,327	23,900	47,000
India	450	836	1,600	4,500	1,069	1,905	3,500	14,100
Japan	50,501	37,393	39,900	42,300	373,481	351,658	355,000	362,900
Republic of Korea	13,005	10,756	10,700	11,800	61,576	68,420	73,600	94,000
Taiwan, Province of China	4,096	4,307			15,464	19,204		
Thailand	1,458	1,102			2,472	3,574		
Other Asia	1,163	812			11,095	11,385		
Australia/New Zealand	913	772			4,938	5,554		
Europe	**28,432**	**31,536**	**35,000**	**39,000**	**296,918**	**315,624**	**329,800**	**380,000**
Austria	485	498			4,148	4,382		
Benelux	1,097	1,459			9,362	10,128		
Denmark	354	417			2,661	3,013		
Finland	556	321			4,159	4,349		
France	3,077	3,071	3,300	3,200	30,236	32,110	34,000	38,800
Germany	10,075	11,425	12,700	13,000	126,294	132,594	137,900	147,400
Italy	5,425	6,259	6,900	6,400	56,198	60,049	63,800	72,000
Norway	115	181			811	960		
Portugal	144	268			1,542	1,710		
Spain	2,709	2,409			24,141	26,008		
Sweden	939	865			8,028	8,245		
Switzerland	442	458			3,732	3,940		
Turkey	207	368			403	771		
United Kingdom	1,363	1,220	1,000	800	14,948	15,082	15,300	13,800
Central/Eastern European countries	1,287	1,322			9,446	10,781		
other Europe	157	995			809	1,502		
Africa	**204**	**426**	**700**	**900**	**634**	**1,060**	**1,700**	**4,400**
Total	**126,669**	**112,203**	**123,100**	**139,300**	**922,838**	**950,974**	**999,100**	**1,173,300**

Figure 1.5 Shipments and operational stock of multipurpose industrial robots in 2005 and 2006 and forecasts for 2007-2010 [10]

Among a wide range of robots, the interest of this thesis work is in legged locomotor robots which are classified as part of the mobile robots. Mobile robots are dynamic machines that balance themselves autonomously and they can be classified as below depending on the environment in which they locomote:

- Land robots, that are wheeled vehicles, legged vehicles or tracks,
- Unmanned aerial vehicles (UAVs),
- Autonomous underwater vehicles (AUVs),

Indeed, the vehicles that locomote are designed by human in different forms depending on their purposes and operating environments. Even if there are many legged locomotor organisms in our environment to imitate, the “wheeled” vehicles are the ones first invented

and used by human instead of the legged locomotion in the mobile robot technology history.

A wheel mechanism provides fast, energy efficient and smooth locomotion on flat terrain, while a legged locomotor is capable of moving in an uneven environment and also able to avoid obstacles, if exist during locomotion. Legged locomotion is very versatile but not as efficient as wheeled locomotion when the terrain is planar such as on rails and roads. However, on rough terrain, legged locomotion is superior to wheeled locomotion and it is a fact that most of the ground terrain has not been asphalted yet. In the world of applications, there is a need for machines that can travel in uneven terrain since about half of the earth's surface is accessible by wheeled and tracked vehicles, but on the other hand, most of this surface is reachable only by legged animals.

What is the reason for such a difference between legged and wheeled locomotion? The answer lays in the difference of the way of locomotion these two go through. In the wheeled robots, the locomotion is continuous and so there is a continuous support surface, whereas in the legged case, the path can be partially decoupled and so it can use separated footholds which provides an optimized support and traction [12]. By using separated support for the foot, the mobility of the legged system is restricted by the best footholds and the wheeled robot is restricted by the flatness of the surface during locomotion. Legged robots also provide active suspension during locomotion by decoupling the path of the body from the paths of the feet which provides increase in its speed and efficiency on uneven surface. On the other hand, the legged locomotion has disadvantage in terms of control, energy consumption and complexity of dynamics and balance. Although, legged locomotors in the nature use their own legs excellently, in the robotics, the research is still at a developing stage in understanding the control principles that underlie legged locomotion.

Legged robot study is largely inspired from legged organisms in the nature and it is interested in the imitation of the legged locomotors. The focus is done to the relations between the manipulator and the objects in its environment. Significant developments have been happened over the past three decades related to the design of legged robots and the coordination, control, balance and stability of legs during locomotion.

In legged robot studies, biped robots (design, locomotion and control) are of particular interest, basically due to the fact that bipeds are the obvious choice for locomotion in environments designed for humans. The biped robots, up to some extent, have the form and the function of the humans (appearance, stance, gait, etc.). That is why biped robot is also called “humanoid”. As a result of this fact, biped robots can perform in a human-oriented environment with a great harmony than any other type of robot. Another reason for a significant interest to bipeds is that a biped robot is more energy-efficient compared to the legged robots with more than two-legs.

As for the application aspect of the biped locomotion, a biped robot is quite adaptable and flexible that they will be rapidly used in many situations and circumstances, such as:

- substituting the human for a part of human work to realize the tasks which are very difficult, hazardous for humans or unreachable to humans, such as:
    - in extreme environmental conditions (earthquake, fire, etc.),
    - when working with toxic gases or chemicals or in nuclear plant investigation,
    - upon working with explosives (mining, geology, etc.),
    - agriculture,
    - forestry, etc.;
- assisting to human in various of tasks, such as:
    - in performing household matters,
    - to be used as a helper in hospitals,
    - aiding to elderly people (in Japan, the biped robots are assumed to be a helper in the future to people in their old age to continue to lead an active and productive life);
- providing enhancement in health care and medical technology such as in the development of prosthesis and orthosis (limb function support);
- in the development of new platforms to study the human body for training in health care (to diagnose locomotion related abnormalities and illnesses);
- optimization of sports techniques;
- education;
- military;
- exploration in space missions; and
- entertaining people just for fun!

That is why efficient, safe and reliable humanoids' development is the purpose in biped research in order to satisfy the high requirements on dexterity necessary for the above applications.

1.2 Terminology

The terminology of biped locomotion is mostly coming from the fields of biology (especially anatomy) and biomechanics. The terminology in the context of this thesis is given below:

Balance	:	The ability to maintain equilibrium and orientation in a gravitational environment
Biped	:	Kinematic chain consisting of two sub-chains called legs and torso, all connected at a common point called hip
Body	:	The major part of the robot
Foot	:	The end of a leg, whether it has links constituting a foot or not
Degrees of freedom (DOF)	:	The number of independent displacements that express completely the displaced or deformed position of the biped system
Gait	:	A manner of moving the legs in walking or running; walking pattern
Sagittal plane	:	The longitudinal plane that divides the body into right and left sections
Frontal plane	:	The plane parallel to the long axis of the body and perpendicular to the sagittal plane that separates the body into front and back portions
Locomotion	:	Legged robot movement
3D locomotion	:	Biped motion taking place in both the sagittal and frontal planes
Single support phase	:	The phase of locomotion where only one foot is in contact with the ground
Double support phase	:	The phase of locomotion where both feet are in contact with the ground
Impact phase	:	The phase of locomotion where the swing foot touches the ground (heel-strike)

Kinematics	:	The geometrical motion (positions, velocities and accelerations) of the robot with respect to a fixed reference coordinate system
Dynamics	:	The mathematical formulation of system equations of motion
COG	:	The specific point in a body at which, the total weight of the body acts as if it were concentrated
COM	:	The specific point in a body at which, the total mass of the body acts as if it were concentrated. In the presence of a uniform and parallel gravitationa field, COM is equivalent to the COG.
Support polygon	:	The convex hull of the vehicle's ground contact points
Stride length	:	The distance between the two successive placement of the same foot on locomotion
Step length	:	The half of a stride length or in other words; the distance taken by one foot step
Hip	:	The link of the body which connects the upper feet to the torso of the body
Gait speed	:	Stepping rate of the biped
Cycle time	:	Number of strides per unit time
Biomechanics	:	The study of the mechanical bases of biological activity, especially as pertaining to muscular activity.

1.3 Biped Locomotion Study

Biped locomotion study includes interdisciplinary work of many disciplines. Before focusing on the topics of interest in this study, some facts related to biped locomotion are summarized as below:

- A biped robot has a torso and two legs.
- Biped system is unstable, non-linear, and subject to restrictions caused by the environment.
- The stability, robustness, controllability and trajectory tracking are the main topics to consider in biped locomotion.
- Complexity. The biped locomotion aims to imitate the human and human motion can only be modeled by high DOF model despite the fact that the walking of the biped robot is a low DOF task. Since the DOF is high, it results in a complex system.

- Impact
    - The aim in biped locomotion is to enable the robot to proceed in a direction without turning over or falling down. This restricts the amount of torque to be applied to the lower leg ankle point to avoid the turn over or fall of the robot, for which the amount of maximum torque depends on the most probably varying ground surface properties.
    - A sudden impact occurs with the walking surface during locomotion and so, robot receives a ground reaction force from the ground. It should be ensured that the biped does not turn over or fall during locomotion in impact phase by proper modeling of the impact phase.
    - As a result of the fact that biped has an impact phase, the biped robot has to be designed as a hybrid model covering the before impact and after impact conditions during the walking cycle.
- Non-linear dynamics. The leg excursions are distinctly outside the linearizable region so that the full non-linear dynamics must be accounted for. The non-linear nature of the system is especially dominant when three dimensional dynamics are considered [13].
- Multi-variable dynamics. Walking systems are modeled as multibody systems with rigid links and low-impedance joints. The interaction between the various degrees of freedom is important and should not be overlooked, especially in three dimensions [13].
- Naturally unstable dynamics. The entire system can be seen as a (naturally unstable) inverted pendulum balancing on the stance leg. This necessitates to study the dynamic balance of the system over the entire walking cycle, which requires a much more involved analysis than the more common study of static balance [13].
- Limited foot-ground interaction. The unilateral nature of the foot-ground contact makes biped systems fundamentally underactuated. The system must use the control over its internal joints to cope also with the uncontrollable foot-ground contact [13].

Biped robot system retains a high complexity to control and difficulty to construct. In its basic sense, the biped locomotion studies include, but not limited to, the following topics: mathematical modeling, reference trajectory generation, dynamic simulation, control, dynamic balance and stability, and learning. The general diagram of a biped locomotion

system is given in Figure 1.6. So the study of legged locomotion is realized by modeling, simulating, building and controlling the humanoids, in general.

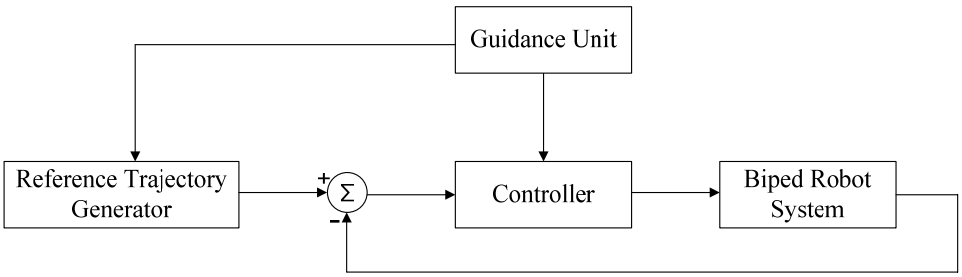

Figure 1.6 Block diagram of the biped system

1.4 Major Contributions

Human beings, together with almost all other creatures on this planet, exhibit modes of locomotion that are far more adaptable, wide ranging and robust than any machine that has yet been developed. The goal of research into walking robots, and bipedal walking research in particular, is to work towards the development of robots that can walk, run and climb as well as a human being, or other animal.

As a contribution toward the objective of developing useful walking machines, this thesis will consider solutions to some of the problems involved with the enhancement of the biped locomotion techniques. The main area of focus involves control system design and implementation.

First of all, full kinematical and dynamical model for 5-link 7 DOF 3D biped robot is derived by analytical calculations and Lagrangian method, respectively. The locomotion of the biped is classified into patterns. These patterns are chosen so that it covers all kinds of walking on different floor conditions, such as even floor walking, stepping over obstacles, stepping up and stepping down motions including staircase walking. Analytical methods (3rd Order Spline Interpolation) is implemented to obtain sagittal and frontal plane reference trajectories during walking on even surface, jumping over obstacles, stepping up and stepping down motions that results in a natural human-like walking. The footstep

planning is realized to ensure the dynamic stability measure (ZMP) for non-periodic locomotion on uneven surfaces, such as walking on an environment with obstacles or stairs. Global trajectory planning (high level controller) is realized for a given desired path, by controlling and planning the step trajectory by using optimization techniques (genetic algorithms), while ensuring the stability by using ZMP as a stability measure. Generation of footstep trajectories resulting in energy optimal foot step parameters such as step length, step speed, etc. for a given desired path as per the different environmental conditions is realized. Implementation of optimal footstep planner is done by using the classified patterns identified for non-periodic locomotion. As low level controller (supervisory control), PID, Computed Torque Control and Improved Computed Torque Control (added an integral term) methods are implemented successfully. The overall system, including the forward dynamics integrator, high level controller (guidance unit), trajectory planner, low level controller (supervisory unit), and animator is implemented in MATLAB.

1.5 Literature Survey

The concept of biped robot design has been first introduced by Leonardo da Vinci on 1497. He designed a mechanical armored knight robot on paper aiming to move like as if there was a real person inside (Figure 1.7) [14].

Figure 1.7 A biped knight robot model based on drawings by Leonardo da Vinci (owned by Ben Sweeney and was loaned for exhibit to the San Diego Museum of Man in 2003)

As can be seen from the ancient manuscripts, the history of human passion testifies the desire for autonomous machines that could look like human and could apply human skills for specific tasks. The very first example of such a human-like autonomous machine that is implemented and achieved to walk is the “steam man” (George Moore, 1893) as shown in (Figure 1.8). The steam man, 1.82 meters in height, was able to walk with a firm, steady gait by exerting considerable tractive power [15].

Although the biped robot studies had been started more than 500 years ago, it had been speeded up and achieved maturity only in the past thirty years. During the development phases in the last 500 years, the studies were limited to the parts of the overall system due to the complexity of the robotic implementation of human locomotion. The research of the entire system became feasible only with the development of high performance computers. However, the complete modeling and enhanced performance implementation of the human locomotion is still stays as a goal to achieve in the future. Despite the fact that there have been thousands of examples produced which achieved to walk and realized some more tasks, the practical use of the models up to now is limited to the education, entertainment and to a few cases in medicine - especially in the diagnosis of locomotion abnormalities and in the prosthesis and orthosis development. The utilization of them in the areas stated earlier has not become common in consequence of the immaturity of the robust, reliable and enhanced ready-to-go models. This is due to the fact that it is difficult to achieve simultaneously the robust, reliable, stable and energy efficient biped robots. As a matter of fact, very deep research and more work on the kinematics, dynamics, mechanics, control, stability and dynamic balance of walking should be done in order to improve the capabilities and performance of biped robots and achieve the reliability, robustness, stability, safety and energy efficiency in the biped robots at the same time.

Undoubtedly, the research on the biped locomotion is a very interdisciplinary area that extends across many fields such as control engineering, robotics, cognitive science, linguistic, psychology, computer science and biomedical engineering. Hence, it necessitated the information sharing among these fields and also joint researches to be implemented combining different branches of biped locomotion interest. Thereafter, the practical use of biped robots will be more common in our daily lives. It is apparent that these benefits of biped robots especially in the areas of medicine, space exploration and dangerous zone works (mining, nuclear plant investigation, rescue) are crucial and makes

human life easier. That is why the rapid reproduction of reliable biped robots should be achieved as soon as possible.

Figure 1.8 The Steam Man

Up to now, many types of walking biped robots have been developed with certain success. A number of the leading walking biped robot samples will be emphasized. Waseda University has initiated WABOT Project in 1970 and has become one of the leading research sites that developed the biped robots by Prof. Ichiro Kato and his colleagues. The first biped walker at Waseda University is WL-5, 11 DOF static walker, that had the ability to walk with a speed of 10 cm/minutes with 20 cm step length. Thereafter, a variety of humanoid robots including WABOT-1 which is the first full-scale human-like robot made in 1973, the musician robot WABOT-2 in 1984, Hadaly-2 which works together with a human partner and the biped walking robot WABIAN in 1997 have been developed by integrating the latest key technologies [16].

Miura and Shimoyama at the University of Tokyo have developed five kinds of biped locomotive robots, namely, BIPER-1, 2, 3, 4, and 5 with various DOF [17]. All of them are statically unstable but can perform a dynamically stable walk with suitable control. BIPER-1 and BIPER-2 walk only sideways. BIPER-3 is a stilt-type robot whose foot contacts occur at a point and who can walk sideways, backward, and forward. BIPER-4's

legs have the same degrees of freedom as human legs. BIPER-5 is similar to BIPER-3, but in the case of BIPER-5 all apparatus, such as the computer, are mounted on it.

In 1980s, Raibert worked on two-leg robots with a high focus on study balance & dynamic stability. He built 2-leg hopping machines that can move with a certain speed and keep balance by continuously hopping due to their simple structure. The implementation of these robots was limited since they were unable to stand still [12]. The robot has telescopic legs with no knees and no ankles. The legs contain springs that make the robot bounce when it falls on its feet. By changing the length of the springs, the controller adjusts the energy stored in the robot, thus controls the hopping height and the running speed. Although his robots are not designed in traditional way, his works add an enormous value to biped locomotion studies by his contributions to the concept of dynamic balance during locomotion.

During 1985-1986, Furusho and Masubuchi built the biped robot Kenkyaku. It was a 5-link planar robot with an approximate weight of 23 kg and 0.7 m height. The biped was able to walk at 0.8 m/sec [18]. In 1990, Junji Furusho and Akihito Sano reported their biped robot BLR-G2, which is a 3D nine-link biped weighted 25kg and height of 0.97 m, which was capable of walking at 0.18 m/sec speed. The BLR-G2 is equipped with foot pressure and ankle torque sensors to provide information about the condition of contact with the floor. The sole and ankle driving actuators undergo force/torque feedback control based on the sensor information [19]. Afterwards, during 1996-2000, Furusho and his team developed biped robot, Strut which is a 4 link 14 DOF planar robot [20].

Zheng and his friends built the 4 DOF robot SD-2 [21], [22]. McGeer showed that a planar human-like pair of knee-jointed legs mechanism could be made to walk stably given only a downhill slope as a source of energy with no other energy input or control [23]. This four-link planar passive biped walker weighted 4 kg, was 0.7 m tall (leg length) and could stably walk down an inclined surface. Afterwards, Goswami, Espiau and Keramane demonstrated that the nonlinear dynamics of a simple passive “compass gait” biped robot can exhibit periodic and stable limit cycle with a robot identical to a doube pendulum [24]. In the late 1990s, Collins constructed the 3D passive walker of needing no external energy while walking as with the same purpose of McGeer [25].

In 1990-1996, Kajita, Tani and Kobayashi built a planar biped robot weighing 2.19 kg and 0.37 m in height, which was able to walk with a speed of 30 cm/sec [26]. Thereafter, they build Meltran II, a planar 4 DOF biped weighing 4.7 kg and 0.45 m in height. It was capable of walking successfully over small obstacles at a speed of 0.2 m/sec [27], [28].

At the University of New Hampshire, two-generations of biped robots were built. The first generation biped robot, built in 1993-1994 period by Miller, was connected to off-board electronics through a heavy, non-elastic tether. The robot was approximately 1.04 m tall from foot to the top of the body and weighted approximately 6.8 kg [29], [30]. In the second generation biped robot, built in 1996-1997 period by Miller and Kun, the heavy, non-elastic tether was replaced by a lightweight, flexible tether. This biped was able to walk with variable speed gaits, change gait speed on the fly and walk with continuous motion on flat, non slippery surfaces at forward progression velocities in the range of 21 cm/min to 72 cm/min, with average stride length of 6.5 cm [31].

During 1994, at the Institute of Mechanics at Moscow University, the team of Grishin, Formal'sky, Lensky and Zhitomirsky constructed a planar telescopic leg biped robot with two actuated DOF. The biped was of 7.5 kg weight and 75 cm tall [32].

Dunn and Howe reported in an article dated 1994 that a planar robot, modeled as an inverted pendulum, achieved a smooth bipedal walking on flat terrain at Harvard University. The robot has 4 DOF with 5.6 kg weight, an approximate speed of 0.3 m/sec. and a step length of 20 centimeters [33], [34].

Spring Flamingo, which was designed, built and controlled by Pratt in 1996-2000 at MIT Leg Laboratory, is a planar biped locomotor and weighs in at approximately 13.5 kg and stands 90 cm tall. It can walk by 1.2 m/sec speed with an efficient power and was developed as an experimental platform for implementing various walking algorithms and control techniques like Virtual Model Control [35].

In 1986, Honda began a robot research program and currently, the Japanese firm is a leader in developing two-legged robots. The developed robots took many names associated to the different forms up to now. The latest and improved humanoid robot is named ASIMO (Advanced Step in Innovative Mobility), which can walk firmly, run, find its way around obstacles as well as interact with people. ASIMO has 34 DOF, 1.3 m height and 54 kg

weight with a walking speed of 2.7 km/hour, all of which help it walk and perform tasks much like a human. ASIMO is designed to operate in the real world, where it can pick things up, navigate along floors, sidewalks, and even climb stairs. Honda's dream is that ASIMO will help improve life in human society [36].

Sony developed the biped robot QRIO ("Quest for cuRIOsity", originally named Sony Dream Robot or SDR). QRIO stood approximately 0.6 m tall and weighed 7.3 kg and besides walking, it is also capable of voice and face recognition, making it able to remember people as well as their likes and dislikes [37].

Toyota constructed a biped robot designed to function as personal assistants for humans. Toyota aimed its partner robots to have human characteristics, such as being agile, warm and kind and also intelligent enough to skillfully operate a variety of devices in the areas of personal assistance, care for the elderly, manufacturing and mobility. The robot is of 1.2 m height and 35 kg weight. This robot is also capable of playing musical instruments.

HRP-2 is the final robotic platform for the Humanoid Robotics Project headed by the Manufacturing Science and Technology Center (MSTC), which is sponsored by the Ministry of Economy, Trade and Industry (METI) through New Energy and Industrial Technology Development Organization (NEDO). The total robotic system was designed and integrated by Kawada Industries, Inc. together with Humanoid Research Group of National Institute of Advanced Industrial Science and Technology (AIST). Yasukawa Electric Corporation provided the initial concept design for the arms and AIST 3D Vision Research Group and Shimizu Corporation provided the vision system. HRP-2's height is 154 cm and weight is 58 kg including batteries with 30 DOF. The firm stated that HRP-2 demonstrates some unique capabilities such as lying down on its back or stomach and get back up, a task never achieved by a robot of its size. In addition, the robot can carry light loads, move a panel in concert with a human, "see" and balance on one foot. The HRP-2 can also cross one leg in front of the other and walk a narrow line [38].

HOAP (Humanoid for Open Architecture Platform), by Fujitsu Automation, in collaboration with Fujitsu Lab, is a miniature humanoid robot, which strengthens cooperation functions with the external world, such as a communication and an image recognition function. The HOAP-3 provides portability, as it measurees only 60cm in height and weighs a mere 8.8 kg with 28 DOF, the same as its predcessor, the HOAP-2

which has been on the market since 2003. HOAP-3 can be used for research of communication with robots, such as a dialog with people [38].

ZMP Inc. produced the biped robot Nuvo, which is stated as the first home-use-type humanoid robot in the world. It is a small and light (39cm in height and 2.5 kg on weight) biped that is introduced as a safe and mobile at the same time. Nuvo can be controlled by voice recognition, remote control, and web access by using mobile phone [39].

The Korea Advanced Institute of Science and Technology (KAIST) created the biped robot HUBO and claims it is the smartest robot in the world. This robot is linked to a computer via a high-speed wireless connection and the computer does all of the thinking for the robot. Hubo (KHR-3) walks 1.25 km/h by itself, and has 5 fingers and 41 joints [40].

Besides the very little of these pioneering examples of which some of the photos are given in Figure 1.9, there are many other organizations, research labs, companies, projects and individuals that are fully involved in the development and implementation of biped robots towards reaching the ideal form of humanoid robots which really look like human and also capable of performing at least the human performance. Numerous companies are working on consumer robots that can navigate their surroundings, recognize common objects, and perform simple chores without expert custom installation (Figure 1.10). Perhaps about the year 2020, the process will have produced the first broadly competent “universal robots” with lizardlike minds that can be programmed for almost any routine chore [41].

Honda ASIMO

Sony QRIO

Toyota Partner

Fujitsu HOAP-3

ZMP Nuvo

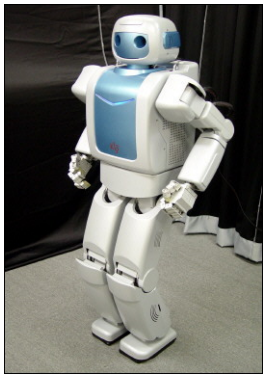

KAIST HUBO

Kawada/AIST HRP-2

MIT Toddler

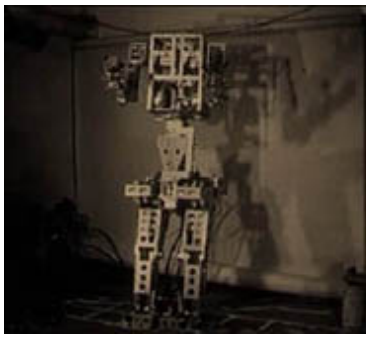

Waseda Wabot

Figure 1.9 Some of the pioneering examples of biped robots developed

Figure 1.10 Two Partner Ballroom Dance Robots face the audience with a human dancer during a demonstration at the Prototype Robot Exhibition, 9 Jun 2005, Nagakute, Japan

1.6 Objective and Organization of the Thesis

The construction of biped robots during recent years has been exploded. It was understood, however, that the further analysis of the system is needed in order to achieve robots very human-like. In the context of this thesis, the focus of the study is done to the development of methods towards the enhancement of biped locomotion and control techniques. In order to achieve this, first of all, each component of the high level overall system design, summarized in Figure 1.6, is realized. The overall system design of interest is composed of biped system's dynamic (mathematical) model, High Level Controller (Guidence Unit), Low Level Controller (Supervisory Unit), and Reference Trajectory Generator. The chapters of this thesis are organized in a way to ease the understanding of overall system and the work done.

First of all, the study is concentrated on the mathematical modeling of the biped robot in Chapter 2. In Chapter 3, the dynamic balance and stability definitions are extended and the stability criterion to be used in High Level Controller design for biped locomotion is defined. Furthermore, Chapter 4 deals with the reference trajectory generation problem. An

analytical method, namely, 3rd order (cubic) spline interpolation method is used to generate the desired walking trajectory in this study. The work was then extended to the control in Chapter 5. This chapter gives a detailed survey on the previous control methods used in the past. It presents the low level controllers designed (PID Controller, Computed Torque Controller and Optimal Contoller) and Guidance Unit. Chapter 6 gives the basics of the biped dynamic simulator programmed in MATLAB, the physical parameters used by the simulator, the algorithms developed, the comparison and evaluation of the methods used and the simulation results. Chapter 7 summarizes the work done and contributions to the biped locomotion studies realized throughout this thesis work.

CHAPTER 2

MATHEMATICAL MODELING

2.1 Background Information on Human Walking

Walking is the human's natural way of changing location and is defined as repetitious sequence of limb motion to move the body forward while keeping the stance balance at the same time [42]. Walking results from a complicated process involving the brain, spinal cord, peripheral nerves, muscles, bones and joints [43]. On the other hand, the gait is defined as the way or style of walking. Walking can be easily understood by analysis of the gait. Gait analysis has been introduced for the first time when the need to understand and diagnose the walking dysfunction and gait abnormalities arose. The gait analysis is described completely by combining the approaches of three scientific disciplines – anatomy, physiology and biomechanics.

The anatomical position of the body is described by the directional terms (superior-interior, left-right, anterior-posterior) and the reference planes (sagittal, frontal and transverse planes) as shown in the Figure 2.1 [43]. A sagittal plane is any plane that divides part of the body into the right and left portions; a frontal plane is any plane that divides a body part into front and back portions; and a transverse plane is any plane that divides a body part into the upper and lower portions. During the walking; bones, joints and muscles form the basic structure of the locomotor, while the brain, spinal cord and nerves are the controlling mechanism of the walking. Especially, the bones of the pelvis and legs play an important role in the structure, and a joint occurs where one bone is in contact with another, whereas the muscles are responsible for movements at joints. The walking is achieved by a complex and coordinated pattern of nerve signals sent to the muscles, which in turn move the joints, the limbs and the remainder of the body.

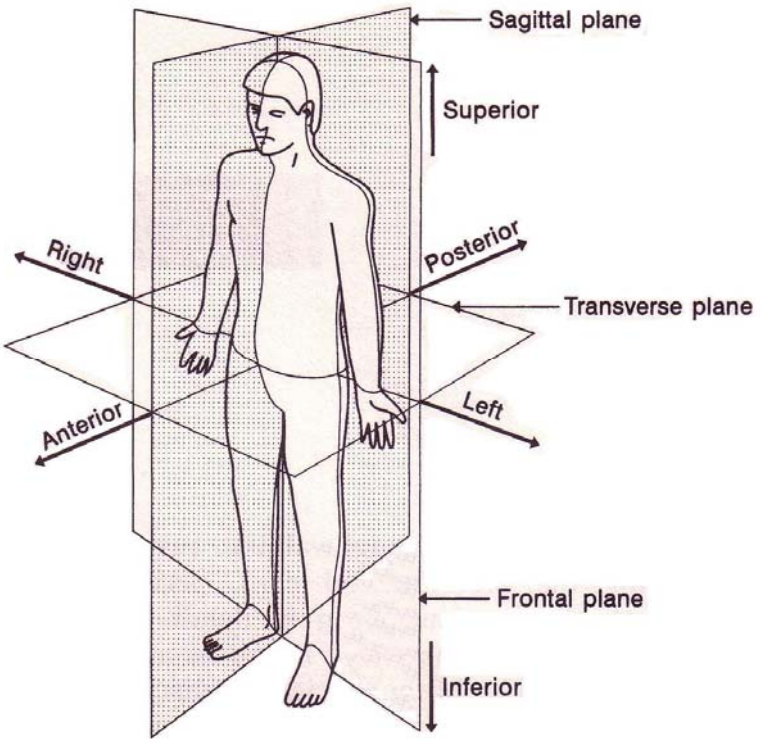

Figure 2.1 The anatomical position, with three reference planes and six fundamental directions [43].

Murray et al. measured and related many kinematics components of the walking act in the sagittal, frontal, and transverse planes by using a simple and inexpensive photographic method over the walking patterns of sixty normal men who ranged in age from 20 to 65 years and in height from 1.55 to 1.88 meters [44]. According to the outcomes of the analysis, there was striking similarity in the duration of successive phases of stance, swing, and double support during the same walking trial and during repeated trials of the same subject. Stride length and stride width showed the same striking similarity. Foot angles, however, showed greater individual variability. The differences in timing and stride dimensions did not relate systematically with age. However, the subjects sixty to sixty-five years old differed from younger subjects in that they took shorter steps and strides and showed a greater degree of out-toeing. The only variables which related systematically with height were the step and stride lengths, with the tall subjects taking the longest steps and strides and the short subjects, the shortest. These results suggested that pelvic and thoracic rotations are not obligatory elements of normal gait. The decreased pelvic rotation

in the group sixty to sixty-five years old may possibly represent another aspect of the presenile pattern of walking.

Growth across the lifespan of males and females produces change in the form and structure of the human body which must be recognized in biomechanical models [45]. The different morphologies for age span, gender and racial groupings have been identified and quantified by anthropometrists working primarily with measuring sticks and tapes. These parameters are not the parameters used to solve the dynamics problems of human movement. Models of the body composed of joints and rigid links have been formed and the inertial properties of the segments are required. The research which has been conducted to estimate these segment inertias is incomplete, dispersed, often flawed and inconclusive. It is clear that there are many interesting differences between age spans and, within these, differences between males and females.

There are several aspects of the gait. One of them is the gait cycle, which is defined as the time interval between two successive occurrences of one of the repetitive events of walking. It's convenient to use the instant at which one foot contacts the ground as a starting point. The major events during the gait cycle are listed as below and depicted in Figure 2.2 [43]:

1) Initial contact
2) Opposite toe off
3) Heel rise
4) Opposite initial contact
5) Toe off
6) Feet adjacent
7) Tibia vertical

The four out of these seven events occur during stance phase, when this foot is on the ground, and the other three in the swing phase, when this foot is moving forward through the air. The duration of the complete gait cycle is called the cycle time. The timings of all portions of a gait cycle are shown in Figure 2.3. The stride length is the distance between two successive placements of the same foot. It consists of two step lengths, left and right. The speed of walking is the distance covered by the whole body in a given time. The

average of the speed is calculated by the stride length divided by cycle time. Figure 2.4 shows the successive positions of the right leg in the sagittal plane [43].

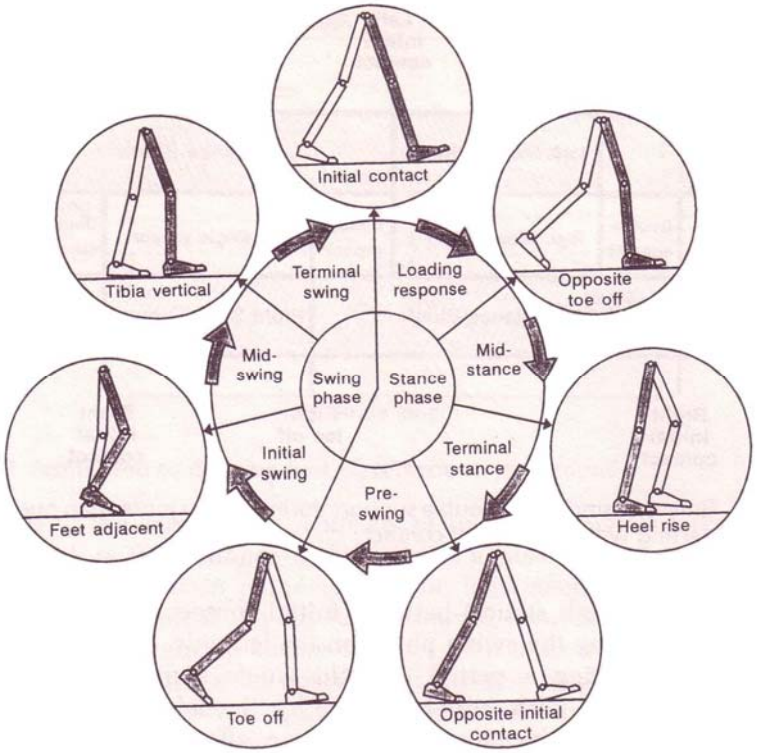

Figure 2.2 Positions of the legs during a single gait cycle by the right leg (shaded) [43].

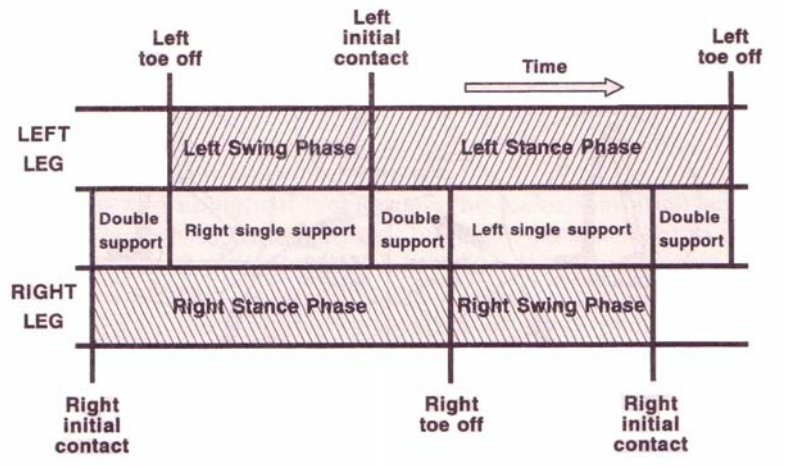

Figure 2.3 Timing of single and double support during a little more than one gait cycle, starting with right leg initial contact [43]

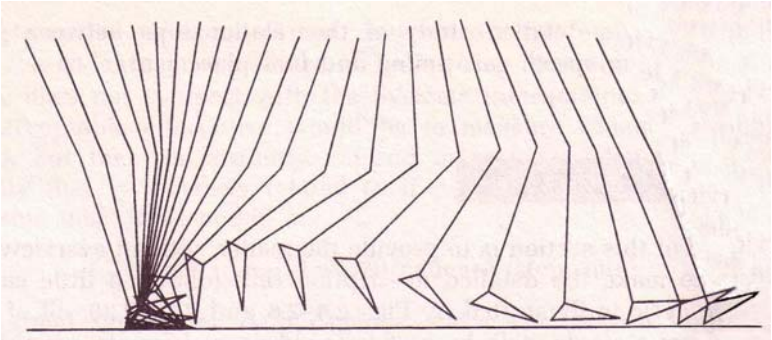

Figure 2.4 Position of the right leg in the sagittal plane during a single gait cycle [43]

2.2 Overview

The human locomotion involves more than 300 muscle pairs and for a natural human locomotion, more than 20 DOF will be gentle. But such a high dimensional system implies very complex dynamics from its mechanical structure and control points of view and results in high order nonlinear differential equations, which is not easy to be solved analytically. In other words, the mathematical representation, modeling of the human locomotion, is highly complex and nonlinear and by increasing the dimension, the modeling suffers from the “curse of dimensionality”, which means that the modeling complexity grows by an exponentially fast rate with increasing dimension. The complexity of the model is caused by the interacting hybrid dynamic nature of the system. As a matter of fact, using very simple models by ignoring the dynamic properties, mass and moment of inertia of some of the human parts is very common since it decreases the order of complexity and nonlinearity. Hence, in order to study the dynamics of biped locomotion, particular simplifications is done in the mechanical model to a compliant level having enough DOF by keeping the basic and important characteristics of human locomotion.

The biped locomotion modeling has roots in the human motion physiology studies based on the observations. The physiology observation of the human movement proceeded one step further by taking photographs of human in motion [46]. There has been profound research on the human locomotion in the fields of anatomy, physiology and biomechanics. Furthermore, the mathematical analysis of biped motion has been intensely implemented by the end of 1960s by using very simple models. As per the studies based on the biped kinematics, several biped robots have been developed. However, these bipeds lacked the

natural walking of the human and also had stability problems due to the fact that the dynamics of the biped locomotion was not taken into account. Including the dynamics of the biped into the calculations carried the system modeling aspect one step forward.

In the work by Vukobratovic, et al., the motion is modeled in the form of two nonlinear differential equations [47], [48]. Frank presented a method for the mathematical modeling of biped locomotion based on the energy efficient walking while maintaining stability. In his study, it is presented that the efficiency in terms of minimum energy has to be sacrificed for the sake of greater stability in the design of biped robots [49]. McGhee, et al. constrained the motion in sagittal plane as a single rigid body, where the biped mass is concentrated, by assuming the single support phase only motion [50], [51]. Thereafter, the modeling of the biped has been accelerated. Hemami, et al. used the inverted pendulum to model the biped locomotion system and analyzed the problems of stability, periodic motion, and locomotion of the inverted pendulum in order to develop useful methods to study the simulation and analysis of more realistic models of biped locomotion systems [52], [53]. Inverted Pendulum is one of the basic and simplest models for biped locomotion. Furthermore, Hemami, with his colleagues, derived the equations of the motion by a simple application of Lagrange's method for generalized coordinates and forces to a massless leg model [54] and to a kneeless leg model [55], and obtained sets of nonlinear differential equations describing the dynamics of biped locomotion for multilink models. Hemami and Zheng have considered 5-link, 3D biped in their studies [56]. Miura and Shimoyama modeled the dynamic walk as a series of inverted pendulum motions with appropriate conditions of connection [17].

After 1980s, the focus was generally on 5-link models in 2D (sagittal plane motion), and 7-link models in 3D considering both sagittal and frontal plane motions . In 5-link models, the links of the system generally consists of an upper body and two legs with 2 links each (thigh and shank links), assuming that the feet are massless so that they are not taken into account in the dynamics calculations. In 7-link models, in addition to the 2D sagittal plane motion, the frontal plane motion is generally considered as well. The links in both of these models are connected with rotational joints.

Furusho and Masubuchi have developed models based on linearizing the equations of motion around the vertical equilibrium for 5-link biped [18], [57]. Kajita proposed a 3-link

global linear dynamics model in single support phase with massless legs of variable lengths and assumed the motion of the model is constrained to the sagittal plane [26].

Hurmuzlu developed a planar, 5-link model, where the links are connected to one another by purely rotational joints. He assumed point contact between the lower limbs and the walking surface [58].

In the research by Gravez, et al., a method in order to completely parameterize the kinematics and the structural modelization of the various bodies constituting anthropomorphic bipeds is proposed [59]. As a result of this research, only stating two parameters of the biped robot, namely, the total mass and total height of the biped system, the virtual models of humanoid bipeds are calculated by means of the measure of dimensions, volume, mass, center of gravity and density of each segment (link) of whole body. The work is carried out within the framework of the digital modeling of humanoid robots for which the inertial and geometrical properties are close to those of the human being. So the aim is to completely parameterize the kinematics and the structural modeling of the various bodies constituting the anthropomorphic bipeds. The awaited result is the automatic creation of digital mockups of humanoid bipeds while respecting structurally the inertial and geometrical distribution of each body as given only two parameters.

Tzafestas, et al., provides the full mathematical model derivation of a 5-link biped robot in sagittal plane [60]. The biped dynamics are derived in single support and biped-in-the-air phases individually. In this thesis, the work of Tzafestas, et al., in [60] is used as a baseline for the dynamic model calculations and the idea is extended to three dimensional (3D) motion by generalizing the biped model. The details of the calculations are given in the next sections. The use of multilink models, Lagrangian dynamics and modern control theory provided a profound understanding of the problems, especially the unstable dynamics of biped locomotion, and also assisted very much in the solution of them.

2.3 Equations of Motion for 5-Link 7 DOF Biped Robot

By keeping the purpose of human-like natural locomotion and the fact of model complexity in mind, the mathematical modeling of biped robot mechanism is realized by a 5-link, 7 DOF motion in 3D space (Figure 2.5). The mechanism consists of a torso and two legs. The torso of the robot represents the head, arm and the trunk of the body and it is

connected to the hip via a rotational joint. The lower part of the body is formed by two legs (right and left). Each leg of the biped is composed of two rigid links as thigh (upper leg) and shank (lower leg), which are connected to each other by a rotational joint acting as the leg's knee. Each leg is connected to the hip via 2 DOF rotational joints acting on the hip. The torso, thigh and shank have dynamic properties since they are individually considered as a massive link and also their moment of inertia is included in the calculations. The feet are assumed to be massless; therefore, the dynamic structures of the feet are ignored (Figure 2.5).

In the sagittal plane (Figure 2.6), the biped robot has 5-link, 5 DOF motion with 2 DOF in each leg's hip and knee joints and 1 DOF in the torso's hip joint. In the frontal plane (Figure 2.7), the biped robot has 3-link, 2 DOF motion with 1 DOF in each leg's hip joint, noting that the torso is jointless in this plane.

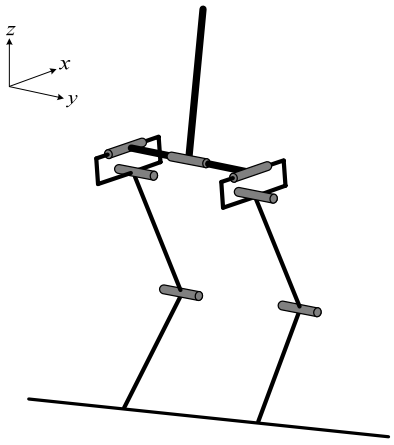

Figure 2.5 The 3D link structure of biped robot

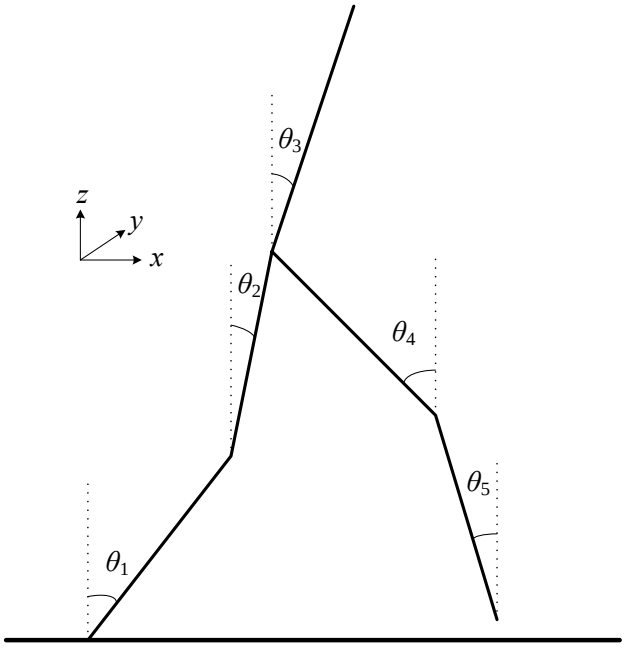

Figure 2.6 The link structure of biped robot in Sagittal Plane

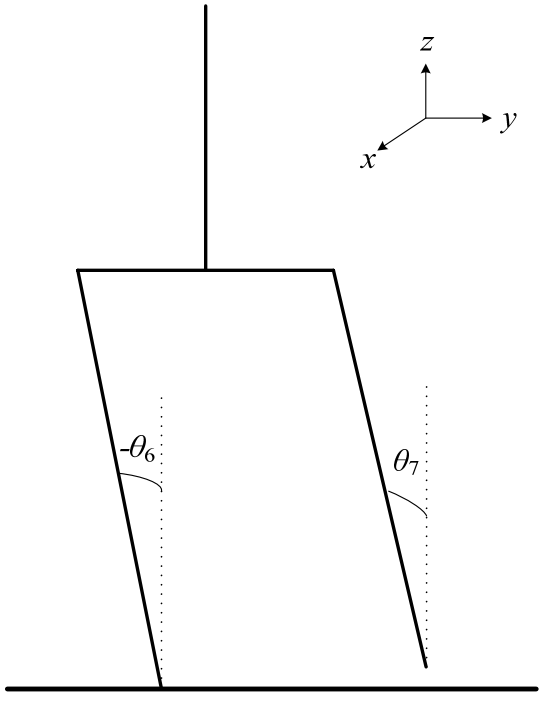

Figure 2.7 The link structure of biped robot in Frontal Plane

In order to obtain the mathematical model of the biped robot with the multilink structure given in Figure 2.5, the course of action taken is first generating the kinematics equations of motion of the biped locomotion and then, developing the dynamic equations of motion by following the procedures of the Lagrangian formulation both in the single-leg support phase and double-leg support phase [60].

2.3.1 Kinematic Equations

The kinematics model of the 5-link 7 DOF biped robot utilized in this study will be presented in this section. In generating the kinematics equations, certain assumptions and simplifications are made in the physical model of the biped robot:

1) Both of the left and right sides of the biped walking are symmetric;
2) The feet are assumed to be massless so that the dynamic structures of the feet are ignored;
3) There is point contact between the stance leg tip and the walking surface;
4) There is no actuation between the tip of the stance leg and the walking surface, and the actuation is at all internal joints of the biped;
5) The base areas of the legs' tips are large enough to maintain its balance at vertical positions (no slippage);
6) The torso oscillates in the frontal plane (in synchronous with the locomotion) to maintain the stability of the biped;
7) The hip strip is always parallel to the ground and there is no twisting motion of hip strip in xy-plane;
8) The friction of the ground is sufficiently large to ensure no slipping of the supporting end.

The biped model consists of 5 rigid links; 1 link for the upper body (torso) and 2 links for the thighs (upper legs), and the 2 links for the shanks (lower legs). These links are connected via 7 rotating joints: 5 hip joints and 2 knee joints.

The variables, given in Figure 2.8, are defined as

m_i – mass of link i $(i = 1,...,5)$

l_i – length of link i $(i = 1,...,5)$

l_6 – width of hip

d_i – distance between the center of mass of link i and its lower joint

I_i – moment of inertia of link i with respect to the axis passing through the center of mass of link i in vertical direction

θ_i – angle of link i with respect to the vertical position, i.e. absolute angle in sagittal plane $(i = 1,...,5)$

θ_{i+5} – angle of link i with respect to the vertical position i.e. absolute angle in frontal plane $(i = 1,2)$

(x_e, y_e, z_e) – the position of the swing leg tip (free end tip)

(x_b, y_b, z_b) – the position of the stance leg tip (point of support)

$O_o - X_o - Y_o - Z_o$ – the fixed coordinate frame

The position of the free end is obtained as

$$\mathrm{x_e} = \mathrm{x_b} + l_1 \sin\theta_1 + l_2 \sin\theta_2 + l_4 \sin\theta_4 + l_5 \sin\theta_5 \tag{2.1}$$

$$\mathrm{y_e} = \mathrm{y_b} + (l_1 + l_2)\sin\theta_6 + l_6 + (l_4 + l_5)\sin\theta_7 \tag{2.2}$$

$$\mathrm{z_e} = \mathrm{z_b} + l_1 \cos\theta_1 + l_2 \cos\theta_2 - l_4 \cos\theta_4 - l_5 \cos\theta_5 \tag{2.3}$$

and the velocity of the free end is obtained as

$$\begin{aligned} \mathrm{v_e} = \begin{Bmatrix} \dot{x}_e \\ \dot{y}_e \\ \dot{z}_e \end{Bmatrix} = & \begin{pmatrix} l_1 \cos\theta_1 \\ 0 \\ -l_1 \sin\theta_1 \end{pmatrix} \dot{\theta}_1 + \begin{pmatrix} l_2 \cos\theta_2 \\ 0 \\ -l_2 \sin\theta_2 \end{pmatrix} \dot{\theta}_2 + \begin{pmatrix} l_4 \cos\theta_4 \\ 0 \\ l_4 \sin\theta_4 \end{pmatrix} \dot{\theta}_4 + \\ & \begin{pmatrix} l_5 \cos\theta_5 \\ 0 \\ l_5 \sin\theta_5 \end{pmatrix} \dot{\theta}_5 + \begin{pmatrix} 0 \\ (l_1 + l_2)\cos\theta_6 \\ 0 \end{pmatrix} \dot{\theta}_6 + \begin{pmatrix} 0 \\ (l_4 + l_5)\cos\theta_7 \\ 0 \end{pmatrix} \dot{\theta}_7 \end{aligned} \tag{2.4}$$

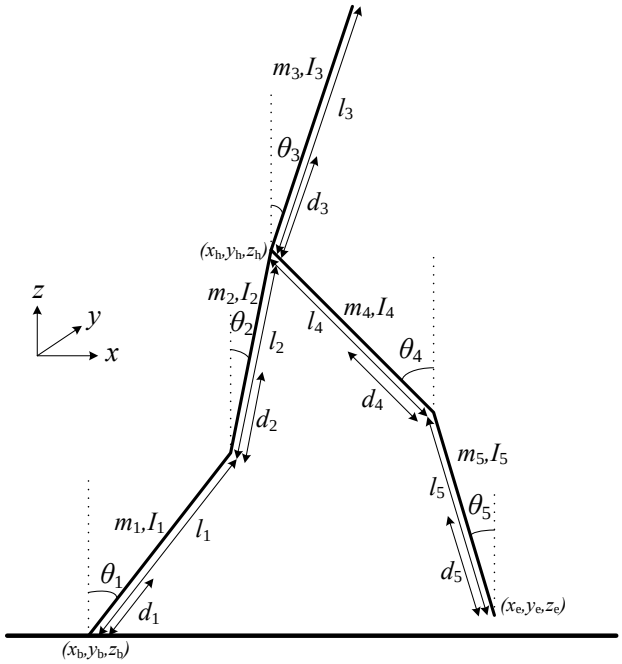

a) in Sagittal Plane

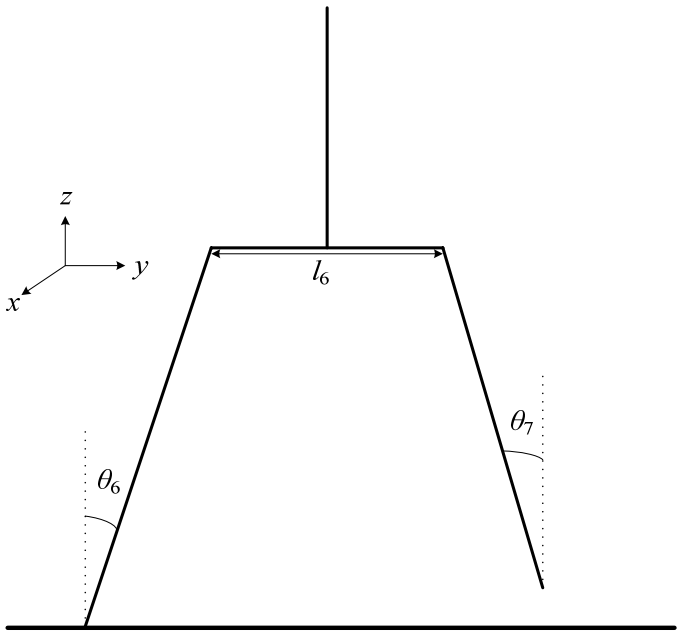

b) in Frontal Plane

Figure 2.8 5-link biped robot model parameters

Now, if (cgx , cgy , cgz) are the coordinates of the biped's center of mass and xc_i , yc_i and zc_i are the coordinates of the center of mass of link i in x-, y- and z- coordinates, respectively, then

$$cgx = \frac{m_1 xc_1 + m_2 xc_2 + m_3 xc_3 + m_4 xc_4 + m_5 xc_5}{m_1 + m_2 + m_3 + m_4 + m_5} \tag{2.5}$$

$$cgy = \frac{m_1 yc_1 + m_2 yc_2 + m_3 yc_3 + m_4 yc_4 + m_5 yc_5}{m_1 + m_2 + m_3 + m_4 + m_5} \tag{2.6}$$

$$cgz = \frac{m_1 zc_1 + m_2 zc_2 + m_3 zc_3 + m_4 zc_4 + m_5 zc_5}{m_1 + m_2 + m_3 + m_4 + m_5} \tag{2.7}$$

and

$$xc_1 = d_1 \sin\theta_1 \tag{2.8}$$

$$yc_1 = d_1 \sin\theta_6 \tag{2.9}$$

$$zc_1 = d_1 \cos\theta_1 \tag{2.10}$$

$$xc_2 = l_1 \sin\theta_1 + d_2 \sin\theta_2 \tag{2.11}$$

$$yc_2 = (l_1 + d_2) \sin\theta_6 \tag{2.12}$$

$$zc_2 = l_1 \cos\theta_1 + d_2 \cos\theta_2 \tag{2.13}$$

$$xc_3 = l_1 \sin\theta_1 + l_2 \sin\theta_2 + d_3 \sin\theta_3 \tag{2.14}$$

$$yc_3 = (l_1 + l_2) \sin\theta_6 + l_6 / 2 \tag{2.15}$$

$$zc_3 = l_1 \cos\theta_1 + l_2 \cos\theta_2 + d_3 \cos\theta_3 \tag{2.16}$$

$$xc_4 = l_1 \sin\theta_1 + l_2 \sin\theta_2 + (l_4 - d_4) \sin\theta_4 \tag{2.17}$$

$$yc_4 = (l_1 + l_2) \sin\theta_6 + l_6 + (l_4 - d_4) \sin\theta_7 \tag{2.18}$$

$$zc_4 = l_1 \cos\theta_1 + l_2 \cos\theta_2 - (l_4 - d_4) \cos\theta_4 \tag{2.19}$$

$$xc_5 = l_1 \sin\theta_1 + l_2 \sin\theta_2 + l_4 \sin\theta_4 + (l_5 - d_5) \sin\theta_5 \tag{2.20}$$

$$yc_5 = (l_1 + l_2) \sin\theta_6 + l_6 + (l_4 + l_5 - d_5) \sin\theta_7 \tag{2.21}$$

$$zc_5 = l_1 \cos\theta_1 + l_2 \cos\theta_2 - l_4 \cos\theta_4 - (l_5 - d_5) \cos\theta_5 \tag{2.22}$$

The linear velocity of every link's center of mass is:

$$vc_1 = \begin{pmatrix} d_1 \cos\theta_1 \\ 0 \\ -d_1 \sin\theta_1 \end{pmatrix} \dot{\theta}_1 + \begin{pmatrix} 0 \\ d_1 \cos\theta_6 \\ 0 \end{pmatrix} \dot{\theta}_6 \tag{2.23}$$

$$vc_2 = \begin{pmatrix} l_1 \cos\theta_1 \\ 0 \\ -l_1 \sin\theta_1 \end{pmatrix} \dot{\theta}_1 + \begin{pmatrix} d_2 \cos\theta_2 \\ 0 \\ -d_2 \sin\theta_2 \end{pmatrix} \dot{\theta}_2 + \begin{pmatrix} 0 \\ (l_1 + d_2) \cos\theta_6 \\ 0 \end{pmatrix} \dot{\theta}_6 \tag{2.24}$$

$$vc_3 = \begin{pmatrix} l_1 \cos\theta_1 \\ 0 \\ -l_1 \sin\theta_1 \end{pmatrix} \dot{\theta}_1 + \begin{pmatrix} l_2 \cos\theta_2 \\ 0 \\ -l_2 \sin\theta_2 \end{pmatrix} \dot{\theta}_2 + \begin{pmatrix} d_3 \cos\theta_3 \\ 0 \\ -d_3 \sin\theta_3 \end{pmatrix} \dot{\theta}_3 + \begin{pmatrix} 0 \\ (l_1 + l_2) \cos\theta_6 \\ 0 \end{pmatrix} \dot{\theta}_6 \tag{2.25}$$

$$\begin{aligned} vc_4 = & \begin{pmatrix} l_1 \cos\theta_1 \\ 0 \\ -l_1 \sin\theta_1 \end{pmatrix} \dot{\theta}_1 + \begin{pmatrix} l_2 \cos\theta_2 \\ 0 \\ -l_2 \sin\theta_2 \end{pmatrix} \dot{\theta}_2 + \begin{pmatrix} (l_4 - d_4) \cos\theta_4 \\ 0 \\ (l_4 - d_4) \sin\theta_4 \end{pmatrix} \dot{\theta}_4 + \\ & \begin{pmatrix} 0 \\ (l_1 + l_2) \cos\theta_6 \\ 0 \end{pmatrix} \dot{\theta}_6 + \begin{pmatrix} 0 \\ (l_4 - d_4) \cos\theta_7 \\ 0 \end{pmatrix} \dot{\theta}_7 \end{aligned} \tag{2.26}$$

$$\begin{aligned} vc_5 = & \begin{pmatrix} l_1 \cos\theta_1 \\ 0 \\ -l_1 \sin\theta_1 \end{pmatrix} \dot{\theta}_1 + \begin{pmatrix} l_2 \cos\theta_2 \\ 0 \\ -l_2 \sin\theta_2 \end{pmatrix} \dot{\theta}_2 + \begin{pmatrix} l_4 \cos\theta_4 \\ 0 \\ l_4 \sin\theta_4 \end{pmatrix} \dot{\theta}_4 + \\ & \begin{pmatrix} (l_5 - d_5) \cos\theta_5 \\ 0 \\ (l_5 - d_5) \sin\theta_5 \end{pmatrix} \dot{\theta}_5 + \begin{pmatrix} 0 \\ (l_1 + l_2) \cos\theta_6 \\ 0 \end{pmatrix} \dot{\theta}_6 + \begin{pmatrix} 0 \\ (l_4 + l_5 - d_5) \cos\theta_7 \\ 0 \end{pmatrix} \dot{\theta}_7 \end{aligned} \tag{2.27}$$

2.3.2 Dynamic Equations

After deciding on the physical model and deriving the kinematics of the biped robot, one of the well known methods can be used to derive the dynamics. The well-known methodologies to develop the equations of motion that describes the dynamics can be classified into two:

1) Newton-Euler Method
2) Lagrangian Method

The Newton-Euler method is comparatively simple to implement but on the other hand, it increases the size of the problem to be solved since it includes additional set of algebraic constraint equations by introducing a set of Lagrange's multipliers of joint reaction forces. An advanced approach to human motion simulation introduces dynamics by using the generalized coordinates with Lagrangian method. The equation of motion of the system is obtained by a direct substitution of the expression for the Lagrangian into the Euler-Lagrange equation. In this method, there is no constraint equation but finding the generalized coordinates may be difficult. In modeling the dynamics of the biped, Lagrangian method is used and the dynamic equations are obtained accordingly in this thesis. The equation of the motion is calculated in single-support and double support phases separately.

2.3.2.1 Single Support Phase

The dynamics of the biped can be written in a general form as in (2.28). The aim is to find the coefficient matrices $D(\underline{\theta})$, $h(\underline{\theta},\underline{\dot{\theta}})$ and $G(\underline{\theta})$ for the link and joint structure given in Figure 2.8 by using the Lagrangian formulation.

$$D(\underline{\theta})\underline{\ddot{\theta}} + h(\underline{\theta},\underline{\dot{\theta}})\underline{\dot{\theta}} + G(\underline{\theta}) = T_\theta \tag{2.28}$$

where

$$\underline{\theta} = \left[\theta_1, \theta_2, \theta_3, \theta_4, \theta_5, \theta_6, \theta_7\right]^T \tag{2.29}$$

$$\underline{T_\theta} = \left[T_{\theta 1}, T_{\theta 2}, T_{\theta 3}, T_{\theta 4}, T_{\theta 5}, T_{\theta 6}, T_{\theta 7}\right]^T \tag{2.30}$$

The configuration in single support phase is schematically shown in Figure 2.9. It is assumed that the friction of the ground is sufficiently large to ensure no slipping of the supporting end.

The Lagrangian method in dynamic modeling is used to describe the motion of the biped and the Lagrangian equation of motion is in the form of

$$L = K - P \tag{2.31}$$

where K is the total kinetic energy and P is the total potential energy of the system.

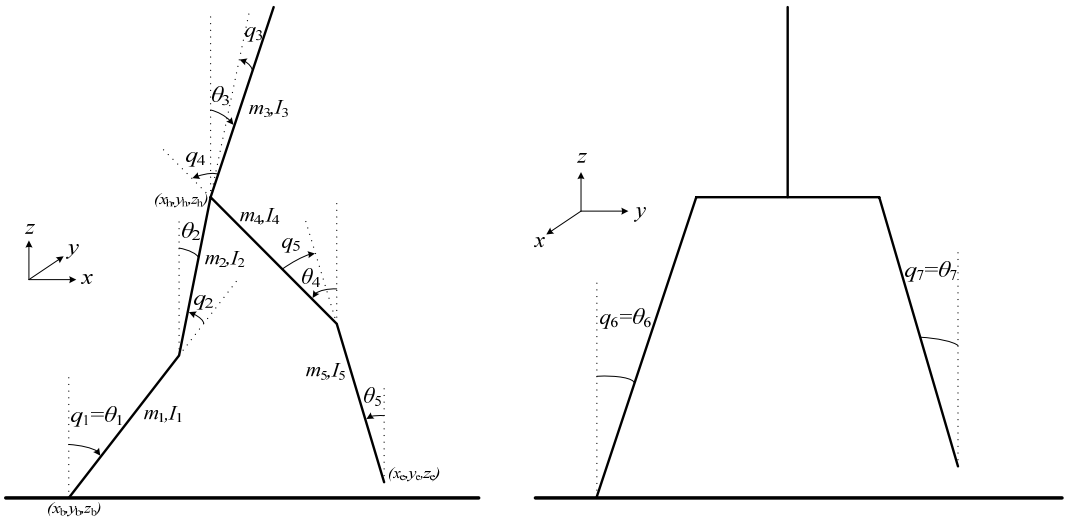

a) Sagittal Plane b) Frontal Plane

Figure 2.9 Biped model in single support phase

The potential energy P is

$$P = \sum_{i=1}^{5} P_i \quad \text{with} \quad \mathrm{P_i} = m_i\, g\, zc_i \tag{2.32}$$

where

g is the gravitational acceleration and

zc_i is determined from equations (2.10), (2.13), (2.16), (2.19) and (2.22).

The kinetic energy K is

$$K = \sum_{i=1}^{5} K_i \ \text{with} \tag{2.33}$$

$$K_{\mathrm{i}} = \frac{1}{2} m_i\, vc_i^{\,2} + \frac{1}{2} I_i (\dot{\theta}_i^{\,2} + \dot{\theta}_6^{\,2}) \ \text{for} \ i = 1, 2 \tag{2.34}$$

$$K_{\mathrm{i}} = \frac{1}{2} m_i\, vc_i^{\,2} + \frac{1}{2} I_i (\dot{\theta}_i^{\,2} + \dot{\theta}_7^{\,2}) \ \text{for} \ i = 4, 5 \tag{2.35}$$

$$K_{\mathrm{i}} = \frac{1}{2} m_i v c_i^{\,2} + \frac{1}{2} I_i \dot{\theta}_i^{\,2} \quad \text{for } i = 3 \tag{2.36}$$

By replacing zc_i from (2.10), (2.13), (2.16), (2.19) and (2.22) into (2.32) and vc_i from (2.23)-(2.27) into (2.33)-(2.36), the kinetic energy and potential energy for each link are obtained as

Link 1:

$$K_1 = \frac{1}{2}(I_1 + m_1 d_1^{\,2})\dot{\theta}_1^{\,2} + \frac{1}{2}(I_1 + m_1 d_1^{\,2}\cos^2\theta_6)\dot{\theta}_6^{\,2} \tag{2.37}$$

$$P_1 = m_1 g d_1 \cos\theta_1 \tag{2.38}$$

where

$$I_1 = \frac{1}{3} m_1 l_1^{\,2} \tag{2.39}$$

Link 2:

$$\begin{aligned} K_2 = {} & \frac{1}{2}(I_2 + m_2 d_2^{\,2})\dot{\theta}_2^{\,2} + \frac{1}{2} m_2 l_1^{\,2}\dot{\theta}_1^{\,2} + m_2 l_1 d_2 \cos(\theta_1 - \theta_2)\dot{\theta}_1\dot{\theta}_2 \\ & + \frac{1}{2}\left[I_2 + m_2 (l_1 + d_2)^2 \cos^2\theta_6 \right]\dot{\theta}_6^{\,2} \end{aligned} \tag{2.40}$$

$$P_2 = m_2 g (l_1 \cos\theta_1 + d_2 \cos\theta_2) \tag{2.41}$$

where

$$I_2 = \frac{1}{3} m_2 l_2^{\,2} \tag{2.42}$$

Link 3:

$$\begin{aligned} K_3 = {} & \frac{1}{2}(I_3 + m_3 d_3^{\,2})\dot{\theta}_3^{\,2} \\ & + \frac{1}{2} m_3 \begin{bmatrix} l_1^{\,2}\dot{\theta}_1^{\,2} + l_2^{\,2}\dot{\theta}_2^{\,2} + 2 l_1 l_2 \cos(\theta_1 - \theta_2)\dot{\theta}_1\dot{\theta}_2 \\ + 2 l_1 d_3 \cos(\theta_1 - \theta_3)\dot{\theta}_1\dot{\theta}_3 + 2 l_2 d_3 \cos(\theta_2 - \theta_3)\dot{\theta}_2\dot{\theta}_3 \end{bmatrix} \\ & + \frac{1}{2} m_3 (l_1 + l_2)^2 \cos^2\theta_6 \dot{\theta}_6^{\,2} \end{aligned} \tag{2.43}$$

$$P_3 = m_3 g(l_1 \cos\theta_1 + l_2 \cos\theta_2 + d_3 \cos\theta_3) \tag{2.44}$$

where

$$I_3 = \frac{1}{3} m_3 l_3^{\,2} \tag{2.45}$$

Link 4:

$$\begin{aligned} K_4 = {} & \frac{1}{2}\left[I_4 + m_4 (l_4 - d_4)^2 \right] \dot{\theta}_4^{\,2} \\ & + \frac{1}{2} m_4 \begin{bmatrix} l_1^{\,2}\dot{\theta}_1^{\,2} + l_2^{\,2}\dot{\theta}_2^{\,2} + 2 l_1 l_2 \cos(\theta_1 - \theta_2)\dot{\theta}_1\dot{\theta}_2 + \\ 2 l_1 (l_4 - d_4)\cos(\theta_1 + \theta_4)\dot{\theta}_1\dot{\theta}_4 + 2 l_2 (l_4 - d_4)\cos(\theta_2 + \theta_4)\dot{\theta}_2\dot{\theta}_4 \end{bmatrix} \\ & + \frac{1}{2} m_4 \left[(l_1 + l_2)^2 \cos^2\theta_6 \right] \dot{\theta}_6^{\,2} + \frac{1}{2}\left[I_4 + m_4 (l_4 - d_4)^2 \cos^2\theta_7 \right] \dot{\theta}_7^{\,2} \\ & + m_4 (l_1 + l_2)(l_4 - d_4)\cos\theta_6 \cos\theta_7 \dot{\theta}_6 \dot{\theta}_7 \end{aligned} \tag{2.46}$$

$$P_4 = m_4 g\left[l_1 \cos\theta_1 + l_2 \cos\theta_2 - (l_4 - d_4)\cos\theta_4 \right] \tag{2.47}$$

where

$$I_4 = \frac{1}{3} m_4 l_4^{\,2} \tag{2.48}$$

Link 5:

$$\begin{aligned} K_5 = {} & \frac{1}{2}\left[I_5 + m_5 (l_5 - d_5)^2 \right] \dot{\theta}_5^{\,2} \\ & + \frac{1}{2} m_5 \begin{bmatrix} l_1^{\,2}\dot{\theta}_1^{\,2} + l_2^{\,2}\dot{\theta}_2^{\,2} + l_4^{\,2}\dot{\theta}_4^{\,2} + 2 l_1 l_2 \cos(\theta_1 - \theta_2)\dot{\theta}_1\dot{\theta}_2 \\ + 2 l_1 l_4 \cos(\theta_1 + \theta_4)\dot{\theta}_1\dot{\theta}_4 + 2 l_1 (l_5 - d_5)\cos(\theta_1 + \theta_5)\dot{\theta}_1\dot{\theta}_5 \\ + 2 l_2 l_4 \cos(\theta_2 + \theta_4)\dot{\theta}_2\dot{\theta}_4 + 2 l_2 (l_5 - d_5)\cos(\theta_2 + \theta_5)\dot{\theta}_2\dot{\theta}_5 \\ + 2 l_4 (l_5 - d_5)\cos(\theta_4 - \theta_5)\dot{\theta}_4\dot{\theta}_5 \end{bmatrix} \\ & + \frac{1}{2} m_5 \left[(l_1 + l_2)^2 \cos^2\theta_6 \right] \dot{\theta}_6^{\,2} + \frac{1}{2}\left[I_5 + m_5 (l_4 + l_5 - d_5)^2 \cos^2\theta_7 \right] \dot{\theta}_7^{\,2} \\ & + m_5 (l_1 + l_2)(l_4 + l_5 - d_5)\cos\theta_6 \cos\theta_7 \dot{\theta}_6 \dot{\theta}_7 \end{aligned} \tag{2.49}$$

$$P_5 = m_5 g\left[l_1 \cos\theta_1 + l_2 \cos\theta_2 - l_4 \cos\theta_4 - (l_5 - d_5)\cos\theta_5 \right] \tag{2.50}$$

where

$$I_5 = \frac{1}{3} m_5 l_5^{\,2} \tag{2.51}$$

The Lagrangian equation of motion, L, is obtained by

$$L = K - P \quad => L = \sum_{i=1}^{5} K_i - \sum_{i=1}^{5} P_i \tag{2.52}$$

Thereafter, the Euler-Lagrange equation is used in order to bring out the dynamics as

$$\frac{d}{dt}\left\{\frac{\partial L}{\partial \dot{q}_i}\right\} - \frac{\partial L}{\partial q_i} = T_i \quad (i = 1, ..., 7) \tag{2.53}$$

The dynamic equations are obtained by inserting (2.52) into (2.53) as

$$\frac{d}{dt}\left\{\frac{\partial K}{\partial \dot{q}_i}\right\} - \frac{d}{dt}\left\{\frac{\partial P}{\partial \dot{q}_i}\right\} - \frac{\partial K}{\partial q_i} + \frac{\partial P}{\partial q_i} = T_i \tag{2.54}$$

$$=> \quad \frac{d}{dt}\left\{\frac{\partial K}{\partial \dot{q}_i}\right\} - \frac{\partial K}{\partial q_i} + \frac{\partial P}{\partial q_i} = T_i \quad (i = 1, ..., 7) \tag{2.55}$$

The equation (2.55) can be adopted to be written in terms of the absolute angles in stead of the relative angles where the conversion between two angles, both representations given in Figure 2.9, is defined as

$$q_1 = \theta_1$$
$$q_2 = \theta_1 - \theta_2$$
$$q_3 = \theta_2 - \theta_3$$
$$q_4 = \theta_3 + \theta_4$$
$$q_5 = \theta_4 - \theta_5$$
$$q_6 = \theta_6$$
$$q_7 = \theta_7$$

in order to express the dynamics in the form of absolute angles as

$$\frac{d}{dt}\left\{\frac{\partial L}{\partial \dot{\theta}_i}\right\}-\frac{\partial L}{\partial \theta_i}=T_{\theta_i} \tag{2.56}$$

Then the equations in terms of absolute angles becomes

$$\text{I. } \frac{d}{dt}\left\{\frac{\partial K}{\partial \dot{\theta}_1}\right\}-\frac{\partial K}{\partial \theta_1}+\frac{\partial P}{\partial \theta_1}=T_1 \tag{2.57}$$

$$\text{II. } \frac{d}{dt}\left\{\frac{\partial K}{\partial \dot{\theta}_1}\right\}-\frac{d}{dt}\left\{\frac{\partial K}{\partial \dot{\theta}_2}\right\}-\frac{\partial K}{\partial \theta_1}+\frac{\partial K}{\partial \theta_2}+\frac{\partial P}{\partial \theta_1}-\frac{\partial P}{\partial \theta_2}=T_2 \tag{2.58}$$

$$\text{III. } \frac{d}{dt}\left\{\frac{\partial K}{\partial \dot{\theta}_2}\right\}-\frac{d}{dt}\left\{\frac{\partial K}{\partial \dot{\theta}_3}\right\}-\frac{\partial K}{\partial \theta_2}+\frac{\partial K}{\partial \theta_3}+\frac{\partial P}{\partial \theta_2}-\frac{\partial P}{\partial \theta_3}=T_3 \tag{2.59}$$

$$\text{IV. } \frac{d}{dt}\left\{\frac{\partial K}{\partial \dot{\theta}_3}\right\}-\frac{d}{dt}\left\{\frac{\partial K}{\partial \dot{\theta}_4}\right\}-\frac{\partial K}{\partial \theta_3}+\frac{\partial K}{\partial \theta_4}+\frac{\partial P}{\partial \theta_3}-\frac{\partial P}{\partial \theta_4}=T_4 \tag{2.60}$$

$$\text{V. } \frac{d}{dt}\left\{\frac{\partial K}{\partial \dot{\theta}_4}\right\}-\frac{d}{dt}\left\{\frac{\partial K}{\partial \dot{\theta}_5}\right\}-\frac{\partial K}{\partial \theta_4}+\frac{\partial K}{\partial \theta_5}+\frac{\partial P}{\partial \theta_4}-\frac{\partial P}{\partial \theta_5}=T_5 \tag{2.61}$$

$$\text{VI. } \frac{d}{dt}\left\{\frac{\partial K}{\partial \dot{\theta}_6}\right\}-\frac{\partial K}{\partial \theta_6}+\frac{\partial P}{\partial \theta_6}=T_6 \tag{2.62}$$

$$\text{VII. } \frac{d}{dt}\left\{\frac{\partial K}{\partial \dot{\theta}_7}\right\}-\frac{\partial K}{\partial \theta_7}+\frac{\partial P}{\partial \theta_7}=T_7 \tag{2.63}$$

Now, we can reorganize these equations in the form of

$$\frac{d}{dt}\left\{\frac{\partial K}{\partial \dot{\theta}_i}\right\}-\frac{\partial K}{\partial \theta_i}+\frac{\partial P}{\partial \theta_i}=T_{\theta_i} \quad i=1,...,7 \tag{2.64}$$

so that each of these Euler-Lagrange equations are to be formulated with respect to θ_i 's as

I*=I:

$$\frac{d}{dt}\left\{\frac{\partial K}{\partial \dot{\theta}_1}\right\}-\frac{\partial K}{\partial \theta_1}+\frac{\partial P}{\partial \theta_1}=T_{\theta_1} \text{ where } T_{\theta_1}=T_1 \tag{2.65}$$

II* = (I-II):

$$\frac{d}{dt}\left\{\frac{\partial K}{\partial \dot{\theta}_2}\right\}+\frac{\partial K}{\partial \theta_2}-\frac{\partial P}{\partial \theta_2}=T_{\theta_2} \text{ where } T_{\theta_2}=T_1-T_2 \tag{2.66}$$

III*= (II*-III):

$$\frac{d}{dt}\left\{\frac{\partial K}{\partial \dot{\theta}_3}\right\}+\frac{\partial K}{\partial \theta_3}-\frac{\partial P}{\partial \theta_3}=T_{\theta_3} \text{ where } T_{\theta_3}=T_1-T_2-T_3 \tag{2.67}$$

IV*=(IV-III*):

$$\frac{d}{dt}\left\{\frac{\partial K}{\partial \dot{\theta}_4}\right\}-\frac{\partial K}{\partial \theta_4}+\frac{\partial P}{\partial \theta_4}=T_{\theta_4} \text{ where } T_{\theta_4}=T_4-T_1+T_2+T_3 \tag{2.68}$$

V*=(IV*-V):

$$\frac{d}{dt}\left\{\frac{\partial K}{\partial \dot{\theta}_5}\right\}-\frac{\partial K}{\partial \theta_5}+\frac{\partial P}{\partial \theta_5}=T_{\theta_5} \text{ where } T_{\theta_5}=T_4-T_1+T_2+T_3-T_5 \tag{2.69}$$

VI*=VI:

$$\frac{d}{dt}\left\{\frac{\partial K}{\partial \dot{\theta}_6}\right\}-\frac{\partial K}{\partial \theta_6}+\frac{\partial P}{\partial \theta_6}=T_{\theta_6} \text{ where } T_{\theta_6}=T_6 \tag{2.70}$$

VII*=VII:

$$\frac{d}{dt}\left\{\frac{\partial K}{\partial \dot{\theta}_7}\right\}-\frac{\partial K}{\partial \theta_7}+\frac{\partial P}{\partial \theta_7}=T_{\theta_7} \text{ where } T_{\theta_7}=T_7 \tag{2.71}$$

Now, let’s drive each term in the above equations as

$$\begin{aligned}\frac{\partial K}{\partial \dot{\theta}_1} &= \left[I_1 + m_1 d_1^{\,2} + (m_2 + m_3 + m_4 + m_5) l_1^{\,2} \right] \dot{\theta}_1 + \\ &+ \left[m_2 l_1 d_2 + (m_3 + m_4 + m_5) l_1 l_2 \right] \cos(\theta_1 - \theta_2) \dot{\theta}_2 \\ &+ m_3 l_1 d_3 \cos(\theta_1 - \theta_3) \dot{\theta}_3 + \left[m_4 l_1 (l_4 - d_4) + m_5 l_1 l_4 \right] \cos(\theta_1 + \theta_4) \dot{\theta}_4 \\ &+ m_5 l_1 (l_5 - d_5) \cos(\theta_1 + \theta_5) \dot{\theta}_5 \end{aligned} \tag{2.72}$$

$$\begin{aligned}\frac{d}{dt}\left\{ \frac{\partial K}{\partial \dot{\theta}_1} \right\} &= \left[I_1 + m_1 d_1^{\,2} + (m_2 + m_3 + m_4 + m_5) l_1^{\,2} \right] \ddot{\theta}_1 \\ &+ \left[m_2 l_1 d_2 + (m_3 + m_4 + m_5) l_1 l_2 \right] \begin{bmatrix} \cos(\theta_1 - \theta_2) \ddot{\theta}_2 - \sin(\theta_1 - \theta_2) \dot{\theta}_1 \dot{\theta}_2 \\ + \sin(\theta_1 - \theta_2) \dot{\theta}_2^2 \end{bmatrix} \\ &+ m_3 l_1 d_3 \left[\cos(\theta_1 - \theta_3) \ddot{\theta}_3 - \sin(\theta_1 - \theta_3) \dot{\theta}_1 \dot{\theta}_3 + \sin(\theta_1 - \theta_3) \dot{\theta}_3^2 \right] \\ &+ \left[m_4 l_1 (l_4 - d_4) + m_5 l_1 l_4 \right] \begin{bmatrix} \cos(\theta_1 + \theta_4) \ddot{\theta}_4 - \sin(\theta_1 + \theta_4) \dot{\theta}_1 \dot{\theta}_4 \\ - \sin(\theta_1 + \theta_4) \dot{\theta}_4^2 \end{bmatrix} \\ &+ m_5 l_1 (l_5 - d_5) \left[\cos(\theta_1 + \theta_5) \ddot{\theta}_5 - \sin(\theta_1 + \theta_5) \dot{\theta}_1 \dot{\theta}_5 - \sin(\theta_1 + \theta_5) \dot{\theta}_5^2 \right] \end{aligned} \tag{2.73}$$

$$\begin{aligned}\frac{\partial K}{\partial \theta_1} &= -\left[m_2 l_1 d_2 + (m_3 + m_4 + m_5) l_1 l_2 \right] \sin(\theta_1 - \theta_2) \dot{\theta}_1 \dot{\theta}_2 \\ &- m_3 l_1 d_3 \sin(\theta_1 - \theta_3) \dot{\theta}_1 \dot{\theta}_3 - \left[m_4 l_1 (l_4 - d_4) + m_5 l_1 l_4 \right] \sin(\theta_1 + \theta_4) \dot{\theta}_1 \dot{\theta}_4 \\ &- m_5 l_1 (l_5 - d_5) \sin(\theta_1 + \theta_5) \dot{\theta}_1 \dot{\theta}_5 \end{aligned} \tag{2.74}$$

$$\frac{\partial P}{\partial \theta_1} = -\left[m_1 d_1 + (m_2 + m_3 + m_4 + m_5) l_1 \right] g \sin \theta_1 \tag{2.75}$$

$$\begin{aligned}\frac{\partial K}{\partial \dot{\theta}_2} &= \left[m_2 l_1 d_2 + (m_3 + m_4 + m_5) l_1 l_2 \right] \cos(\theta_1 - \theta_2) \dot{\theta}_1 \\ &+ \left[I_2 + m_2 d_2^2 + (m_3 + m_4 + m_5) l_2^2 \right] \dot{\theta}_2 + m_3 l_2 d_3 \cos(\theta_2 - \theta_3) \dot{\theta}_3 \\ &+ \left[m_4 l_2 (l_4 - d_4) + m_5 l_2 l_4 \right] \cos(\theta_2 + \theta_4) \dot{\theta}_4 + m_5 l_2 (l_5 - d_5) \cos(\theta_2 + \theta_5) \dot{\theta}_5 \end{aligned} \tag{2.76}$$

$$\frac{d}{dt}\left\{\frac{\partial K}{\partial \dot{\theta}_2}\right\} =$$
$$\begin{aligned}
&\left[m_2 l_1 d_2 + (m_3+m_4+m_5) l_1 l_2\right]\begin{bmatrix}\cos(\theta_1-\theta_2)\ddot{\theta}_1 + \sin(\theta_1-\theta_2)\dot{\theta}_1\dot{\theta}_2 \\ -\sin(\theta_1-\theta_2)\dot{\theta}_1^2\end{bmatrix} \\
&+\left[I_2 + m_2 d_2^2 + (m_3+m_4+m_5) l_2^2\right]\ddot{\theta}_2 \\
&+ m_3 l_2 d_3\left[\cos(\theta_2-\theta_3)\ddot{\theta}_3 - \sin(\theta_2-\theta_3)\dot{\theta}_2\dot{\theta}_3 + \sin(\theta_2-\theta_3)\dot{\theta}_3^2\right] \\
&+\left[m_4 l_2 (l_4-d_4) + m_5 l_2 l_4\right]\begin{bmatrix}\cos(\theta_2+\theta_4)\ddot{\theta}_4 - \sin(\theta_2+\theta_4)\dot{\theta}_2\dot{\theta}_4 \\ -\sin(\theta_2+\theta_4)\dot{\theta}_4^2\end{bmatrix} \\
&+ m_5 l_2 (l_5-d_5)\left[\cos(\theta_2+\theta_5)\ddot{\theta}_5 - \sin(\theta_2+\theta_5)\dot{\theta}_2\dot{\theta}_5 - \sin(\theta_2+\theta_5)\dot{\theta}_5^2\right]
\end{aligned} \tag{2.77}$$

$$\begin{aligned}
\frac{\partial K}{\partial \theta_2} &= \left[m_2 l_1 d_2 + (m_3+m_4+m_5) l_1 l_2\right]\sin(\theta_1-\theta_2)\dot{\theta}_1\dot{\theta}_2 - m_3 l_2 d_3 \sin(\theta_2-\theta_3)\dot{\theta}_2\dot{\theta}_3 \\
&\quad -\left[m_4 l_2 (l_4-d_4) + m_5 l_2 l_4\right]\sin(\theta_2+\theta_4)\dot{\theta}_2\dot{\theta}_4 - m_5 l_2 (l_5-d_5)\sin(\theta_2+\theta_5)\dot{\theta}_2\dot{\theta}_5
\end{aligned} \tag{2.78}$$

$$\frac{\partial P}{\partial \theta_2} = -\left[m_2 d_2 + (m_3+m_4+m_5) l_2\right] g \sin\theta_2 \tag{2.79}$$

$$\frac{\partial K}{\partial \dot{\theta}_3} = m_3 l_1 d_3 \cos(\theta_1-\theta_3)\dot{\theta}_1 + m_3 l_2 d_3 \cos(\theta_2-\theta_3)\dot{\theta}_2 + \left[I_3 + m_3 d_3^2\right]\dot{\theta}_3 \tag{2.80}$$

$$\begin{aligned}
\frac{d}{dt}\left\{\frac{\partial K}{\partial \dot{\theta}_3}\right\} &= m_3 l_1 d_3\left[\cos(\theta_1-\theta_3)\ddot{\theta}_1 - \sin(\theta_1-\theta_3)\dot{\theta}_1^2 + \sin(\theta_1-\theta_3)\dot{\theta}_1\dot{\theta}_3\right] \\
&\quad + m_3 l_2 d_3\left[\cos(\theta_2-\theta_3)\ddot{\theta}_2 - \sin(\theta_2-\theta_3)\dot{\theta}_2^2 + \sin(\theta_2-\theta_3)\dot{\theta}_2\dot{\theta}_3\right] \\
&\quad + \left[I_3 + m_3 d_3^2\right]\ddot{\theta}_3
\end{aligned} \tag{2.81}$$

$$\frac{\partial K}{\partial \theta_3} = m_3 l_1 d_3 \sin(\theta_1-\theta_3)\dot{\theta}_1\dot{\theta}_3 + m_3 l_2 d_3 \sin(\theta_2-\theta_3)\dot{\theta}_2\dot{\theta}_3 \tag{2.82}$$

$$\frac{\partial P}{\partial \theta_3} = -m_3 d_3 g \sin\theta_3 \tag{2.83}$$

$$\frac{\partial K}{\partial \dot{\theta}_4} = \left[m_4 l_1 (l_4 - d_4) + m_5 l_1 l_4\right] \cos(\theta_1 + \theta_4)\dot{\theta}_1 + \\ + \left[m_4 l_2 (l_4 - d_4) + m_5 l_2 l_4\right] \cos(\theta_2 + \theta_4)\dot{\theta}_2 + \left[I_4 + m_4 (l_4 - d_4)^2 + m_5 l_4^2\right]\dot{\theta}_4 \\ + m_5 l_4 (l_5 - d_5) \cos(\theta_4 - \theta_5)\dot{\theta}_5 \tag{2.84}$$

$$\frac{d}{dt}\left\{\frac{\partial K}{\partial \dot{\theta}_4}\right\} = \left[m_4 l_1 (l_4 - d_4) + m_5 l_1 l_4\right] \begin{bmatrix} \cos(\theta_1 + \theta_4)\ddot{\theta}_1 - \sin(\theta_1 + \theta_4)\dot{\theta}_1^2 \\ -\sin(\theta_1 + \theta_4)\dot{\theta}_1\dot{\theta}_4 \end{bmatrix} \\ + \left[m_4 l_2 (l_4 - d_4) + m_5 l_2 l_4\right] \begin{bmatrix} \cos(\theta_2 + \theta_4)\ddot{\theta}_2 - \sin(\theta_2 + \theta_4)\dot{\theta}_2^2 \\ -\sin(\theta_2 + \theta_4)\dot{\theta}_2\dot{\theta}_4 \end{bmatrix} \\ + \left[I_4 + m_4 (l_4 - d_4)^2 + m_5 l_4^2\right]\ddot{\theta}_4 \\ + m_5 l_4 (l_5 - d_5)\left[\cos(\theta_4 - \theta_5)\ddot{\theta}_5 - \sin(\theta_4 - \theta_5)\dot{\theta}_4\dot{\theta}_5 + \sin(\theta_4 - \theta_5)\dot{\theta}_5^2\right] \tag{2.85}$$

$$\frac{\partial K}{\partial \theta_4} = -\left[m_4 l_1 (l_4 - d_4) + m_5 l_1 l_4\right] \sin(\theta_1 + \theta_4)\dot{\theta}_1\dot{\theta}_4 \\ -\left[m_4 l_2 (l_4 - d_4) + m_5 l_2 l_4\right] \sin(\theta_2 + \theta_4)\dot{\theta}_2\dot{\theta}_4 - m_5 l_4 (l_5 - d_5) \sin(\theta_4 - \theta_5)\dot{\theta}_4\dot{\theta}_5 \tag{2.86}$$

$$\frac{\partial P}{\partial \theta_4} = \left[m_4 (l_4 - d_4) + m_5 l_4\right] g \sin\theta_4 \tag{2.87}$$

$$\frac{\partial K}{\partial \dot{\theta}_5} = m_5 l_1 (l_5 - d_5) \cos(\theta_1 + \theta_5)\dot{\theta}_1 + m_5 l_2 (l_5 - d_5) \cos(\theta_2 + \theta_5)\dot{\theta}_2 \\ + m_5 l_4 (l_5 - d_5) \cos(\theta_4 - \theta_5)\dot{\theta}_4 + \left[I_5 + m_5 l_1 (l_5 - d_5)^2\right]\dot{\theta}_5 \tag{2.88}$$

$$\frac{d}{dt}\left\{\frac{\partial K}{\partial \dot{\theta}_5}\right\} = m_5 l_1 (l_5 - d_5)\left[\cos(\theta_1 + \theta_5)\ddot{\theta}_1 - \sin(\theta_1 + \theta_5)\dot{\theta}_1^2 - \sin(\theta_1 + \theta_5)\dot{\theta}_1\dot{\theta}_5\right] \\ + m_5 l_2 (l_5 - d_5)\left[\cos(\theta_2 + \theta_5)\ddot{\theta}_2 - \sin(\theta_2 + \theta_5)\dot{\theta}_2^2 - \sin(\theta_2 + \theta_5)\dot{\theta}_2\dot{\theta}_5\right] \\ + m_5 l_4 (l_5 - d_5)\left[\cos(\theta_4 - \theta_5)\ddot{\theta}_4 - \sin(\theta_4 - \theta_5)\dot{\theta}_4^2 + \sin(\theta_4 - \theta_5)\dot{\theta}_4\dot{\theta}_5\right] \\ + \left[I_5 + m_5 (l_5 - d_5)^2\right]\ddot{\theta}_5 \tag{2.89}$$

$$\frac{\partial K}{\partial \theta_5} = -m_5 l_1 (l_5 - d_5)\sin(\theta_1 + \theta_5)\dot{\theta}_1\dot{\theta}_5 - m_5 l_2 (l_5 - d_5)\sin(\theta_2 + \theta_5)\dot{\theta}_2\dot{\theta}_5 + m_5 l_4 (l_5 - d_5)\sin(\theta_4 - \theta_5)\dot{\theta}_4\dot{\theta}_5 \tag{2.90}$$

$$\frac{\partial P}{\partial \theta_5} = m_5 (l_5 - d_5) g \sin\theta_5 \tag{2.91}$$

$$\frac{\partial K}{\partial \dot{\theta}_6} = (I_1 + I_2)\dot{\theta}_6 + \left[m_1 d_1^{\,2} + m_2 (l_1 + d_2)^2 + (m_3 + m_4 + m_5)(l_1 + l_2)^2 \right]\cos^2\theta_6\dot{\theta}_6 + \left[m_4 (l_1 + l_2)(l_4 - d_4) + m_5 (l_1 + l_2)(l_4 + l_5 - d_5) \right]\cos\theta_6 \cos\theta_7\dot{\theta}_7 \tag{2.92}$$

$$\frac{d}{dt}\left\{\frac{\partial K}{\partial \dot{\theta}_6}\right\} = (I_1 + I_2)\ddot{\theta}_6 + \begin{bmatrix} m_1 d_1^{\,2} + m_2 (l_1 + d_2)^2 \\ +(m_3 + m_4 + m_5)(l_1 + l_2)^2 \end{bmatrix}\left[\cos^2\theta_6\ddot{\theta}_6 - 2\sin\theta_6\cos\theta_6\dot{\theta}_6^{\,2}\right] + \begin{bmatrix} m_4 (l_1 + l_2)(l_4 - d_4) \\ +m_5 (l_1 + l_2)(l_4 + l_5 - d_5) \end{bmatrix}\begin{bmatrix} \cos\theta_6\cos\theta_7\ddot{\theta}_7 - \sin\theta_6\cos\theta_7\dot{\theta}_6\dot{\theta}_7 \\ -\cos\theta_6\sin\theta_7\dot{\theta}_7^{\,2} \end{bmatrix} \tag{2.93}$$

$$\frac{\partial K}{\partial \theta_6} = -\left[m_1 d_1^{\,2} + m_2 (l_1 + d_2)^2 + (m_3 + m_4 + m_5)(l_1 + l_2)^2 \right]\sin\theta_6\cos\theta_6\dot{\theta}_6^{\,2} - \left[m_4 (l_1 + l_2)(l_4 - d_4) + m_5 (l_1 + l_2)(l_4 + l_5 - d_5) \right]\sin\theta_6\cos\theta_7\dot{\theta}_6\dot{\theta}_7 \tag{2.94}$$

$$\frac{\partial P}{\partial \theta_6} = 0 \tag{2.95}$$

$$\frac{\partial K}{\partial \dot{\theta}_7} = \left[m_4 (l_1 + l_2)(l_4 - d_4) + m_5 (l_1 + l_2)(l_4 + l_5 - d_5) \right]\cos\theta_6\cos\theta_7\dot{\theta}_6 + (I_4 + I_5)\dot{\theta}_7 + \left[m_4 (l_4 - d_4)^2 + m_5 (l_4 + l_5 - d_5)^2 \right]\cos^2\theta_7\dot{\theta}_7 \tag{2.96}$$

$$\frac{d}{dt}\left\{\frac{\partial K}{\partial \dot{\theta}_7}\right\} = \begin{bmatrix} m_4(l_1+l_2)(l_4-d_4) \\ +m_5(l_1+l_2)(l_4+l_5-d_5) \end{bmatrix}\begin{bmatrix} \cos\theta_6\cos\theta_7\ddot{\theta}_6 - \sin\theta_6\cos\theta_7\dot{\theta}_6^{\,2} \\ -\cos\theta_6\sin\theta_7\dot{\theta}_6\dot{\theta}_7 \end{bmatrix}$$
$$+(I_4+I_5)\ddot{\theta}_7 + \begin{bmatrix} m_4(l_4-d_4)^2 \\ +m_5(l_4+l_5-d_5)^2 \end{bmatrix}\left[\cos^2\theta_7\ddot{\theta}_7 - 2\sin\theta_7\cos\theta_7\dot{\theta}_7^{\,2}\right] \tag{2.97}$$

$$\frac{\partial K}{\partial \theta_7} = -\left[m_4(l_4-d_4)^2 + m_5(l_4+l_5-d_5)^2\right]\sin\theta_7\cos\theta_7\dot{\theta}_7^{\,2}$$
$$-\left[m_4(l_1+l_2)(l_4-d_4) + m_5(l_1+l_2)(l_4+l_5-d_5)\right]\cos\theta_6\sin\theta_7\dot{\theta}_6\dot{\theta}_7 \tag{2.98}$$

$$\frac{\partial P}{\partial \theta_7} = 0 \tag{2.99}$$

So inserting these equations into

$$\frac{d}{dt}\left\{\frac{\partial K}{\partial \dot{\theta}_i}\right\} - \frac{\partial K}{\partial \theta_i} + \frac{\partial P}{\partial \theta_i} = T_{\theta_i} \text{ equations for } i = 1,...,7 \tag{2.100}$$

results in

I^*:

$$\frac{d}{dt}\left\{\frac{\partial K}{\partial \dot{\theta}_1}\right\} - \frac{\partial K}{\partial \theta_1} + \frac{\partial P}{\partial \theta_1} = T_{\theta_1} \tag{2.101}$$

$$\Rightarrow \begin{bmatrix} \left[I_1 + m_1 d_1^{\,2} + (m_2+m_3+m_4+m_5)l_1^{\,2}\right]\ddot{\theta}_1 \\ +\left[m_2 l_1 d_2 + (m_3+m_4+m_5)l_1 l_2\right]\cos(\theta_1-\theta_2)\ddot{\theta}_2 \\ +m_3 l_1 d_3\cos(\theta_1-\theta_3)\ddot{\theta}_3 \\ +\left[m_4 l_1(l_4-d_4) + m_5 l_1 l_4\right]\cos(\theta_1+\theta_4)\ddot{\theta}_4 \\ +m_5 l_1(l_5-d_5)\cos(\theta_1+\theta_5)\ddot{\theta}_5 \\ +\left[m_2 l_1 d_2 + (m_3+m_4+m_5)l_1 l_2\right]\sin(\theta_1-\theta_2)\dot{\theta}_2^2 \\ +m_3 l_1 d_3\sin(\theta_1-\theta_3)\dot{\theta}_3^2 \\ -\left[m_4 l_1(l_4-d_4) + m_5 l_1 l_4\right]\sin(\theta_1+\theta_4)\dot{\theta}_4^2 \\ -m_5 l_1(l_5-d_5)\sin(\theta_1+\theta_5)\dot{\theta}_5^2 \\ -\left[m_1 d_1 + (m_2+m_3+m_4+m_5)l_1\right]g\sin\theta_1 \end{bmatrix} = T_{\theta_1} \tag{2.102}$$

II* :

$$\frac{d}{dt}\left\{\frac{\partial K}{\partial \dot{\theta}_2}\right\}-\frac{\partial K}{\partial \theta_2}+\frac{\partial P}{\partial \theta_2}=T_{\theta_2} \tag{2.103}$$

$$\Rightarrow \begin{bmatrix} \left[m_2 l_1 d_2+(m_3+m_4+m_5)l_1 l_2\right]\cos(\theta_1-\theta_2)\ddot{\theta}_1 \\ +\left[I_2+m_2 d_2^2+(m_3+m_4+m_5)l_2^2\right]\ddot{\theta}_2+m_3 l_2 d_3\cos(\theta_2-\theta_3)\ddot{\theta}_3 \\ +\left[m_4 l_2(l_4-d_4)+m_5 l_2 l_4\right]\cos(\theta_2+\theta_4)\ddot{\theta}_4 \\ +m_5 l_2(l_5-d_5)\cos(\theta_2+\theta_5)\ddot{\theta}_5 \\ -\left[m_2 l_1 d_2+(m_3+m_4+m_5)l_1 l_2\right]\sin(\theta_1-\theta_2)\dot{\theta}_1^2 \\ +m_3 l_2 d_3\sin(\theta_2-\theta_3)\dot{\theta}_3^2 \\ -\left[m_4 l_2(l_4-d_4)+m_5 l_2 l_4\right]\sin(\theta_2+\theta_4)\dot{\theta}_4^2 \\ -m_5 l_2(l_5-d_5)\sin(\theta_2+\theta_5)\dot{\theta}_5^2 \\ -\left[m_2 d_2+(m_3+m_4+m_5)l_2\right]g\sin\theta_2 \end{bmatrix}=T_{\theta_2} \tag{2.104}$$

III* :

$$\frac{d}{dt}\left\{\frac{\partial K}{\partial \dot{\theta}_3}\right\}-\frac{\partial K}{\partial \theta_3}+\frac{\partial P}{\partial \theta_3}=T_{\theta_3} \tag{2.105}$$

$$\Rightarrow \begin{bmatrix} m_3 l_1 d_3\cos(\theta_1-\theta_3)\ddot{\theta}_1+m_3 l_2 d_3\cos(\theta_2-\theta_3)\ddot{\theta}_2+\left[I_3+m_3 d_3^2\right]\ddot{\theta}_3 \\ -m_3 l_1 d_3\sin(\theta_1-\theta_3)\dot{\theta}_1^2-m_3 l_2 d_3\sin(\theta_2-\theta_3)\dot{\theta}_2^2-m_3 d_3 g\sin\theta_3 \end{bmatrix}=T_{\theta_3} \tag{2.106}$$

IV* :

$$\frac{d}{dt}\left\{\frac{\partial K}{\partial \dot{\theta}_4}\right\}-\frac{\partial K}{\partial \theta_4}+\frac{\partial P}{\partial \theta_4}=T_{\theta_4} \tag{2.107}$$

$$
\Rightarrow \begin{bmatrix}
\left[m_4 l_1 (l_4 - d_4) + m_5 l_1 l_4\right]\cos(\theta_1 + \theta_4)\ddot{\theta}_1 \\
+\left[m_4 l_2 (l_4 - d_4) + m_5 l_2 l_4\right]\cos(\theta_2 + \theta_4)\ddot{\theta}_2 \\
+\left[I_4 + m_4 (l_4 - d_4)^2 + m_5 l_4^2\right]\ddot{\theta}_4 \\
+m_5 l_4 (l_5 - d_5)\cos(\theta_4 - \theta_5)\ddot{\theta}_5 \\
-\left[m_4 l_1 (l_4 - d_4) + m_5 l_1 l_4\right]\sin(\theta_1 + \theta_4)\dot{\theta}_1^2 \\
-\left[m_4 l_2 (l_4 - d_4) + m_5 l_2 l_4\right]\sin(\theta_2 + \theta_4)\dot{\theta}_2^2 \\
+m_5 l_4 (l_5 - d_5)\sin(\theta_4 - \theta_5)\dot{\theta}_5^2 \\
+\left[m_4 (l_4 - d_4) + m_5 l_4\right] g \sin\theta_4
\end{bmatrix} = T_{\theta_4} \tag{2.108}
$$

V*:

$$
\frac{d}{dt}\left\{\frac{\partial K}{\partial \dot{\theta}_5}\right\} - \frac{\partial K}{\partial \theta_5} + \frac{\partial P}{\partial \theta_5} = T_{\theta_5} \tag{2.109}
$$

$$
\Rightarrow \begin{bmatrix}
\left[m_5 l_1 (l_5 - d_5)\right]\cos(\theta_1 + \theta_5)\ddot{\theta}_1 + m_5 l_2 (l_5 - d_5)\cos(\theta_2 + \theta_5)\ddot{\theta}_2 + \\
+m_5 l_4 (l_5 - d_5)\cos(\theta_4 - \theta_5)\ddot{\theta}_4 + \left[I_5 + m_5 (l_5 - d_5)^2\right]\ddot{\theta}_5 \\
-\left[m_5 l_1 (l_5 - d_5)\right]\sin(\theta_1 + \theta_5)\dot{\theta}_1^2 - m_5 l_2 (l_5 - d_5)\sin(\theta_2 + \theta_5)\dot{\theta}_2^2 \\
-m_5 l_4 (l_5 - d_5)\sin(\theta_4 - \theta_5)\dot{\theta}_4^2 + m_5 (l_5 - d_5) g \sin\theta_5
\end{bmatrix} = T_{\theta_5} \tag{2.110}
$$

VI*:

$$
\frac{d}{dt}\left\{\frac{\partial K}{\partial \dot{\theta}_6}\right\} - \frac{\partial K}{\partial \theta_6} + \frac{\partial P}{\partial \theta_6} = T_{\theta_6} \tag{2.111}
$$

$$
\Rightarrow \begin{bmatrix}
\left[(I_1 + I_2) + \begin{pmatrix} m_1 d_1^{\,2} + m_2 (l_1 + d_2)^2 \\ +(m_3 + m_4 + m_5)(l_1 + l_2)^2 \end{pmatrix}\cos^2\theta_6\right]\ddot{\theta}_6 \\
+\left[m_4 (l_1 + l_2)(l_4 - d_4) + m_5 (l_1 + l_2)(l_4 + l_5 - d_5)\right]\cos\theta_6 \cos\theta_7 \ddot{\theta}_7 \\
-\begin{bmatrix} m_1 d_1^{\,2} + m_2 (l_1 + d_2)^2 \\ +(m_3 + m_4 + m_5)(l_1 + l_2)^2 \end{bmatrix}\sin\theta_6 \cos\theta_6 \dot{\theta}_6^{\,2} \\
-\left[m_4 (l_1 + l_2)(l_4 - d_4) + m_5 (l_1 + l_2)(l_4 + l_5 - d_5)\right]\cos\theta_6 \sin\theta_7 \dot{\theta}_7^{\,2}
\end{bmatrix} = T_{\theta_6} \tag{2.112}
$$

VII* :

$$\frac{d}{dt}\left\{\frac{\partial K}{\partial \dot{\theta}_7}\right\}-\frac{\partial K}{\partial \theta_7}+\frac{\partial P}{\partial \theta_7}=T_{\theta_7} \tag{2.113}$$

$$\Rightarrow \begin{bmatrix} \left[m_4(l_1+l_2)(l_4-d_4)+m_5(l_1+l_2)(l_4+l_5-d_5)\right]\cos\theta_6\cos\theta_7\ddot{\theta}_6 \\ +\left[(I_4+I_5)+(m_4(l_4-d_4)^2+m_5(l_4+l_5-d_5)^2)\cos^2\theta_7\right]\ddot{\theta}_7 \\ -\left[m_4(l_1+l_2)(l_4-d_4)+m_5(l_1+l_2)(l_4+l_5-d_5)\right]\sin\theta_6\cos\theta_7\dot{\theta}_6{}^2 \\ -\left[m_4(l_4-d_4)^2+m_5(l_4+l_5-d_5)^2\right]\sin\theta_7\cos\theta_7\dot{\theta}_7{}^2 \end{bmatrix} = T_{\theta_7} \tag{2.114}$$

Now, rearranging (2.100)-(2.114) into the standard form (2.28) results

$D(\underline{\theta})=[D_{ij}(\underline{\theta})]\quad (i,j=1,...,7)$, 7x7 symmetric, positive-definite inertia matrix

where

$$\begin{aligned}
D_{11} &= I_1+m_1d_1{}^2+(m_2+m_3+m_4+m_5)l_1^2 \\
D_{12} &= \left[m_2l_1d_2+(m_3+m_4+m_5)l_1l_2\right]\cos(\theta_1-\theta_2) \\
D_{13} &= \left[m_3l_1d_3\right]\cos(\theta_1-\theta_3) \\
D_{14} &= \left[m_4l_1(l_4-d_4)+m_5l_1l_4\right]\cos(\theta_1+\theta_4) \\
D_{15} &= \left[m_5l_1(l_5-d_5)\right]\cos(\theta_1+\theta_5) \\
D_{21} &= D_{12} \\
D_{22} &= I_2+m_2d_2{}^2+(m_3+m_4+m_5)l_2{}^2 \\
D_{23} &= \left[m_3l_2d_3\right]\cos(\theta_2-\theta_3) \\
D_{24} &= \left[m_4l_2(l_4-d_4)+m_5l_2l_4\right]\cos(\theta_2+\theta_4) \\
D_{25} &= \left[m_5l_2(l_5-d_5)\right]\cos(\theta_2+\theta_5) \\
D_{31} &= D_{13} \\
D_{32} &= D_{23} \\
D_{33} &= I_3+m_3d_3{}^2 \\
D_{34} &= D_{35}=0
\end{aligned}$$

$$D_{41} = D_{14}$$
$$D_{42} = D_{24}$$
$$D_{43} = D_{34}$$
$$D_{44} = I_4 + m_4(l_4 - d_4)^2 + m_5 l_4^{\,2}$$
$$D_{45} = \left[m_5 l_4 (l_5 - d_5)\right]\cos(\theta_4 - \theta_5)$$

$$D_{51} = D_{15}$$
$$D_{52} = D_{25}$$
$$D_{53} = D_{35}$$
$$D_{54} = D_{45}$$
$$D_{55} = I_5 + m_5(l_5 - d_5)^2$$

$$D_{16} = D_{61} = 0$$
$$D_{17} = D_{71} = 0$$
$$D_{26} = D_{62} = 0$$
$$D_{27} = D_{72} = 0$$
$$D_{36} = D_{63} = 0$$
$$D_{37} = D_{73} = 0$$

$$D_{46} = D_{64} = 0$$
$$D_{47} = D_{74} = 0$$
$$D_{56} = D_{65} = 0$$
$$D_{57} = D_{75} = 0$$

$$D_{66} = (I_1 + I_2) + [m_1 d_1^{\,2} + m_2(l_1 + d_2)^2 + (m_3 + m_4 + m_5)(l_1 + l_2)^2]\cos^2\theta_6$$
$$D_{67} = D_{76} = \left[m_4(l_1 + l_2)(l_4 - d_4) + m_5(l_1 + l_2)(l_4 + l_5 - d_5)\right]\cos\theta_6 \cos\theta_7$$
$$D_{77} = (I_4 + I_5) + [m_4(l_4 - d_4)^2 + m_5(l_4 + l_5 - d_5)^2]\cos^2\theta_7$$

Similarly,

$$h(\underline{\theta}, \underline{\dot{\theta}})\underline{\dot{\theta}} = \underset{i}{col}[\sum_{\substack{j=1 \\ j\neq i}}^{7} h_{ij}\dot{\theta}_j^{\,2}] \quad (i = 1,...,7), \tag{2.115}$$

7x1 column vector consisting of Coriolis and Centrifugal torques with

$$h_{ii} = 0 \quad (i, j = 1,2,...,5)$$

$$h_{12} = \left[m_2 l_1 d_2 + (m_3 + m_4 + m_5) l_1 l_2\right] \sin(\theta_1 - \theta_2)\dot{\theta}_2$$
$$h_{13} = (m_3 l_1 d_3) \sin(\theta_1 - \theta_3)\dot{\theta}_3$$
$$h_{14} = -\left[m_4 l_1 (l_4 - d_4) + m_5 l_1 l_4\right] \sin(\theta_1 + \theta_4)\dot{\theta}_4$$
$$h_{15} = -\left[m_5 l_1 (l_5 - d_5)\right] \sin(\theta_1 + \theta_5)\dot{\theta}_5$$

$$h_{21} = -\left[m_2 l_1 d_2 + (m_3 + m_4 + m_5) l_1 l_2\right] \sin(\theta_1 - \theta_2)\dot{\theta}_1$$
$$h_{23} = (m_3 l_2 d_3) \sin(\theta_2 - \theta_3)\dot{\theta}_3$$
$$h_{24} = -\left[m_4 l_2 (l_4 - d_4) + m_5 l_2 l_4\right] \sin(\theta_2 + \theta_4)\dot{\theta}_4$$
$$h_{25} = -\left[m_5 l_2 (l_5 - d_5)\right] \sin(\theta_2 + \theta_5)\dot{\theta}_5$$

$$h_{31} = -(m_3 l_1 d_3) \sin(\theta_1 - \theta_3)\dot{\theta}_1$$
$$h_{32} = -(m_3 l_2 d_3) \sin(\theta_2 - \theta_3)\dot{\theta}_2$$
$$h_{34} = 0$$
$$h_{35} = 0$$

$$h_{41} = -\left[m_4 l_1 (l_4 - d_4) + m_5 l_1 l_4\right] \sin(\theta_1 + \theta_4)\dot{\theta}_1$$
$$h_{42} = -\left[m_4 l_2 (l_4 - d_4) + m_5 l_2 l_4\right] \sin(\theta_2 + \theta_4)\dot{\theta}_2$$
$$h_{43} = 0$$
$$h_{45} = \left[m_5 l_4 (l_5 - d_5)\right] \sin(\theta_4 - \theta_5)\dot{\theta}_5$$

$$h_{51} = -\left[m_5 l_1 (l_5 - d_5)\right] \sin(\theta_1 + \theta_5)\dot{\theta}_1$$
$$h_{52} = -\left[m_5 l_2 (l_5 - d_5)\right] \sin(\theta_2 + \theta_5)\dot{\theta}_2$$
$$h_{53} = 0$$
$$h_{54} = -\left[m_5 l_4 (l_5 - d_5)\right] \sin(\theta_4 - \theta_5)\dot{\theta}_4$$

$$h_{16} = h_{61} = 0$$
$$h_{26} = h_{62} = 0$$
$$h_{36} = h_{63} = 0$$
$$h_{46} = h_{64} = 0$$
$$h_{56} = h_{65} = 0$$
$$h_{66} = -\left[m_1 d_1^{\,2} + m_2 (l_1 + d_2)^2 + (m_3 + m_4 + m_5)(l_1 + l_2)^2\right] \sin\theta_6 \cos\theta_6 \dot{\theta}_6$$
$$h_{67} = -\left[m_4 (l_1 + l_2)(l_4 - d_4) + m_5 (l_1 + l_2)(l_4 + l_5 - d_5)\right] \cos\theta_6 \sin\theta_7 \dot{\theta}_7$$
$$h_{17} = h_{71} = 0$$
$$h_{27} = h_{72} = 0$$
$$h_{37} = h_{73} = 0$$
$$h_{47} = h_{74} = 0$$
$$h_{57} = h_{75} = 0$$

$$h_{76} = -\left[m_4(l_1+l_2)(l_4-d_4)+m_5(l_1+l_2)(l_4+l_5-d_5)\right]\sin\theta_6\cos\theta_7\dot{\theta}_6$$
$$h_{77} = -\left[m_4(l_4-d_4)^2+m_5(l_4+l_5-d_5)^2\right]\sin\theta_7\cos\theta_7\dot{\theta}_7$$

Also,

$$G(\underline{\theta}) = [G_i(\underline{\theta})] \quad (i=1,...,7),\ 7\text{x}1 \tag{2.116}$$

column vector consisting of gravitational torques with

$$G_1 = -\left[m_1d_1+(m_2+m_3+m_4+m_5)l_1\right]g\sin\theta_1$$
$$G_2 = -\left[m_2d_2+(m_3+m_4+m_5)l_2\right]g\sin\theta_2$$
$$G_3 = -(m_3d_3)g\sin\theta_3$$
$$G_4 = \left[m_4(l_4-d_4)+m_5l_4\right]g\sin\theta_4$$
$$G_5 = \left[m_5(l_5-d_5)\right]g\sin\theta_5$$
$$G_6(\underline{\theta}) = 0$$
$$G_7(\underline{\theta}) = 0$$

The dynamic equations of motion formulated as above are used for both the left leg stance and right leg stance motion during the single support phase.

2.3.2.2 Double Support Phase

At the moment that the swing leg completes the motion in air and gets into contact with the ground, it is assumed that the stance leg leaves the ground immediately. At that point of contact, the angular velocity of each joint is exposed to jump discontinuities and the supporting leg becomes the swing leg and the swing leg becomes the supporting leg. At that moment, the biped robot assumed to be in the state that both legs are in the air. In this phase of motion, the two constraints x_b, y_b and z_b are constant and $\dot{x}_b = \dot{y}_b = \dot{z}_b = 0$, which were valid in the single support phase, are no longer satisfied. As a result of this fact, the equations of motion (2.28) can not be employed in this phase and therefore, a set of new equations of motion is derived for the phase both legs in air as the configuration is shown in Figure 2.10. In addition to the joint angle variable, θ_i, the coordinates x_b, y_b and z_b of support leg in single support phase are also used as variables in the calculations.

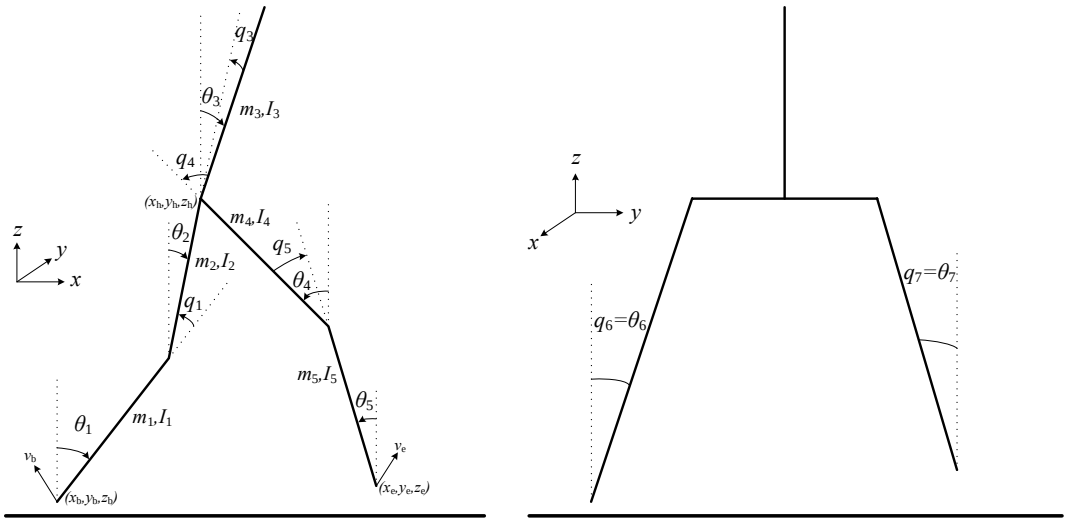

Figure 2.10 Biped with both legs in air

The configuration of the robot with both legs in air is given in Figure 2.10 and as per this configuration, the center of mass of each link and their velocities are obtained as

$$xc_1 = x_b + d_1 \sin\theta_1 \tag{2.117}$$

$$yc_1 = y_b + d_1 \sin\theta_6 \tag{2.118}$$

$$zc_1 = z_b + d_1 \cos\theta_1 \tag{2.119}$$

$$xc_2 = x_b + l_1 \sin\theta_1 + d_2 \sin\theta_2 \tag{2.120}$$

$$yc_2 = y_b + (l_1 + d_2)\sin\theta_6 \tag{2.121}$$

$$zc_2 = z_b + l_1 \cos\theta_1 + d_2 \cos\theta_2 \tag{2.122}$$

$$xc_3 = x_b + l_1 \sin\theta_1 + l_2 \sin\theta_2 + d_3 \sin\theta_3 \tag{2.123}$$

$$yc_3 = y_b + (l_1 + l_2)\sin\theta_6 + l_6 / 2 \tag{2.124}$$

$$zc_3 = z_b + l_1 \cos\theta_1 + l_2 \cos\theta_2 + d_3 \cos\theta_3 \tag{2.125}$$

$$xc_4 = x_b + l_1 \sin\theta_1 + l_2 \sin\theta_2 + (l_4 - d_4)\sin\theta_4 \tag{2.126}$$

$$yc_4 = y_b + (l_1 + l_2)\sin\theta_6 + l_6 + (l_4 - d_4)\sin\theta_7 \tag{2.127}$$

$$zc_4 = z_b + l_1 \cos\theta_1 + l_2 \cos\theta_2 - (l_4 - d_4)\cos\theta_4 \tag{2.128}$$

$$xc_5 = x_b + l_1 \sin\theta_1 + l_2 \sin\theta_2 + l_4 \sin\theta_4 + (l_5 - d_5)\sin\theta_5 \tag{2.129}$$

$$yc_5 = y_b + (l_1 + l_2)\sin\theta_6 + l_6 + (l_4 + l_5 - d_5)\sin\theta_7 \tag{2.130}$$

$$zc_5 = z_b + l_1\cos\theta_1 + l_2\cos\theta_2 - l_4\cos\theta_4 - (l_5 - d_5)\cos\theta_5 \tag{2.131}$$

and

$$vc_1 = \begin{pmatrix}\dot{x}_b\\ \dot{y}_b\\ \dot{z}_b\end{pmatrix} + \begin{pmatrix}d_1\cos\theta_1\\ 0\\ -d_1\sin\theta_1\end{pmatrix}\dot{\theta}_1 + \begin{pmatrix}0\\ d_1\cos\theta_6\\ 0\end{pmatrix}\dot{\theta}_6 \tag{2.132}$$

$$vc_2 = \begin{pmatrix}\dot{x}_b\\ \dot{y}_b\\ \dot{z}_b\end{pmatrix} + \begin{pmatrix}l_1\cos\theta_1\\ 0\\ -l_1\sin\theta_1\end{pmatrix}\dot{\theta}_1 + \begin{pmatrix}d_2\cos\theta_2\\ 0\\ -d_2\sin\theta_2\end{pmatrix}\dot{\theta}_2 + \begin{pmatrix}0\\ (l_1 + d_2)\cos\theta_6\\ 0\end{pmatrix}\dot{\theta}_6 \tag{2.133}$$

$$\begin{aligned} vc_3 = &\begin{pmatrix}\dot{x}_b\\ \dot{y}_b\\ \dot{z}_b\end{pmatrix} + \begin{pmatrix}l_1\cos\theta_1\\ 0\\ -l_1\sin\theta_1\end{pmatrix}\dot{\theta}_1 + \begin{pmatrix}l_2\cos\theta_2\\ 0\\ -l_2\sin\theta_2\end{pmatrix}\dot{\theta}_2 + \begin{pmatrix}d_3\cos\theta_3\\ 0\\ -d_3\sin\theta_3\end{pmatrix}\dot{\theta}_3 \\ &+ \begin{pmatrix}0\\ (l_1 + l_2)\cos\theta_6\\ 0\end{pmatrix}\dot{\theta}_6 \end{aligned} \tag{2.134}$$

$$\begin{aligned} vc_4 = &\begin{pmatrix}\dot{x}_b\\ \dot{y}_b\\ \dot{z}_b\end{pmatrix} + \begin{pmatrix}l_1\cos\theta_1\\ 0\\ -l_1\sin\theta_1\end{pmatrix}\dot{\theta}_1 + \begin{pmatrix}l_2\cos\theta_2\\ 0\\ -l_2\sin\theta_2\end{pmatrix}\dot{\theta}_2 + \begin{pmatrix}(l_4 - d_4)\cos\theta_4\\ 0\\ (l_4 - d_4)\sin\theta_4\end{pmatrix}\dot{\theta}_4 \\ &+ \begin{pmatrix}0\\ (l_1 + l_2)\cos\theta_6\\ 0\end{pmatrix}\dot{\theta}_6 + \begin{pmatrix}0\\ (l_4 - d_4)\cos\theta_7\\ 0\end{pmatrix}\dot{\theta}_7 \end{aligned} \tag{2.135}$$

$$\begin{aligned} vc_5 = &\begin{pmatrix}\dot{x}_b\\ \dot{y}_b\\ \dot{z}_b\end{pmatrix} + \begin{pmatrix}l_1\cos\theta_1\\ 0\\ -l_1\sin\theta_1\end{pmatrix}\dot{\theta}_1 + \begin{pmatrix}l_2\cos\theta_2\\ 0\\ -l_2\sin\theta_2\end{pmatrix}\dot{\theta}_2 + \begin{pmatrix}l_4\cos\theta_4\\ 0\\ l_4\sin\theta_4\end{pmatrix}\dot{\theta}_4 \\ &+ \begin{pmatrix}(l_5 - d_5)\cos\theta_5\\ 0\\ (l_5 - d_5)\sin\theta_5\end{pmatrix}\dot{\theta}_5 + \begin{pmatrix}0\\ (l_1 + l_2)\cos\theta_6\\ 0\end{pmatrix}\dot{\theta}_6 + \begin{pmatrix}0\\ (l_4 + l_5 - d_5)\cos\theta_7\\ 0\end{pmatrix}\dot{\theta}_7 \end{aligned} \tag{2.136}$$

So the equations of motion in double support phase, just after the impact is also derived using the same procedure as in single support phase by using Lagrangian formulation. In this phase, the kinetic energy and the potential energy equations for each link is derived in a similar way as below and the additional indexes 8, 9, 10 in these calculations correspond to x_b, y_b & z_b, respectively:

Link 1:

$$K_1 = \frac{1}{2}(I_1 + m_1 d_1^{\,2})\dot{\theta}_1^{\,2} + \frac{1}{2}(I_1 + m_1 d_1^{\,2}\cos^2\theta_6)\dot{\theta}_6^{\,2} + \frac{1}{2}m_1\left[\dot{x}_b^{\,2} + \dot{y}_b^{\,2} + \dot{z}_b^{\,2} + 2d_1\dot{\theta}_1(\dot{x}_b\cos\theta_1 - \dot{z}_b\sin\theta_1) + 2d_1\dot{\theta}_6\dot{y}_b\cos\theta_6\right] \tag{2.137}$$

$$P_1 = m_1 g(z_b + d_1\cos\theta_1) \tag{2.138}$$

Link 2:

$$\begin{aligned} K_2 = {} & \frac{1}{2}(I_2 + m_2 d_2^{\,2})\dot{\theta}_2^{\,2} + \frac{1}{2}m_2 l_1^{\,2}\dot{\theta}_1^{\,2} + m_2 l_1 d_2\cos(\theta_1 - \theta_2)\dot{\theta}_1\dot{\theta}_2 \\ & + \frac{1}{2}m_2\left[2l_1\dot{\theta}_1(\dot{x}_b\cos\theta_1 - \dot{z}_b\sin\theta_1) + 2d_2\dot{\theta}_2(\dot{x}_b\cos\theta_2 - \dot{z}_b\sin\theta_2)\right] \\ & + \frac{1}{2}m_2(\dot{x}_b^{\,2} + \dot{z}_b^{\,2}) + \frac{1}{2}\left[I_2 + m_2(l_1 + d_2)^2\cos^2\theta_6\right]\dot{\theta}_6^{\,2} \\ & + \frac{1}{2}m_2\dot{y}_b^{\,2} + m_2\dot{y}_b(l_1 + d_2)\cos\theta_6\dot{\theta}_6 \end{aligned} \tag{2.139}$$

$$P_2 = m_2 g(z_b + l_1\cos\theta_1 + d_2\cos\theta_2) \tag{2.140}$$

Link 3:

$$\begin{aligned} K_3 = {} & \frac{1}{2}(I_3 + m_3 d_3^{\,2})\dot{\theta}_3^{\,2} \\ & + \frac{1}{2}m_3\begin{bmatrix} l_1^{\,2}\dot{\theta}_1^{\,2} + l_2^{\,2}\dot{\theta}_2^{\,2} + 2l_1 l_2\cos(\theta_1 - \theta_2)\dot{\theta}_1\dot{\theta}_2 \\ +2l_1 d_3\cos(\theta_1 - \theta_3)\dot{\theta}_1\dot{\theta}_3 + 2l_2 d_3\cos(\theta_2 - \theta_3)\dot{\theta}_2\dot{\theta}_3 \end{bmatrix} \\ & + \frac{1}{2}m_3\begin{bmatrix} \dot{x}_b^{\,2} + \dot{z}_b^{\,2} + 2l_1\dot{\theta}_1(\dot{x}_b\cos\theta_1 - \dot{z}_b\sin\theta_1) \\ +2l_2\dot{\theta}_2(\dot{x}_b\cos\theta_2 - \dot{z}_b\sin\theta_2) + 2d_3\dot{\theta}_3(\dot{x}_b\cos\theta_3 - \dot{z}_b\sin\theta_3) \end{bmatrix} \\ & + \frac{1}{2}m_3(l_1 + l_2)^2\cos^2\theta_6\dot{\theta}_6^{\,2} + \frac{1}{2}m_3\left[\dot{y}_b^{\,2} + 2\dot{y}_b(l_1 + l_2)\cos\theta_6\dot{\theta}_6\right] \end{aligned} \tag{2.141}$$

$$P_3 = m_3 g(z_b + l_1\cos\theta_1 + l_2\cos\theta_2 + d_3\cos\theta_3) \tag{2.142}$$

Link 4:

$$
\begin{aligned}
K_4 &= \frac{1}{2}\left[I_4 + m_4 (l_4 - d_4)^2 \right] \dot{\theta}_4^{\,2} \\
&+ \frac{1}{2} m_4 \begin{bmatrix} l_1^{\,2}\dot{\theta}_1^{\,2} + l_2^{\,2}\dot{\theta}_2^{\,2} + 2 l_1 l_2 \cos(\theta_1 - \theta_2)\dot{\theta}_1\dot{\theta}_2 \\ +2 l_1 (l_4 - d_4)\cos(\theta_1 + \theta_4)\dot{\theta}_1\dot{\theta}_4 + 2 l_2 (l_4 - d_4)\cos(\theta_2 + \theta_4)\dot{\theta}_2\dot{\theta}_4 \end{bmatrix} \\
&+ \frac{1}{2} m_4 \begin{bmatrix} \dot{x}_b^{\,2} + 2 l_1 \dot{\theta}_1 (\dot{x}_b \cos\theta_1 - \dot{z}_b \sin\theta_1) + 2 l_2 \dot{\theta}_2 (\dot{x}_b \cos\theta_2 - \dot{z}_b \sin\theta_2) \\ +\dot{z}_b^{\,2} + 2(l_4 - d_4)\dot{\theta}_4 (\dot{x}_b \cos\theta_4 + \dot{z}_b \sin\theta_4) \end{bmatrix} \\
&+ \frac{1}{2} m_4 \left[(l_1 + l_2)^2 \cos^2\theta_6 \right] \dot{\theta}_6^{\,2} + \frac{1}{2}\left[I_4 + m_4 (l_4 - d_4)^2 \cos^2\theta_7 \right] \dot{\theta}_7^{\,2} \\
&+ \frac{1}{2} m_4 [\dot{y}_b^{\,2} + 2\dot{y}_b (l_1 + l_2)\cos\theta_6 \dot{\theta}_6 + 2\dot{y}_b (l_4 - d_4)\cos\theta_7 \dot{\theta}_7] \\
&+ m_4 (l_1 + l_2)(l_4 - d_4)\cos\theta_6 \cos\theta_7 \dot{\theta}_6 \dot{\theta}_7
\end{aligned}
\tag{2.143}
$$

$$
P_4 = m_4 g \left[z_b + l_1 \cos\theta_1 + l_2 \cos\theta_2 - (l_4 - d_4)\cos\theta_4 \right] \tag{2.144}
$$

Link 5:

$$
\begin{aligned}
K_5 &= \frac{1}{2}\left[I_5 + m_5 (l_5 - d_5)^2 \right] \dot{\theta}_5^{\,2} \\
&+ \frac{1}{2} m_5 \begin{bmatrix} l_1^{\,2}\dot{\theta}_1^{\,2} + l_2^{\,2}\dot{\theta}_2^{\,2} + l_4^{\,2}\dot{\theta}_4^{\,2} + 2 l_1 l_2 \cos(\theta_1 - \theta_2)\dot{\theta}_1\dot{\theta}_2 \\ +2 l_1 l_4 \cos(\theta_1 + \theta_4)\dot{\theta}_1\dot{\theta}_4 + 2 l_1 (l_5 - d_5)\cos(\theta_1 + \theta_5)\dot{\theta}_1\dot{\theta}_5 \\ +2 l_2 l_4 \cos(\theta_2 + \theta_4)\dot{\theta}_2\dot{\theta}_4 + 2 l_2 (l_5 - d_5)\cos(\theta_2 + \theta_5)\dot{\theta}_2\dot{\theta}_5 \\ +2 l_4 (l_5 - d_5)\cos(\theta_4 - \theta_5)\dot{\theta}_4\dot{\theta}_5 \end{bmatrix} \\
&+ \frac{1}{2} m_5 \begin{bmatrix} \dot{x}_b^{\,2} + \dot{z}_b^{\,2} + 2 l_1 \dot{\theta}_1 (\dot{x}_b \cos\theta_1 - \dot{z}_b \sin\theta_1) \\ +2 l_2 \dot{\theta}_2 (\dot{x}_b \cos\theta_2 - \dot{z}_b \sin\theta_2) + 2 l_4 \dot{\theta}_4 (\dot{x}_b \cos\theta_4 + \dot{z}_b \sin\theta_4) \\ +2(l_5 - d_5)\dot{\theta}_5 (\dot{x}_b \cos\theta_5 + \dot{z}_b \sin\theta_5) \end{bmatrix} \\
&+ \frac{1}{2}\left[m_5 (l_1 + l_2)^2 \cos^2\theta_6 \right] \dot{\theta}_6^{\,2} + \frac{1}{2}\left[I_5 + m_5 (l_4 + l_5 - d_5)^2 \cos^2\theta_7 \right] \dot{\theta}_7^{\,2} \\
&+ \frac{1}{2} m_5 [\dot{y}_b^{\,2} + 2\dot{y}_b (l_1 + l_2)\cos\theta_6 \dot{\theta}_6 + 2\dot{y}_b (l_4 + l_5 - d_5)\cos\theta_7 \dot{\theta}_7] \\
&+ m_5 (l_1 + l_2)(l_4 + l_5 - d_5)\cos\theta_6 \cos\theta_7 \dot{\theta}_6 \dot{\theta}_7
\end{aligned}
\tag{2.145}
$$

$$
P_5 = m_5 g \left[z_b + l_1 \cos\theta_1 + l_2 \cos\theta_2 - l_4 \cos\theta_4 - (l_5 - d_5)\cos\theta_5 \right] \tag{2.146}
$$

Thereafter, the Euler-Lagrange equation is used in order to express the dynamics by substituting (2.137)-(2.146) into (2.147)

$$\frac{d}{dt}\left\{\frac{\partial K}{\partial \dot{\theta}_i}\right\}-\frac{\partial K}{\partial \theta_i}+\frac{\partial P}{\partial \theta_i}=T_i \ (i=1,...,10) \tag{2.147}$$

Each term in the Euler-Lagrange equation in double support phase just after the impact is derived as

$$\begin{aligned}\frac{d}{dt}\left\{\frac{\partial K}{\partial \dot{\theta}_1}\right\} &= \left[I_1+m_1 d_1^{\,2}+(m_2+m_3+m_4+m_5)l_1^{\,2}\right]\ddot{\theta}_1 \\ &+\left[m_2 l_1 d_2+(m_3+m_4+m_5)l_1 l_2\right]\begin{bmatrix}\cos(\theta_1-\theta_2)\ddot{\theta}_2-\sin(\theta_1-\theta_2)\dot{\theta}_1\dot{\theta}_2\\ +\sin(\theta_1-\theta_2)\dot{\theta}_2^2\end{bmatrix} \\ &+m_3 l_1 d_3\left[\cos(\theta_1-\theta_3)\ddot{\theta}_3-\sin(\theta_1-\theta_3)\dot{\theta}_1\dot{\theta}_3+\sin(\theta_1-\theta_3)\dot{\theta}_3^2\right] \\ &+\left[m_4 l_1(l_4-d_4)+m_5 l_1 l_4\right]\begin{bmatrix}\cos(\theta_1+\theta_4)\ddot{\theta}_4-\sin(\theta_1+\theta_4)\dot{\theta}_1\dot{\theta}_4\\ -\sin(\theta_1+\theta_4)\dot{\theta}_4^2\end{bmatrix} \\ &+m_5 l_1(l_5-d_5)\left[\cos(\theta_1+\theta_5)\ddot{\theta}_5-\sin(\theta_1+\theta_5)\dot{\theta}_1\dot{\theta}_5-\sin(\theta_1+\theta_5)\dot{\theta}_5^2\right] \\ &+\left[m_1 d_1+(m_2+m_3+m_4+m_5)l_1\right]\begin{bmatrix}\ddot{x}_b\cos\theta_1-\dot{x}_b\sin\theta_1\dot{\theta}_1\\ -\ddot{z}_b\sin\theta_1-\dot{z}_b\cos\theta_1\dot{\theta}_1\end{bmatrix}\end{aligned} \tag{2.148}$$

$$\begin{aligned}\frac{\partial K}{\partial \theta_1} &= -\left[m_2 l_1 d_2+(m_3+m_4+m_5)l_1 l_2\right]\sin(\theta_1-\theta_2)\dot{\theta}_1\dot{\theta}_2 \\ &-m_3 l_1 d_3\sin(\theta_1-\theta_3)\dot{\theta}_1\dot{\theta}_3-\left[m_4 l_1(l_4-d_4)+m_5 l_1 l_4\right]\sin(\theta_1+\theta_4)\dot{\theta}_1\dot{\theta}_4 \\ &-m_5 l_1(l_5-d_5)\sin(\theta_1+\theta_5)\dot{\theta}_1\dot{\theta}_5 \\ &-\left[m_1 d_1+(m_2+m_3+m_4+m_5)l_1\right](\dot{x}_b\sin\theta_1+\dot{z}_b\cos\theta_1)\dot{\theta}_1\end{aligned} \tag{2.149}$$

$$\frac{\partial P}{\partial \theta_1}=-\left[m_1 d_1+(m_2+m_3+m_4+m_5)l_1\right]g\sin\theta_1 \tag{2.150}$$

$$\frac{d}{dt}\left\{\frac{\partial K}{\partial \dot{\theta}_2}\right\} =$$
$$\begin{aligned}
&\left[m_2 l_1 d_2 + (m_3+m_4+m_5) l_1 l_2\right]\begin{bmatrix}\cos(\theta_1-\theta_2)\ddot{\theta}_1 + \sin(\theta_1-\theta_2)\dot{\theta}_1\dot{\theta}_2 \\ -\sin(\theta_1-\theta_2)\dot{\theta}_1^2\end{bmatrix} \\
&+\left[I_2 + m_2 d_2^2 + (m_3+m_4+m_5) l_2^2\right]\ddot{\theta}_2 \\
&+ m_3 l_2 d_3\left[\cos(\theta_2-\theta_3)\ddot{\theta}_3 - \sin(\theta_2-\theta_3)\dot{\theta}_2\dot{\theta}_3 + \sin(\theta_2-\theta_3)\dot{\theta}_3^2\right] \\
&+\left[m_4 l_2 (l_4-d_4) + m_5 l_2 l_4\right]\begin{bmatrix}\cos(\theta_2+\theta_4)\ddot{\theta}_4 - \sin(\theta_2+\theta_4)\dot{\theta}_2\dot{\theta}_4 \\ -\sin(\theta_2+\theta_4)\dot{\theta}_4^2\end{bmatrix} \\
&+ m_5 l_2 (l_5-d_5)\left[\cos(\theta_2+\theta_5)\dot{\theta}_5 - \sin(\theta_2+\theta_5)\dot{\theta}_2\dot{\theta}_5 - \sin(\theta_2+\theta_5)\dot{\theta}_5^2\right] \\
&+\left[m_2 d_2 + (m_3+m_4+m_5) l_2\right]\begin{bmatrix}\ddot{x}_b\cos\theta_2 - \dot{x}_b\sin\theta_2\dot{\theta}_2 \\ -\ddot{z}_b\sin\theta_2 - \dot{z}_b\cos\theta_2\dot{\theta}_2\end{bmatrix}
\end{aligned} \tag{2.151}$$

$$\begin{aligned}
\frac{\partial K}{\partial \theta_2} &= \left[m_2 l_1 d_2 + (m_3+m_4+m_5) l_1 l_2\right]\sin(\theta_1-\theta_2)\dot{\theta}_1\dot{\theta}_2 - m_3 l_2 d_3 \sin(\theta_2-\theta_3)\dot{\theta}_2\dot{\theta}_3 \\
&-\left[m_4 l_2 (l_4-d_4) + m_5 l_2 l_4\right]\sin(\theta_2+\theta_4)\dot{\theta}_2\dot{\theta}_4 - m_5 l_2 (l_5-d_5)\sin(\theta_2+\theta_5)\dot{\theta}_2\dot{\theta}_5 \\
&-\left[m_2 d_2 + (m_3+m_4+m_5) l_2\right](\dot{x}_b\sin\theta_2 + \dot{z}_b\cos\theta_2)\dot{\theta}_2
\end{aligned} \tag{2.152}$$

$$\frac{\partial P}{\partial \theta_2} = -\left[m_2 d_2 + (m_3+m_4+m_5) l_2\right] g \sin\theta_2 \tag{2.153}$$

$$\begin{aligned}
\frac{d}{dt}\left\{\frac{\partial K}{\partial \dot{\theta}_3}\right\} &= m_3 l_1 d_3\left[\cos(\theta_1-\theta_3)\ddot{\theta}_1 - \sin(\theta_1-\theta_3)\dot{\theta}_1^2 + \sin(\theta_1-\theta_3)\dot{\theta}_1\dot{\theta}_3\right] \\
&+ m_3 l_2 d_3\left[\cos(\theta_2-\theta_3)\ddot{\theta}_2 - \sin(\theta_2-\theta_3)\dot{\theta}_2^2 + \sin(\theta_2-\theta_3)\dot{\theta}_2\dot{\theta}_3\right] \\
&+\left[I_3 + m_3 d_3^2\right]\ddot{\theta}_3 + m_3 d_3\begin{bmatrix}\ddot{x}_b\cos\theta_3 - \dot{x}_b\sin\theta_3\dot{\theta}_3 \\ -\ddot{z}_b\sin\theta_3 - \dot{z}_b\cos\theta_3\dot{\theta}_3\end{bmatrix}
\end{aligned} \tag{2.154}$$

$$\begin{aligned}
\frac{\partial K}{\partial \theta_3} &= m_3 l_1 d_3 \sin(\theta_1-\theta_3)\dot{\theta}_1\dot{\theta}_3 + m_3 l_2 d_3 \sin(\theta_2-\theta_3)\dot{\theta}_2\dot{\theta}_3 \\
&- m_3 d_3(\dot{x}_b\sin\theta_3 + \dot{z}_b\cos\theta_3)\dot{\theta}_3
\end{aligned} \tag{2.155}$$

$$\frac{\partial P}{\partial \theta_3} = -m_3 d_3 g \sin\theta_3 \tag{2.156}$$

$$\begin{aligned}\frac{d}{dt}\left\{\frac{\partial K}{\partial \dot{\theta}_4}\right\} &= \left[m_4 l_1 (l_4 - d_4) + m_5 l_1 l_4\right]\begin{bmatrix}\cos(\theta_1+\theta_4)\ddot{\theta}_1 - \sin(\theta_1+\theta_4)\dot{\theta}_1^2 \\ -\sin(\theta_1+\theta_4)\dot{\theta}_1\dot{\theta}_4\end{bmatrix} \\ &+ \left[m_4 l_2 (l_4 - d_4) + m_5 l_2 l_4\right]\begin{bmatrix}\cos(\theta_2+\theta_4)\ddot{\theta}_2 - \sin(\theta_2+\theta_4)\dot{\theta}_2^2 \\ -\sin(\theta_2+\theta_4)\dot{\theta}_2\dot{\theta}_4\end{bmatrix} \\ &+ \left[I_4 + m_4(l_4 - d_4)^2 + m_5 l_4^2\right]\ddot{\theta}_4 \\ &+ m_5 l_4 (l_5 - d_5)\left[\cos(\theta_4 - \theta_5)\ddot{\theta}_5 - \sin(\theta_4 - \theta_5)\dot{\theta}_4\dot{\theta}_5 + \sin(\theta_4 - \theta_5)\dot{\theta}_5^2\right] \\ &+ \left[m_4(l_4 - d_4) + m_5 l_4\right]\begin{bmatrix}\ddot{x}_b\cos\theta_4 - \dot{x}_b\sin\theta_4\dot{\theta}_4 \\ +\ddot{z}_b\sin\theta_4 + \dot{z}_b\cos\theta_4\dot{\theta}_4\end{bmatrix}\end{aligned} \tag{2.157}$$

$$\begin{aligned}\frac{\partial K}{\partial \theta_4} &= -\left[m_4 l_1 (l_4 - d_4) + m_5 l_1 l_4\right]\sin(\theta_1+\theta_4)\dot{\theta}_1\dot{\theta}_4 \\ &-\left[m_4 l_2 (l_4 - d_4) + m_5 l_2 l_4\right]\sin(\theta_2+\theta_4)\dot{\theta}_2\dot{\theta}_4 - m_5 l_4 (l_5 - d_5)\sin(\theta_4 - \theta_5)\dot{\theta}_4\dot{\theta}_5 \\ &-\left[m_4(l_4 - d_4) + m_5 l_4\right](\dot{x}_b\sin\theta_4 - \dot{z}_b\cos\theta_4)\dot{\theta}_4\end{aligned} \tag{2.158}$$

$$\frac{\partial P}{\partial \theta_4} = \left[m_4(l_4 - d_4) + m_5 l_4\right] g \sin\theta_4 \tag{2.159}$$

$$\begin{aligned}\frac{d}{dt}\left\{\frac{\partial K}{\partial \dot{\theta}_5}\right\} &= m_5 l_1 (l_5 - d_5)\left[\cos(\theta_1+\theta_5)\ddot{\theta}_1 - \sin(\theta_1+\theta_5)\dot{\theta}_1^2 - \sin(\theta_1+\theta_5)\dot{\theta}_1\dot{\theta}_5\right] \\ &+ m_5 l_2 (l_5 - d_5)\left[\cos(\theta_2+\theta_5)\ddot{\theta}_2 - \sin(\theta_2+\theta_5)\dot{\theta}_2^2 - \sin(\theta_2+\theta_5)\dot{\theta}_2\dot{\theta}_5\right] \\ &+ m_5 l_4 (l_5 - d_5)\left[\cos(\theta_4 - \theta_5)\ddot{\theta}_4 - \sin(\theta_4 - \theta_5)\dot{\theta}_4^2 + \sin(\theta_4 - \theta_5)\dot{\theta}_4\dot{\theta}_5\right] \\ &+ \left[I_5 + m_5(l_5 - d_5)^2\right]\ddot{\theta}_5 + m_5(l_5 - d_5)\begin{bmatrix}\ddot{x}_b\cos\theta_5 - \dot{x}_b\sin\theta_5\dot{\theta}_5 \\ +\ddot{z}_b\sin\theta_5 + \dot{z}_b\cos\theta_5\dot{\theta}_5\end{bmatrix}\end{aligned} \tag{2.160}$$

$$\begin{aligned}\frac{\partial K}{\partial \theta_5} &= -m_5 l_1 (l_5 - d_5)\sin(\theta_1+\theta_5)\dot{\theta}_1\dot{\theta}_5 - m_5 l_2 (l_5 - d_5)\sin(\theta_2+\theta_5)\dot{\theta}_2\dot{\theta}_5 \\ &+ m_5 l_4 (l_5 - d_5)\sin(\theta_4 - \theta_5)\dot{\theta}_4\dot{\theta}_5 \\ &- m_5(l_5 - d_5)(\dot{x}_b\sin\theta_5 - \dot{z}_b\cos\theta_5)\dot{\theta}_5\end{aligned} \tag{2.161}$$

$$\frac{\partial P}{\partial \theta_5} = m_5(l_5 - d_5)g\sin\theta_5 \tag{2.162}$$

$$\frac{d}{dt}\left\{\frac{\partial K}{\partial \dot{\theta}_6}\right\} = \begin{bmatrix} (I_1 + I_2)\ddot{\theta}_6 + \left[m_1 d_1^{\,2} + m_2(l_1 + d_2)^2 \right. \\ \left. +(m_3 + m_4 + m_5)(l_1 + l_2)^2\right]\begin{bmatrix} -2\cos\theta_6 \sin\theta_6 \ddot{\theta}_6 \\ +\cos^2\theta_6 \ddot{\theta}_6 \end{bmatrix} \\ +\begin{bmatrix} m_1 d_1 + m_2(l_1 + d_2) \\ +(m_3 + m_4 + m_5)(l_1 + l_2) \end{bmatrix}\begin{bmatrix} \ddot{y}_b \cos\theta_6 \\ -\dot{y}_b \sin\theta_6 \dot{\theta}_6 \end{bmatrix} \end{bmatrix} \tag{2.163}$$

$$\begin{aligned} \frac{\partial K}{\partial \theta_6} = -\begin{bmatrix} m_1 d_1^{\,2} + m_2(l_1 + d_2)^2 + m_3(l_1 + l_2)^2 \\ +m_4(l_1 + l_2)^2 + m_5(l_1 + l_2)^2 \end{bmatrix}\sin\theta_6 \cos\theta_6 \dot{\theta}_6^{\,2} + \\ -\left[m_1 d_1 + m_2(l_1 + d_2) + (m_3 + m_4 + m_5)(l_1 + l_2)\right]\sin\theta_6 \dot{\theta}_6 \dot{y}_b \end{aligned} \tag{2.164}$$

$$\frac{\partial P}{\partial \theta_6} = 0 \tag{2.165}$$

$$\frac{d}{dt}\left\{\frac{\partial K}{\partial \dot{\theta}_7}\right\} = \begin{bmatrix} (I_4 + I_5)\ddot{\theta}_7 \\ +\begin{bmatrix} m_4(l_4 - d_4)^2 \\ +m_5(l_4 + l_5 - d_5)^2 \end{bmatrix}\begin{bmatrix} \cos^2\theta_7 \ddot{\theta}_7 \\ -2\cos\theta_7 \sin\theta_7 \dot{\theta}_7^{\,2} \end{bmatrix} \\ +\begin{bmatrix} m_4(l_4 - d_4) \\ +m_5(l_4 + l_5 - d_5) \end{bmatrix}(\ddot{y}_b \cos\theta_7 - \dot{y}_b \sin\theta_7 \dot{\theta}_7) \end{bmatrix} \tag{2.166}$$

$$\begin{aligned} \frac{\partial K}{\partial \theta_7} = -\left[m_4(l_4 - d_4)^2 + m_5(l_4 + l_5 - d_5)^2\right]\sin\theta_7 \cos\theta_7 \dot{\theta}_7^{\,2} + \\ -\left[m_4(l_4 - d_4) + m_5(l_4 + l_5 - d_5)\right]\sin\theta_7 \dot{\theta}_7 \dot{y}_b \end{aligned} \tag{2.167}$$

$$\frac{\partial P}{\partial \theta_7} = 0 \tag{2.168}$$

$$\frac{d}{dt}\left\{\frac{\partial K}{\partial \dot{x}_b}\right\} = \begin{bmatrix} (m_1+m_2+m_3+m_4+m_5)\ddot{x}_b + \\ \begin{bmatrix} m_1 d_1 \\ +(m_2+m_3+m_4+m_5)l_1 \end{bmatrix}(\cos\theta_1\ddot{\theta}_1 - \sin\theta_1\dot{\theta}_1^{\,2}) + \\ (m_2 d_2 + (m_3+m_4+m_5)l_2)(\cos\theta_2\ddot{\theta}_2 - \sin\theta_2\dot{\theta}_2^{\,2}) + \\ m_3 d_3(\cos\theta_3\ddot{\theta}_3 - \sin\theta_3\dot{\theta}_3^{\,2}) + \\ (m_4(l_4-d_4)+m_5 l_4)(\cos\theta_4\ddot{\theta}_4 - \sin\theta_4\dot{\theta}_4^{\,2}) + \\ m_5(l_5-d_5)(\cos\theta_5\ddot{\theta}_5 - \sin\theta_5\dot{\theta}_5^{\,2}) \end{bmatrix} \tag{2.169}$$

$$\frac{\partial K}{\partial x_b} = 0 \tag{2.170}$$

$$\frac{\partial P}{\partial x_b} = 0 \tag{2.171}$$

$$\frac{d}{dt}\left\{\frac{\partial K}{\partial \dot{y}_b}\right\} = \begin{bmatrix} (m_1+m_2+m_3+m_4+m_5)\ddot{y}_b + \\ \begin{bmatrix} m_1 d_1 + m_2(l_1+d_2) \\ +(m_3+m_4+m_5)(l_1+l_2) \end{bmatrix}(\cos\theta_6\ddot{\theta}_6 - \sin\theta_6\dot{\theta}_6^{\,2}) + \\ (m_4(l_4-d_4)+m_5(l_4+l_5-d_5))(\cos\theta_7\ddot{\theta}_7 - \sin\theta_7\dot{\theta}_7^{\,2}) \end{bmatrix} \tag{2.172}$$

$$\frac{\partial K}{\partial y_b} = 0 \tag{2.173}$$

$$\frac{\partial P}{\partial y_b} = 0 \tag{2.174}$$

$$\frac{d}{dt}\left\{\frac{\partial K}{\partial \dot{z}_b}\right\} = \begin{bmatrix} (m_1+m_2+m_3+m_4+m_5)\ddot{z}_b \\ -\begin{bmatrix} m_1 d_1 \\ +(m_2+m_3+m_4+m_5)l_1 \end{bmatrix}(\sin\theta_1\ddot{\theta}_1 + \cos\theta_1\dot{\theta}_1^{\,2}) \\ -(m_2 d_2 + (m_3+m_4+m_5)l_2)(\sin\theta_2\ddot{\theta}_2 + \cos\theta_2\dot{\theta}_2^{\,2}) \\ -m_3 d_3(\sin\theta_3\ddot{\theta}_3 + \cos\theta_3\dot{\theta}_3^{\,2}) \\ +(m_4(l_4-d_4)+m_5 l_4)(\sin\theta_4\ddot{\theta}_4 + \cos\theta_4\dot{\theta}_4^{\,2}) \\ +m_5(l_5-d_5)(\sin\theta_5\ddot{\theta}_5 + \cos\theta_5\dot{\theta}_5^{\,2}) \end{bmatrix} \tag{2.175}$$

$$\frac{\partial K}{\partial z_b} = 0 \tag{2.176}$$

$$\frac{\partial P}{\partial z_b} = (m_1 + m_2 + m_3 + m_4 + m_5)g \tag{2.177}$$

So, let's insert these equations into:

$$\frac{d}{dt}\left\{\frac{\partial K}{\partial \dot{\theta}_i}\right\} - \frac{\partial K}{\partial \theta_i} + \frac{\partial P}{\partial \theta_i} = T_{\theta_i} \text{ equations for } i = 1,...,10 \tag{2.178}$$

Ia* :

$$\frac{d}{dt}\left\{\frac{\partial K}{\partial \dot{\theta}_1}\right\} - \frac{\partial K}{\partial \theta_1} + \frac{\partial P}{\partial \theta_1} = T_{\theta_1} \tag{2.179}$$

$$\Rightarrow \left[\begin{array}{l} \left[I_1 + m_1 d_1^{\,2} + (m_2 + m_3 + m_4 + m_5) l_1^{\,2}\right]\ddot{\theta}_1 \\ +\left[m_2 l_1 d_2 + (m_3 + m_4 + m_5) l_1 l_2\right]\cos(\theta_1 - \theta_2)\ddot{\theta}_2 \\ +m_3 l_1 d_3 \cos(\theta_1 - \theta_3)\ddot{\theta}_3 + \left[m_4 l_1 (l_4 - d_4) + m_5 l_1 l_4\right]\cos(\theta_1 + \theta_4)\ddot{\theta}_4 \\ +m_5 l_1 (l_5 - d_5)\cos(\theta_1 + \theta_5)\ddot{\theta}_5 \\ +\left[m_2 l_1 d_2 + (m_3 + m_4 + m_5) l_1 l_2\right]\sin(\theta_1 - \theta_2)\dot{\theta}_2^2 \\ +m_3 l_1 d_3 \sin(\theta_1 - \theta_3)\dot{\theta}_3^2 - \left[m_4 l_1 (l_4 - d_4) + m_5 l_1 l_4\right]\sin(\theta_1 + \theta_4)\dot{\theta}_4^2 \\ -m_5 l_1 (l_5 - d_5)\sin(\theta_1 + \theta_5)\dot{\theta}_5^2 \\ +\left[m_1 d_1 + (m_2 + m_3 + m_4 + m_5) l_1\right]\left[\ddot{x}_b \cos\theta_1 - \ddot{z}_b \sin\theta_1\right] \\ -\left[m_1 d_1 + (m_2 + m_3 + m_4 + m_5) l_1\right] g \sin\theta_1 \end{array}\right] = T_{\theta_1} \tag{2.180}$$

IIa* :

$$\frac{d}{dt}\left\{\frac{\partial K}{\partial \dot{\theta}_2}\right\} - \frac{\partial K}{\partial \theta_2} + \frac{\partial P}{\partial \theta_2} = T_{\theta_2} \tag{2.181}$$

$$
\Rightarrow \begin{bmatrix}
\left[m_2 l_1 d_2 + (m_3+m_4+m_5) l_1 l_2\right]\cos(\theta_1-\theta_2)\ddot{\theta}_1 \\
+\left[I_2 + m_2 d_2^2 + (m_3+m_4+m_5) l_2^2\right]\ddot{\theta}_2 + m_3 l_2 d_3 \cos(\theta_2-\theta_3)\ddot{\theta}_3 \\
+\left[m_4 l_2 (l_4-d_4) + m_5 l_2 l_4\right]\cos(\theta_2+\theta_4)\ddot{\theta}_4 \\
+m_5 l_2 (l_5-d_5)\cos(\theta_2+\theta_5)\ddot{\theta}_5 \\
-\left[m_2 l_1 d_2 + (m_3+m_4+m_5) l_1 l_2\right]\sin(\theta_1-\theta_2)\dot{\theta}_1^2 \\
+m_3 l_2 d_3 \sin(\theta_2-\theta_3)\dot{\theta}_3^2 - \left[m_4 l_2 (l_4-d_4) + m_5 l_2 l_4\right]\sin(\theta_2+\theta_4)\dot{\theta}_4^2 \\
-m_5 l_2 (l_5-d_5)\sin(\theta_2+\theta_5)\dot{\theta}_5^2 \\
+\left[m_2 d_2 + (m_3+m_4+m_5) l_2\right]\left[\ddot{x}_b \cos\theta_2 - \ddot{z}_b \sin\theta_2\right] \\
-\left[m_2 d_2 + (m_3+m_4+m_5) l_2\right] g \sin\theta_2
\end{bmatrix} = T_{\theta_2} \qquad (2.182)
$$

IIIa*:

$$
\frac{d}{dt}\left\{\frac{\partial K}{\partial \dot{\theta}_3}\right\} - \frac{\partial K}{\partial \theta_3} + \frac{\partial P}{\partial \theta_3} = T_{\theta_3} \qquad (2.183)
$$

$$
\Rightarrow \begin{bmatrix}
m_3 l_1 d_3 \cos(\theta_1-\theta_3)\ddot{\theta}_1 + m_3 l_2 d_3 \cos(\theta_2-\theta_3)\ddot{\theta}_2 + \left[I_3 + m_3 d_3^2\right]\ddot{\theta}_3 \\
-m_3 l_1 d_3 \sin(\theta_1-\theta_3)\dot{\theta}_1^2 - m_3 l_2 d_3 \sin(\theta_2-\theta_3)\dot{\theta}_2^2 \\
+m_3 d_3 \left[\ddot{x}_b \cos\theta_3 - \ddot{z}_b \sin\theta_3\right] - m_3 d_3 g \sin\theta_3
\end{bmatrix} = T_{\theta_3} \qquad (2.184)
$$

IVa*:

$$
\frac{d}{dt}\left\{\frac{\partial K}{\partial \dot{\theta}_4}\right\} - \frac{\partial K}{\partial \theta_4} + \frac{\partial P}{\partial \theta_4} = T_{\theta_4} \qquad (2.185)
$$

$$
\Rightarrow \begin{bmatrix}
\left[m_4 l_1 (l_4 - d_4) + m_5 l_1 l_4\right]\cos(\theta_1 + \theta_4)\ddot{\theta}_1 \\
+\left[m_4 l_2 (l_4 - d_4) + m_5 l_2 l_4\right]\cos(\theta_2 + \theta_4)\ddot{\theta}_2 \\
+\left[I_4 + m_4 (l_4 - d_4)^2 + m_5 l_4^2\right]\ddot{\theta}_4 \\
+m_5 l_4 (l_5 - d_5)\cos(\theta_4 - \theta_5)\ddot{\theta}_5 \\
-\left[m_4 l_1 (l_4 - d_4) + m_5 l_1 l_4\right]\sin(\theta_1 + \theta_4)\dot{\theta}_1^2 \\
-\left[m_4 l_2 (l_4 - d_4) + m_5 l_2 l_4\right]\sin(\theta_2 + \theta_4)\dot{\theta}_2^2 \\
+m_5 l_4 (l_5 - d_5)\sin(\theta_4 - \theta_5)\dot{\theta}_5^2 \\
+\left[m_4 (l_4 - d_4) + m_5 l_4\right]\left[\ddot{x}_b \cos\theta_4 + \ddot{z}_b \sin\theta_4\right] \\
+\left[m_4 (l_4 - d_4) + m_5 l_4\right] g \sin\theta_4
\end{bmatrix} = T_{\theta_4} \tag{2.186}
$$

Va* :

$$
\frac{d}{dt}\left\{\frac{\partial K}{\partial \dot{\theta}_5}\right\} - \frac{\partial K}{\partial \theta_5} + \frac{\partial P}{\partial \theta_5} = T_{\theta_5} \tag{2.187}
$$

$$
\Rightarrow \begin{bmatrix}
\left[m_5 l_1 (l_5 - d_5)\right]\cos(\theta_1 + \theta_5)\ddot{\theta}_1 + m_5 l_2 (l_5 - d_5)\cos(\theta_2 + \theta_5)\ddot{\theta}_2 + \\
+m_5 l_4 (l_5 - d_5)\cos(\theta_4 - \theta_5)\ddot{\theta}_4 + \left[I_5 + m_5 (l_5 - d_5)^2\right]\ddot{\theta}_5 \\
-\left[m_5 l_1 (l_5 - d_5)\right]\sin(\theta_1 + \theta_5)\dot{\theta}_1^2 - m_5 l_2 (l_5 - d_5)\sin(\theta_2 + \theta_5)\dot{\theta}_2^2 \\
-m_5 l_4 (l_5 - d_5)\sin(\theta_4 - \theta_5)\dot{\theta}_4^2 + m_5 (l_5 - d_5)\left[\ddot{x}_b \cos\theta_5 + \ddot{z}_b \sin\theta_5\right] \\
+m_5 (l_5 - d_5) g \sin\theta_5
\end{bmatrix} = T_{\theta_5} \tag{2.188}
$$

VIa* :

$$
\frac{d}{dt}\left\{\frac{\partial K}{\partial \dot{\theta}_6}\right\} - \frac{\partial K}{\partial \theta_6} + \frac{\partial P}{\partial \theta_6} = T_{\theta_6} \tag{2.189}
$$

$$
\Rightarrow \begin{bmatrix}
(I_1 + I_2)\ddot{\theta}_6 \\
+\begin{bmatrix} m_1 d_1{}^2 + m_2 (l_1 + d_2)^2 \\ +(m_3 + m_4 + m_5)(l_1 + l_2)^2 \end{bmatrix} \left[\cos^2 \theta_6 \ddot{\theta}_6 - \cos\theta_6 \sin\theta_6 \ddot{\theta}_6 \right] \\
+\begin{bmatrix} m_1 d_1 + m_2 (l_1 + d_2) \\ +(m_3 + m_4 + m_5)(l_1 + l_2) \end{bmatrix} \ddot{y}_b \cos\theta_6 \\
+\begin{bmatrix} m_4 (l_1 + l_2)(l_4 - d_4) \\ +m_5 (l_1 + l_2)(l_4 + l_5 - d_5) \end{bmatrix} \begin{bmatrix} -\cos\theta_6 \sin\theta_7 \dot{\theta}_7^2 \\ +\cos\theta_6 \cos\theta_7 \ddot{\theta}_7 \end{bmatrix}
\end{bmatrix} = T_{\theta_6} \qquad (2.190)
$$

VIIa* :

$$
\frac{d}{dt}\left\{\frac{\partial K}{\partial \dot{\theta}_7}\right\} - \frac{\partial K}{\partial \theta_7} + \frac{\partial P}{\partial \theta_7} = T_{\theta_7} \qquad (2.191)
$$

$$
\Rightarrow \begin{bmatrix}
(I_4 + I_5)\ddot{\theta}_7 + \begin{bmatrix} m_4 (l_4 - d_4)^2 \\ +m_5 (l_4 + l_5 - d_5)^2 \end{bmatrix} \begin{bmatrix} \cos^2 \theta_7 \ddot{\theta}_7 \\ -\cos\theta_7 \sin\theta_7 \dot{\theta}_7{}^2 \end{bmatrix} \\
+[m_4 (l_4 - d_4) + m_5 (l_4 + l_5 - d_5)]\ddot{y}_b \cos\theta_7 \\
+\begin{bmatrix} m_4 (l_1 + l_2)(l_4 - d_4) \\ +m_5 (l_1 + l_2)(l_4 + l_5 - d_5) \end{bmatrix} \begin{bmatrix} -\sin\theta_6 \cos\theta_7 \dot{\theta}_6^2 \\ +\cos\theta_6 \cos\theta_7 \ddot{\theta}_6 \end{bmatrix}
\end{bmatrix} = T_{\theta_7} \qquad (2.192)
$$

VIIIa* :

$$
\frac{d}{dt}\left\{\frac{\partial K}{\partial \dot{x}_b}\right\} - \frac{\partial K}{\partial x_b} + \frac{\partial P}{\partial x_b} = T_{\theta_8} \text{ where } T_{\theta_{a8}} = T_{x_b} \qquad (2.193)
$$

$$
\Rightarrow \begin{bmatrix}
(m_1 + m_2 + m_3 + m_4 + m_5)\ddot{x}_b \\
+(m_1 d_1 + (m_2 + m_3 + m_4 + m_5) l_1)(\cos\theta_1 \ddot{\theta}_1 - \sin\theta_1 \dot{\theta}_1{}^2) \\
+(m_2 d_2 + (m_3 + m_4 + m_5) l_2)(\cos\theta_2 \ddot{\theta}_2 - \sin\theta_2 \dot{\theta}_2{}^2) \\
+m_3 d_3 (\cos\theta_3 \ddot{\theta}_3 - \sin\theta_3 \dot{\theta}_3{}^2) \\
+(m_4 (l_4 - d_4) + m_5 l_4)(\cos\theta_4 \ddot{\theta}_4 - \sin\theta_4 \dot{\theta}_4{}^2) \\
+m_5 (l_5 - d_5)(\cos\theta_5 \ddot{\theta}_5 - \sin\theta_5 \dot{\theta}_5{}^2)
\end{bmatrix} = T_{\theta_8} \qquad (2.194)
$$

IXa* :

$$\frac{d}{dt}\left\{\frac{\partial K}{\partial \dot{y}_b}\right\}-\frac{\partial K}{\partial y_b}+\frac{\partial P}{\partial y_b}=T_{\theta_9} \text{ where } T_{\theta_{a9}}=T_{y_b} \tag{2.195}$$

$$\Rightarrow \begin{bmatrix} (m_1+m_2+m_3+m_4+m_5)\ddot{y}_b \\ +\begin{bmatrix} m_1d_1+m_2(l_1+d_2) \\ +(m_3+m_4+m_5)(l_1+l_2) \end{bmatrix}(\cos\theta_6\ddot{\theta}_6-\sin\theta_6\dot{\theta}_6{}^2) \\ +(m_4(l_4-d_4)+m_5(l_4+l_5-d_5))(\cos\theta_7\ddot{\theta}_7-\sin\theta_7\dot{\theta}_7{}^2) \end{bmatrix}=T_{\theta_9} \tag{2.196}$$

Xa* :

$$\frac{d}{dt}\left\{\frac{\partial K}{\partial \dot{z}_b}\right\}-\frac{\partial K}{\partial z_b}+\frac{\partial P}{\partial z_b}=T_{\theta_{10}} \text{ where } T_{\theta_{a10}}=T_{z_b} \tag{2.197}$$

$$\Rightarrow \begin{bmatrix} (m_1+m_2+m_3+m_4+m_5)\ddot{z}_b \\ -(m_1d_1+(m_2+m_3+m_4+m_5)l_1)(\sin\theta_1\ddot{\theta}_1+\cos\theta_1\dot{\theta}_1{}^2) \\ -(m_2d_2+(m_3+m_4+m_5)l_2)(\sin\theta_2\ddot{\theta}_2+\cos\theta_2\dot{\theta}_2{}^2) \\ -m_3d_3(\sin\theta_3\ddot{\theta}_3+\cos\theta_3\dot{\theta}_3{}^2) \\ +(m_4(l_4-d_4)+m_5l_4)(\sin\theta_4\ddot{\theta}_4+\cos\theta_4\dot{\theta}_4{}^2) \\ +m_5(l_5-d_5)(\sin\theta_5\ddot{\theta}_5+\cos\theta_5\dot{\theta}_5{}^2) \\ +(m_1+m_2+m_3+m_4+m_5)g \end{bmatrix}=T_{\theta_{10}} \tag{2.198}$$

Now, let's arrange the equation

$$\frac{d}{dt}\left\{\frac{\partial L}{\partial \dot{\theta}_i}\right\}-\frac{\partial L}{\partial \theta_i}+\frac{\partial P}{\partial \theta_i}=T_{\theta_i} \quad i=1,...,10 \tag{2.199}$$

where

$$\begin{aligned} \theta_8 &= x_b \\ \theta_9 &= y_b \\ \theta_{10} &= z_b \end{aligned} \tag{2.200}$$

into the following standard form:

$$D_a(\underline{\theta_a})\underline{\ddot{\theta}_a} + h_a(\underline{\theta_a}, \underline{\dot{\theta}_a})\underline{\dot{\theta}_a} + G_a(\underline{\theta_a}) = \underline{T_{\theta_a}} \tag{2.201}$$

where

$\underline{\theta_a} = [\theta_{1a}, \ldots, \theta_{7a}, x_b, y_b, z_b]^T$, the 10x1 vector of angles of links with respect to the vertical axis (z-axis) for i=1,...,7 and (x_b, y_b, z_b) stance leg foot tip position during the double support phase;

$\underline{\mathrm{T}_{\theta_a}} = [\mathrm{T}_{\theta_1}, \ldots, \mathrm{T}_{\theta_{10}}]^T$, the 10x1 vector of control torque applied at each joint for $i = 1, ..., 7$ & $T_{\theta_8} = T_{\theta_9} = T_{\theta_{10}} = 0$ during double support phase; and

$$D_a(\underline{\theta_a}) = [D_{aij}(\underline{\theta_a})] \quad (i = 1, ..., 10) \tag{2.202}$$

is a 10x10 symmetric, positive-definite inertia matrix where D_{aij}'s for $i = 1, ..., 7$ are exactly same as in the single support phase, i.e. $D_{aij} = D_{ij}$ for $i = 1, ..., 7$ and the rest of terms for $i = 8, 9, 10$ are obtained as

$$\begin{aligned}
D_{a18} &= D_{a81} = \left[m_1 d_1 + (m_2 + m_3 + m_4 + m_5) l_1\right] \cos\theta_1 \\
D_{a28} &= D_{a82} = \left[m_2 d_2 + (m_3 + m_4 + m_5) l_2\right] \cos\theta_2 \\
D_{a38} &= D_{a83} = m_3 d_3 \cos\theta_3 \\
D_{a48} &= D_{a84} = \left[m_4 (l_4 - d_4) + m_5 l_4\right] \cos\theta_4 \\
D_{a58} &= D_{a85} = m_5 (l_5 - d_5) \cos\theta_5 \\
D_{a68} &= D_{a86} = 0 \\
D_{a78} &= D_{a87} = 0 \\
D_{a88} &= m_1 + m_2 + m_3 + m_4 + m_5 \\
D_{a89} &= D_{a98} = 0 \\
D_{a810} &= D_{a108} = 0 \\
D_{a19} &= D_{a91} = 0 \\
D_{a29} &= D_{a92} = 0 \\
D_{a39} &= D_{a93} = 0
\end{aligned}$$

$$D_{a49} = D_{a94} = 0$$
$$D_{a59} = D_{a95} = 0$$
$$D_{a69} = D_{a96} = \left[m_1 d_1 + m_2(l_1 + d_2) + (m_3 + m_4 + m_5)(l_1 + l_2)\right]\cos\theta_6$$
$$D_{a79} = D_{a97} = \left[m_4(l_4 - d_4) + m_5(l_4 + l_5 - d_5)\right]\cos\theta_7$$
$$D_{a99} = m_1 + m_2 + m_3 + m_4 + m_5$$
$$D_{a910} = D_{a109} = 0$$
$$D_{a110} = D_{a101} = -\left[m_1 d_1 + (m_2 + m_3 + m_4 + m_5) l_1\right]\sin\theta_1$$
$$D_{a210} = D_{a102} = -\left[m_2 d_2 + (m_3 + m_4 + m_5) l_2\right]\sin\theta_2$$
$$D_{a310} = D_{a103} = -m_3 d_3 \sin\theta_3$$
$$D_{a410} = D_{a104} = \left[m_4(l_4 - d_4) + m_5 l_4\right]\sin\theta_4$$
$$D_{a510} = D_{a105} = m_5(l_5 - d_5)\sin\theta_5$$
$$D_{a6-10} = D_{a10-6} = 0$$
$$D_{a710} = D_{a107} = 0$$
$$D_{a1010} = m_1 + m_2 + m_3 + m_4 + m_5$$

Similarly,

$$h_a(\underline{\theta_a}, \underline{\dot{\theta}_a})\underline{\dot{\theta}_a} = \underset{i}{col}[\sum_{\substack{j=1 \\ j\neq i}}^{10} h_{aijj}\dot{\theta}_j^{\,2}] \quad (i = 1,...,10) \text{ is a 10x1 column vector} \tag{2.203}$$

where

h_{aijj} for $i, j = 1,...,7$ are exactly same as in single support phase, i.e.

$h_{aijj} = h_{ijj}$ for $i, j = 1,...,7$

and rest of the terms are obtained as

$$h_{188} = 0 \qquad h_{199} = 0 \qquad h_{11010} = 0$$
$$h_{288} = 0 \qquad h_{299} = 0 \qquad h_{21010} = 0$$
$$h_{388} = 0 \qquad h_{399} = 0 \qquad h_{31010} = 0$$

$$h_{488}=0 \qquad h_{499}=0 \qquad h_{41010}=0$$
$$h_{588}=0 \qquad h_{599}=0 \qquad h_{51010}=0$$
$$h_{688}=0 \qquad h_{699}=0 \qquad h_{61010}=0$$
$$h_{788}=0 \qquad h_{799}=0 \qquad h_{71010}=0$$

$$h_{811}=-\left[m_1 d_1+(m_2+m_3+m_4+m_5)l_1\right]\sin\theta_1$$
$$h_{822}=-\left[m_2 d_2+(m_3+m_4+m_5)l_2\right]\sin\theta_2$$
$$h_{833}=-m_3 d_3\sin\theta_3$$
$$h_{844}=-\left[m_4(l_4-d_4)+m_5 l_5\right]\sin\theta_4$$
$$h_{855}=-m_5(l_5-d_5)\sin\theta_5$$
$$h_{866}=0$$
$$h_{877}=0$$
$$h_{899}=0$$
$$h_{81010}=0$$

$$h_{911}=0$$
$$h_{922}=0$$
$$h_{933}=0$$
$$h_{944}=0$$
$$h_{955}=0$$
$$h_{966}=-\left[m_1 d_1+m_2(l_1+d_2)+(m_3+m_4+m_5)(l_1+l_2)\right]\sin\theta_6$$
$$h_{977}=-\left[m_4(l_4-d_4)+m_5(l_4+l_5-d_5)\right]\sin\theta_7$$
$$h_{988}=0$$
$$h_{91010}=0$$

$$h_{1011}=-\left[m_1 d_1+(m_2+m_3+m_4+m_5)l_1\right]\cos\theta_1$$
$$h_{1022}=-\left[m_2 d_2+(m_3+m_4+m_5)l_2\right]\cos\theta_2$$
$$h_{1033}=-m_3 d_3\cos\theta_3$$
$$h_{1044}=-\left[m_4(l_4-d_4)+m_5 l_5\right]\cos\theta_4$$
$$h_{1055}=-m_5(l_5-d_5)\cos\theta_5$$
$$h_{1066}=0$$
$$h_{1077}=0$$
$$h_{1088}=0$$
$$h_{1099}=0$$

$G_a(\underline{\theta_a}) = [G_{ai}(\underline{\theta_a})]$ ($i = 1,...,10$) is a 10x1 column vector (2.204)

where $G_{ai}(\underline{\theta})$ for $i = 1,...,7$ are exactly same as in single support phase, i.e. $G_{ai} = G_i$ for $i = 1,...,7$ and rest of the terms are obtained as

$$G_{a8}(\underline{\theta_a}) = 0$$
$$G_{a9}(\underline{\theta_a}) = 0$$
$$G_{a10}(\underline{\theta_a}) = (m_1 + m_2 + m_3 + m_4 + m_5)g$$

$$T_{ai} = T_{\theta i} \quad (i = 1,2,...,5)$$
$$T_{a6} = T_{a7} = 0$$

The dynamic equations of motion formulated as above in this section are used for both the left leg and right leg in the calculations during the double support phase.

During the single support phase, the free end of the swing leg is in motion towards the forward direction, it moves from back of the body towards the ahead of it and just at the moment of end of single support phase, the free end of the biped swing leg comes into a sudden contact with the ground and an instantaneous exchange of the support of the biped takes place. At the time when the free end of the swing leg collides with the ground, the joint angle velocities change discontinuously. Finally, the free end becomes the support and the support end leaves immediately the ground and becomes the free end. The interval of exchange of legs during the impact is assumed to be infinitely small and perfectly plastic collision takes place, which means the tip of the swing leg does not leave the walking surface after impact with the walking surface and the velocity of the tip of the swing leg immediately becomes zero. During the impact phase, no change in the joint angular positions is assumed.

The instantaneous change in the joint angular velocities of the links can be derived based on the collision formula and is given with proof by Theorem 2.1.

Theorem 2.1: The sudden change in the angular velocity of each joint is given by

$$\Delta\underline{\dot{\theta}} = \underline{D}_a^{-1}\,\underline{J}_a^{T}\,(\underline{J}_a\;\underline{D}_a^{-1}\;\underline{J}_a^{T})^{-1}\,\Delta\underline{v}_e \tag{2.205}$$

where

$\Delta\underline{\dot{\theta}} = \underline{\dot{\theta}}_{after} - \underline{\dot{\theta}}_{before}$ is the 7x1 vector of instantaneous change in the angular velocities before and after the impact;

$\Delta\underline{v}_e = \underline{v}_{e,\,after} - \underline{v}_{e,\,before}$ is the 3x1 vector of instantaneous change in the swing leg tip point velocities before and after the impact;

$\underline{D}_a$ is the 10x10 inertia matrix of the model as obtained in (2.202);

$\underline{J}_a$ is the 3x10 Jacobian matrix of the biped in air defined by;

$\underline{J}_a = \dfrac{\partial \underline{P}_e}{\partial \underline{\theta}_a}$ where $\underline{P}_e = (\underline{x}_e, \underline{y}_e, \underline{z}_e)$ is the position of the free end of the swing leg with respect to the fixed coordinate frame

Proof: The equation representing the collision can be formulated by the following procedure [60].

$\underline{P}_e = (\underline{x}_e, \underline{y}_e, \underline{z}_e)$, the instantaneous position of the free end of the swing leg coming into contact with the environment, can be expressed with respect to the fixed coordinate as

$$\underline{P}_e = \underline{P}_e(\underline{\theta}) \tag{2.206}$$

where $\underline{\theta} = \left[\theta_1, ..., \theta_7\right]^T$ is the vector of angular joint positions of the system.

If $\underline{P}_s$ is the contact point, the impact occurs when

$$\underline{P}_e(\theta) = \underline{P}_s \tag{2.207}$$

This equation (2.207) represents an external constraint to the motion, which implies that a generalized constraint force $\underline{F}_{\delta}$ is introduced into the system and

$$\underline{F}_{\delta} = \left[\frac{\partial \underline{P}_e}{\partial \underline{\theta}_a}\right]^T \underline{\lambda} \tag{2.208}$$

where $\underline{\lambda}$ is a suitable column vector of Lagrange multipliers.

By defining the Jacobian matrix $\underline{J}_a$ at the swing leg tip point as

$$\underline{J}_a = \left[\frac{\partial \underline{P}_e}{\partial \underline{\theta}_a}\right] \tag{2.209}$$

the equation (2.208) becomes

$$\underline{F}_{\delta} = \underline{J}_a{}^T \underline{\lambda} \tag{2.210}$$

The equations of motion just before the impact are the same as in (2.201):

$$\underline{D}_a(\underline{\theta}_a)\ddot{\underline{\theta}}_a + \underline{h}_a(\underline{\theta}_a, \dot{\underline{\theta}}_a)\dot{\underline{\theta}}_a + \underline{G}_a(\underline{\theta}_a) = \underline{T}_a \tag{2.211}$$

and the equations of motion just after the impact becomes as

$$\underline{D}_a(\underline{\theta}_a)\ddot{\underline{\theta}}_a + \underline{h}_a(\underline{\theta}_a, \dot{\underline{\theta}}_a)\dot{\underline{\theta}}_a + \underline{G}_a(\underline{\theta}_a) = \underline{T}_a + \underline{F}_{\delta} \tag{2.212}$$

By integrating (2.212) over the infinitesimal interval $\left[t_0, t_0 + \Delta t\right]$ where t_0 is the instant of impact, the following is obtained

$$\begin{aligned} \lim_{\Delta t \to 0} \int_{t_0}^{t_0+\Delta t} \underline{D}_a(\underline{\theta}_a)\ddot{\underline{\theta}}_a dt + \lim_{\Delta t \to 0} \int_{t_0}^{t_0+\Delta t} \left[\underline{h}_a(\underline{\theta}_a, \dot{\underline{\theta}}_a)\dot{\underline{\theta}}_a + \underline{G}_a(\underline{\theta}_a) - \underline{T}_a\right] dt \\ = \lim_{\Delta t \to 0} \int_{t_0}^{t_0+\Delta t} \underline{F}_{\delta} dt \end{aligned} \tag{2.213}$$

As $\Delta t \to 0$, $\lim_{\Delta t \to 0} \int_{t_0}^{t_0+\Delta t} \left[h_a(\underline{\theta}_a, \dot{\underline{\theta}}_a)\dot{\underline{\theta}}_a + G_a(\underline{\theta}_a) - \underline{T}_a \right] dt \to 0$ and as a result, (2.213) reduces to

$$\underline{D}_a(\underline{\theta}_a)\Delta\dot{\underline{\theta}}_a = \int_{t_0}^{t_0+\Delta t} \underline{F}_\delta dt \tag{2.214}$$

where $\Delta\dot{\underline{\theta}}_a = \dot{\underline{\theta}}_a(t_0 + \Delta t) - \dot{\underline{\theta}}_a(t_0)$

By using the equality (2.208) in (2.214), it becomes

$$\underline{D}_a(\underline{\theta}_a)\Delta\dot{\underline{\theta}}_a = \underline{J}_a^{\ T} \int_{t_0}^{t_0+\Delta t} \underline{\lambda} dt \tag{2.215}$$

The equation (2.215) forms an expression of the theorem of conservation of momentum. It allows the computation of $\Delta\dot{\underline{\theta}}_a$ if the right-hand side of the equation is known and can be written as

$$\Delta\dot{\underline{\theta}}_a = \underline{D}_a^{-1}(\underline{\theta}_a)\underline{J}_a^{\ T} \int_{t_0}^{t_0+\Delta t} \underline{\lambda} dt \tag{2.216}$$

Assuming that the relative velocity

$$\Delta\underline{v}_e = \underline{v}_e(t_0 + \Delta t) - \underline{v}_e(t_0) \tag{2.217}$$

is known where $\underline{v}_e$ is the velocity of the swing leg tip point $\underline{P}_e$; and by using the fact that

$$\underline{v}_e = \underline{J}_a \dot{\underline{\theta}}_a \tag{2.218}$$

the following can be obtained

$$\underline{v}_e(t_0 + \Delta t) - \underline{v}_s(t_0) = \underline{J}_a \left[\dot{\underline{\theta}}_a(t_0 + \Delta t) - \dot{\underline{\theta}}_a(t_0) \right] \tag{2.219}$$

Hence,

$$\underline{J}_a \Delta\dot{\underline{\theta}}_a = \Delta\underline{v}_e \tag{2.220}$$

is obtained.

Therefore, replacing $\Delta\dot{\underline{\theta}}_a$ in (2.220) with (2.216), the below is found

$$\underline{J}_a \left[\underline{D}_a{}^{-1}(\underline{\theta}_a)\, \underline{J}_a{}^{T} \int_{t_0}^{t_0+\Delta t} \underline{\lambda} dt \right] = \Delta\underline{v}_e \tag{2.221}$$

Rearrangement of (2.221) results in

$$\int_{t_0}^{t_0+\Delta t} \underline{\lambda} dt = \left[\underline{J}_a \underline{D}_a{}^{-1} \underline{J}_a{}^{T} \right]^{-1} \Delta\underline{v}_e \tag{2.222}$$

As a result, putting (2.119) into (2.216) concludes the proof

$$\Delta\dot{\underline{\theta}}_a = \underline{D}_a^{-1}(\underline{\theta}_a)\, \underline{J}_a{}^{T} \left[\underline{J}_a \underline{D}_a{}^{-1} \underline{J}_a{}^{T} \right]^{-1} \Delta\underline{v}_e \tag{2.223}$$

■

In order to calculate $\Delta\dot{\underline{\theta}}_a$ by using (2.205) as obtained by Theorem 2.1, $\underline{J}_a$ needs to be calculated in advance. $\underline{J}_a$ is the Jacobian calculated for point $\underline{P}_e = (\underline{x}_e, \underline{y}_e, \underline{z}_e)$, the position of the free end of the swing leg with respect to the fixed coordinate frame and it is easily acquired by writing down the point $\underline{P}_e$ in terms of the elements of the joint angle vectore, $\underline{\theta}_a$ and then taking the necessary derivatives as given in (2.4). As a result, the Jacobian $\underline{J}_a$ is obtained as

$$\underline{J}_a^T = \begin{pmatrix} l_1\cos\theta_1 & 0 & -l_1\sin\theta_1 \\ l_2\cos\theta_2 & 0 & -l_2\sin\theta_2 \\ 0 & 0 & 0 \\ l_4\cos\theta_4 & 0 & l_4\sin\theta_4 \\ l_5\cos\theta_5 & 0 & l_5\sin\theta_5 \\ 0 & (l_1+l_2)\cos\theta_6 & 0 \\ 0 & (l_4+l_5)\cos\theta_7 & 0 \\ 1 & 0 & 0 \\ 0 & 1 & 0 \\ 0 & 0 & 1 \end{pmatrix} \tag{2.224}$$

After the impact with the ground, the velocity $\underline{v}_e$ becomes zero and so,

$$\Delta\underline{v}_e(0) = -\underline{v}_{e,\,before} \tag{2.225}$$

Therefore, (2.205) becomes:

$$\underline{\dot{\theta}}_{after} = \underline{\dot{\theta}}_{before} + \underline{D}_a^{-1}\,\underline{J}_a^{\,T}(\underline{J}_a\,\underline{D}_a^{-1}\,\underline{J}_a^{\,T})^{-1}(-\underline{v}_{e,\,before}) \tag{2.226}$$

where $\underline{\dot{\theta}}_{before}$ and $\underline{\dot{\theta}}_{after}$ are the link velocities just before and just after the impact, respectively. It is a fact that the joint angles during the time interval of the impact do not change and as a result, $\underline{D}_a$ and $\underline{J}_a$ in (2.226) are evaluated at the moment of impact.

After the impact, the roles of the swing and stance legs are to be exchanged just before the consecutive single support phase by relabeling the links in order to be able to use the same set of equations of motion for both left and right leg swing and stance phases as below. The joint angles and velocities to be used as initial conditions for the next step can be calculated as

$$\begin{aligned} &\theta_1(0) = -\theta_5(T), \quad \theta_2(0) = -\theta_4(T), \quad \theta_3(0) = \theta_3(T), \quad \theta_4(0) = -\theta_2(T), \\ &\theta_5(0) = -\theta_1(T), \quad \theta_6(0) = -\theta_7(T), \quad \theta_7(0) = -\theta_6(T) \end{aligned} \tag{2.227}$$

$$\dot{\theta}_1(0) = -\dot{\theta}_{5,\,after}(T), \quad \dot{\theta}_2(0) = -\dot{\theta}_{4,\,after}(T), \quad \dot{\theta}_3(0) = \dot{\theta}_{3,\,after}(T),$$
$$\dot{\theta}_4(0) = -\dot{\theta}_{2,\,after}(T), \quad \dot{\theta}_5(0) = -\dot{\theta}_{1,\,after}(T), \quad \dot{\theta}_6(0) = -\dot{\theta}_{7,\,after}(T),$$
$$\dot{\theta}_7(0) = -\dot{\theta}_{6,\,after}(T)$$

where

$\underline{\theta}(0)$ and $\underline{\dot{\theta}}(0)$ are the initial conditions of the following (next) step,

$\underline{\theta}(T)$ is the terminal posture of the completion of each step before switching support leg,

$\underline{\dot{\theta}}_{after}(T)$ is the angular velocities after impact at the completion of each step.

It is a fact that such relabeling deduces discontinuities in the joint angles and velocities.

CHAPTER 3

DYNAMIC BALANCE AND STABILITY

3.1 Overview

The behavior that is called balance results from an interaction of many systems and subsystems. In dynamical system terms, balance is a collective variable, a measure of the way a system or organism reduces a huge number of potential postural responses to a finite set of possibilities [61]. Bipedal walking, naturally, compels good balance to prevent falling down during locomotion. Balance is essential for continuation of life in the sense that it is necessary to carry out acts of daily living independently while avoiding falls causing injuries. Walking on two legs also requires certain adjustments to body proportions. On the other hand, animals with more than two legs have relatively more advantage as per ensuring stability during locomotion.

The biped locomotion control requires a more complex control problem and detailed knowledge of the biped's structure and dynamics. Precise positioning and timing to achieve coordinated movement is essential in biped locomotion stability. It is difficult to stabilize the biped robot when dynamics of the environment is unknown.

In biped locomotion terminology, there are two kinds of locomotion stability, namely:

- Static stability,
- Dynamic stability.

Static stability is the stability when the biped remains balanced during locomotion by keeping its COM vertically projected over the polygon of support formed by feet on the ground surface [12]. This means that, if the robot stops motion at any point of time of locomotion, it will remain in a stable position for an indefinite period of time. The polygon of support is the area of the stance foot on the ground in the single support phase; and the minimum convex area containing both foot surfaces touching wholly to the ground in the

double support phase as the details are depicted in Figure 3.1. Note that, in this figure, the direction of motion is from left to right, ■ indicates the COM position and polygons indicate the area of support formed by the feet. Static walking is easier to develop since it only requires taking into account the biped kinematical structure. Statically stable walking necessitates large feet, strong ankle joints and can achieve only slow walking speeds [63].

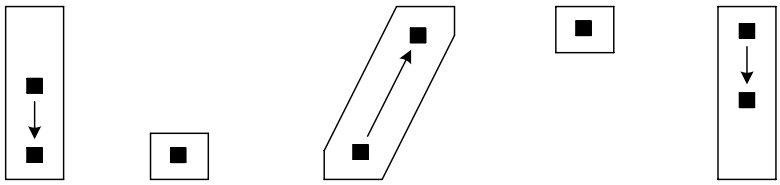

Figure 3.1 Static biped walking [62]

On the other hand, in dynamic stability, the COM may leave the feet support area boundaries for limited amount of time as depicted in Figure 3.2. This causes the biped to experience tipping moments. So the biped may be falling during parts of the gait. The effect of tipping moment can be counteracted by the joint torques. The biped could overturn around the edge of the stance foot on the ground unless the feet are controlled correctly. Hence, the walking gait is designed to have feet move in a manner that catches the walker when it is falling. Dynamic stability means that biped never falls down on the ground during walking. Dynamic walking permits smaller feet size, faster walking speeds and greater efficiency with more mobility and versatility (increased leg motion and foot placement flexibility). These are significant advantages compared to static walking.

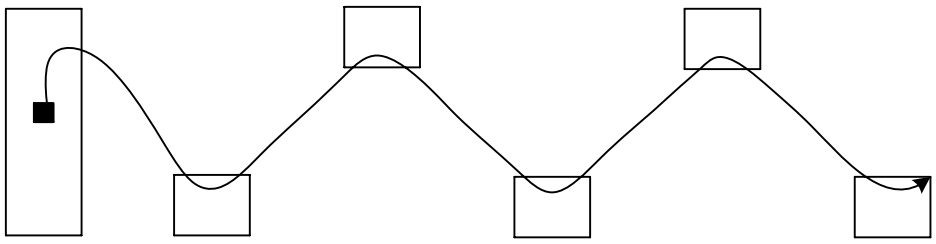

Figure 3.2 Dynamic biped walking [62]

Human walking is usually of dynamical gait type when walking – very rarely human exhibits static walking. Hence, ensuring dynamic stability in biped robot is more realistic. It also permits faster walking speeds and is more efficient than static walking. When walking slowly, it is difficult for biped to employ dynamic walking gait since at slow speeds, the time in which the COM is outside of the support polygon is longer, and as a result the tipping moment have a stronger effect on walking.

In the literature, there are many approaches that examined the statically stable biped walking motions [64], [65], [66]. Hemami et al. studied the upright stability of bipeds modeled as inverted pendulums using Lyapunov's second method [67], [68]. Katoh and Mori considered the stability of the walking motion by proving convergence to the dynamics prescribed by the van der Pol equations [69]. The biped robots by Furusho achieve the stability of steady walking by using the reduced order biped model [18].

Hurmuzlu proposed an approach that applies discrete mapping techniques to study the stability of bipedal locomotion [70]. The method is based on the construction of a first return map by considering the intersection of periodic orbits. Hurmuzlu also studied the role of impact in the stability of biped locomotion [71].

Raibert designed biped hopping machines that can move with a certain speed and keep balance due to their simple structure [12]. Raibert studied the dynamic balance of the biped by modeling it as an inverted pendulum.

The first biped robot to be successfully created and use dynamic balance was developed by Kato in 1983 and improved afterwards [76], [77]. Miura & Shimoyama built a walking machine that can balance itself dynamically [17]. Hodgins et. al. developed a dynamic running robot [78]. Miller and Kun also studied walking with dymanic balance [79], [80].

Vukobratovic contributed to the development of stability of bipeds in early stages of the biped robot technology [48]. Furthermore, he introduced a concept of stability called the Zero Moment Point (ZMP), which is closely tied to the biped dynamic stability criteria [72]. ZMP criteria is, thereafter, very commonly used by many other researchers in biped research [73], [74], [75]. There are many other authors contributed to the stability analysis of passive dynamic bipedal walking [81], [82], [24], [83], [84], [85].

3.2 Biped Stability Criterion

There is no definite criterion that decides whether the dynamic biped walking is stable or not. Vukobratovic, et al. proposed the concept of ZMP to study the dynamic stability of bipedal locomotion [86]. In this thesis, ZMP is used as the stability criterion.

ZMP is the point where the sum of all the moments of active forces acting on the biped is equal to zero along the horizontal axis. When the ZMP of the biped is inside the support polygon, the walking is defined to be dynamically stable. ZMP is only defined under the foot contacting to the ground. Mathematically, ZMP condition for biped can be written as:

$$x_{ZMP} = \frac{\sum_{i=1}^{5} m_i(\ddot{z}_i + g)x_i - \sum_{i=1}^{5} m_i \ddot{x}_i z_i - \sum_{i=1}^{5} I_{iy}\ddot{\Omega}_{iy}}{\sum_{i=1}^{5} m_i(\ddot{z}_i + g)} \tag{3.1}$$

$$y_{ZMP} = \frac{\sum_{i=1}^{5} m_i(\ddot{z}_i + g)y_i - \sum_{i=1}^{5} m_i \ddot{y}_i z_i - \sum_{i=1}^{5} I_{ix}\ddot{\Omega}_{ix}}{\sum_{i=1}^{5} m_i(\ddot{z}_i + g)} \tag{3.2}$$

where

m_i : the mass of link i

I_{ix}, I_{iy} : the inertial component around the x-axis and the y-axis at the center of gravity of link i

$\ddot{\Omega}_{ix}$, $\ddot{\Omega}_{iy}$: the absolute angular velocity components around the x-axis and y-axis at the center of gravity of link i

$p_i = (x_i, y_i, z_i)$: the coordinate of the mass center of link i on an absolute Cartesian coordinate system

$p_{ZMP} = (x_{ZMP}, y_{ZMP}, 0)$: is the coordinate of the ZMP

In this thesis, the ZMP condition is used as a stability constraint by the high level controller.

CHAPTER 4

REFEFENCE TRAJECTORY GENERATION

4.1 Overview

Reference gait trajectory generation is a critical issue and another challenging problem in the biped locomotion and control study. The aim of the reference trajectory generation is to produce the desired gait to the biped control system so that the purpose of the control becomes to enable the biped system to follow this trajectory throughout the locomotion (straight, step over obstacles, step up/down). As a parallel fact to the locomotion of humans, biped trajectory generation also involves the capabilities of enhancement through learning, minimization of dissipated energy, and finding the optimal trajectory. The basic purpose is to generate gait trajectory that is natural and similar to human locomotion. In other words, an algorithm to design the reference gait trajectory that results in joint angle profiles coherent with the human-like motion is desired.

The joint angle profile of a normal human in sagittal plane is given in Figure 4.1 [87]. When designing the reference trajectory, some basic facts about the human gait should be taken into account in order to obtain a natural walking pattern:

- Knee joint angle is limited so that the knee does not bend backward during walking,
- Biped realizes continuous (of time) and steady gait,
- The generated profile satisfies the condition of being repeatable.

The biped robot reference trajectory synthesis is hard due to the fact that it necessiates a complete comprehension and analysis of the system characteristics. In the past 40 years, considerable improvement has been realized in the biped reference trajectory generation and in the literature, many methods for trajectory generation have been proposed. Some works have been focused on the generation of desired trajectory via trial-error or simple methods. Tzafestas et al. generated reference walking pattern consisting of several phases

(single-leg-supporting phase with non-kick or kick-action, leg support-exchange, collision of the swing leg with the ground), and derived intuitively the corresponding joint angle trajectories for the 9-link planar biped [88]. The reference signals are chosen so as to use the effects of the gravity in a way that increases the angular momentum during the single leg supporting phase, assuming that the body is always kept upright.

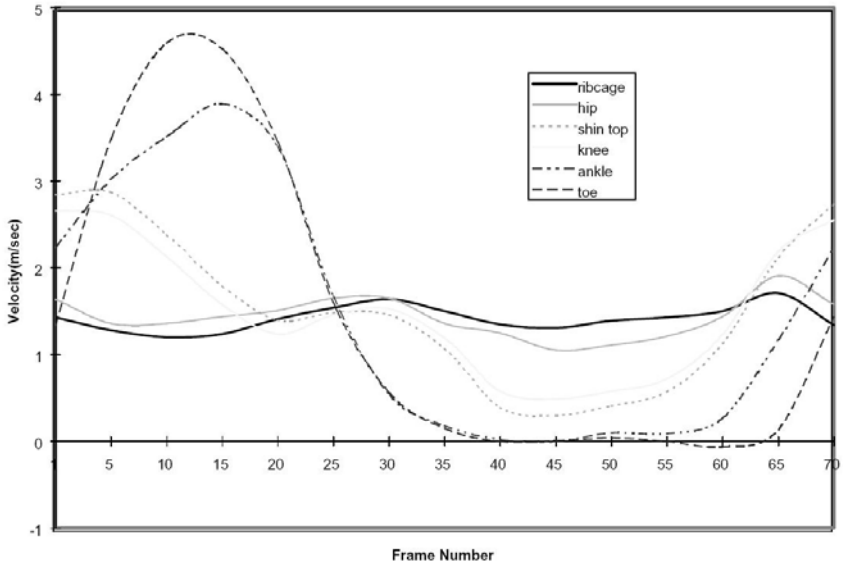

Figure 4.1 The locomotion velocity profile of a normal human in Sagittal Plane

In general, a systematic method is required to generate the reference gait trajectory. These methods, used in the literature, can be classified as below:

1) Analytical
2) COG Based
3) Measured Human Walking Data Based
4) Stability Based
5) Optimality Based
6) Computational Intelligence Based

The review of the corresponding literature as per the above classification is given in the rest of this section.

4.1.1 Analytical Gait Trajectory

4.1.1.1 Constraint Based Design

Hurmuzlu developed a set of kinematic relations in the form of constraint functions from the human walking physical attributes (erect posture, overall progression velocity, trajectory of the swing limb during the single support phase, bias of the stance knee, and coordination of the motion of the limbs) and generated a methodical approach by parametric formulation that connects the constraint equations to desired joint angle profiles for five-link planar biped robot. Hurmuzlu's constraint functions automatically produce a repeatable gait [58].

4.1.1.2 Oscillatory Gait Trajectory

4.1.1.2.1 Sinusoidal Gait Generation

Golliday and Hemami generated the reference gait trajectory as a periodic response (undamped oscillator-simple pendulum) whereas the oscillator parameters are obtained from the human body parameters for the linearized dynamic model to be controlled by a state feedback controller [55]. Kurematsu et al. used a cycloidal profile for generating the trajectories of the hip and ankle joints of the swinging leg. The trajectory is described by a simple periodic sinusoidal function, which shows an analog to human's hip and ankle trajectory in normal walking [89]. Juang et al. also used the same method for generating the pre-defined reference trajectories to a multi-layered neural network control architecture [90].

4.1.1.2.2 Coupled Oscillator Pattern Generator

Coupled oscillators are first used by Bay et al. [91] and then by Zielinska [92]. Thereafter, Jalics et al. developed five coupled oscillators (each modeled as a Van der Pol oscillator), which is analogous to the oscillators that are conjectured to exist in humans and animals, with equal importance based on an independent master oscillator assigned to torso to which the other oscillators, assigned to upper and lower legs, adjust in order to produce joint angle reference trajectory of a five link planar biped. The goal of Jalics's research is to combine the skeletal and muscle models with a coupled pattern generator and a controller to achieve adaptable rhythmic motion [93]. Benbrahim et al. developed a central pattern generator, which uses a CMAC neural network algorithm to generate the desired

reference trajectory for a six joint seven link biped robot. The inputs to the CMAC are time, step length and walking period [94].

Kurematsu et al. designed the trajectory of a biped by using a neuro oscillator pattern generator, which consists of four neuron cells which are mutually coupled with inhibitory connections and shows a stationary periodic oscillation for an appropriate set of parameters. This periodic oscillation generates a trajectory for stationary walking by assigning the state variables of neuron cells to joint angles of robot [95].

4.1.1.3 Interpolation Based Design

The trajectory planning by interpolation has been widely used for biped reference trajectory generation. Initially, it has started to be used very commonly in situations such as “Keyframe Animation”, which is the synthesis of a sequence of images portraying continuous motion interpolating between a set of keyframes that are specified by parameters at several instants of time and then the trajectory at the intermediate instants of time is found. These intermediate trajectories are constructed either by interpolating each of the motion parameters independently or by minimizing the energy [96]. Initially, using polynomial interpolation method was used for simple biped configuration and planar flat plane motion but when there are various constraints like walking surface conditions (inclined surface, rough terrain, environment containing obstacles, etc.), different locomotion types (running, turning, etc.), the order of the polynomial becomes very high that causes computational difficulties.

Silva et al. completely characterized the reference trajectory in terms of five locomotion variables: step length, hip height, maximum hip ripple, maximum foot clearance and link lengths [97]. The kinematic characteristics and the system performance during walking were determined. Hereafter, the relation between the locomotion variables and the trajectories physically admissible are decided and the reference trajectory is accomplished by prescribing the Cartesian trajectories of the body and the lower extremities of the leg. The hip trajectory is assumed to maintain a fixed height with constant forward velocity, where the stance leg adjusts itself accordingly. In accordance, the equation of the tip of the swing leg along the axis of motion is computed by summing a linear function with a sinusoidal function. By means of an inverse kinematics algorithm, the related reference joint trajectories are generated from these hip and feet trajectories.

Shih generated the reference gait trajectories of the biped's body and its two feet as a piecewise cubic polynomials in order to realize the walking on even floor, sloping surfaces and stairs for a biped with variable-length legs [98]. Also, Shih developed the reference gait trajectories for the variable-length leg 7 DOF biped when ascending and descending stairs [99]. Polynomials of third order are chosen as being of minimum complexity to allow the positions and velocities at the two ends of a time interval to be freely allocated.

Huang first formulated the constraints of a complete foot trajectory which includes the ground conditions, dynamic stability constraint, and relationship between walking patterns and actuator specifications; hereafter generated the reference trajectory by 3rd order spline interpolation [100], [101]. In [100], the hip trajectory is generated using a 3rd order periodic spline function in order to satisfy the high stability. Later in [101], the hip trajectory is generated by 3rd order spline interpolation and then reviewed by iterative computation in order to obtain a smooth hip motion with the largest stability margin using two parameters. Huang also presented work to generate reference trajectory that requires small torque and velocity of the joint actuators.

Tang et al. presented trajectory planning methods for walking and penalty kicking both in Cartesian and joint spaces. The trajectory is generated by first designing the hip and ankle trajectories as a 3rd order spline function in Cartesian space and then the joint angle profiles are obtained by inverse kinematics. The designed trajectory has first-order derivative continuity, guaranteeing smoothness of joint velocity, and second-order derivative continuity, providing smoothness of acceleration or torque of joint [102].

Lee derived the reference trajectory for a five-link biped robot at first by dividing the motion into phases of single-support and double-support and also assuming that the torso is always desired to be in upright position and then obtained the joint angle trajectories by polynomial interpolation. The coefficients of the polynomial are obtained by minimizing the squared joint angle error [103]. Tang et al. presented trajectory planning methods for walking and penalty kicking both in Cartesian and joint spaces. The trajectory in joint space is generated by directly applying the 3rd order spline interpolation method to the joint angles [102].

4.1.2 COG Based Gait Trajectory

4.1.2.1 Modeling as an Inverted Pendulum

It is a common observation that the motion of the biped robot is similar to an inverted pendulum. Generally, the inverted pendulum model is linearized about the upright position in order to obtain the reference trajectory generation. But the inverted pendulum simplification is not generally applicable for rough terrain locomotion or for the biped systems that aims to bend the knee.

Kitamura, Kurematsu et al. generated joint angle trajectory by introducing a hierarchical structure [104], [105]. The motion of the center of gravity of the robot is modeled as an inverted pendulum and a Hopfield type neural network is used to solve the inverse kinematics in order to obtain the desired joint reference trajectory of biped robot on flat surface [104] and on stairs [105] from the position of the center of gravity and the position of toes calculated from the equation of an inverted pendulum. Note that, the only a priori given to the reference trajectory generation system is the position and the velocity of the center of gravity of the robot for each step.

Kajita et al. derived the reference trajectory from the COG trajectory of the body, where the body moves horizontally and this horizontal motion is expressed by a simple linear differential equation [26]. Furthermore, Kajita et al. assumed that the body of the biped which has massless legs moves on a straight line in sagittal plane and rotates at a constant angular velocity and as a result of this assumption, the COM motion is modeled as a linear inverted pendulum. By applying this model, it is stated that the walking of biped in rugged ground becomes equivalent to walking on a level ground [106], [107]. Kajita et al. considered the ideal biped model consisting of a single rigid body with massless legs and solved the motion of the COG of the biped robot body to find the reference trajectory, which is described as the potential energy conserving orbit [26], [27].

4.1.3 Measured Human Walking Data Based Gait Trajectory

Motion capture is a way used to generate the reference trajectory to the biped control system. A common way to capture the human locomotion is to attach a series of markers to the limbs and joints of the human subject and then record the motion of the markers by video cameras and/or sensory devices. In Hemami’s work, all reference angles are

measured with the help of a television camera/computer system and this television recording of angles and angle rates of all five segments of a human in normal walk is used as reference gait trajectory to the planar five link biped system [64].

Dasgupta et al. adapted Human Motion Capture Data (HMCD) to the biped system in order to achieve a human-like locomotion [108]. The HMCD is the human locomotion joint angle data recorded from a human subject, to whom the markers are attached at the limbs and joints. The HMCD was not used directly to control the robot because of kinematic and dynamic inconsistencies between the human whose motion is recorded and the biped robot locomotion, which is due to the presence of underactuation in biped robots compared to the human. The kinematic inconsistencies are handled by kinematic corrections to the data and the dynamic inconsistencies are solved by setting the desired Zero Moment Point (ZMP) trajectory (from the stability point of view) based on the foot motion data in the HMCD and taking into accout the ground reaction force; and then using the periodic joint motion corrections at selected joints to approximately match the desired ZMP trajectory. The method is simulated numerically by using a 40 DOF biped model.

4.1.4 Stability Based Gait Trajectory

Since the stability is an important criteria in biped locomotion and biped tends to tip over easily, it is very useful to take into account the stability when deciding a reference gait trajectory. Zheng et al. studied a method to generate trajectory of the center of mass using stability margin criteria that satisfies the static stability for an 8 DOF biped, named SD-2 [22], [21].

It is very common to use the ZMP concept from the stability aspect in designing the reference gait trajectoy for biped robot. If the ZMP is within the convex hull of all contact points between the feet and the ground, then the system is in dynamic equilibrium [72]. There are several ways to design the reference gait trajectory by using ZMP concept. One of them is first designing the desired ZMP trajectory and then calculating the hip motion ensuring the desired ZMP trajectory. Hirai et al. produced the reference ZMP trajectory and used it as an input to the complex control of the Honda humanoid robot for ground level walking, up and down stair walking, etc [109]. Shih used the ZMP method to generate the reference gait trajectory for a 7 link, 12 DOF biped robot in the single-support phase [110]. The trajectory of the ZMP on the ground is designed to be in stable region of

the supporting sole. The reference gait trajectory is specified by eight pattern parameters and derived through the inverse kinematics. ZMP trajectories for different walking patterns and the influence of the pattern parameters on the ZMP trajectories are also investigated. Zhou synthesized the biped walking motion by solving an optimization problem in which the desired ZMP trajectory is forced to be followed. The proposed gait synthesizer is trained by reinforcement learning that uses a multi-valued scalar signal to evaluate the degrees of failure or success for the biped locomotion by means of the ZMP [111], [112], [113].

Kun and Miller developed a multi-stage reference trajectory generation for variable-speed gait biped [114]. The posture generation is realized based on ensuring the stability by using a simplified model of the biped.

4.1.5 Optimal Gait Trajectory

The optimal trajectory generation aims to find reference gait paths that satisfies some definite gait parameter constraints (walking speed, step length, maximum/minimum hip height, maximum height of the tip of the swing leg, the angular range giving the limits of the knee angle, etc.) when minimizing input energy or any other performance measure. In optimal trajectory generation, the minimization function is generally chosen to be the summation of square of the control torques aiming to minimize the energy. The optimal trajectories are generally found numerically.

Chevallereau studied impulsive torque at the beginning and end of the ballistic motion between these two instants that gives energetically optimal motion for a pendulum by assuming that a motion defined by ballistic motion and impulsive control at double support instant will lead to an energetically economical trajectory which can be followed with finite torques [115]. Chevallereau et al. generated optimal reference trajectories for the walking of a planar biped robot without an actuated ankle joint and four actuators [116]. The evolution of four joint variables is assumed to be polynomial functions of the fourth order. The coefficients of the polynomial functions are chosen to optimize the criteria and insure cyclic motion of the biped. The criteria chosen are maximal motion velocity, minimal torque, and minimal energy.

Chevallereau and Aoustin [117] and Channon et al. [118] produced the Cartesian coordinates of the hip, the swing leg tip point and the trunk angle as a time polynomial function and realized the optimization on coefficients of the polynomial that minimizes the energy. Then, the joint angle trajectories are obtained from this polynomial function. Chevallereau and Aoustin obtained optimal cyclic gaits for a biped robot without actuated ankles [117]. During each phase the evolution of joints variables is assumed to be polynomial functions, where the coefficients of the polynomial functions are chosen to optimize the criterion (maximal advance velocity, minimal torque and minimal energy) and to ensure cyclic motion of the biped.

Channon developed energy optimal walking motions for a planar 7 link bipedal walking robot with feet. Motions of the hip and feet during a regular step are modelled by 3rd order polynomials, the coefficients of which are obtained by numerically minimising an energy cost function for the specific cases of motion over level ground, motion up and down of an incline, and varying payload [118]. Channon et al. presented a method for optimizing the walking motions of a planar five-link biped [119]. The technique starts with non-linear kinematic and dynamic models for both the single-support and impact stages of motion. A variational technique is then used to derive joint trajectories that minimize a simple cost function. The resulting two-point boundary value problem is solved using a finite difference technique, with trajectories obtained from a simple linearized model as initial conditions. Families of optimal trajectories for different step periods and step lengths are presented.

Nagurka and Yen [120], and Cabodevila and Abba [121] solved an algebraic nonlinear problem by approximating each generalized coordinate as a Fourier series expansion. Roussel et al. developed energy optimal reference trajectories by optimization from the unconstrained piecewise constant input trajectories [122], [123]. Anderson et al. examined the feasibility of using massively-parallel and vector-processing supercomputers to solve large-scale optimization problems for the biped modeled as a 14 DOF linkage actuated by 46 musculotendinous units [124]. Wu and Chan generated the joint reference trajectory using five constraint functions for a 5-link biped robot walking on a horizontal surface. These constraint functions are designed to constrain the walking speed, support knee bias angle, coordination of the motion of the legs, upright posture of the upper body and energy conservation of the biped robot [125].

Silva presented the energy analysis of a bipedal walking system in order to understand the movement strategies in walking and to search for the optimal locomotion variables that minimise a cost function related to energy. Based on a set of locomotion variables (step length, hip height, hip ripple, hip offset, foot clearance and link lengths) and their influence on the energy flow, the performance measures are discussed and the results compared with those observed in nature [126].

Shih designed the reference trajectory by first developing the COG reference trajectory and then computing the joint angle trajectories from inverse kinematics [127]. It is assumed that the body maintains a constant upright posture during motion, and both feet stay parallel to the walking plane. Shih et al. treated the optimization of the 13 link biped walking trajectory so that it can be used as a reference trajectory for control [128]. The inverse kinematics of the biped is derived for the specified positions of the body and feet. The objective is stated as the optimization of the location of the ZMP. Shih generated an inverted pendulum like reference trajectory for a 5 link planar biped on an even floor with consideration of various objectives such as satisfying a frictional constraint, balancing itself, reducing the impact effect and consuming less energy [129]. The trajectory is designed with five basic quantities: step length, locomotion cycle, height of COG, maximum clearance of the swing leg and inverted pendulum factor.

Cheng and Lin designed the biped reference trajectory by formulating as a parameter search problem, and a genetic algorithm is applied to help to obtain the optimal design [130]. Capi et al. proposed a prismatic joint biped robot trajectory generation method with minimum consumed energy used as a criterion by using a real number genetic algorithm as an optimization tool [131]. Rostami and Bessonnet proposed a reference gait generation method by minimizing the energy consumption [132].

Ono and Liu described an optimal trajectory planning of walking locomotion for a planar biped mechanism which has thighs, shanks and small feet [133]. The one step walking locomotion is divided into two phases. The motion of the swing and stance legs in the first phase is solved by the optimal trajectory planning based on the function approximation method that minimizes the square integral of input torque. Lee et al. formulated the trajectory generation problem of biped as a multi-objective optimal problem to keep walking stably [134], [135]. The walking trajectories resulted in best performance of the

biped robot is generated by using multi-objective evolutionary algorithm, although only mechanical information for a biped robot is known.

Chemori and Loria dealt with the generation of optimal reference trajectories for a planar under-actuated biped robot [136]. The basic feature of the proposed strategy is to generate, for the actuated joints, on-line optimal reference trajectories with respect to the zero dynamics. Djoud et al. obtained optimal cyclic gaits for a biped without actuated ankle [137]. During each phase the evolution of the joint variables is assumed to be polynomial functions of a scalar path parameter. The coefficients of the polynomial functions are chosen to optimize a torque criterion and to ensure a cyclic motion for the biped.

Yoon et al. proposed the adaptation of the genetic algorithm for minimizing energy consumption by using the Real Coded Genetic Algorithms (RCGA) to generate locomotion trajectory for biped [138]. The trajectory is represented by 4th order polynomials whose coefficients are chromosomes. The repeatability condition for stable walking is used with inequality conditions to describe kinematics constraints for swing motion and ZMP. Hase and Huang proposed an energy optimal trajectory planning method based on a function approximation method for a 2D biped walking model [139].

4.1.6 Computational Intelligence Based Gait Trajectory

In the recent years, use of the artificial intelligence techniques in biped trajectory generation apparently becomes very common. Zheng designed a gait reference trajectory generator in the form of a central pattern generator that creates reference motion patterns of voluntary and involuntary motions [140]. If the motion is voluntary, the generated pattern goes directly to the biped. Otherwise, the pattern goes to an adaptive network that modifies the reflexive motion patterns in accordance with terrain conditions.

Arakawa and Fukuda researched natural motion of the biped robot to walk like a human in various environments [141]. The genetic algorithm is applied to the reference trajectory generation through energy optimization. Cheng and Lin formulated the reference trajectory generation as a parameter search problem and applied the genetic algorithm to assist the optimal design in order to achieve walking on an inclined surface, walking at a high speed, or walking with a specified step size [130].

4.2 Walking Pattern Classification

The main objective of this chapter is to develop a systematical method for reference gait trajectory generation of a 5-link 7 DOF biped robot during walking on even surface, stepping over obstacles, stepping up and stepping down motions which results in a natural human-like walking.

Based on the assumption that the environment that robot interacts is formed of even surfaces, obstacles that the robot can step over directly or by stepping, and up/down stairs, the walking of robot is classified into 9 patterns. Each walking pattern class corresponds to one step motion of the biped. The aim is to classify the walking steps of the biped so that by realizing the consequence of these classified patterns in a predefined order extracted from the desired path information, robot can achieve any given path in such an environment.

The pattern classes are extracted as per the biped's current and next steps' floor conditions in sagittal plane. In other words, the patterns are designed depending on the stance foot's current floor position and swing foot's transitioning floor conditions. The pattern classification is done in 9 classes as below and depicted by means of Figure 4.1 to Figure 4.10 in detail:

- Pattern 1: Walking on even floor
- Pattern 2: Stair up – first step
- Pattern 3: Stair up – second step
- Pattern 4: Stair up – second periodic step
- Pattern 5: Stair down – first step
- Pattern 6: Stair down – second step
- Pattern 7: Stair down – second periodic step
- Pattern 8: Stepping on up
- Pattern 9: Stepping on down

Note that stepping over an obstacle directly corresponds to Pattern 1 with proper step height as shown in Figure 4.11.

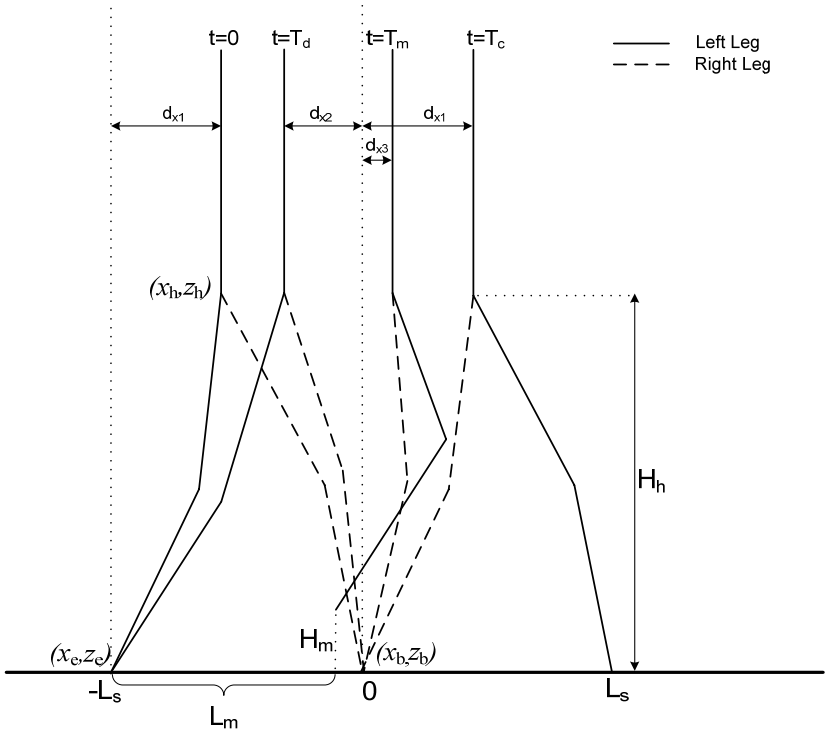

Figure 4.2 Pattern 1: Walking on Even Floor

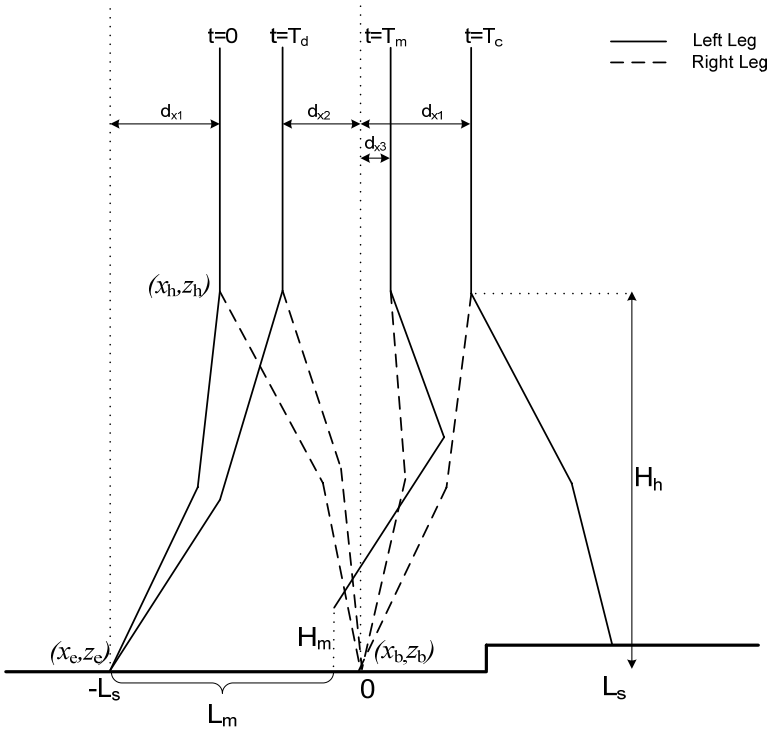

Figure 4.3 Pattern 2: Stair Up – First Step

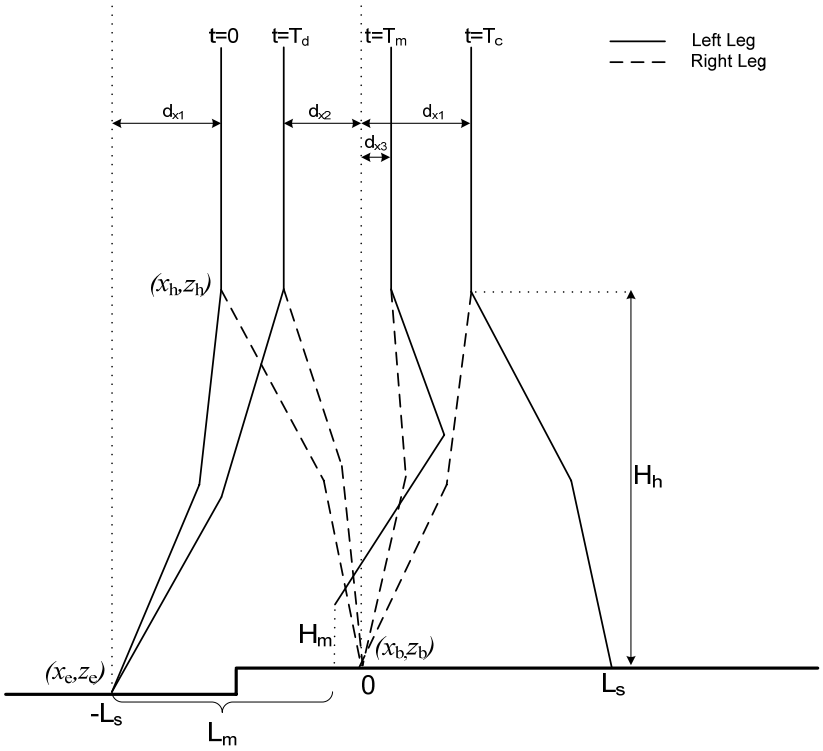

Figure 4.4 Pattern 3: Stair Up – Second Step

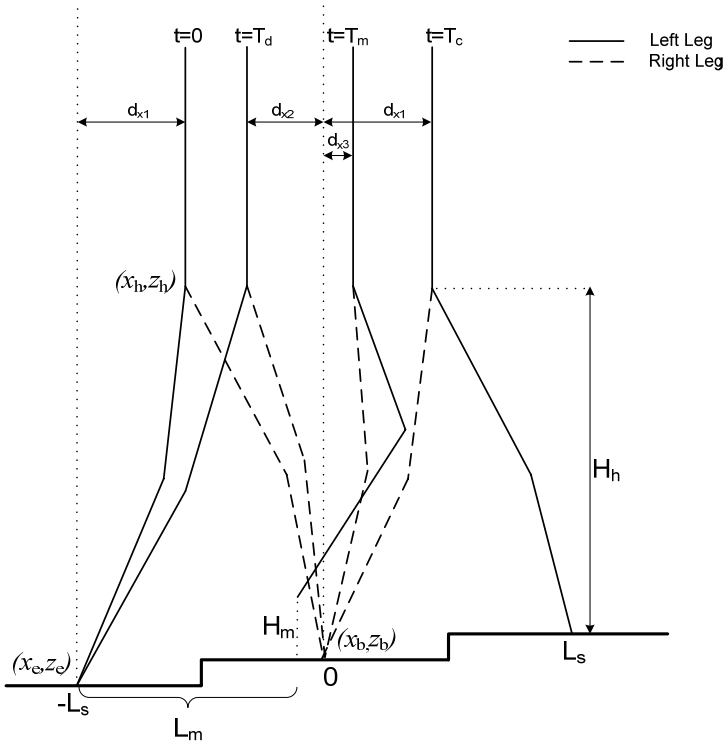

Figure 4.5 Pattern 4: Stair Up – Second Periodic Step

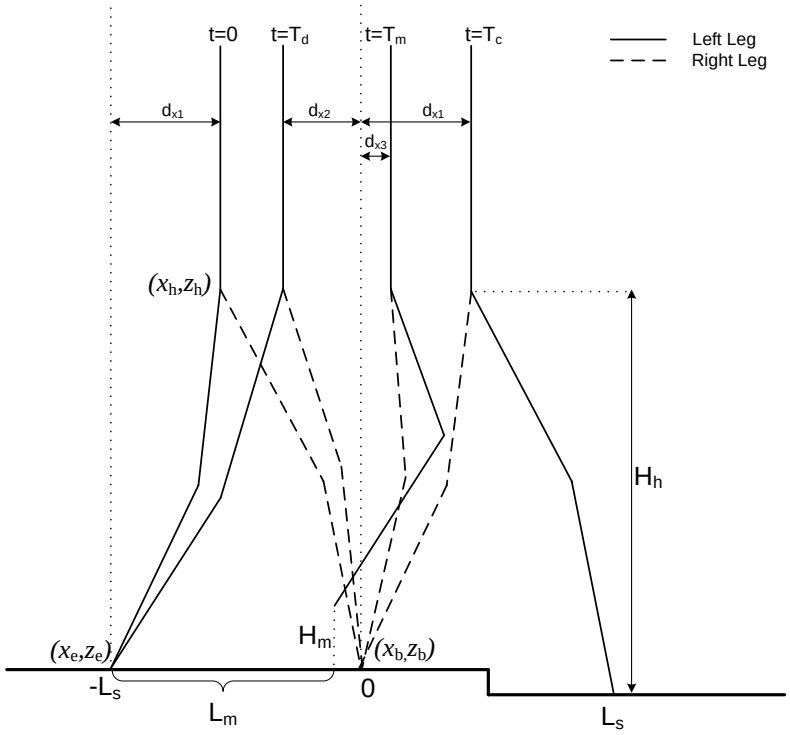

Figure 4.6 Pattern 5: Stair Down – First Step

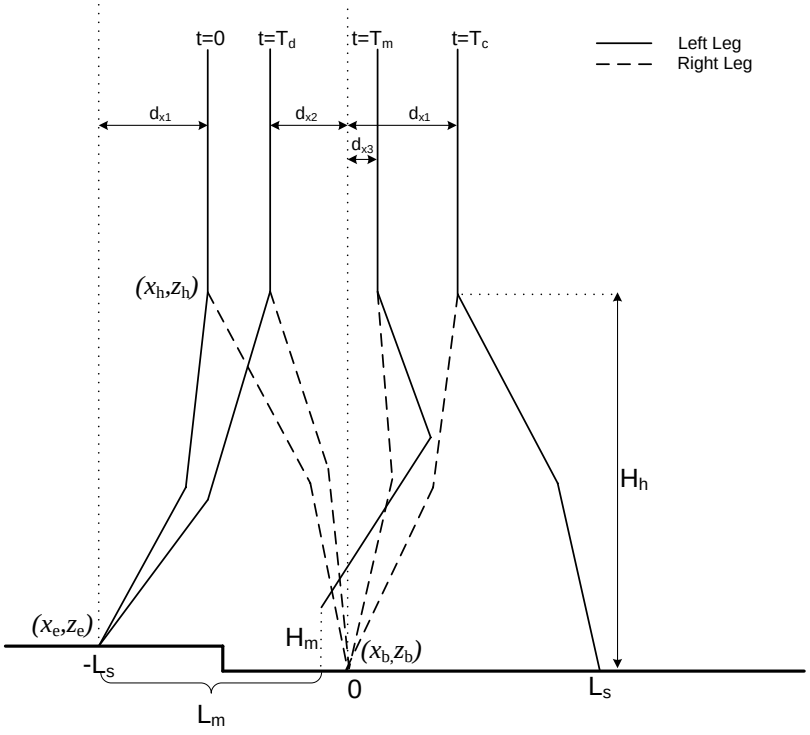

Figure 4.7 Pattern 6: Stair Down – Second Step

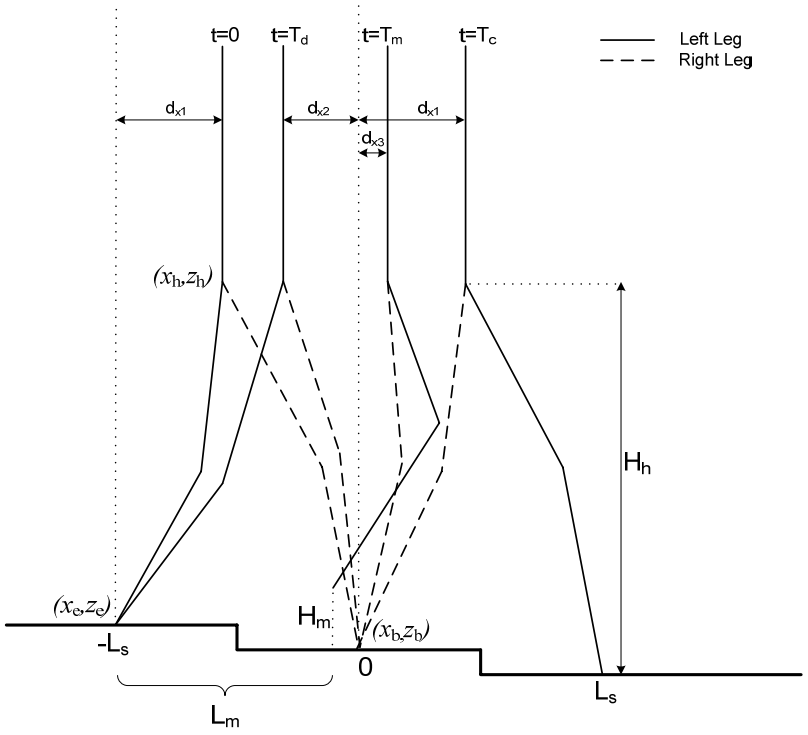

Figure 4.8 Pattern 7: Stair Down – Second Periodic Step

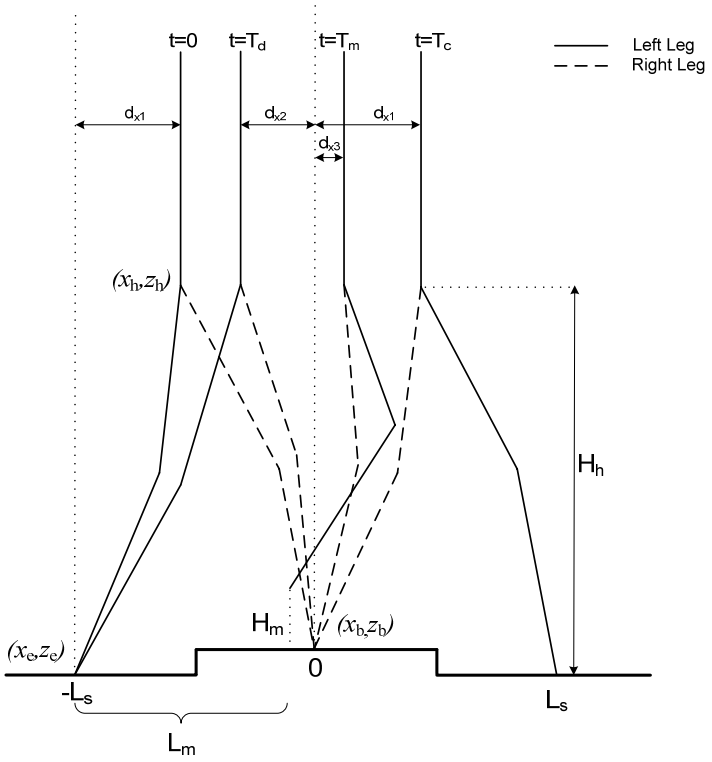

Figure 4.9 Pattern 8: Stepping on Up

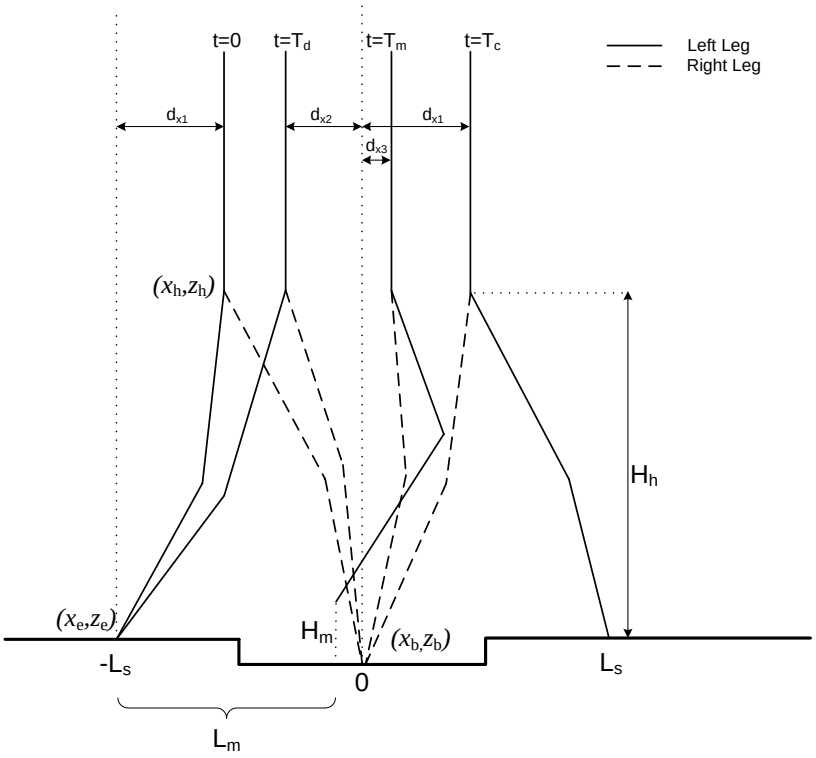

Figure 4.10 Pattern 9: Sepping on Down

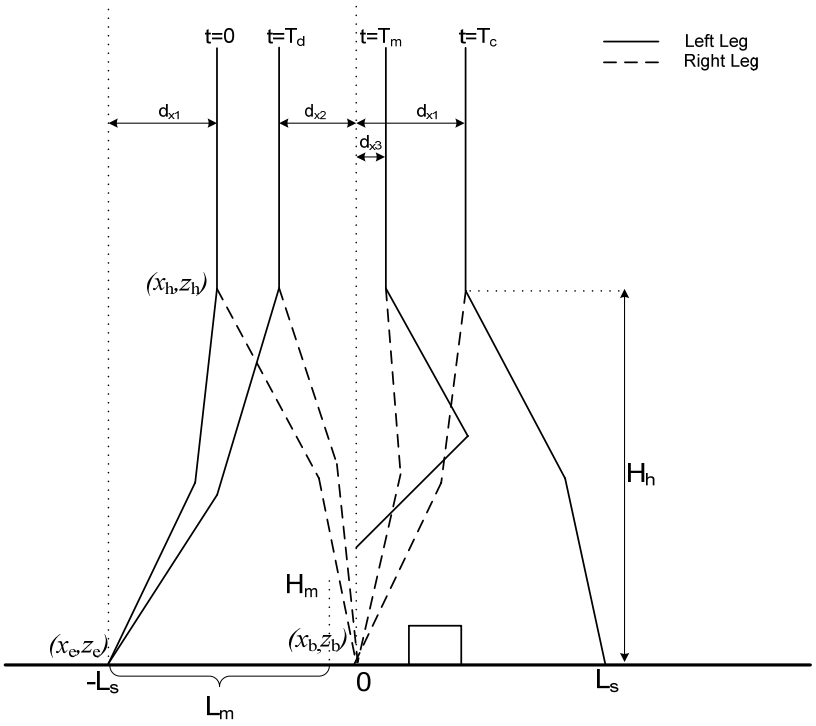

Figure 4.11 Pattern 1: Stepping over an Obstacle

4.3 Trajectory Generation by Spline Interpolation

The reference trajectory in sagittal (Figure 4.12) and frontal (Figure 4.13) planes of biped robot for all pattern classes is obtained by using 3rd Order (Cubic) Spline Interpolation. In the context of reference trajectory generation, determination of the whole trajectory for all t as shown in Figure 4.14 is realized by obtaining the spline function for one step time, T_c both in sagittal and frontal planes for each pattern of the given path with predefined initial and final conditions so that the right and left leg trajectories can be obtained from one to other by simple transition as explained in Chapter 2.

Consequently, the development of the reference walking trajectory for each pattern, as Pattern 1 shown in Figure 4.12 and Figure 4.13 for illustration purposes, by using the theory of 3rd order spline interpolation, where the details of the theory are explained in Appendix A, is realized for the hip and ankle points.

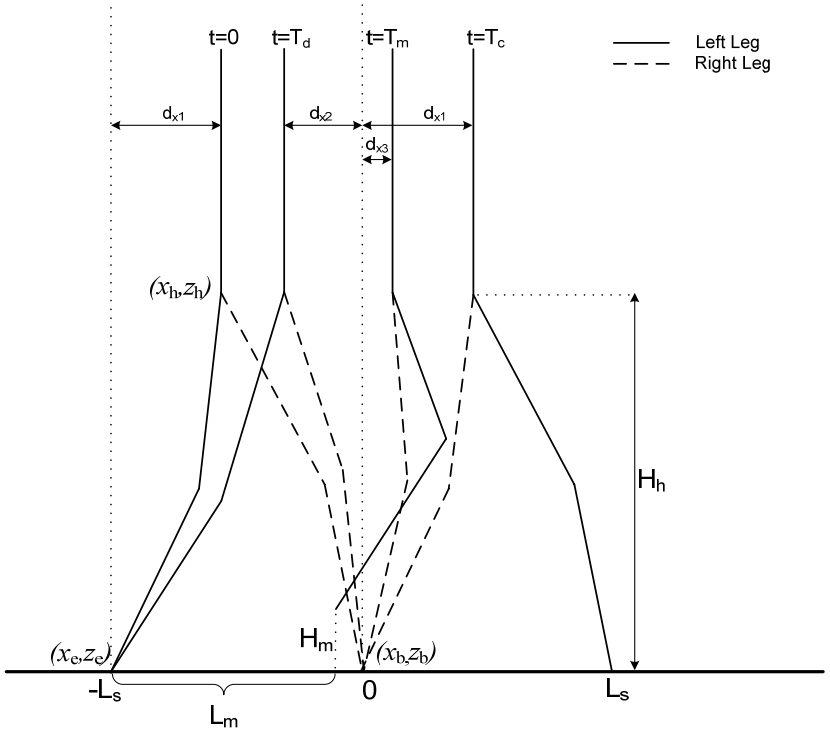

Figure 4.12 Sagittal Plane Walking Cycle for Pattern Class 1

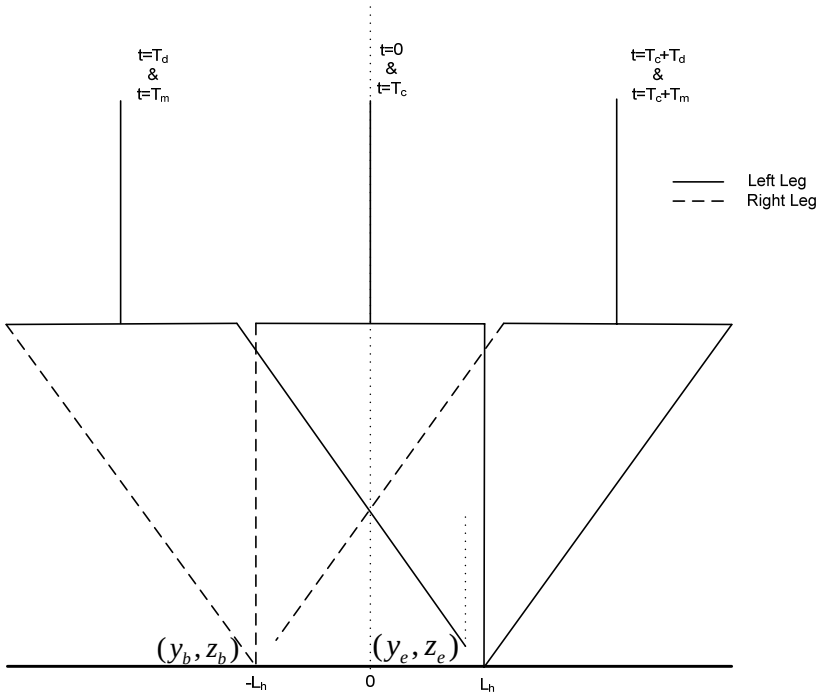

Figure 4.13 Frontal PlaneWalking Cycle for Pattern Class 1

As discussed before, the complete gait cycle of the biped consists two phases, namely, single support phase and double support phase. The generation of the reference trajectory is realized based on the assumption that each step starts after the impact that occurs with the ground, and right after the impact, the double support phase starts with both feet on the ground. In this phase, the hip trajectory proceeds in the direction of motion, whereas both ankle point trajectories are fixed on the ground and so do not change. After this phase, the single support phase starts. In this phase, one leg keeps attaching to the ground (stance leg) and other leg starts to move forward over ground (swing leg). The hip and swing leg ankle point trajectories will change whereas the stance leg ankle point trajectory stays constant during the single support phase. Without loss of generality, the one step reference trajectory generation is realized for the hip point $(x_{\mathrm{h}}, y_{\mathrm{h}}, z_{\mathrm{h}})$ and left leg ankle point $(x_{\mathrm{e}}, y_{\mathrm{e}}, z_{\mathrm{e}})$ assuming that the stance leg is the right one and the swing leg is the left one in single support phase of the walking step and similarly, the trajectory generation is explained for Pattern 1, where it can be easily calculated in a very similar way for the other pattern classes.

In the Figure 4.14 above, the parameters are:

n is the number of steps,

T_c is the time duration for one step,

T_d is the elapsed time in double support phase,

T_m is the time when the swinging foot reaches the maximum height.

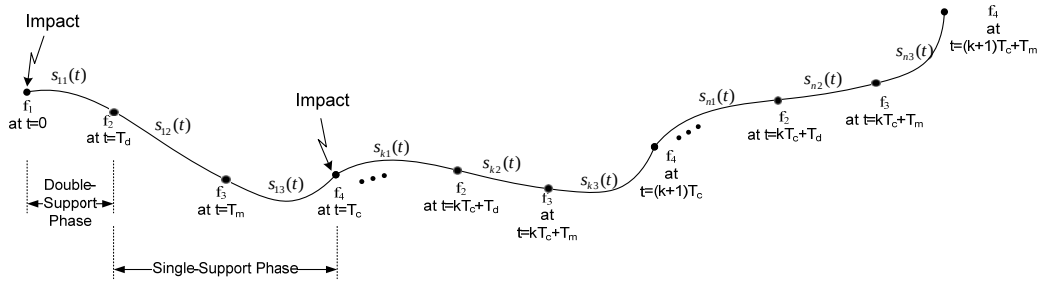

Figure 4.14 The schematic diagram for t dependent periodic cubic spline generation

For each spline generation case, there are 4 breakpoints for each step:

For hip point;

$$f_1\left(\begin{bmatrix} x_h \\ y_h \\ z_h \end{bmatrix}\right) = \begin{bmatrix} -L_s + d_{x1} \\ 0 \\ H_h \end{bmatrix} \tag{4.1}$$

$$f_2\left(\begin{bmatrix} x_h \\ y_h \\ z_h \end{bmatrix}\right) = \begin{bmatrix} -d_{x2} \\ -L_h / 4 \\ H_h \end{bmatrix} \tag{4.2}$$

$$f_3\left(\begin{bmatrix} x_h \\ y_h \\ z_h \end{bmatrix}\right) = \begin{bmatrix} d_{x3} \\ -L_h / 4 \\ H_h \end{bmatrix} \tag{4.3}$$

$$f_4\left(\begin{bmatrix} x_h \\ y_h \\ z_h \end{bmatrix}\right) = \begin{bmatrix} d_{x1} \\ 0 \\ H_h \end{bmatrix} \tag{4.4}$$

For left leg ankle point;

$$f_1\left(\begin{bmatrix} x_e \\ y_e \\ z_e \end{bmatrix}\right) = \begin{bmatrix} -L_s \\ L_h \\ 0 \end{bmatrix} \tag{4.5}$$

$$f_2\left(\begin{bmatrix} x_e \\ y_e \\ z_e \end{bmatrix}\right) = \begin{bmatrix} -L_s \\ L_h \\ 0 \end{bmatrix} \tag{4.6}$$

$$f_3\left(\begin{bmatrix} x_e \\ y_e \\ z_e \end{bmatrix}\right) = \begin{bmatrix} -L_s + L_m \\ L_h \\ H_m \end{bmatrix} \tag{4.7}$$

$$f_4\left(\begin{bmatrix} x_e \\ y_e \\ z_e \end{bmatrix}\right) = \begin{bmatrix} L_s \\ L_h \\ 0 \end{bmatrix} \tag{4.8}$$

From these 4 breakpoints data (time and function values), we can obtain the spline path for each period as below:

$$s_k(t) = \left\{\begin{matrix} s_{k1} & if\ (k-1)T_c \le t \le (k-1)T_c + T_d \\ s_{k2} & if\ (k-1)T_c + T_d \le t \le (k-1)T_c + T_m \\ s_{k3} & if\ (k-1)T_c + T_m \le t \le kT_c \end{matrix}\right\} \quad for\ k = 1,...,3 \tag{4.9}$$

where

$$s_{k1}(t) = a_1(t-(k-1)T_c)^3 + b_1(t-(k-1)T_c)^2 + c_1(t-(k-1)T_c) + d_1 \tag{4.10}$$

$$s_{k2}(t) = a_2(t-(k-1)T_c)^3 + b_2(t-(k-1)T_c)^2 + c_2(t-(k-1)T_c) + d_2 \tag{4.11}$$

$$s_{k3}(t) = a_3(t-(k-1)T_c)^3 + b_3(t-(k-1)T_c)^2 + c_3(t-(k-1)T_c) + d_3 \tag{4.12}$$

and a_1, b_1, c_1 and d_1 in these equations are calculated using the formulation derived in Appendix A.

4.4 Joint Angle Profile Generation by Inverse Kinematics

The reference trajectories corresponding to each pattern class in sagittal (Figure 4.12) and frontal (Figure 4.13) planes are calculated in terms of the hip and swing leg ankle point cubic spline functions of time in Cartesian coordinates in the previous section. In fact, the purpose of the reference trajectory generation is to find the joint angle trajectories as a function of time corresponding to the biped model's joint angles at the hip and ankle joints as defined in Chapter 2. Knowing the hip point and swing leg ankle point trajectories, the inverse kinematics is used to calculate the reference joint angle trajectories for each pattern class. The detailed inverse kinematics calculation in frontal and sagittal planes is given in Appendix B.

CHAPTER 5

CONTROLLER DESIGN

5.1 Overview

Why a biped is able to walk or fail to walk continuously is a challenging control task to be explained despite the highly nonlinear, naturally unstable, multi input, multi output and both continuous and discrete characteristics of the biped system.

To achieve biped robot locomotion without control does not result in a good solution so, the need for control turned into a fact in the biped history by the early 1970s. By the development of high speed computers, the control of the biped robot became broad. A wide variety of approaches has been developed and so the biped locomotion has been improved.

The aim in control, in the context of this thesis, is to sustain the response of the system in accordance with the reference walking trajectory of the biped robot by ensuring the stability. The reference trajectory is chosen as a human like motion. Generally, the reference and real trajectories differ due to the dynamic model inaccuracies and walking surface conditions.

The control of biped robot is a challenge since the biped system is complex and preserving balance is difficult. The biped mechanism is composed of distributed masses. Even the simplified physical model of the biped is used, the biped includes several coupled masses or links. In order to achieve high speed locomotion, more complex multi-body or multi-link rigid body models are needed to be developed. Also the leg inertia has an effect on the dynamics of the system. In order to overcome these coupled dynamics, complex control algorithms are needed to obtain more accurate results and good performance. In general, distinctive control methods solve different problems and these methods are also weighted with the complexity of model of the system under control. As a result, the structure of the controllers varies in specific or general sense with the structure describing the operations to be executed in creating the desired control.

In controlling the biped, first, the reference trajectory of joint angles is provided with local angle feedback to the control system and then, the controller provides the corresponding joint torques to the system as shown in Figure 5.1.

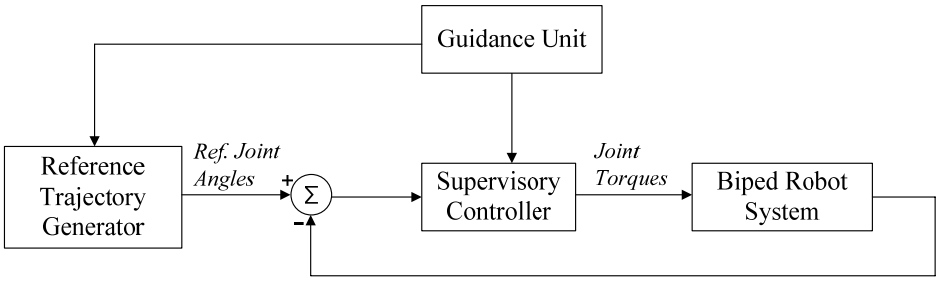

Figure 5.1 A representative block diagram of biped locomotion control

The control of locomotion in bipeds necessitates accurate positioning and timing to achieve the commanded locomotion. The first task in control is to achieve walking without turning over and also imitating human like motion. In addition to these tasks, it is also important to remain upright and possess several other desirable attributes. Control also used to impose gaits that guaratee the stability under some assumptions. In order to provide a stable biped body platform, the body's height and orientation should be controlled.

In summary, the controller for biped locomotion purposes is designed to satisfy one or more criteria given below [142]:

- reference trajectory tracking
- conserving dynamic stability
- maintaining the upright posture
- being robust to small perturbations
- using minimum energy

Many solution techniques to the biped locomotion control problem have been developed in the past. These methods mostly depend on the models used for the dynamics of the biped and it ranges if the model describing the complete dynamics is used or a simplified version of the model is used. One of the methods used is the implementation of the linear control

to biped locomotion by linearizing the system. In the literature, many well known control methods are developed for the linear systems. So when the linearized biped model is used, these techniques can be applied easily to the biped. Since the actual system is highly nonlinear, the biped locomotion can only be treated linear in a predefined range of operation. Unfortunately, linearization approximation does not usually result in a stable and firm walking. Another class of controllers used in biped locomotion control is a state feedback controller. The state of the biped is the variables specifying the position and velocity of every point of trajectory at any time instant of operation. The state feedback provides the position and velocity information of the biped to the controller. Instead of state feedback, a sensory feedback can also be used. But the entire state of the system is not guaranteed by the sensor-based feedback. The controller can also be classified in accordance with its optimality that ensures a motion performing a desired evaluation metric for natural, stable looking motions. Generally, achieving a globally optimal solution is difficult and calculating the solution is expensive, especially as the system to be controlled becomes more complex. In controlling biped, integrating different control methods are also useful. For this reason, hierarchical and hybrid methods are also developed in the history. As a result, two main approaches are developed in the history to solve the biped locomotion control problem. First one is the conventional way that uses control theory techniques by providing the system input to run the system in the required/wanted behavior. The disadvantage of this method is difficulty to adapt to the changing conditions. The other approach is the intelligent control method that generally does not require the equations of the system and instead, a learning algorithm that enables robot to learn from experience is developed. Intelligent control methods provide flexibility in the sense that the robot can adapt to changing conditions resulting in a high range of operability. The pros and cons of these two methods directed the researches to combine both methods and generate “hybrid” control techniques.

5.1.1 Conventional Control

Vukobratovic et al. used a trajectory control algorithm based on one fixed program of kinematic-dynamic character [47]. The simplified mathematical model is formed by using the kinematic connection between the levers of the locomotion system. Then the control problem is formalized as a repetition of the motion cycle on the basis of satisfying the initial and end conditions. The feedback is introduced at the level of maintaining the achieved mathematical gait. Sano and Furusho adapted a control method which divides the

walking into motions in the sagittal and frontal planes seperately [143]. The control problem in sagittal plane is designed to keep the angular momentum close to a smooth reference function given in advance by controlling the ankle torque of the supporting leg. On the other hand, the control in the frontal plane is treated as a regulator problem with two equilibrium states.

Golliday and Hemami developed a multivariable feedback to design locomotion controls by using a robot model, which has no knee joints or feet in sagital plane [55]. The actuator torque waveforms required to produce the desired state space joint angle trajectories is computed in a complete state feedback control form that is designed to decouple the general dynamics into several independent subsystems each having three independent second-order systems. Lee et al. used the model following and Variable Structure Systems techniques in the sagittal plane, and nonlinear feedback and modified α-comuted torque techniques in the frontal plane in order to implement a robust trajectory tracking control that achieves biped robot steady walking even in the presence of system modeling errors [103]. Takanishi and Takeya introduced a control method for dynamic biped walking under unknown external forces and moments [144]. The control method for compensating the external force reacts so that its ZMP follows the reference trajectory by the trunk motion controlled. Shih and Gruver implemented an advanced control system based on feedforward compensation and linear state feedback to track reference joint trajectories for a 7 link 12 DOF biped robot in double support phase [145].

Fujimoto et al. proposed an autonomous walking control algorithm with hierarchical structure in which 3D inverted pendulum model that is considered as the motion of COG, and the tip position of swing leg are controlled autonomously [146]. Fujimoto et al. designed a walking control algorithm based on force control for 19 axes biped robot [147]. A hierarchical control system that can stabilize the contact force between the foot and the ground under some restrictions is proposed. Fujimoto et al. described a biped walking control system based on the reactive force interaction control on foothold for a 14-axis biped robot [148]. The control system is composed of a reactive force/torque controller and a posture controller. Ono et al. contolled the biped walking of a planar 4 link robot with knees locked with a single actuator located on the hip [149]. Chemori and Loria dealt with a control approach for a planar under-actuated biped robot based on partial feedback linearization [136]. The partial feedback linearizing control enables the tracking of these trajectories, which results in the convergence of the zero dynamics to a stable limit cycle.

5.1.1.1 Linear Feedback Control

Linear feedback control is applied to a biped system that is linearized. Given the reference gait trajectory of the biped locomotion, the nonlinear system is linearized about a selected point on the trajectory and then a feedback control law is designed for the linearized system. The linearization is only valid in a vicinity of the operating point. Golliday and Hemami generated a multivariable feedback control algorithm for the biped to produce a walking gait having a velocity and stride length similar to those of a human walking gait [55]. The equations of the motion is linearized into a state space representation and pole assignment is used to compute the feedback control gain. Hemami and Wyman considered the general problem of control of state space constrained dynamic systems for a three link biped model [150]. The dynamic system is linearized for an equilibrium point where the constraints are satisfied and the control is applied by using a linear feedback so that the equilibrium point is stable under disturbances in the state that may or may not satisfy the constraints. Zheng developed three different control methods for a 3D 5 link biped robot control problem [151]. The first one is linear feedback control whereas the nonlinear biped system is linearized about zero velocity operating point. The state feebdback matrices are calculated to obtain the desired properties of the linearized system. The linear feedback gains that decouples the motion of each link and assigns the system poles are calculated.

5.1.1.2 Feedforward Control

Miura and Shimoyama designed a feedforward controller by approximating the biped robot dynamics as an inverted pendulum in the single support phase. They treated the entire gait cycle as a function and sampled once per step for the controller. They considered the dynamic walk as a series of inverted-pendulum motions with appropriate conditions of connection [17]. Their model used trajectory tracking and resulted in a statically unstable walk but dynamically stable limit cycles with suitable control.

5.1.1.3 PID Control

Furusho and Masubuchi controlled walking by tracking piecewise linear joint reference trajectories using PID control [18]. Kajita et al. formulated the control laws for walk initiation, walk continuation, and walk termination [26], [27]. The walking motion is controlled by support leg exchange and the control is applied to the joint angles by PD controller. In addition, robust realization of the walking control is also considered. Furusho

and Sano controlled 3D biped walking by using decoupled control for the frontal and sagittal planes [19], [143]. PID control is used in frontal plane to stabilize the upright form and joint trajectory tracking was used in sagittal plane to regulate the robot's angular momentum in the form of an inverted pendulum. Raibert et al. provided a comparative study of the effectiveness of three control methods, namely, local decoupled PD control, the computed torque control and the sliding mode robust control in the tracking of piecewise linear joint trajectories for a planar 5 link biped robot [152]. Grishin et al. used PID control to track pre-computed trajectories that were modified online for the walking control of a three-link 3 DOF planar biped robot with telescoping legs [32].

Kajita and Tani proposed direct control of COM for a 6 DOF biped robot modeled as a linear varying length inverted pendulum and walking on rugged terrain [28]. The motion is controlled by a PID controller to move the COM of the biped body, which is modeled as an inverted pendulum, on a constraint straight line and keep its posture vertical. The pendulum's length was varied to maintain the biped's COM at a constant height above the walking surface. Biped is assumed to know the profile of the ground before the motion begins. Local position feedback is applied to the joints of the support leg to follow the reference trajectory.

Pratt and Pratt exploited the natural dynamics of bipedal walking in the control of a 7 link planar biped [153] and 3D biped [154]. The control algorithm using these natural mechanisms requiring very little computation, and the necessary sensing consisting of joint angles, joint velocities and ground reaction forces are described. In the design, the legs act separately, have a simple state machine and are controlled by a PD controller at joints. Pratt and Pratt used a number of intuitive control strategies in order to achieve five objectives for walking related to stability and walking transitions of a 7 link planar biped robot [155]. Yuksel et al. analyzed the ground reaction force in terms of smooth transition and landing impact under the parametric change of frontal gait trajectory that is realized by inverted pendulum model and the parametric change in the proportional gain of PID feedback controller [156].

5.1.1.4 Computed Torque Control

Computed torque control method is a feedback control method for nonlinear systems. Zheng developed three different control methods for a 3D 5 link biped robot [151]. The

second method is computed torque control and the nonlinear model is controlled by a feedback controller, following the computed torque technique. Mitobe et al. used computed torque control technique to regulate the planar 5 DOF biped's COM and swing leg end position [157]. Tzafestas et al. applied the computed torque control method for robust control of a 5 link biped robot [60]. The comparison of this method to PD and sliding mode control methods are also presented. Park and Kim presented the computed torque control method with gravity compensation in order to track the reference joint angle trajectory generated by a length varying inverted pendulum applied on the swing leg of a 3D biped and to stabilize the error dynamics of the base link position of the support leg [158]. Chevallereau et al. used a modified computed torque control for biped robot control [114]. The physical constraints of reaction force that prevent the foot from sliding or taking off is taken into account.

5.1.1.5 Sliding Mode Control

Chang and Hurmuzlu developed a sliding mode control method for a 5 link biped robot [159]. Tzafestas et al. developed a robust sliding mode control method for a 5-link biped robot model and also compared it to pure computed torque control, assuming that the locomotion of the biped is constrained on the sagittal plane [60]. The rotating joints are considered to be friction-free and driven by independent d.c. motors. In his work, the results obtained through the sliding mode control is found superior to those obtained with the computed torque control. This superiority is found to become stronger as the degree of uncertainty and the size of the biped increases. Tzafestas et al. developed a nonlinear robust control approach for the control of 9 link biped, motivated by the fact that the control which has to guarantee the stability of the biped robot must take into account its exact nonlinear dynamics [88]. This method provides a successful way to preserve stability despite the presence of strong modeling imprecision or uncertainties.

5.1.1.6 CPG Based Control

Bay and Hemami designed the Central Pattern Generator (CPG) model including a set of van der Pol oscillators arranged in a network in which each oscillator is coupled to each other oscillator [91]. The CPG model generates the control signals for simulated walking and jumping maneuvers. Katoh and Mori was one of the first to deal with a control method of a dynamic biped locomotion by utilizing a dynamical system having a stable limit cycle [69]. The control method for a planar walking model having four DOF with prismatic legs

separately studied for the double support phase and the single support phase. The control strategy used the bifurcation of a set of coupled van der Pol's equations, which has a stable limit cycle. Using PID control to track reference trajectories generated by a van der Pol's oscillator induced walking in a model of BIPMAN is demonstrated.

5.1.1.7 Adaptive Control

Zheng developed three different control methods for a 3D 5 link biped robot control problem [151]. The third method is a multivariable model-referenced adaptive control method that adjusts the parameters of the controller to account for changes in plant dynamics or disturbances in the environment. As a result, the system is stabilized and behaves like a referenced model. Wang et al. investigated the bipedal walking control by using adaptive control based on neurocomputing [149]. The neuro-controllers are designed as a several hidden layer feedforward neural network and trained by using multi link model deterministic controller as reference. The knowledge to the neuro controller is provided by a deterministic controller or by using a learning algorithm. Kajita and Tani developed a realtime control algorithm for dynamic biped locomotion by PID controller using sensor information and a control architecture based on the Linear Inverted Pendulum Mode [160].

5.1.2 Intelligent Control

The intelligent control methods in biped robot locomotion are developed to imitate the functions of the human locomotion that consist of adaptation, learning and planning under uncertainty. The artificial intelligence based methods, such as, neural networks, genetic algorithm and fuzzy logic are widely used to improve the implementation of automatic control systems.

5.1.2.1 Fuzzy Control

Murakami et al. designed a fuzzy control algorithm to control dynamic biped walking robot and used it to simulate the locomotion of biped without a mathematical model [161]. Shih et al. determined force and position control gains by using fuzzy logic control leading to improved performance of the 12 DOF biped system [162]. Magdalena and Monasterio developed a fuzzy control method based on the hierarchically intelligent control approach with three levels: organization, coordination and execution to perform gait synthesis [163]. The walk coordinator has been designed as a rule based fuzzy logic control system of

prescription and compensation rule levels based on prescribed synergy method, where the initial rules are obtained from biomechanical studies of human walking. Zhou and Jagannathan proposed an Adaptive-Network-Based Fuzzy Inference System (ANFIS) control strategy based on a hierarchy of walking planning level, gait generating level and joint control level, which do not require detailed kinematics or dynamic biped model [164]. The ANFIS controller is verified through a 5 link biped robot simulation.

5.1.2.2 Neural Network Control

Kurematsu et al. suggested a multi-layer neural network control model by using the center of gravity concept on reference trajectory generation [89]. Juang et al. developed a multi-layered feedforward neural network architecture combined with a linearized inverse biped model for the control of a five link biped [90]. Miller applied a Cerebellar Model Arithmetic Computer (CMAC) neural networks to control the biped walking with dynamic balance [30]. The control strategies based on a hierarchy of simple gait oscillators, PID controllers and neural network learning that do not require detailed kinematic or dynamic models are applied. Doerschuk et al. used CMAC neural network to enforce a previously generated gait into a simulated 7 link biped robot [165], [166]. Miller and Kun developed multiple layer CMAC neural networks in order to produce a controller with wider operating range by adapting various walking parameters [30], [80], [167]. Taga proposed a new principle in control of legged locomotion based on the neurophysiological knowledge and a theory of nonlinear dynamics [168]. A global limit cycle is generated by a global entrainment between the rhythmic activities of a nervous system composed of coupled neural oscillators and the rhythmic movements of a musculo-skeletal system including interaction with its environment. The transitions between the gait patterns occurred with hysteresis.

5.1.2.3 Neuro-Fuzzy Control

Juang presented a five link planar biped locomotion scheme using a multi-layered fuzzy modeling neural network with back-propagation through time in order to control the biped by defining the desired step width, height and period in several stages [169]. Juang generated a bipedal control technique based on a neurofuzzy controller, which is a five-layered neurofuzzy network providing the control signals in each stage of a walking gait, and a neural network emulator, which is a conventional three-layered feedforward neural network emulating the robot dynamics and providing the error signals for back

propogation through controller in each stage [170]. This technique is stated to be able to generate dynamic walking on inclined surface. Zhou designed a reinforcement learning-based neuro-fuzzy gait synthesizer based on the Generalized Approximate Reasoning for Intelligent Control (GARIC) architecture aiming to ensure the dynamic balance of a 5 link biped robot [111]. The proposed controller is trained by reinforcement learning by taking the ZMP criteria as a measure of success and failure.

5.1.3 Hierarchical Control

Wagner et al. proposed a knowledge based multi layer control strategy that supports dynamic stability of biped locomotion [171]. A generalized set of solutions are optimized via simulation. One of the common methods used in trajectory tracking controllers or to analyze the stability is the ZMP criteria. The ZMP based control is a method used in biped locomotion for stability control, which is based on the D'Alembert Principle stating that in order to ensure the stability, the total forces and moments acting on the robot must be zero. When the ZMP trajectory is designed so that the D'Alembert Principle applies, the robot will walk firmly. Vukobratovic et al. considered the control of biped as a two stage problem [64]. At the first stage, the control is applied to ensure the system's motion in the absence of any disturbance along the reference trajectories calculated in advance in order to satisfy the conditions of both the desired gait and overall system stability. At the second stage, only the deviation of the actual state vector from its nominal value is considered and the additional control is applied to force the system state to its nominal. Deviation of the ZMP point from its nominal position is adopted as a measure of the system's overall deviation from nominal trajectories. Yamaguchi et al. proposed a model based walking control (ZMP and yaw axis moment control) for dynamic biped walking aiming to obtain high stability [172], [173], [174]. Li et al. proposed a learning control algorithm for the compensative trunk motion of a biped walking robot based on the ZMP stability criterion [175], [176].

5.1.4 Virtual Model Control

Virtual Model Control (VMC) is a language to depict the interactive force conduction and it uses simulations of mechanical components which are virtual to produce real actuator torques/forces. Pratt and Pratt described a control scheme, called VMC that address the transformation from high level task specification to low level motion control [177]. The VMC motion control language uses the simulations of imagined mechanical components to

create forces, which are applied through real joint torques. Pratt et al. controlled the dynamic walking of Spring Flamingo via VMC method by using ad hoc designed intuitive constraints that are switched based on the robot's state machine [178].

5.1.5 Optimal Control

The optimal control is used for the calculation of walking control generated on the basis of its optimality. Cheng and Lin obtained the optimal or near optimal biped controller through parameter search. Genetic algorithm is applied to determine the optimal solution [130]. Saidouni generated optimal gait cycles in the sagittal plane of a biped [179]. Both single and double support phases are globally optimized, considering incompletely specified transition postural configurations from one phase to the other. A parametric optimisation method is implemented. The biped joint coordinates are approximated by cubic spline functions connected at uniformly distributed knots along the motion time. The finite set of unknowns consists of the joint coordinate values at knots, some gait pattern parameters at phase transitions and the motion time of each phase. The step length is adjusted to the prescribed gait speed by the optimization process.

Rostami and Bessonnet generated optimal swing motions during the single-support phase of sagittal gait for a 7 link planar biped with active joints [180]. The optimization problem is solved by using Pontryagin's Maximum Principle by implementing a shooting method. Roussel et al. addressed the problem of energy-optimal control input generation for biped robot locomotion by minimizing the energy robot uses during walking [123]. Schiehlen investigated the limit cycle of passive motions as well as the related stability using shooting approaches with optimization techniques [181]. The active machines proposed are controlled using the principles of inverse dynamics and advanced linear control strategies. In particular, the energy consumption between passive and active walking machines is compared by a coefficient of efficiency.

Capi et al. solved the problem of humanoid robot gait generation by using neural networks modules in unknown environments by creating an autonomous humanoid robot, able to take decisions and generate the appropriate optimal gait based on the information received by the eye system [182]. Cheng and Lin designed the biped controller by formulating the problem as a parameter search problem, and a genetic algorithm is applied to help to obtain the optimal design [130]. Hardt et al. investigated the problem of constructing a nonlinear

controller for a 5 link biped robot optimal with respect to a minimal energy performance criteria [183]. Westervelt and Grizzle designed a controller for a closed-loop, asymptotically stable walking motions of a 5 link, planar biped robot [184]. Parameter optimization is applied to the hybrid zero dynamics in order to create asymptotically stable orbits. The optimization process uses a Sequential Quadratic Programming (SQP) algorithm and is able to satisfy kinematic and dynamic constraints while approximately minimizing energy consumption and ensuring stability.

5.1.6 Hybrid Control

Zheng developed motion control mechanism that is centered on a neural gait synthesizer consisting of a number of functional unit including a CPG, an adaptive neural network, a knowledge base, a learning unit and a switch mechanism for biped robot [140]. Vukobratovic and Timcenko proposed a control method for biped robot that combines the model-based and fuzzy logic control techniques [185]. The model-based decentralized control algorithm is extended by fuzzy logic in order to modify the parameters of joint servo controllers. Park and Chung proposed a hybrid control method of the combination of impedance and computed torque control for biped locomotion control [186]. The impedance control is used for the control of the swing leg and the computed torque control is applied to the support leg. Yuksel et al. designed a fuzzy PD controller in order to achieve a balanced biped walking and controlled the overall biped system modeled as a 3D Inverted Pendulum [187].

5.1.7 Passive Walking Control

Passive dynamic walking is a class of biped robot walking mechanisms where the biped walks down a gentle slope smoothly and stably without any active feedback control or energy input other than gravity [85], [23], [82], [24], [188], [83], [189], [84]. These passive dynamic walkers exhibit a steady walking cycle which is smooth and effcient, and appears natural. The legs swing like a coupled pendulum so as to produce a stepping motion resembling that of humans and the impact of the swing leg with the ground is controlled by the conservation of the angular momentum. The completion of a step automatically produces the appropriate conditions for the initiation of another step. This periodic motion is locally stable in that it passively suppresses small perturbations from its nominal walking trajectory.

5.2 Supervisory Control System for Biped Robot

5.2.1 Preliminary Work

In the initial phases of this thesis work, the author visited Singapore Polytechnic's Advanced Robotic and Intelligent Control Centre (ARICC) in Singapore under the supervision of Dr. Changjiu Zhou, whereas the research trip is supported by the Scientific and Technical Research Council of Turkey (TUBITAK). During the author's visit to Singapore, a preliminary work, that aided the development of initial thoughts on supervisory control system design is realized.

5.2.1.1 Ground Reaction Force Analysis in Biped Locomotion

The biped model used in this research is 3D 7-link robot with 10 DOFs where 2 DOFs in each ankle, 1 DOF in each knee and 2 DOFs in each hip joints. The model has 6 DOFs in sagittal plane and 4 DOFs in frontal plane as shown in Figure 5.2.

In order to control the stability of gait and investigate the resultant ZMP trajectory, the focus is done to the frontal plane trajectory generation. The gait planning in frontal plane is achieved by using inverted pendulum model (Figure 5.3). The inverted pendulum model parameters are discretely chosen in different regions of the motion.

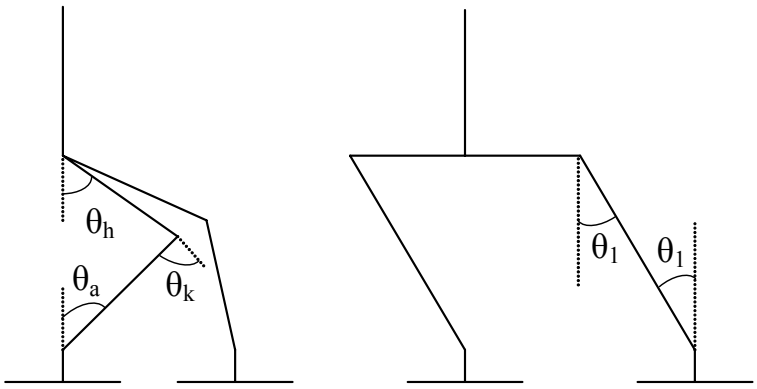

Figure 5.2 Sagittal and frontal plane views of biped structure

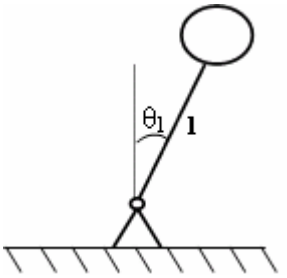

Figure 5.3 Inverted pendulum model

The approximated equation of motion of Inverted Pendulum Model is as below:

$$\ddot{\theta}_l = \frac{g}{l}\theta_l \tag{5.1}$$

The solution of this equation is in the following form:

$$\theta_l(t) = C_1 e^{(\sqrt{\frac{g}{l}})t} + C_2 e^{-(\sqrt{\frac{g}{l}})t} \tag{5.2}$$

where g is the gravitational acceleration and l is the length of inverted pendulum.

In biped locomotion, the main aim is to reach dynamically balanced walking since with two feet, the dynamic balance is not satisfied by default on walking. When designing and controlling the gait, the desired trajectory is also required to satisfy the dynamic balance. So there is a need of a measure to make sure that a dynamically balanced gait is obtained and also to control the dynamic stability of the gait.

In this work, ZMP concept is used in order to investigate the dynamic stability and the effect of the interaction with ground in biped locomotion. ZMP can also be defined as the center of pressure at the feet where Ground Reaction Force (GRF) acts on the ground (Figure 5.4). ZMP is only defined under the foot contacting to the ground.

The ZMP condition for the biped robot structure can be written as [108]:

$$\sum_i (r_i \times m_i a_i + I_i \alpha_i + \omega_i \times I_i \omega_i) - \sum_i (r_i \times m_i g_i) = (0,0,*)^T \tag{5.3}$$

where

$r_i = p_i - p_{ZMP}$

I_i : moment of inertia of the i^{th} link

ω_i : the angular velocity of the i^{th} link

α_i : the angular acceleration of the i^{th} link

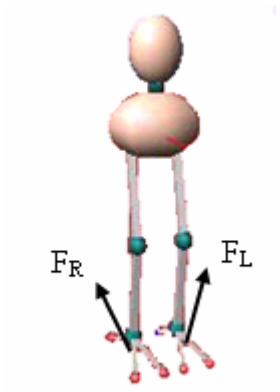

Figure 5.4 Ground reaction forces under the right and left foot

The rate of change of moment of momentum of the whole system about the ZMP, in the double-support phase, can be written as [108]:

$$-\sum_i (r_i \times m_i (a_i - g) + I_i \alpha_i + \omega_i \times I_i \omega_i) + r_L \times f_L + r_R \times f_R + n_L + n_R = 0 \tag{5.4}$$

where

$r_{L/R} = p_{L/R} - p_{ZMP}$, $p_{L/R}$ is the position of the left/right foot contact point,

$f_{L/R}$ and $n_{L/R}$ represent the GRF and moment at the left/right foot, respectively.

Using (5.3) and (5.4),

$$r_L \times f_L + r_R \times f_R + n_L + n_R = (0,0,*)^T \tag{5.5}$$

which gives the relation of GRF.

In order to investigate the GRF distribution under both feet, let's focus on single-support phase and double support phase separately. In single support phase, one foot is swinging and the other is touching to the ground. The GRF under the swinging foot is zero, and the total GRF is under the foot touching to the ground. The total GRF can be obtained from the following equation, which is derived from the motion of center of mass of biped robot:

$$m_{cm} a_{cm} = f_L + f_R + m_{cm} g \tag{5.6}$$

where

m_{cm} : the total mass of biped robot

a_{cm} : the acceleration of the center of mass of biped

On the other hand, in double support phase, only the total force, $f_L + f_R$ can be calculated from (5.6). So an approximate solution to resolve total force is needed. Dasgupta and Nakamura proposed a method to resolve the total force in double support phase by defining a constrained optimization problem [108]. In this phase, the vertical component of the force is determined from (5.5) that is:

$$y_L f_{LZ} + y_R f_{RZ} = y_{ZMP}(f_{LZ} + f_{RZ}) \tag{5.7}$$

$$x_L f_{LZ} + x_R f_{RZ} = x_{ZMP}(f_{LZ} + f_{RZ}) \tag{5.8}$$

where $x_{L/R}$ and $y_{L/R}$ are the x and y coordinates of the foot contacting to the ground in the world coordinate frame. In (5.7) and (5.8), the total force, that is $f_{LZ} + f_{RZ}$ in the right hand side of both equations is known so that the vertical component of the right and left forces can be calculated. On the other hand, the tangential components of the forces can be approximately calculated by forming a constrained optimization problem, where the

constraints include the (5.6) condition and the friction constrained between foot and ground at contact point, by minimizing the internal force in the closed-loop double-support phase structure and maximizing the contact stability margin.

The plot of the desired GRF to be obtained from above calculations is given in Figure 5.5. The repeated loop for gait trajectory is also given in Figure 5.6. In single support phase, GRF under the foot is desired to be constant and during the double support phase, the force under one foot is desired to be transferred smoothly to the other.

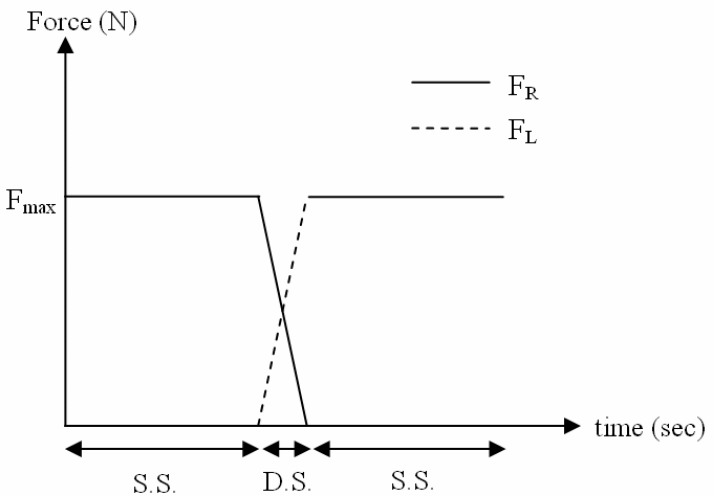

Figure 5.5 Desired GRF

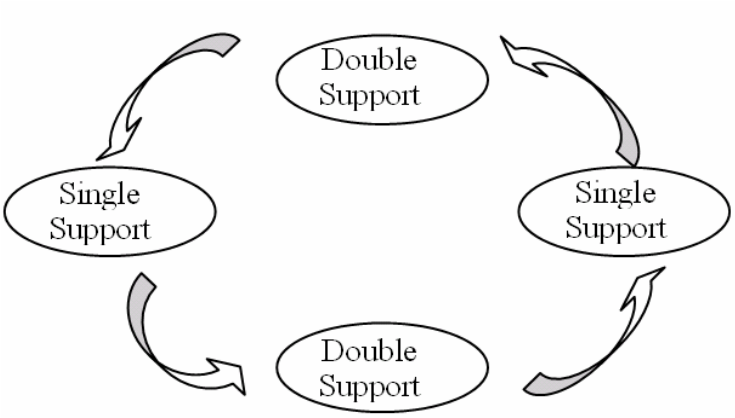

Figure 5.6 Gait trajectory finite state machine

In order to test the algorithm and analyze the corresponding results, a dynamic simulator, namely, SL Simulator is used [191]. SL allows creating complex rigid-body dynamic simulations easily and in a short time so that the biped robot algorithms can be tested in the simulation before they are tried on the actual robot. Both in simulation and real-time robot setup, SL allows collecting related data into a file after simulating the robot in simulation or after testing the algorithms in real robot. SL can also be used just for creating graphic animations. The visual appearance of the simulation in SL looks like as depicted in Figure 5.7. The User Interface (UI) of SL has commands that allow the user to control the simulation. There are some functions that can be used from UI command line. SL Simulation allows the user to use a robot model that the robot specific parameters and simulation conditions can be changed, to implement gait trajectories and to collect data from the simulation. After collecting the data from the simulation, it can be analyzed and plotted using MATLAB or any other relevant program.

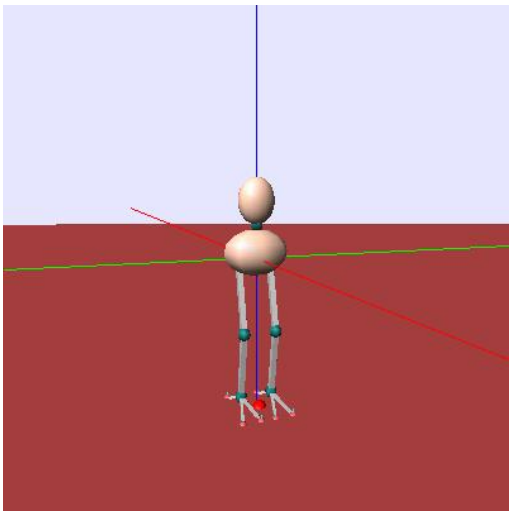

Figure 5.7 *SL* simulation

The aim of the simulation is to analyze the effects of low-level controller parameters and frontal plane desired gait trajectory parameters on the resultant GRF. Main aim is to tune the parameters so that the landing impact can be analyzed and the effects of parameters to reach a smooth transition between two phases of bipedal locomotion, namely, single support phase and double support phase, can be observed. So in this study, under different

parameter constraints, the resultant GRF is analyzed. The simulation results and the comparison are given in Chapter 6.

5.2.1.2 Hybrid Fuzzy Control Using 3D Inverted Pendulum Model

In this work, first the biped walking is modelled by 3D Inverted Pendulum (IP). In the IP model, ZMP and COG points of biped robot are used for both sagittal and frontal planes. One way to generate biped walking motion is, given the constraints of motion, calculating the ZMP and COG trajectories. The motions in sagittal and frontal planes are considered as independent motions. By solving the equations of biped approximated by IP model, COG, ZMP and GRF trajectories are obtained to achieve the desired sagittal and frontal plane motions. In order to achieve a stable biped walking, a fuzzy PD controller is designed to control the overall biped system. Fuzzy controller parameters are extracted by using intuitive control knowledge. The biped robot used is a 3D 6-link 10 DOF robot manipulator. The robot model is assumed to be independent in x-z (sagittal) and y-z (frontal) planes. In the sagittal plane, robot has 6 DOF and in the frontal plane, it has 4 DOF. It has 2 DOF in each hip joint, 1 DOF in each knee joint and 2 DOF in each ankle joint as shown in Figure 5.8.

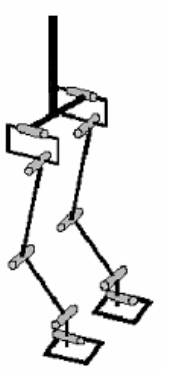

Figure 5.8 Link structure of biped robot

3D Inverted Pendulum Model (IPM) is formulated such as the base point of IP is located at the ZMP on the ground and the mass point of IP is located at the COG of the biped robot [192]. In the IPM, the motion in x and y directions (in sagittal and frontal planes, respectively) are assumed to be independent. So the differential equation describing the

motion of COG (x_{COG} , y_{COG}) in sagittal and frontal planes can be written as below, respectively:

$$\ddot{x}_{COG} = \frac{g}{H}(x_{COG} - x_{ZMP}) \tag{5.9}$$

$$\ddot{y}_{COG} = \frac{g}{H}(y_{COG} - y_{ZMP}) \tag{5.10}$$

where H is the height of COG that is assumed to be constant through the motion as shown in Figure 5.9, g is the gravitational acceleration constant (g = 9.81) and x_{COG} and y_{COG} are the positions of COG in x- and y-directions, respectively.

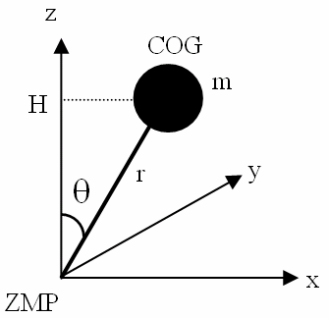

Figure 5.9 3D inverted pendulum model

The ZMP of the biped system in x-direction (sagittal plane) is approximated by:

$$x_{ZMP} = ax_{COG} + b \tag{5.11}$$

where the relation between COG and ZMP in SSP and DSP can be written as [192]:

$$x_{ZMP} = \begin{cases} a_S x_{COG} & \text{(in SSP)} \\ a_D x_{COG} & \text{(in DSP)} \end{cases} \tag{5.12}$$

Combining (5.9) and (5.11) , the differential equation describing the motion of COG in x-direction becomes:

$$\ddot{x}_{COG} = \frac{g}{H}(x_{COG} - ax_{COG} - b) \tag{5.13}$$

So the solution of the above differential equation can be written as:

$$x_{COG} = x_0 \cosh\frac{t}{T_{C1}} + \dot{x}_0 T_{C1} \sinh\frac{t}{T_{C1}} + \frac{b}{1-a} \tag{5.14}$$

where $T_{C1} = \sqrt{H/(g(1-a))}$ is time constant, x_0 and $\dot{x}_0$ are the initial values of position and velocity in x-direction. Then, the Ground Reaction Force (GRF) in x-direction can be written as:

$$F_X = m\ddot{x}_{COG} = m(\frac{x_0}{T_{C1}^2}\cosh\frac{t}{T_{C1}} + \frac{\dot{x}_0}{T_{C1}}\sinh\frac{t}{T_{C1}}) \tag{5.15}$$

where m is the total mass of the system, so also the mass of IPM.

In frontal plane, the ZMP of the biped system in y-direction is approximated by:

$$y_{ZMP} = cy_{COG} + d \tag{5.16}$$

where the relation between COG and ZMP in SSP and DSP can be written as [192]:

$$y_{ZMP} = \begin{cases} 0 & \text{(in SSP)} \\ c_D y_{COG} & \text{(in DSP)} \end{cases} \tag{5.17}$$

where $c_D = \frac{\beta + s}{\beta}$

Combining the (5.10) and (5.16), the differential equation describing the motion of COG in y-direction becomes:

$$\ddot{y}_{COG} = \frac{g}{H}(y_{COG} - cy_{COG} - d) \tag{5.18}$$

So the solution of the above differential equation can be written as:

$$y_{COG} = y_0 \cosh\frac{t}{T_{C2}} + \dot{y}_0 T_{C2} \sinh\frac{t}{T_{C2}} + \frac{d}{1-c} \tag{5.19}$$

where $T_{C2} = \sqrt{H/(g(1-c))}$ is time constant, y_0 and $\dot{y}_0$ are the initial values of position and velocity in y-direction.

Then, GRF can be written as:

$$F_Y = m\ddot{y}_{COG} = m(\frac{y_0}{T_{C2}^2}\cosh\frac{t}{T_{C2}} + \frac{\dot{y}_0}{T_{C2}}\sinh\frac{t}{T_{C2}}) \tag{5.20}$$

where m is the total mass of the system, so also the mass of IPM.

After modelling and obtaining the COG, ZMP and GRF trajectories, joint dynamics of the robot by using inverse kinematics is calculated as described below. From ZMP and COG knowledge, θ_X and θ_Y, the lean angle of IPM in sagittal and frontal planes, respectively, can be easily calculated by using inverse kinematics.

Since the analysis is focused on the neighbourhood of the vertical position of IPM, the system dynamics is linearized in this neighbourhood by using the approximation $\cos\theta \approx 1-\theta^2/2$, $\sin\theta \approx \theta$ and $\theta^2 \approx 0$ so that the approximated dynamics of the system in sagittal and frontal plane is obtained by reorganizing the equations obtained before. From Figure 5.9, the relationship between x_{COG}, θ_X and y_{COG}, θ_Y can be easily obtained.

In sagittal plane;

$$\frac{\cos\theta_X}{\sin\theta_X} = \frac{H}{x_{COG} - x_{ZMP}} \tag{5.21}$$

By using the angle approximations;

$$x_{COG} - x_{ZMP} = H\theta_X \tag{5.22}$$

After inserting x_{ZMP} in this equation in terms of x_{COG} as derived above, x_{COG} is found as

$$x_{COG} = \begin{cases} \dfrac{H}{(1-a_S)}\theta_X & in\ SSP \\ \dfrac{H}{(1-a_D)}\theta_X & in\ DSP \end{cases} \tag{5.23}$$

From these differential equations, GRF equation is also obtained in terms of sagittal plane angle

$$F_X = m\ddot{x}_{COG} = \begin{cases} \dfrac{mH}{(1-a_S)}\ddot{\theta}_X & in\ SSP \\ \dfrac{mH}{(1-a_D)}\ddot{\theta}_X & in\ DSP \end{cases} \tag{5.24}$$

Thus, applying a PD control law for the IPM

$$F_X = -k_p\theta_X - k_d\dot{\theta}_X \tag{5.25}$$

which, substituted into (5.24), yields

$$\begin{aligned} &\ddot{\theta}_X + \frac{(1-a_S)}{mH}k_d\dot{\theta}_X + \frac{(1-a_S)}{mH}k_p\theta_X = 0 \quad in\ SSP \\ &\ddot{\theta}_X + \frac{(1-a_D)}{mH}k_d\dot{\theta}_X + \frac{(1-a_D)}{mH}k_p\theta_X = 0 \quad in\ DSP \end{aligned} \tag{5.26}$$

In order to guarantee the stability of (5.26), both coefficients of the above differential equation must be positive:

$$\frac{(1-a_S)}{mH}k_d > 0 \quad and \quad \frac{(1-a_S)}{mH}k_p > 0 \quad in\ SSP$$
$$\frac{(1-a_D)}{mH}k_d > 0 \quad and \quad \frac{(1-a_D)}{mH}k_p > 0 \quad in\ DSP \tag{5.27}$$

where $a_S < 1$ and $a_D > 1$ so that the following results for sagittal plane is obtained:

$$k_d > 0 \quad and \quad k_p > 0 \quad in\ SSP$$
$$k_d < 0 \quad and \quad k_p < 0 \quad in\ DSP \tag{5.28}$$

And also in frontal plane, the above procedure is applied:

$$\frac{\cos\theta_Y}{\sin\theta_Y} = \frac{H}{y_{COG} - y_{ZMP}} \tag{5.29}$$

By using the angle approximations;

$$y_{COG} - y_{ZMP} = H\theta_Y \tag{5.30}$$

After inserting y_{ZMP} in this equation in terms of y_{COG} as derived above, y_{COG} is found as

$$y_{COG} = \begin{cases} 0 & in\ SSP \\ \dfrac{H}{(1-c_D)}\theta_Y & in\ DSP \end{cases} \tag{5.31}$$

From these differential equations, GRF equation is obtained in terms of frontal plane angle

$$F_Y = m\ddot{y}_{COG} = \begin{cases} 0 & in\ SSP \\ \dfrac{mH}{(1-c_D)}\ddot{\theta}_Y & in\ DSP \end{cases} \tag{5.32}$$

Thus, applying a PD control law for the IPM

$$F_Y = -k_p\theta_Y - k_d\dot{\theta}_Y \tag{5.33}$$

which, substituted into (5.32), yields

$$\begin{aligned} &-k_p\theta_Y - k_d\dot{\theta}_Y = 0 && \textit{in SSP} \\ &\ddot{\theta}_Y + \frac{(1-c_D)}{mH}k_d\dot{\theta}_Y + \frac{(1-c_D)}{mH}k_p\theta_Y = 0 && \textit{in DSP} \end{aligned} \tag{5.34}$$

In order to guarantee the stability of (5.34), both coefficients of the above differential equation must be positive:

$$\frac{(1-c_D)}{mH}k_d > 0 \quad \textit{and} \quad \frac{(1-c_D)}{mH}k_p > 0 \quad \textit{in DSP} \tag{5.35}$$

where $a_S < 1$ so that the following results for frontal plane is obtained:

$$\begin{aligned} &\textit{no constraints} && \textit{in SSP} \\ &k_d < 0 \quad \textit{and} \quad k_p < 0 && \textit{in DSP} \end{aligned} \tag{5.36}$$

Now, the expert knowledge will be used to construct a fuzzy control system to control and stabilize the biped robot. Since the IPM designed has an independent dynamic structure in sagittal and frontal planes, two equivalent PD-based fuzzy controllers will be designed, each of which works independently in these two planes with different controller parameters.

In designing the fuzzy controller, the control laws are constructed by employing intuitive expert knowledge in the form of if-then rules by using a rule-base fuzzy control system to stabilize and control the IP via horizontal ground reaction forces in x and y directions in sagittal and frontal planes, respectively.

The controller has two inputs, namely, $(\theta, \dot{\theta})$, the lean angle and angular velocity of inverted pendulum and one output, namely, F, ground reaction force. The construction of the if-then rules of the controller is based on the values of two inputs and the heuristic knowledge. In Figure 5.10, the four possible IP states are represented [193]. When the pendulum is moving away from the vertical position, the lean angle and velocity have the same sign and when the pendulum is coming back to the vertical position, the lean angle and the velocity have opposite signs as shown in Figure 5.10 with horizontal ground reaction force.

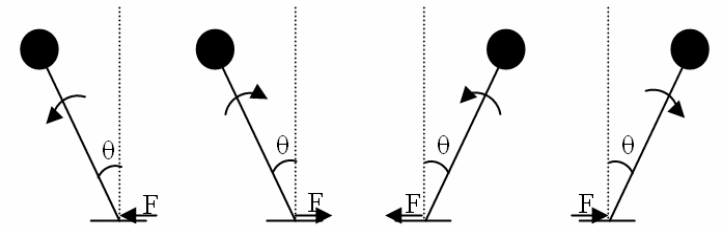

Figure 5.10 Four possible IP states

Using the intuitive control knowledge, the fuzzy rules listed below are applied to control the position of pendulum:

(1) If the pendulum is far then

$$F_1 = -(k_{pFar}\theta + k_{dFar}\dot{\theta})$$

(2) If the pendulum is near then

$$F_2 = -(k_{pNear}\theta + k_{dNear}\dot{\theta})$$

Based on the if-then rules given above, a fuzzy partition for the IP state space $(\theta, \dot{\theta})$ is proposed as shown in Figure 5.11.

In the realization of these fuzzy control rules, the Sugeno-Takagi (S-T) type fuzzy controller is used. The S-T fuzzy control method is applied to the PD controller.

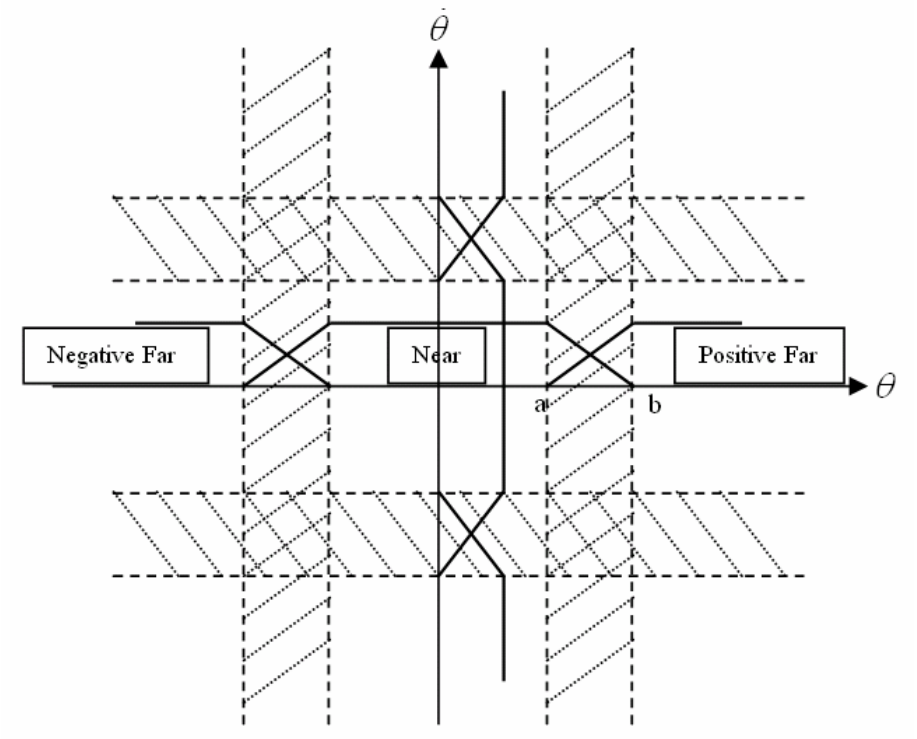

Figure 5.11 Fuzzy IP $(\theta, \dot{\theta})$ State Space Partition

By applying defuzzification in S-T PD controller [194], the below equation is obtained:

$$\mathrm{F} = \frac{\sum_{i=1}^{2} w_i F_i}{\sum_{i=1}^{2} w_i} \tag{5.37}$$

where

$$w_1 = \begin{Bmatrix} 0 & \theta \le a \\ \dfrac{|\theta| - a}{b - a} & a < \theta \le b \\ 1 & b < \theta \end{Bmatrix} \tag{5.38}$$

and

$$w_2 = \begin{Bmatrix} 1 & \theta \le a \\ \dfrac{b-|\theta|}{b-a} & a < \theta \le b \\ 0 & b < \theta \end{Bmatrix} \tag{5.39}$$

In the above equations, w_1 and w_2 are obtained for positive θ values. Similarly, it is obtained for negative values of θ. In the designed fuzzy controller, F_1 is valid on a region where θ is far from the vertical position in IPM and $\theta > b$. In this region, a PD controller with $k_p = k_{pFar}$ *and* $k_d = k_{dFar}$ is in use. Similarly, F_2 is valid on a region where θ is near to the vertical position in IPM and $a < \theta$. In this region, a PD controller with $k_p = k_{pNear}$ *and* $k_d = k_{dNear}$ is in use. In between, i.e., when $a \le \theta \le b$, the controller is fuzzy and the control rule is as in (5.37). In this region of operation, S-T type fuzzy system provides a heuristic representation of the controller as a nonlinear interpolation between two linear PD controllers. The simulation results and the analysis of the results are given in Chapter 6.

5.2.2 PID Control

5.2.2.1 PID Controller Design

Proportional-Integral-Derivative (PID) control is a close loop feedback controller that attemps to correct the error between the output of the process (system under control) and the reference signal input by producing the corrective action to adjust the process accordingly.

The output signal from the controller to the process is calculated as the proportional gain (K_P) times the magnitude of the error plus the integral gain (K_I) times the integral of the error plus the derivative gain (K_D) times the derivative of the error.

5.2.2.2 Effect of the PID Parameter Change on the Overall System Performance

In general, it is a well known fact that the change in the PID controller parameters affects the performance of the system:

- Larger K_P generally indicate a faster response time since the larger the error the larger the feedback to compensate. But the large proportional gain results in process instability;
- Larger K_I generally indicates the elimination of the steady state error quicker but a larger overshoot;
- Larger K_D generally indicates a decrease in the overshoot but slow transient response and possibly process instability.

Table 5-1 gives the summary of the change in PID parameters and its effect in the system response.

Table 5-1 The effects of the increase in PID parameters to the system response

PID Controller					
	Rise Time	Overshoot	Settling Time	Steady-State Error	Stability
K_P	⇓	⇑	⇔	⇓	Degrade
K_I	⇓	⇑	⇑	eliminates	Degrade
K_D	⇔	⇓	⇓	⇔	Improve

5.2.2.3 Adjustment of the PID Parameters

In order to adjust the PID parameters, Ziegler-Nichols method can be used as the details of the method is given in the Table 5-2. In this method, first of all, the proportional gain is increased until it reaches the "critical gain" K_c at which the output of the loop starts to oscillate. K_c and the oscillation period P_c are used to set the gains as the details given in the Table 5-2.

Table 5-2 The Ziegler-Nichols method summary

	K_P	K_I	K_D
P	$0.5K_C$	-	-
PI	$0.45K_C$	$1.2K_C / P_C$	-
PID	$0.6K_C$	$2K_P / P_C$	$K_P P_C / 8$

5.2.2.4 PID Controller for Biped Locomotion

Given the system dynamics

$$D(\underline{\theta})\ddot{\underline{\theta}} + h(\underline{\theta}, \dot{\underline{\theta}})\dot{\underline{\theta}} + G(\underline{\theta}) = \underline{T}_\theta \tag{5.40}$$

The joint torque vector (input vector) T_θ is calculated as

$$\underline{T}_\theta = K_p \underline{e}(t) + K_i \int_0^t \underline{e}(\tau) d\tau + K_d \frac{d\underline{e}}{dt} \tag{5.41}$$

where

$$\underline{e} = \underline{\theta}_d - \underline{\theta}$$

5.2.3 Computed Torque Control

In order to generate the joint torque vector, the computed torque control method is used as details given below:

The system dynamics are formulated previously in Chapter 2 as

$$D(\underline{\theta})\ddot{\underline{\theta}} + h(\underline{\theta}, \dot{\underline{\theta}})\dot{\underline{\theta}} + G(\underline{\theta}) = T_\theta \tag{5.42}$$

Let's define T_θ as

$$T_\theta = D(\underline{\theta})\underline{\lambda} + h(\underline{\theta}, \underline{\dot{\theta}})\underline{\dot{\theta}} + G(\underline{\theta}) \tag{5.43}$$

where $\underline{\lambda}$ is the acceleration related vector and is defined as below according to the PD control law:

$$\underline{\lambda} = \underline{\ddot{\theta}}_d + \underline{K}_d(\underline{\dot{\theta}}_d - \underline{\dot{\theta}}) + \underline{K}_p(\underline{\theta}_d - \underline{\theta}) \tag{5.44}$$

where subscribe "d" in joint angles and velocities represents the desired reference trajectory values.

By using this method, the error equation which is defined as the difference between the desired and actual joint angle trajectories can be written as below from the above equations:

$$\underline{\ddot{e}} + \underline{K}_d\underline{\dot{e}} + \underline{K}_p\underline{e} = 0 \tag{5.45}$$

where

$$\underline{e} = \underline{\theta}_d - \underline{\theta}$$

So the second order system equations of the error can be assumed to realize a critically damped behaviour [195]. As a result, the control gain matrices are formulated as below:

$$\begin{aligned} &\underline{K}_p = diag[w_1^2, w_2^2, ..., w_7^2] \text{ and} \\ &\underline{K}_d = 2diag[w_1, w_2, ..., w_7] \end{aligned} \tag{5.46}$$

Furthermore, the computed torque control method is extended to "modified" computed torque control method by adding an integral term to the control law.

5.2.4 Optimal Controller Design

Many environmental activities engage with the “control” of a process and “law” on achieving this goal. Control theory is involved with mathematical models of physical or biological systems. In order to find a solution of a control problem, classical control system design deals generally with a trial-and-error process in which various methods of analysis are used iteratively to determine the design parameters of an “acceptable” system.

In the applied sciences, many theories can be expressed by optimality approach that provides the most economical description, in some sense, of the rules controlling a system's manner of acting. In motor control problems, optimality has also played a fundamental role in order to provide the necessary control mechanism to the system. The efficiency to achieve the desired system behavior and experimental accomplishment of optimal control models in biological movement increased the interest on the subject.

The process belonging to a specific motor system behavior is, in fact, an optimization process and leads to the system to act better and better as time passes. Hence, the use of optimality approach in the motor control of such systems is a natural fact. More specifically, in biological systems, the motor behavior is controlled by muscles and the number of muscles is a lot more than the number of joints and so, the posture is generated by an infinite variety of muscle activation patterns. In other words, this redundancy of biological systems causes the motor system to be very flexible and in parallel, in biomechanical systems, this necessitates a very well designed controller that can generate the desired intelligent behavior among the huge amount of possible candidates. At this point, optimal control theory ensures a practical solution.

Optimal control deals with the determination of the control law for a given system such that a certain optimality criterion is achieved and at the same time, the physical constraints are satisfied. That is why, in most of the nonlinear control problems such as in robotics, optimal control approach is used. In optimal control, the computed controls are aimed to achieve to the good numerical convergence, acceptable performance (peak overshoot, gain, rise time, settling time, phase margin and bandwidth), robustness and stability criteria in addition to the satisfaction of system constraints and minimum performance measure.

5.2.4.1 Optimal Control Problem

In biped locomotion, optimal control theory objective is to decide on the joint torques (control signals) resulting in a gait walking pattern so that the acceptable performance measure is achieved, the physical constraints, robustness and stability criteria are all satisfied.

In this work, the optimal controller is designed by using three different methods: the variational techniques with iterative numerical determination, Linear Quadratic Regulator (LQR) with system linearization and Hooke & Jeeves method.

The formulation of an optimal control problem requires [196]:

- Mathematical model of the process to be controlled
- Physical Constraints
- Performance Criterion

5.2.4.1.1 Mathematical Model of the Biped Robot

The robot dynamics for the biped locomotion was derived previously in Chapter 2. Now, the aim is to change the form of these derived equations into state space representation in order to use them in controlling the biped system and producing the control signals to result in the optimal path for one step of biped locomotion.

The dynamic model of the biped is:

$$D_\theta(\underline{\theta})\ddot{\underline{\theta}} + h_\theta(\underline{\theta},\dot{\underline{\theta}})\dot{\underline{\theta}} + G_\theta(\underline{\theta}) = \underline{T}_\theta \tag{5.47}$$

where

$\underline{\theta} = \left[\theta_1, \theta_2, \theta_3, \theta_4, \theta_5, \theta_6, \theta_7\right]^T$, the 7x1 vector of control torque applied at each joint

$\underline{T_\theta} = \left[T_{\theta 1}, T_{\theta 2}, T_{\theta 3}, T_{\theta 4}, T_{\theta 5}, T_{\theta 6}, T_{\theta 7}\right]^T$, the 7x1 vector of relative angles between links

$D_\theta(\underline{\theta}) = \left[D_{\theta ij}(\underline{\theta}) \right] \quad (i, j = 1, 2, ..., 7)$ is a 7x7 symmetric, positive-definite inertia matrix,

$h_\theta(\underline{\theta}) = \left[h_{\theta ij}(\underline{\theta}, \dot{\underline{\theta}}) \right]$ $(i, j = 1, 2, ..., 7)$ is a 7x7 vector consisting of coriolis and centripetal torques, and

$G_\theta(\underline{\theta}) = \left[G_{\theta i}(\underline{\theta}) \right]$ $(i = 1, 2, ..., 7)$ is a 7x1 gravity vector consisting of gravitational torques.

These equations can be formulated in the state variable form in order to obtain the ordinary differential equations:

$$\begin{aligned} &\underline{x_1} = \underline{\theta} \quad and \quad \dot{\underline{x_1}} = \dot{\underline{\theta}} \\ &\underline{x_2} = \dot{\underline{\theta}} \quad and \quad \dot{\underline{x_2}} = D^{-1}{}_\theta(\underline{\theta}) \left[T_\theta - h_\theta(\underline{\theta}, \dot{\underline{\theta}}) \dot{\underline{\theta}} - G_\theta(\underline{\theta}) \right] \end{aligned} \tag{5.48}$$

So,

$$\underline{x} = \begin{bmatrix} \underline{x}_1 \\ \underline{x}_2 \end{bmatrix} \tag{5.49}$$

and

$$\dot{\underline{x}} = \begin{bmatrix} \underline{x}_2 \\ D^{-1}{}_{x_1}(\underline{x}_1) \left[\underline{u} - h_{x_1}(\underline{x}_1, \underline{x}_2) \underline{x}_2 - G_{x_1}(\underline{x}_1) \right] \end{bmatrix} \tag{5.50}$$

where

$\underline{u} = T_{x_1}$

Hence, the mathematical equations are obtained in the below ordinary 14-dimensional differential equations form:

$$\dot{\underline{x}} = \underline{f}(\underline{x}(t), \underline{u}(t), t) \tag{5.51}$$

where

$\underline{x}(t) = \begin{bmatrix} \underline{x}_1(t) \\ \underline{x}_2(t) \end{bmatrix}$ is the 14-dimensional state vector of the process at time t

and

$$\underline{u}(t) = \begin{bmatrix} u_1(t) \\ u_2(t) \\ . \\ . \\ . \\ u_7(t) \end{bmatrix}$$ are the 7-dimensional control vector to the process at time t.

Furthermore, in biological systems, the joint variables are bounded by the lower and upper limits. So, in biped system, these limits are defined as below:

$$\begin{aligned}
&\theta_{1\min} \le \theta_1 \le \theta_{1\max} \\
&\theta_{2\min} \le \theta_2 \le \theta_{2\max} \\
&\theta_{3\min} \le \theta_3 \le \theta_{3\max} \\
&\theta_{4\min} \le \theta_4 \le \theta_{4\max} \\
&\theta_{5\min} \le \theta_5 \le \theta_{5\max} \\
&\theta_{6\min} \le \theta_6 \le \theta_{6\max} \\
&\theta_{7\min} \le \theta_7 \le \theta_{7\max}
\end{aligned} \tag{5.52}$$

$$z_h \ge z_{h\min} \Rightarrow l_1 \cos\theta_1 + l_2 \cos\theta_2 \ge z_{h\min}$$

(imposed by the hip point vertical limits)

$$z_e \ge 0 \Rightarrow l_1 \cos\theta_1 + l_2 \cos\theta_2 - l_4 \cos\theta_4 - l_5 \cos\theta_5 \ge 0$$

(imposed by the end-effector kinematics with gorund level)

These inequality constraints are enforced to the system and so, the system controller provides signals that result a configuration satisfying this limitations. In order to achieve this, a new state variable, called, constraint-state, is added to the system dynamics as a last state variable:

$$\underline{x} = \begin{bmatrix} \underline{x}_1 \\ \underline{x}_2 \\ x_c \end{bmatrix}$$ where x_c, the constraint state is defined as below: (5.53)

$$\dot{x}_c(t) = f_c(\underline{x}(t), t) \tag{5.54}$$

The constraint-state represents the constraints on joint variables. The inequality constraints on the joint variable as given in (5.52) can be written as below:

$$\begin{aligned}
&\theta_{i\min} \le \theta_i \le \theta_{i\max} \text{ for } i = 1,...,7 \\
&l_1 \cos\theta_1 + l_2 \cos\theta_2 \ge z_{h\min} \\
&l_1 \cos\theta_1 + l_2 \cos\theta_2 - l_4 \cos\theta_4 - l_5 \cos\theta_5 \ge 0
\end{aligned} \tag{5.55}$$

The joint angle inequalities can be written in different format and can be defined in a new function representation form:

$$\begin{aligned}
&f_{ci}(\underline{x}(t),t) = \theta_i - \theta_{i\min} \ge 0 \text{ for } i = 1,...,7 \\
&f_{ci}(\underline{x}(t),t) = \theta_{(i-7)\max} - \theta_{i-7} \ge 0 \text{ for } i = 8,...,14 \\
&f_{c15}(\underline{x}(t),t) = l_1 \cos\theta_1 + l_2 \cos\theta_2 - z_{h\min} \ge 0 \\
&f_{c16}(\underline{x}(t),t) = l_1 \cos\theta_1 + l_2 \cos\theta_2 - l_4 \cos\theta_4 - l_5 \cos\theta_5 \ge 0
\end{aligned} \tag{5.56}$$

Now, let's write the dynamics of the constraint-state as

$$\underline{\dot{x}_c} = f_c(\underline{x}(t),t) \tag{5.57}$$

and

$$f_c(\underline{x}(t),t) = \sum_{i=1}^{16} \left[f_{ci}(\underline{x}(t),t) \right]^2 \psi(-f_{ci}(\underline{x}(t),t)) \text{ for } i = 1,...,16 \tag{5.58}$$

where

$$\psi(-f_{ci}(\underline{x}(t),t)) = \begin{cases} 0 & for \quad f_{ci}(\underline{x}(t),t) \ge 0 \\ 1 & for \quad f_{ci}(\underline{x}(t),t) < 0 \end{cases} \tag{5.59}$$

Fact 1: $\underline{\dot{x}_c}(t) \ge 0$ for $\forall t$ and that $\underline{\dot{x}_c}(t) = 0$ only for times when all of the constraints are satisfied.

Fact 2: The initial and final conditions for the constraint state are set to 0.

Fact 1 and 2, together, result in the constraint state being 0 throughout the interval, only when the constraints are satisfied for all $t \in [t_0, t_f]$.

5.2.4.1.2 Physical Constraints

Physical constraints are to be defined on the state and control values. The known parameters of this problem are assumed to be:

- Initial time and initial state variable constraints: The initial time, t_0, and the initial state variable, $\underline{x}(t_0)$ are given to the optimal control problem as an input constraint.

- Final time and final state variable constraints: The final time, t_f, is given to the optimal control problem as an input constraint.

- Note that the final state variable seems to be free since it is not imposed to the system as a constraint but this is not the actual case. This constraint is included in the performance measure as a penalty function.

- System dynamics: In control problems, the system trajectory is determined by the applied control and so the optimal control problem here is also constrained by the dynamics of the process, which is:

$$\dot{\underline{x}} = \underline{f}(\underline{x}(t), \underline{u}(t), t)$$

- Joint angle constraints: These constraints are imposed into the system dynamics as a constraint state as described above.

- Control input constraints: Control inputs (acceleration) can also be a physical constraint. The acceleration can be bounded by some upper limit which depends on the capability of joint angles, i.e. $\underline{\tau}_{\min} \leq \underline{\tau} \leq \underline{\tau}_{\max}$

The initial time and state variable, and final time constraints are enforced to the Optimal Control Problem as boundary conditions; the final state variable constraint is imposed to the system in the objective function; the system dynamics are included in the mathematical representation; joint angle constraints are imposed as a constraint state in the state equations.

5.2.4.1.3 Derivation of the Performance Measure for Biped Robot Locomotion:

At this point, it is important to give some definitions related to this subject.

Definition: A history of control input values during the interval $[t_0, t_f]$ is called control history denoted by $\underline{u}$ and the history of state values in the interval $[t_0, t_f]$ is called a state trajectory and is denoted by $\underline{x}$.

A control history which satisfies the control constraints during the entire time interval $[t_0, t_f]$ is called an admissible control and is denoted by U.

Note that, the notation $\underline{u} \in U$ means that the control history $\underline{u}$ is admissible.

Definition: (Biped Robot Locomotion Optimal Control Problem) Finding an admissible control $\underline{u}^*$ which causes the system

$$\dot{\underline{x}} = \underline{f}(\underline{x}(t), \underline{u}(t), t) \tag{5.60}$$

to follow an admissible trajectory $\underline{x}^*$ that minimizes the performance measure

$$J = h(\underline{x}(t_f), t_f) + \int_{t_0}^{t_f} g(\underline{x}(t), \underline{u}(t), t)dt \tag{5.61}$$

This admissible control $\underline{u}^*$ is called the optimal control and the admissible trajectory $\underline{x}^*$ is called the optimal trajectory.

Hence, if a functional relationship of the form

$$\underline{u}^*(t) = \underline{a}(\underline{x}(t), t) \tag{5.62}$$

can be found for the optimal control at time t, then the function $\underline{a}$ is called the optimal control law.

In order to solve this problem, first the performance measure is determined. The performance measure has been chosen to minimize the dissipated energy at the joints of the biped robot, to minimize the error between the actual and desired trajectory and to minimize the error in the desired final trajectory as a penalty. The final trajectory, $\underline{x}(t_f)$ is not included as a boundary condition but is included in the performance measure as a penalty function. Hence, the performance measure, by which the performance of the biped system is evaluated, becomes as below:

$$J = h(\underline{x}(t_f), t_f) + \int_{t_0}^{t_f} g(\underline{x}(t), \underline{u}(t), t)dt \tag{5.63}$$

where

t_0 = initial time of one step motion
t_f = final time of one step motion
$\underline{x}(t_f)$ = desired state at final time
$h(\underline{x}(t_f), t_f)$ = a scalar function of free leg state evaluated at final time
$g(\underline{x}(t), \underline{u}(t), t)$ = a scalar function of a measure for the dissipated energy at the joints of the biped robot plus a measure for the error between the actual and desired trajectory

Also,

$$h(\underline{x}(t_f), t_f) = \frac{1}{2}\left[\underline{x}(t_f) - \underline{x}_d(t_f)\right]^T F\left[\underline{x}(t_f) - \underline{x}_d(t_f)\right], \tag{5.64}$$

$$g(\underline{x}(t), \underline{u}(t), t) = \frac{1}{2}(\underline{x}(t) - \underline{x}_d(t))^T Q(\underline{x}(t) - \underline{x}_d(t)) + \frac{1}{2}\alpha.\underline{u}^T(t) R\,\underline{u}(t), \tag{5.65}$$

and F, Q and R are real symmetric, positive semi-definite weight matrices. The elements of these matrices are chosen to weight the different components of the system elements that each of them affecting according to their relative importance.

5.2.4.2 Variational Approach to Optimal Control in Biped Locomotion Problem

The use of variational techniques leads to a nonlinear two-point boundary value problem. The analytical solution of such problems cannot be achieved and so, the steepest descent procedure, which is a typical iterative gradient based numerical method, is used. It is a well-known fact that, the gradient based optimal control leads to stick to local optimums.

5.2.4.2.1 Necessary Conditions for Optimal Control in Biped Locomotion Problem

Given the optimal control problem

$$\begin{aligned} &\text{minimize } J(\underline{u}) = h(\underline{x}(t_f), t_f) + \int_{t_0}^{t_f} g(\underline{x}(t), \underline{u}(t), t)dt \\ &\text{subject to} \\ &\qquad \dot{\underline{x}} = \underline{f}(\underline{x}(t), \underline{u}(t), t) \\ &\qquad \underline{x}(t_0) = \underline{x}_0 \end{aligned} \tag{5.66}$$

where $\underline{x}$ is the state variable and $\underline{u}$ is control variable continuous first derivative and the problem is finding the function $\underline{u}$ for which the functional J has a relative extremum.

The variational approach results in a nonlinear two-point boundary-value problem (2P-BVP). According to the assumption that the state and control variables are not constrained by any boundaries, the final time t_f is fixed and final state $\underline{x}(t_f)$ is free, then the 2P-BVP with the necessary and boundary conditions can be summarized as below:

Necessary Conditions:

$$\dot{\underline{x}}^* = \underline{f}(\underline{x}^*(t), \underline{u}^*(t), t) \tag{5.67}$$

$$\dot{\underline{p}}^* = -\left[\frac{\partial \underline{\underline{f}}}{\partial \underline{x}}(\underline{x}^*(t),\underline{u}^*(t),t)\right]^T \underline{p}^*(t) - \frac{\partial \underline{\underline{g}}}{\partial \underline{x}}(\underline{x}^*(t),\underline{u}^*(t),t)$$

$$0 = \left[\frac{\partial \underline{\underline{f}}}{\partial \underline{u}}(\underline{x}^*(t),\underline{u}^*(t),t)\right]^T \underline{p}^*(t) + \frac{\partial \underline{\underline{g}}}{\partial \underline{u}}(\underline{x}^*(t),\underline{u}^*(t),t)$$

Boundary Conditions:

$$\begin{aligned} &\dot{\underline{x}}^*(t_0) = \underline{x}_0 \\ &\dot{\underline{p}}^*(t_f) = \frac{\partial \underline{h}}{\partial \underline{x}}(\underline{x}^*(t_f)) \end{aligned} \tag{5.68}$$

The aim is, from these five sets of the conditions, to obtain an explicit relationship for $\underline{x}^*(t)$ and $\underline{u}^*(t)$, $t \in [t_0, t_f]$.

In this case, it is convenient to use the function H, called Hamiltonian, as defined below:

$$H(\underline{x}(t),\underline{u}(t),\underline{p}(t),t) = g(\underline{x}(t),\underline{u}(t),t) + p^T(t)[\underline{f}(\underline{x}(t),\underline{u}(t),t)] \tag{5.69}$$

The above 2P-BVP can be written as below using the Hamiltonian:

Necessary Conditions:

$$\begin{aligned} &\dot{\underline{x}}^* = \frac{\partial H}{\partial p}(\underline{x}^*(t),\underline{u}^*(t),\underline{p}^*(t),t) \\ &\dot{\underline{p}}^* = -\frac{\partial H}{\partial \underline{x}}(\underline{x}^*(t),\underline{u}^*(t),\underline{p}^*(t),t) \\ &0 = \frac{\partial H}{\partial \underline{u}}(\underline{x}^*(t),\underline{u}^*(t),\underline{p}^*(t),t) \end{aligned} \tag{5.70}$$

for all $t \in [t_0, t_f]$.

Boundary Conditions:

$$\dot{\underline{x}}^*(t_0) = \underline{x}_0$$
$$\dot{\underline{p}}^*(t_f) = \frac{\partial \underline{h}}{\partial \underline{x}}(\underline{x}^*(t_f)) \tag{5.71}$$

Also note that, the costate equation corresponding to the constraint state is:

$$\dot{p}_c^*(t) = -\frac{\partial H}{\partial \underline{x}_c}(\underline{x}(t), \underline{u}(t), t) = 0 \text{ for all } t \in [t_0, t_f] \tag{5.72}$$

since $x_c(t)$ does not appear explicitly in the Hamiltonian. As a result,

$$p_c(t) = \text{a constant} \tag{5.73}$$

Let's take the final condition, $p_c(t_f) = 0$.

Note that, the calculations of $\frac{\partial H}{\partial \underline{u}}$, $\frac{\partial H}{\partial \underline{x}}$ and $\frac{\partial h}{\partial \underline{x}}$ are given in Appendix C.

5.2.4.2.2 Steepest Descent Method Applied to Biped Locomotion

The above state and costate (adjoint) equations, of the necessary conditions formed two differential equations with initial and final conditions and these initial and final conditions are defined as the boundary conditions of the steepest descent optimal control problem.

Initial guess for input vector $\underline{u}(t)$ is assumed to be a dense discretization of N samples of time. Starting with an initial guess for input trajectory, the state and costate equations are solved. These Euler-Lagrange equations are difficult to be solved analytically. In the biped locomotion problem, numerical algorithm is used for the solution of these two equations. So by using the numerical integration methods (refer to Appendix D for the details), the state and costate equations are solved by forward and backward integrations, respectively. At this point, the objective function for the whole trajectory can be calculated. The right hand side of the third equation of the necessary conditions is equal to the gradient of the

objective function with respect to the input variable. So, $\underline{u}(t)$ is updated in negative direction of the gradient (steepest descent) in order to minimize the objective function.

After a number of iterations, the input trajectory that makes the right hand side of the third equation of the necessary conditions close to zero will be achieved and the iteration will be stopped.

5.2.4.2.3 The Steepest Descent Algorithm:

1) Select a discrete approximation to the nominal control history $\underline{u}^{(0)}(t)$, $t \in [t_0, t_f]$, and store it in the memory. This will be achieved by subdividing the interval $[t_0, t_f]$ into N subintervals of equal duration and considering the control $\underline{u}^{(0)}$ as a piecewise-constant during each of these subintervals; that is:

$$\underline{u}^{(0)}(t) = \underline{u}^{(0)}(t_k),\ t \in [t_k, t_{k+1}),\ k = 0,1,...,N-1 \tag{5.74}$$

Let's assume the iteration index, i is zero in this step.

2) Using the nominal control history $\underline{u}^{(i)}$, integrate the state equations from t_0 to t_f with initial conditions $\underline{x}(t_0) = \underline{x}_0$ and store the resulting state trajectory $\underline{x}^{(i)}$ as a piecewise constant vector function.

3) Calculate $\underline{p}^{(i)}(t_f)$ by substituting $\underline{x}^{(i)}(t_f)$ from Step 2 into

$$\underline{p}^{(i)}(t_f) = \frac{\partial h}{\partial x}(\underline{x}^{(i)}(t_f)) \tag{5.75}$$

Using the value of $\underline{p}^{(i)}(t_f)$ as the "initial condition" and the piecewise-constant values of $\underline{x}^{(i)}$ stored in Step 2, integrate the costate equations from t_0 to t_f, evaluate $\partial H^{(i)}(t) / \partial \underline{u}$, $t \in [t_0, t_f]$, and store this function in piecewise-constant fashion.

4) If $\left\| \frac{\partial H^{(i)}}{\partial u} \right\| \leq \gamma$

where γ is a preselected positive constant and

$$\left\| \frac{\partial H^{(i)}}{\partial u} \right\|^2 = \int_{t_0}^{t_f} \left[\frac{\partial H^{(i)}}{\partial u}(t) \right]^T \left[\frac{\partial H^{(i)}}{\partial u}(t) \right] dt \tag{5.76}$$

terminate the iterative procedure, and output the extremal state and control.

If the stopping criterion $\left\| \frac{\partial H^{(i)}}{\partial u} \right\| \leq \gamma$ is not satisfied, generate a new piecewise-constant control function given by

$$\underline{u}^{(i+1)}(t_k) = \underline{u}^{(i)}(t_k) - \varepsilon \frac{\partial H^{(i)}}{\partial u}, \; k = 0,1,...,N-1 \tag{5.77}$$

where

$$\underline{u}^{(i)}(t) = \underline{u}^{(i)}(t_k) \text{ for } t \in [t_k, t_{k+1}), \; k = 0,1,...,N-1 \tag{5.78}$$

Replace $\underline{u}^{(i)}(t_k)$ by $\underline{u}^{(i+1)}(t_k)$, $k = 0,1,...,N-1$, and return to Step 2.

5.2.4.3 LQR Approach in Biped Locomotion Control

5.2.4.3.1 Introduction

The optimal control theory deals with finding the control input that minimizes the cost function defined for a dynamic system. If the system dynamics are defined by a set of linear differential equations and the cost function is in a quadratic form then the problem is called Linear Quadratic (LQ) problem. One of the main types of LQ problem is defined if the solution of the optimal control LQ problem is a feedback controller of the Linear Quadratic Regulator (LQR) type. The results of a (regulating) controller is achieved by a process extracted by using an algorithm that minimizes the cost function which is defined by the deviations of some system variables from their desired values and also the key

measurements, such as the energy, which is wanted to be as small as possible. As a result, the algorithm finds the control input that minimizes the undesired deviations and also some key system values, such as energy. Most of the time, the adjustment of the control input requires comparison of the results with the specified design goals, which means, most of the time, that controller synthesis is an iterative process to achieve the design goals and required system behavior. Hence, the LQR algorithm is, in summary, a systematic procedure that finds an appropriate state-feedback controller.

In this work, the LQR algorithm is applied iteratively. At the beginning, the iteration starts with a predefined control input trajectory. By solving the system dynamics, the corresponding state variable trajectory will be obtained. Afterwards, the linearized system dynamics equation will be calculated using this initial control input and state variable trajectories. In other words, the linearized system dynamics is obtained by linearizing the system around the initial control input and state variable trajectories. Then, the linearized system dynamics will be used in order to solve the LQR problem with the given cost function. The LQR problem is solved in order to find the deviations from the initial control input and state variable trajectories by minimizing the cost function.

5.2.4.3.2 The Discretization of System Dynamics

The continuous-time ordinary differential equation of the biped system in state-space representation was found as below:

$$\dot{\underline{x}} = \underline{f}(\underline{x}(t), \underline{u}(t), t) \tag{5.79}$$

Let's first approximate this system dynamics by a discrete system, using the Taylor Series Expansion of the form:

$$\dot{\underline{x}} \approx \frac{\underline{x}(t + \Delta t) - \underline{x}(t)}{\Delta t} \tag{5.80}$$

and

$$\Delta t = \frac{t_f - t_0}{N - 1} \tag{5.81}$$

where

$t_0 =$ initial time of one step motion

$t_f =$ final time of one step motion

$N =$ number of points where the discretization is relaized

From (5.79) and (5.80),

$$\frac{\underline{x}(t+\Delta t)-\underline{x}(t)}{\Delta t} \approx \underline{f}(\underline{x}(t),\underline{u}(t),t)$$

$$\Rightarrow \ \underline{x}(t+\Delta t) = \underline{x}(t) + \Delta t\, \underline{f}(\underline{x}(t),\underline{u}(t),t) \tag{5.82}$$

is obtained.

Let us define $t = k\Delta t$ where $k = 0,...,N-1$ and so the equation becomes:

$$\underline{x}((k+1)\Delta t) = \underline{x}(k\Delta t) + \Delta t\, \underline{f}(\underline{x}(k\Delta t),\underline{u}(k\Delta t)) \ \text{ for } k = 0,...,N-1 \tag{5.83}$$

Without causing confusion, the indexing k, instead of $k\Delta t$, is used so that the equation becomes:

$$\underline{x}(k+1) = \underline{x}(k) + \Delta t\, \underline{f}(\underline{x}(k),\underline{u}(k)) \ \text{ for } k = 0,...,N-1 \tag{5.84}$$

Now let us define $\underline{f_d}(\underline{x}(k),\underline{u}(k)) = \underline{x}(k) + \Delta t\, \underline{f}(\underline{x}(k),\underline{u}(k))$ and as a result the equation takes its final form as:

$$\underline{x}(k+1) = \underline{f_d}(\underline{x}(k),\underline{u}(k)) \ \text{ for } k = 0,...,N-1 \tag{5.85}$$

5.2.4.3.3 Linearization of Nonlinear System Dynamics

First of all, the system dynamics will be linearized. It is important to mention at this point that, the aim is to slove the LQR problem so that the deviations from the initial control input and state variable trajectories can be obtained by minimizing the cost function. So let

us continue accordingly and define the deviations from the initial control input and state variable trajectories as below:

$$\begin{aligned}\delta \underline{x}^{i}(k) &= \underline{x}^{i}(k) - \underline{x}^{(i-1)^*}(k) \\ \delta \underline{u}^{i}(k) &= \underline{u}^{i}(k) - \underline{u}^{i-1}(k)\end{aligned} \quad \text{for } k = 0,...,N-1 \text{ and } \mathrm{i} = 1,...,Iter_{\max} \tag{5.86}$$

where $\underline{x}^{i}(k)$ and $\underline{u}^{i}(k)$ denotes the state variable and control input trajectories obtained as a solution of LQR problem after i th iteration, respectively for $\mathrm{i} = 1,...,Iter_{\max}$ with an exception that at the beginning of first iteration, $\underline{u}^{0}(k)$ is assigned and $\underline{x}^{0^*}(k)$ is obtained by solving the system dynamics. Also, $\underline{x}^{i^*}(k)$ for $\mathrm{i} = 1,...,Iter_{\max} - 1$ is obtained by using the $\underline{u}^{i}(k)$ found by the previous iteration and solving the system dynamics accordingly.

The same equations can be written as below:

$$\begin{aligned}\underline{x}^{i}(k) &= \underline{x}^{(i-1)^*}(k) + \delta \underline{x}^{i}(k) \\ \underline{u}^{i}(k) &= \underline{u}^{i-1}(k) + \delta \underline{u}^{i}(k)\end{aligned} \quad \text{for } k = 0,...,N-1 \text{ and } \mathrm{i} = 1,...,Iter_{\max} \tag{5.87}$$

The Taylor Series Expansion is used around the initial trajectory on the discretized system dynamics function and as a result, the following equations are obtained:

$$\begin{aligned}&\underline{f_d}(\underline{x}^{(i-1)^*}(k) + \delta \underline{x}^{i}(k), \underline{u}^{i-1}(k) + \delta \underline{u}^{i}(k)) = \\ &\quad \underline{f_d}(\underline{x}^{(i-1)}(k), \underline{u}^{i-1}(k)) + \frac{\partial \underline{f_d}}{\partial \underline{x}}(\underline{x}^{(i-1)}(k), \underline{u}^{i-1}(k)) \delta \underline{x}^{i}(k) + \\ &\quad \frac{\partial \underline{f_d}}{\partial \underline{u}}(\underline{x}^{(i-1)}(k), \underline{u}^{i-1}(k)) \delta \underline{u}^{i}(k) + H.O.T\end{aligned} \tag{5.88}$$

for $k = 0,...,N-1$ where $\frac{\partial \underline{f_d}}{\partial \underline{x}}(\underline{x}^{(i-1)^*}(k), \underline{u}^{i-1}(k))$ and $\frac{\partial \underline{f_d}}{\partial \underline{u}}(\underline{x}^{(i-1)^*}(k), \underline{u}^{i-1}(k))$ are the gradient of $\underline{f_d}$ with respect to $\underline{x}$ and $\underline{u}$ that are evaluated along $\underline{x}^{(i-1)^*}(k)$ and $\underline{u}^{i-1}(k)$, respectively.

$$\Rightarrow \underline{f_d}(\underline{x}^{(i-1)^*}(k)+\delta\underline{x}^i(k),\underline{u}^{i-1}(k)+\delta\underline{u}^i(k)) = \underline{f_d}(\underline{x}^{(i-1)^*}(k),\underline{u}^{i-1}(k)) + \frac{\partial \underline{f_d}}{\partial \underline{x}}(\underline{x}^{(i-1)^*}(k),\underline{u}^{i-1}(k))\delta\underline{x}^i(k) + \frac{\partial \underline{f_d}}{\partial \underline{u}}(\underline{x}^{(i-1)^*}(k),\underline{u}^{i-1}(k))\delta\underline{u}^i(k) + H.O.T \tag{5.89}$$

Note that;

$$\underline{f_d}(\underline{x}^{(i-1)^*}(k)+\delta\underline{x}^i(k),\underline{u}^{i-1}(k)+\delta\underline{u}^i(k)) = \underline{x}^{(i-1)^*}(k+1)+\delta\underline{x}^i(k+1) \tag{5.90}$$

and

$$\underline{f_d}(\underline{x}^{(i-1)^*}(k),\underline{u}^{i-1}(k)) = \underline{x}^{(i-1)^*}(k+1) \tag{5.91}$$

If the higher order terms are ignored, the equation becomes:

$$\Rightarrow \underline{x}^{(i-1)^*}(k+1)+\delta\underline{x}^i(k+1) = \underline{x}^{(i-1)^*}(k+1) + \frac{\partial \underline{f_d}}{\partial \underline{x}}(\underline{x}^{(i-1)^*}(k),\underline{u}^{i-1}(k))\delta\underline{x}^i(k) + \frac{\partial \underline{f_d}}{\partial \underline{u}}(\underline{x}^{(i-1)^*}(k),\underline{u}^{i-1}(k))\delta\underline{u}^i(k) + H.O.T \tag{5.92}$$

$$\Rightarrow \delta\underline{x}^i(k+1) = \frac{\partial \underline{f_d}}{\partial \underline{x}}(\underline{x}^{(i-1)^*}(k),\underline{u}^{i-1}(k))\delta\underline{x}^i(k) + \frac{\partial \underline{f_d}}{\partial \underline{u}}(\underline{x}^{(i-1)^*}(k),\underline{u}^{i-1}(k))\delta\underline{u}^i(k) \tag{5.93}$$

for $k = 0,...,N-1$

Equation (5.93) can be written as

$$\delta\underline{x}^i(k+1) = A(k)\delta\underline{x}^i(k) + B(k)\delta\underline{u}^i(k) \tag{5.94}$$

where

$$A(k) = \frac{\partial \underline{\underline{f_d}}}{\partial \underline{x}}(\underline{x}^{(i-1)^*}(k), \underline{u}^{i-1}(k))$$

$$B(k) = \frac{\partial \underline{\underline{f_d}}}{\partial \underline{u}}(\underline{x}^{(i-1)^*}(k), \underline{u}^{i-1}(k)) \tag{5.95}$$

This, finally, gives the discrete-time linear dynamical system equation for the deviation of the LQR system.

5.2.4.3.4 Discretization of the Performance Measure

After the linearization of the system dynamics and finally, obtaining the discrete-time linear dynamical system equations, main aim is to formulate the LQR problem.

As in any optimal control problem, the main purpose of the problem is to find a control input trajectory, $\underline{u}^*(k)$, for a given system, that minimizes the performance measure. The performance measure in biped locomotion problem is formulated as a continuous-time quadratic function:

$$J = \frac{1}{2}\left[\underline{x}(t_f) - \underline{x}_d(t_f)\right]^T F\left[\underline{x}(t_f) - \underline{x}_d(t_f)\right] + \frac{1}{2}\int_{t_0}^{t_f} ((\underline{x}(t) - \underline{x}_d(t))^T Q(\underline{x}(t) - \underline{x}_d(t)) + \alpha \underline{u}^T(t) R \underline{u}(t)) dt \tag{5.96}$$

Now, let us write the cost function in discrete form keeping in mind that the process aims to find

$$\underline{x}^i(k) = \underline{x}^{(i-1)^*}(k) + \delta \underline{x}^i(k) \text{ and } \underline{u}^i(k) = \underline{u}^{i-1}(k) + \delta \underline{u}^i(k) \tag{5.97}$$

for $k = 0, ..., N-1$, $i = 1, ..., Iter_{\max}$ so that the cost function will be minimized.

Based on the discrete-time linear dynamic system, let us find the optimal control input by minimizing the cost function:

$$\Rightarrow J_0^i(\delta\underline{u}^i)=\frac{1}{2}\begin{bmatrix}\underline{x}^{(i-1)^*}(N)\\+\delta\underline{x}^i(N)-\underline{x}_d(N)\end{bmatrix}^T F\begin{bmatrix}\underline{x}^{(i-1)^*}(N)\\+\delta\underline{x}^i(N)-\underline{x}_d(N)\end{bmatrix}+$$
$$\frac{1}{2}\Delta t\sum_{k=0}^{N-1}\left\{\begin{matrix}\begin{bmatrix}\underline{x}^{(i-1)^*}(k)\\+\delta\underline{x}^i(k)-\underline{x}_d(k)\end{bmatrix}^T Q\begin{bmatrix}\underline{x}^{(i-1)^*}(k)\\+\delta\underline{x}^i(k)-\underline{x}_d(k)\end{bmatrix}\\+\alpha\left[\underline{u}^{i-1}(k)+\delta\underline{u}^i(k)\right]^T R\left[\underline{u}^{i-1}(k)+\delta\underline{u}^i(k)\right]\end{matrix}\right\} \tag{5.98}$$

Now, define

$$Q_d=\Delta tQ \text{ and } R_d=\alpha\Delta tR \tag{5.99}$$

so that the equation becomes

$$\Rightarrow J_0^i(\delta\underline{u}^i)=\frac{1}{2}\begin{bmatrix}\underline{x}^{(i-1)^*}(N)\\+\delta\underline{x}^i(N)-\underline{x}_d(N)\end{bmatrix}^T F\begin{bmatrix}\underline{x}^{(i-1)^*}(N)\\+\delta\underline{x}^i(N)-\underline{x}_d(N)\end{bmatrix}+$$
$$\sum_{k=0}^{N-1}\left\{\begin{matrix}\frac{1}{2}\begin{bmatrix}\underline{x}^{(i-1)^*}(k)\\+\delta\underline{x}^i(k)-\underline{x}_d(k)\end{bmatrix}^T Q_d\begin{bmatrix}\underline{x}^{(i-1)^*}(k)\\+\delta\underline{x}^i(k)-\underline{x}_d(k)\end{bmatrix}\\+\frac{1}{2}\left[\underline{u}^{i-1}(k)+\delta\underline{u}^i(k)\right]^T R_d\left[\underline{u}^{i-1}(k)+\delta\underline{u}^i(k)\right]\end{matrix}\right\} \tag{5.100}$$

where the paranthesis inside the summation is named as $L(\underline{x}^i(k),\underline{u}^i(k))$.

5.2.4.3.5 LQR Problem Solution

Now, let us begin with the formulation of the Hamiltonian:

$$H(\underline{x}^i(k),\underline{u}^i(k))\triangleq L(\underline{x}^i(k),\underline{u}^i(k))+\underline{\lambda}^{iT}(k+1)\begin{bmatrix}A(k)\delta\underline{x}^i(k)\\+B(k)\delta\underline{u}^i(k)\end{bmatrix} \tag{5.101}$$

$$
\begin{aligned}
\Rightarrow H(\underline{x}^i(k),\underline{u}^i(k)) = \\
&\frac{1}{2}\begin{bmatrix}\underline{x}^{(i-1)^*}(k)\\ +\delta\underline{x}^i(k)-\underline{x}_d(k)\end{bmatrix}^T Q_d \begin{bmatrix}\underline{x}^{(i-1)^*}(k)\\ +\delta\underline{x}^i(k)-\underline{x}_d(k)\end{bmatrix}+\\
&\frac{1}{2}\left[\underline{u}^{i-1}(k)+\delta\underline{u}^i(k)\right]^T R_d\left[\underline{u}^{i-1}(k)+\delta\underline{u}^i(k)\right]+\\
&\underline{\lambda}^{iT}(k+1)(A(k)\delta\underline{x}^i(k)+B(k)\delta\underline{u}^i(k))
\end{aligned}
\tag{5.102}
$$

So the corresponding costate equation is given by:

$$
\underline{\lambda}^i(k) = A^T(k)\underline{\lambda}^i(k+1) + Q_d\left[\underline{x}^{(i-1)^*}(k)+\delta\underline{x}^i(k)-\underline{x}_d(k)\right] \tag{5.103}
$$

The boundary conditions are given by

$$
\underline{\lambda}^i(N) = F(\underline{x}^{(i-1)^*}(N)+\delta\underline{x}^i(N)-\underline{x}_d(N)) \tag{5.104}
$$

The stationary condition is that:

$$
\begin{aligned}
&\underline{u}^i(k) = -R_d^{-1}B^T(k)\underline{\lambda}(k+1)\\
&\Rightarrow \delta\underline{u}^i(k) = -R_d^{-1}B^T(k)\underline{\lambda}^i(k+1)-\underline{u}^{i-1}(k)
\end{aligned}
\tag{5.105}
$$

and inserting this into (5.94) and (5.103) yields:

$$
\begin{aligned}
\begin{bmatrix}\delta\underline{x}^i(k+1)\\ \underline{\lambda}^i(k)\end{bmatrix} &= \begin{bmatrix}A(k) & -B(k)R_d^{-1}B^T(k)\\ Q_d & A^T(k)\end{bmatrix}\begin{bmatrix}\delta\underline{x}^i(k)\\ \underline{\lambda}^i(k+1)\end{bmatrix}\\
&+\begin{bmatrix}-B(k)\underline{u}^i(k)\\ Q_d(\underline{x}^{(i-1)^*}(k)-\underline{x}_d^i(k))\end{bmatrix}
\end{aligned}
\tag{5.106}
$$

The optimal control is a linear costate feedback, but in fact, due to the forcing term in the costate equation and (5.104), it is not possible to express the control law as a linear state feedback as can be done in ideal LQR case.

It is assumed that [197], for all $k \le N$, so that

$$\underline{\lambda}^i(k) = S^i(k)\delta\underline{x}^i(k) - v^i(k) \tag{5.107}$$

for some auxiliary sequences $S^i(k)$ and $v^i(k)$ where $S^i(k)$ is nxn matrix and $v^i(k)$ is an n dimensional vector .

Inserting this equation into (5.106) yields:

$$\delta\underline{x}^i(k+1) = A(k)\delta\underline{x}^i(k) - B(k)R_d^{-1}B^T(k)\begin{bmatrix} S^i(k+1)\delta\underline{x}^i(k+1) \\ -v^i(k+1) \end{bmatrix} - B(k)\underline{u}^i(k)$$

$$\Rightarrow \delta\underline{x}^i(k+1) = A(k)\delta\underline{x}^i(k) - B(k)R_d^{-1}B^T(k)S^i(k+1)\delta\underline{x}^i(k+1) + B(k)R_d^{-1}B^T(k)v^i(k+1) - B(k)\underline{u}^i(k) \tag{5.108}$$

$$\Rightarrow \delta\underline{x}^i(k+1) = (I + B(k)R_d^{-1}B^T(k)S^i(k+1))^{-1}(A(k)\delta\underline{x}^i(k) + B(k)R_d^{-1}B^T(k)v^i(k+1) - B(k)\underline{u}^i(k))$$

$$S^i(k)\delta\underline{x}^i(k) - v^i(k) = Q_d\delta\underline{x}^i(k) + A^T(k)\begin{bmatrix} S^i(k+1)\delta\underline{x}^i(k+1) \\ -v^i(k+1) \end{bmatrix} + Q_d(\underline{x}^{(i-1)^*}(k) - \underline{x}_d^i(k)) \tag{5.109}$$

Now, let's insert (5.108) and (5.109):

$$\begin{aligned} S^i(k)\delta\underline{x}^i(k) - v^i(k) = {} & Q_d\delta\underline{x}^i(k) + \\ & A^T(k)(S^i(k+1)(I + B(k)R_d^{-1}B^T(k)S^i(k+1))^{-1} \\ & (A(k)\delta\underline{x}^i(k) + B(k)R_d^{-1}B^T(k)v^i(k+1) - B(k)\underline{u}^i(k)) - v^i(k+1)) - \\ & Q_d(\underline{x}^{(i-1)^*}(k) - \underline{x}_d^i(k)) \end{aligned} \tag{5.110}$$

$$\Rightarrow S^i(k)\delta\underline{x}^i(k) - v^i(k) = Q_d\delta\underline{x}^i(k) + A^T(k)S^i(k+1)(I + B(k)R_d^{-1}B^T(k)S^i(k+1))^{-1} (A(k)\delta\underline{x}^i(k) + B(k)R_d^{-1}B^T(k)v^i(k+1) - B(k)\underline{u}^i(k)) + - A^T(k)v^i(k+1) + Q_d(\underline{x}^{(i-1)^*}(k) - \underline{x}_d^i(k)) \quad (5.111)$$

$$\Rightarrow \delta\underline{x}^i(k)\begin{bmatrix} -S^i(k) + Q_d + \\ A^T(k)S^i(k+1)(I + B(k)R_d^{-1}B^T(k)S^i(k+1))^{-1}A(k) \end{bmatrix} + \begin{bmatrix} v^i(k) + A^T(k)S^i(k+1)(I + B(k)R_d^{-1}B^T(k)S^i(k+1))^{-1} \\ (B(k)R_d^{-1}B^T(k)v^i(k+1) - B(k)\underline{u}^i(k)) - A^T(k)v^i(k+1) + \\ Q_d(\underline{x}^{(i-1)^*}(k) - \underline{x}_d^i(k)) \end{bmatrix} = 0 \quad (5.112)$$

It is necessary that (5.112) holds for all $\delta\underline{x}^i(k)$ sequences for any given $\delta\underline{x}^i(0)$ which yields the bracketed "[ ]" terms to vanish:

$$S^i(k) = Q_d + A^T(k)S^i(k+1)(I + B(k)R_d^{-1}B^T(k)S^i(k+1))^{-1}A(k) = 0 \quad (5.113)$$

and

$$v^i(k) = \begin{bmatrix} A^T(k) - A^T(k)S^i(k+1)(I + B(k) \\ R_d^{-1}B^T(k)S^i(k+1))^{-1}B(k)R_d^{-1}B^T(k) \end{bmatrix} v^i(k+1) + A^T(k)S^i(k+1)(I + B(k)R_d^{-1}B^T(k)S^i(k+1))^{-1} (B(k)\underline{u}^i(k) - Q_d(\underline{x}^{(i-1)^*}(k) - \underline{x}_d^i(k)) = 0 \quad (5.114)$$

Using the matrix inversion lemma, that is;

$$(A^{-1} + BCD)^{-1} = A - AB(DAB + C^{-1})DA \quad (5.115)$$

equation (5.113) and (5.114) can be written as below:

$$S^i(k) = Q_d + A^T(k)\left[\begin{array}{l} S^i(k+1) - \\ S^i(k+1)B(k)\left[\begin{array}{l} B^T(k)S^i(k+1) \\ +R_d \end{array}\right]^{-1} B^T(k)S^i(k+1) \end{array}\right]A(k) \qquad (5.116)$$

$$\begin{aligned} v^i(k) = -A^T(k)&\left[\begin{array}{l} S^i(k+1)B(k)R_d^{-1} - \\ S^i(k+1)B(k)(B^T(k)S^i(k+1)B(k)+R_d)^{-1} \\ B^T(k)S^i(k+1)B(k)R_d^{-1} - I \end{array}\right]v^i(k+1) + \\ &A^T(k)S^i(k+1)\left[\begin{array}{l} I - B(k)(B^T(k)S^i(k+1)B(k)+R_d)^{-1} \\ B^T(k)S^i(k+1) \end{array}\right]B(k)\underline{u}^i(k) - \\ &Q_d(\underline{x}^{(i-1)^*}(k) - \underline{x}_d^i(k)) \end{aligned} \qquad (5.117)$$

$$\begin{aligned} \Rightarrow v^i(k) = & \\ &- A^T(k)S^i(k+1)B(k)\left[\begin{array}{l} R_d^{-1} - \\ (R_d + B^T(k)S^i(k+1)B(k))^{-1} \\ B^T(k)S^i(k+1)B(k)R_d^{-1} \end{array}\right]B^T(k)v^i(k+1) \\ &+ A^T(k)v^i(k+1) \\ &+ A^T(k)S^i(k+1)B(k)\left[\begin{array}{l} R_d^{-1} - (R_d + B^T(k)S^i(k+1) \\ B(k))^{-1}B^T(k)S^i(k+1)B(k)R_d^{-1} \end{array}\right]R_d\underline{u}^i(k) \\ &- Q_d(\underline{x}^{(i-1)^*}(k) - \underline{x}_d^i(k)) \end{aligned} \qquad (5.118)$$

In order to further simplify this equation, let us use the following fact:

Fact 3:

$$\begin{aligned} R_d^{-1} - (R_d + B^T(k)S^i(k+1)B(k))^{-1}B^T(k)S^i(k+1)B(k)R_d^{-1} = & \\ \left[R_d + B^T(k)S^i(k+1)B(k)\right]^{-1} & \end{aligned} \qquad (5.119)$$

Proof:

$$\left[R_d + B^T(k)S^i(k+1)B(k)\right]^{-1}\left[R_d + B^T(k)S^i(k+1)B(k)\right] = I \qquad (5.120)$$

$$\Rightarrow \left[R_d + B^T(k) S^i(k+1) B(k) \right]^{-1} \left[I + B^T(k) S^i(k+1) B(k) R_d^{-1} \right] R_d = I$$

$$\Rightarrow \left[R_d + B^T(k) S^i(k+1) B(k) \right]^{-1} \left[I + B^T(k) S^i(k+1) B(k) R_d^{-1} \right] = R_d^{-1}$$

$$\Rightarrow \left[R_d + B^T(k) S^i(k+1) B(k) \right]^{-1} +$$
$$\left[R_d + B^T(k) S^i(k+1) B(k) \right]^{-1} B^T(k) S^i(k+1) B(k) R_d^{-1} = R_d^{-1}$$

$$\Rightarrow \left[R_d + B^T(k) S^i(k+1) B(k) \right]^{-1} =$$
$$R_d^{-1} - \left[R_d + B^T(k) S^i(k+1) B(k) \right]^{-1} B^T(k) S^i(k+1) B(k) R_d^{-1} \quad \square$$

By using Fact 3, the above equation becomes:

$$\begin{aligned} \Rightarrow v^i(k) = & \\ & - A^T(k) S^i(k+1) B(k) \left[R_d^{-1} + B^T(k) S^i(k+1) B(k) \right]^{-1} B^T(k) v^i(k+1) \\ & + A^T(k) v^i(k+1) + \\ & + A^T(k) S^i(k+1) B(k) \left[R_d^{-1} + B^T(k) S^i(k+1) B(k) \right]^{-1} R_d \underline{u}^i(k) \\ & - Q_d (\underline{x}^{(i-1)^*}(k) - \underline{x}_d^i(k)) \end{aligned} \tag{5.121}$$

Assuming $S^i(N) = F$ and $v^i(N) = F(-\underline{x}^{(i-1)^*} + \underline{x}_d(N))$ satisfies (5.107) and so these are assumed to be the boundary conditions for $S^i(k)$ and $v^i(k)$.

Now, by inserting (5.107) into the stationary condition, the following is obtained:

$$\delta \underline{u}^i(k) = -R_d^{-1} B^T(k) \left[S^i(k+1) \delta \underline{x}^i(k+1) - v^i(k+1) \right] - \underline{u}^{i-1}(k) \tag{5.122}$$

Since this control depends on $\delta \underline{x}^i(k+1)$, which is not known at time k, substitute (5.94) and (5.122) in order to eliminate this term:

$$\delta \underline{u}^i(k) = -R_d^{-1} B^T(k) S^i(k+1)\Big[A(k)\delta \underline{x}^i(k) + B(k)\delta \underline{u}^i(k) \Big] + R_d^{-1} B^T(k) v^i(k+1) - \underline{u}^{i-1}(k) \tag{5.123}$$

If this equation is rearranged,

$$\delta \underline{u}^i(k) = \Big[B^T(k) S^i(k+1) B(k) + R_d \Big]^{-1} \Big[-B^T(k) S^i(k+1) A(k) \delta \underline{x}^i(k) + B^T(k) v^i(k+1) - R_d \underline{u}^{i-1}(k) \Big] \tag{5.124}$$

is obtained.

For convenience, the above equation can be written as:

$$\delta \underline{u}^i(k) = -K_x(k)\delta \underline{x}^i(k) + K_v(k) v^i(k+1) - K_u(k)\underline{u}^{i-1}(k) \tag{5.125}$$

where

- $K_x(k) = \Big[B^T(k) S^i(k+1) B(k) + R_d \Big]^{-1} B^T(k) S^i(k+1) A(k)$
- $K_v(k) = \Big[B^T(k) S^i(k+1) B(k) + R_d \Big]^{-1} B^T(k)$
- $K_u(k) = \Big[B^T(k) S^i(k+1) B(k) + R_d \Big]^{-1} R_d$
- $S^i(k+1)$ & $v^i(k+1)$ are the solutions of (5.116) and (5.121) with BCs given above.

Before solving the LQR problem for $\delta \underline{u}^i(k)$, first the $\delta \underline{x}^i(k)$ should be obtained and to do so, let us rearrange the (5.108) as below:

$$\delta \underline{x}^i(k+1) = \Big[I - B(k)(B^T(k) S^i(k+1) B(k) + R_d)^{-1} B^T(k) S^i(k+1) \Big] \Big[A(k)\delta \underline{x}^i(k) + B(k) R_d^{-1} B^T(k) v^i(k+1) - B(k)\underline{u}^i(k) \Big] \tag{5.126}$$

$$\Rightarrow \delta \underline{x}^i(k+1) = \begin{bmatrix} A(k) - B(k)(B^T(k)S^i(k+1)B(k) + R_d)^{-1} \\ B^T(k)S^i(k+1)A(k) \end{bmatrix} \delta \underline{x}^i(k) + \begin{bmatrix} B(k)R_d^{-1}B^T(k) \\ -B(k)(B^T(k)S^i(k+1)B(k) + R_d)^{-1} \\ B^T(k)S^i(k+1)B(k)R_d^{-1}B^T(k) \end{bmatrix} v^i(k+1) + - \begin{bmatrix} B(k) - B(k)(B^T(k)S^i(k+1)B(k) + R_d)^{-1} \\ B^T(k)S^i(k+1)B(k) \end{bmatrix} \underline{u}^i(k) \tag{5.127}$$

$$\Rightarrow \delta \underline{x}^i(k+1) = \left[A(k) - B(k)K_x(k)\right] \delta \underline{x}^i(k) + B(k) \begin{bmatrix} R_d^{-1} + \\ -(B^T(k)S^i(k+1)B(k) + R_d)^{-1} \\ B^T(k)S^i(k+1)B(k)R_d^{-1} \end{bmatrix} B^T(k)v^i(k+1) + - B(k) \begin{bmatrix} R_d^{-1} - (B^T(k)S^i(k+1)B(k) + R_d)^{-1} \\ B^T(k)S^i(k+1)B(k)R_d^{-1} \end{bmatrix} R_d \underline{u}^i(k) \tag{5.128}$$

where from Fact 3

$$\left[R_d^{-1} - (B^T(k)S^i(k+1)B(k) + R_d)^{-1} B^T(k)S^i(k+1)B(k)R_d^{-1} \right] = \left[R_d + B^T(k)S^i(k+1)B(k) \right]^{-1} \tag{5.129}$$

So inserting this fact into the above equation yields:

$$\Rightarrow \delta \underline{x}^i(k+1) = \left[A(k) - B(k)K_x(k)\right] \delta \underline{x}^i(k) + B(k) \left[R_d + B^T(k)S^i(k+1)B(k) \right]^{-1} B^T(k)v^i(k+1) + - B(k) \left[R_d + B^T(k)S^i(k+1)B(k) \right]^{-1} R_d \underline{u}^i(k) \tag{5.130}$$

$$\Rightarrow \delta \underline{x}^i(k+1) = \left[A(k) - B(k)K_x(k)\right] \delta \underline{x}^i(k) + B(k)K_v(k)v^i(k+1) - B(k)\, K_u(k)\underline{u}^i(k) \tag{5.131}$$

5.2.4.3.6 Implementation Algorithm for LQR Problem in Biped Locomotion

Step a:

The algorithm to solve the discrete-time LQR will start with a guess for the initial control input trajectory, $\underline{u}^0(k) \quad \forall k$ which is obtained from the results of PID controller simulations.

Step b:

By solving the system dynamics for the initial control input, $\underline{u}^{i-1}(k)$, the initial state variable trajectory, $\underline{x}^{(i-1)^*}(k)$, is found.

Step c:

Obtain the discrete-time linear dynamical system equation for the deviation $\delta\underline{x}^i(k+1)$ by linearizing the system around $\underline{x}^{(i-1)^*}(k)$ and $\underline{u}^{i-1}(k)$ as given in (5.94).

Step d:

In order to solve (5.125) for $\delta\underline{u}^i(k)$, first find the trajectory of $S^i(k)$ by solving (5.116) with the boundary condition $S^i(N) = F$ by backward integration.

Step e:

After finding $S^i(k)$ trajectory, $K_x(k)$, $K_v(k)$ and $K_u(k)$ trajectories can be calculated by using the definitions given in (5.125).

Step f:

In parallel, the trajectory for $v^i(k)$ can also be obtained with the BC $v^i(N) = F\underline{x}_d^i(N)$ by backward integration algorithm applied to (5.121).

Step g:

In order to calculate the deviation in the state variable trajectory, $\delta\underline{x}^i(k)$, the (5.131) is to be solved.

Step h:

$\delta \underline{u}^i(k)$, the deviation in the input control trajectory can be calculated by using (5.125).

Step i:

The updated input control trajectory, $\underline{u}^i(k)$, after iteration i, can be calculated from the output of discrete-time LQR method as below:

$$\underline{u}^i(k) = \underline{u}^{i-1}(k) + \delta \underline{u}^i(k) \quad \forall k$$

and is obtained so that the cost function given by (5.100) is minimized.

Step j:

As the updated control input trajectory $\underline{u}^i(k)$ is obtained, go back to the step b of the algorithm and continue iteration until convergence.

5.2.4.4 Hooke & Jeeves Method in Biped Locomotion Control Problem

5.2.4.4.1 Introduction

The method of Hooke and Jeeves carries out two search types in an iteration cycle consecutively; namely, exploratory search and pattern search, in order to find the minimum of a multidimensional problem as shown in Figure 5.12 [198]. In exploratory search method, starting with an initial guess for control input trajectory, line search as discrete steps along the coordinate directions along one-direction-at-a-time is taken, each of which leads to a new starting point for the next step. After ending up the line search for each of the coordinate axis during the exploratory search, a pattern search along the direction of the control input trajectory of the exploratory moves dictated by the control input trajectory just before the exploratory moves has taken. The iteration cycle including the exploratory seach followed by a pattern search continues until convergence. The main advantage of this method is that it provides multidimensional search without using derivatives.

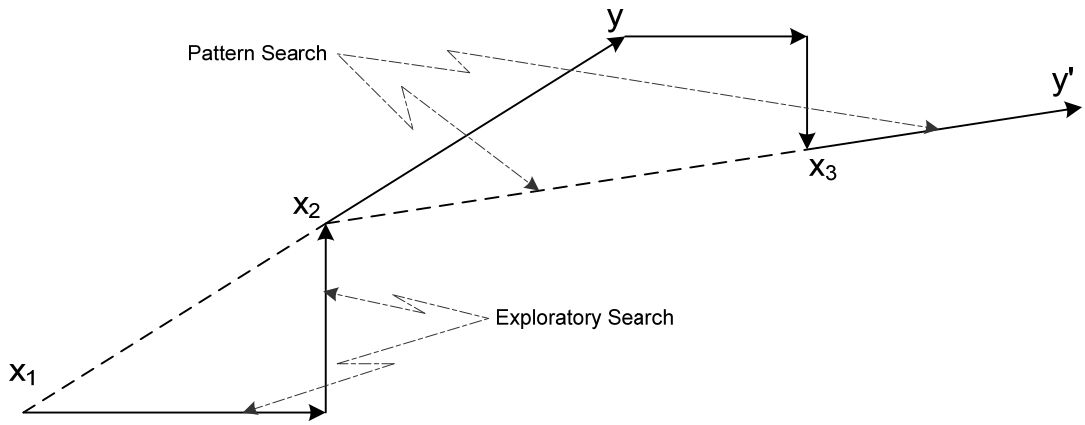

Figure 5.12 Illustration of the Hooke and Jeeves Method

5.2.4.4.2 Hooke & Jeeves Algorithm

Step a: (Initialization)

1) The algorithm to solve the Hooke & Jeeves method starts with a guess for the initial control input trajectory, $\underline{u}_x^0(k) \quad \forall k$.
2) Assign $\underline{u}_y(k) = \underline{u}_x^0(k) \quad \forall k$
3) Let $k = j = 1$

Step b: (Exploratory Search)

1) Find λ_j for

$$\underline{u}_y^{j+1}(k) = \underline{u}_y^j(k) + \lambda_j \, d_j \quad \forall k \tag{5.132}$$

by using "Parabolic Fit" method that gives the optimal solution by minimizing the cost function given by (5.63) for $\underline{u}_y^{j+1}$ control input trajectory, where d_j is the coordinate direction.

2) If $j < n$ being the number of elements in $\underline{u}_y^j$, replace j by $j+1$, and repeat the Step b-1. Otherwise, if $j = n$, let $\underline{u}_x^{i+1} = \underline{u}_y^{j+1}$
3) If $\left\| \underline{u}_x^{i+1} - \underline{u}_x^i \right\| < \varepsilon$, stop; otherwise go to Step c.

Step c: (Pattern Search)

1) Define $\underline{d} = \underline{u}_x^{i+1} - \underline{u}_x^{i}$, and find $\hat{\lambda}$ for

$$\underline{u}_y^{1} = \underline{u}_x^{i+1} + \hat{\lambda}\,\underline{d} \tag{5.133}$$

by using "Parabolic Fit" method that gives the optimal solution by minimizing the cost function given by (5.63) for $\underline{u}_y^{1}$ control input trajectory .

2) Set $j = 1$, replace i by $i+1$, and repeat Step b.

5.3 Guidance Control System for Biped Robot

5.3.1 Introduction

The human walking is controlled by muscles that are trained to walk through a learning process. Furthermore, the human walking is normally not under the central nervous system's conscious control and so there is a spinal cord's low level control on human walking. The limitation of unconscious walking reaction is until there is a disturbance to the normal walking (such as periodic even floor walking) and so until there is a need for control to step over obstacles, to step on the objects, to go up/down stairs, etc. In a similar sense, the biped robot's control structure is designed based on the same idea of two-level controller; namely, High Level Control (or Guidance Control such as Intelligent Control) and Low Level Control (or Supervisory Control such as PID Controller), as depicted in Figure 5.13. The Supervisory Control of biped robot is explained in Section 5.2 of this chapter. Therefore, the focus of this section is Guidance Control System of biped robot.

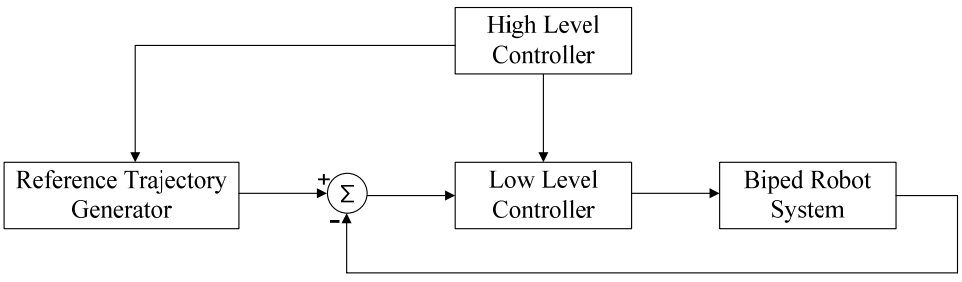

Figure 5.13 Block diagram representation of the overall system

The Guidance Controller is designed as a Genetic Algorithm based HLC that determines the biped system's reference footstep walking trajectory from a given global path data while minimizing a performance measure by ensuring the stability of biped.

5.3.2 Genetic Algorithm Based Optimization Process

Genetic algorithm (GA) is an evolutionary technique that uses crossover and mutation operators to solve optimization problems using a survival of the fittest idea. There is a large class of interesting problems for which no reasonably fast algorithms have been developed. Many of these problems are optimization problems that arise frequently in applications. Given such a hard optimization problem, it is often possible to find an efficient algorithm whose solution is approximately optimal. For some hard optimization problems, probabilistic algorithms can be used as well – these algorithms do not guarantee the optimal value, but by randomly choosing sufficiently many candidates, the probability of error can be made as small as possible. GAs are among stochastic algorithms whose search methods model some natural phenomena.

The GA searchs the optimum from a population of points in parallel and posses more chances to find the global optimum than the classical optimization methods. The robustness of the search process and the effectiveness of their genetic operators, such as crossover, mutation, and the selection, etc., make this method full of vitality. Many of the engineering problems can apply the GAs, such as function optimization, pattern recognition, signal processing, robotics, feature extraction, etc. The GAs have become one of the basic tools in artificial intelligence together with the expert systems and the artificial neural networks.

GA performs a multi-directional search by maintaining a population of potential solutions and encourages information formation and exchange between these directions. The population undergoes a simulated evolution: at each generation the relatively "good" solutions reproduce, while the relatively "bad" solutions die. To distinguish between different solutions, an objective (evaluation) function is used, which plays the role of an environment.

5.3.3 Guidance Control System Design

The aim of the guidance control system is to define certain walking parameters to be used by the biped robot system and to determine the sequence of pattern classes to be followed by the biped robot by using optimality principle and stability of biped for a given path. When a global path composed of stairs, obstacles, etc. and certain walking parameters, such as the speed of walking and total walking time, are given to the system as a task to achieve, the Guidance Controller determines each consequence step trajectory in terms of step patterns by using a genetic algorithm based optimization process while ensuring biped's stability criterion.

In biped robot guidance control system, the genetic algorithm based optimization problem can be stated as below:

Given a global path to be followed by the biped, find sequence of pattern classes with its properties by minimizing the energy consumed by the biped while ensuring the stability criterion.

So, in order to solve this problem, the genetic algorithm based optimization process minimizes a performance function that gives a measure for the biped energy consumed during walking by ensuring the biped stability constraints. The output of the process is a sequential set of pattern classes, whereas each element of this set corresponds to a pattern class and its necessary parameters such as step size, speed, etc. As an example, for the global path given in Figure 5.14, that is desired to be walked smoothly by the biped, the global path input data to the guidance unit is formulated from this figure as in Table 5-3. Then, the guidance unit produces the biped path in the form of sequence of patterns as demonstrated in Table 5-4. So, Table 5-4 is the output of the guidance control system. The sequence of pattern classes and parametric information in this table is found by using genetic algorithm method that minimizes the performance measure in the form of energy while ensuring the stability.

The biped robot limitations such as the maximum and the minimum step length, upper and lower bound for step time, total distance to travel (determined from the given global path), stability criterion, etc. are given to the genetic algorithm optimization problem as constraints. In solving this problem, the stability criterion is taken to ensure ZMP measure,

as the details are given in Chapter 3. As a result, guidance control unit achieves to find the footstep trajectory resulting in energy optimal foot step parameters such as step length, step speed, etc. for a given desired global path as per the different environmental conditions.

Table 5-3 An exemplary global path input to the HLC

Corner Point	Height of Stair
0	0
0.45	Hs1
1.35	-Hs2
2.25	Hs3
2.55	Hs3
3.45	-Hs4
3.75	-Hs4
4.5	0

Table 5-4 An exemplary output of the HLC in the form of footstep trajectory

Pattern Class	Step Time	Step Length	Stair Height	x-coord of Stair	Stair Up/Down
1	Tc1	Ls1	0	0	0
2	Tc2	Ls2	Hs1	Lx2	1
3	Tc3	Ls3	Hs1	-Lx3	0
1	Tc4	Ls4	0	0	0
5	Tc5	Ls5	Hs2	Lx5	-1
6	Tc6	Ls6	Hs2	-Lx6	0
1	Tc7	Ls7	0	0	0
2	Tc8	Ls8	Hs3	Lx8	1
4	Tc9	Ls9	Hs3	Lx9	1
3	Tc10	Ls10	Hs3	-Lx10	0
1	Tc11	Ls11	0	0	0
5	Tc12	Ls12	Hs4	Lx12	-1
7	Tc13	Ls13	Hs4	Lx13	-1
6	Tc14	Ls14	Hs4	-Lx14	0
1	Tc15	Ls15	0	0	0

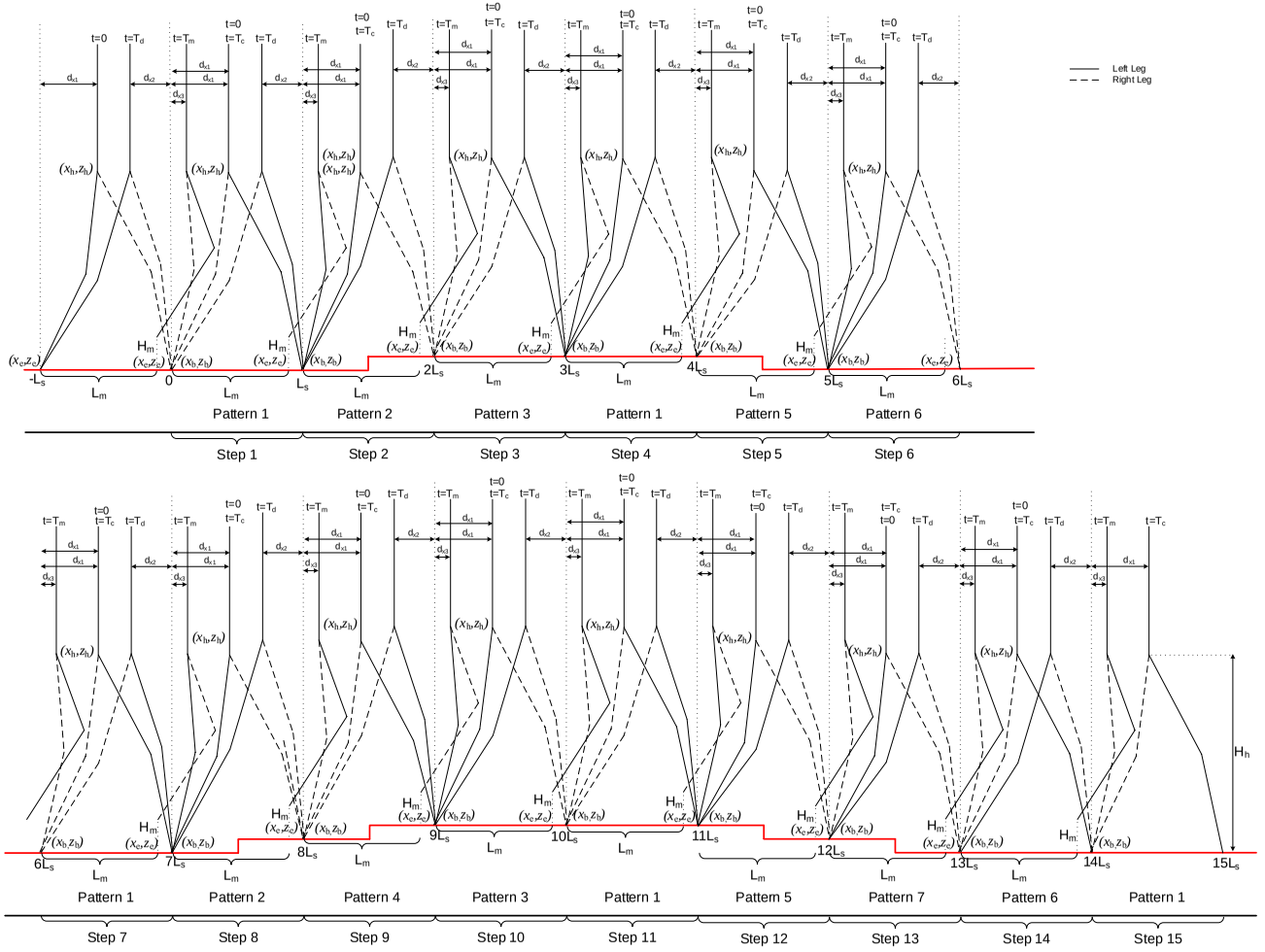

Figure 5.14 Desired Biped Path

CHAPTER 6

BIPED DYNAMIC SIMULATION AND RESULTS

6.1 Overview

The controlled biped system is created and simulated in MATLAB and the simulation results are presented in this chapter. The biped system used in the simulations is 5-link 7 DOF biped with the mathematical model as presented in Chapter 2.

6.2 Physical Parameters of 5-Link Biped Robot

The biped robot's physical parameters are identified in Chapter 2 as depicted in Figure 6.1. The physical parameters of the biped used in the simulations are given in Table 6-1.

Table 6-1 The physical parameters of the 5-link 7 DOF biped

Link		**Mass, *m*, (kg)**	**Moment of Inertia, *I*, (kg-m2)**	**Length, *l*, (m)**	**Location of center of mass, *d*, (m)**
1, 5	Shank	2.23	3.30e-2	0.332	0.189
2, 4	Thigh	5.28	3.30e-2	0.302	0.236
3	Upper Body	14.79	3.30e-2	0.486	0.282

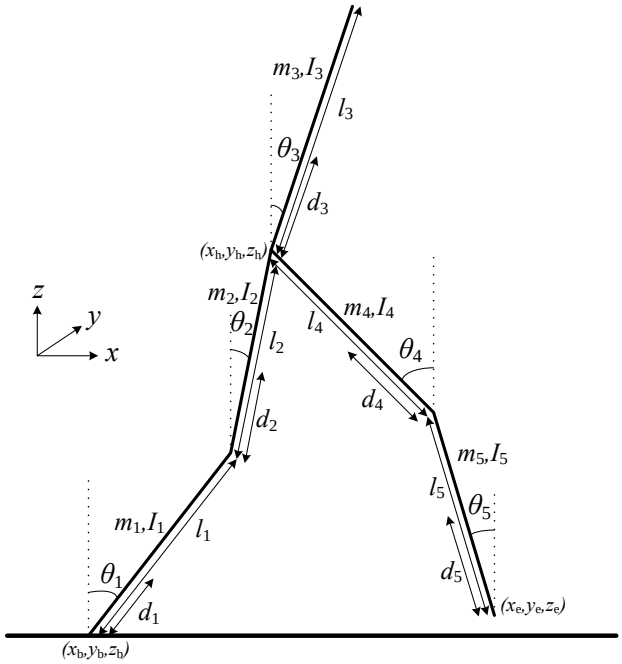

a) in Sagittal Plane

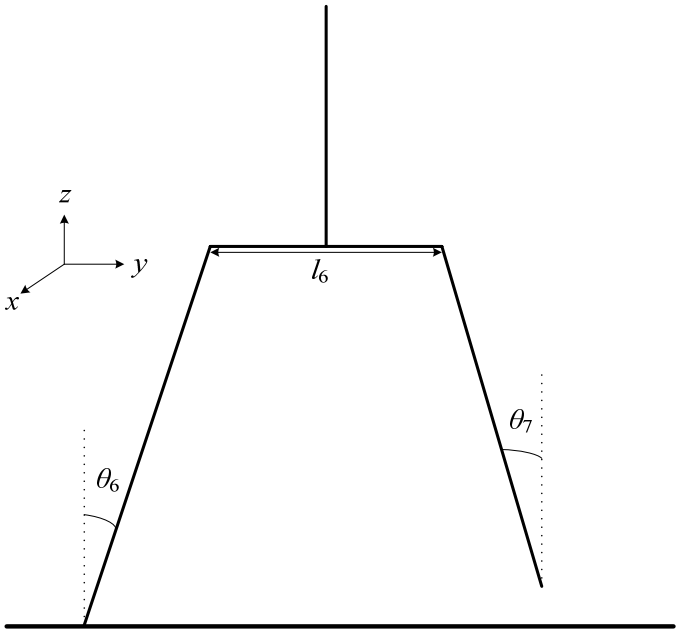

b) in Frontal Plane

Figure 6.1 5-Link 7 DOF biped robot physical parameters

6.3 Biped Dynamic Simulator

The biped dynamic simulator is implemented in MATLAB. The simulator, called BipedWalker3D, is composed of the following components:

1) Forward Dynamics Integrator (FDI)
2) High Level Controller (HLC)
3) Trajectory Planner (TP)
4) Low Level Controller (LLC)
5) Animator

Forward Dynamics Integrator is designed to solve the motion equations of the biped in differential equation form. The differential equation is solved in three different ways; by using MATLAB ODE Solver, Runge-Kutta (4,5) Solver and Forward Integration. These methods are compared and the results are given in the following sections of this chapter.

High Level Controller is the guidance unit of the system. The first step taken during the simulation is the generation of the guidance commands by HLC. For the desired global walking path given, the HLC creates the foot step trajectory (sequence of pattern classes with their parameter properties) by minimizing the energy of the system while ensuring the stability criterion. Genetics Algorithm method is used to find the foot step trajectory.

Trajectory Planner generates swing leg ankle and hip point trajectories for a given pattern class by using 3rd Order Spline Interpolation method. Thereafter, all limb trajectories in Cartesian coordinates and also corresponding joint angle and velocity trajectories (by inverse kinematics) are also calculated by TP. These trajectories are then used by the low level controller as reference to run the biped dynamics.

Low Level Controller produces the control input to the biped system in order to enable the system run as desired and ruled. Many control methods, namely, PID Control, Computed Torque Control, Modified Computed Torque Control and Optimal Control (Steepest Descent Method, Hooke and Jeeves Method, LQR) methods are applied to the system. Some of these methods produced more successful results compared to others. The results and comparison of these methods are all presented in the following sections of this chapter.

Animator presents a visual demonstration for biped locomotion. It generates sagittal and frontal plane views of biped, separately but simultaneously while walking (Figure 6.2). Upon to desire, the view can be switched to a 3D view (Figure 6.3). Animator also visualizes the environment and desired walking path. In other words, it animates the biped robot while walking and depicts the environment (path) it interacts while walking.

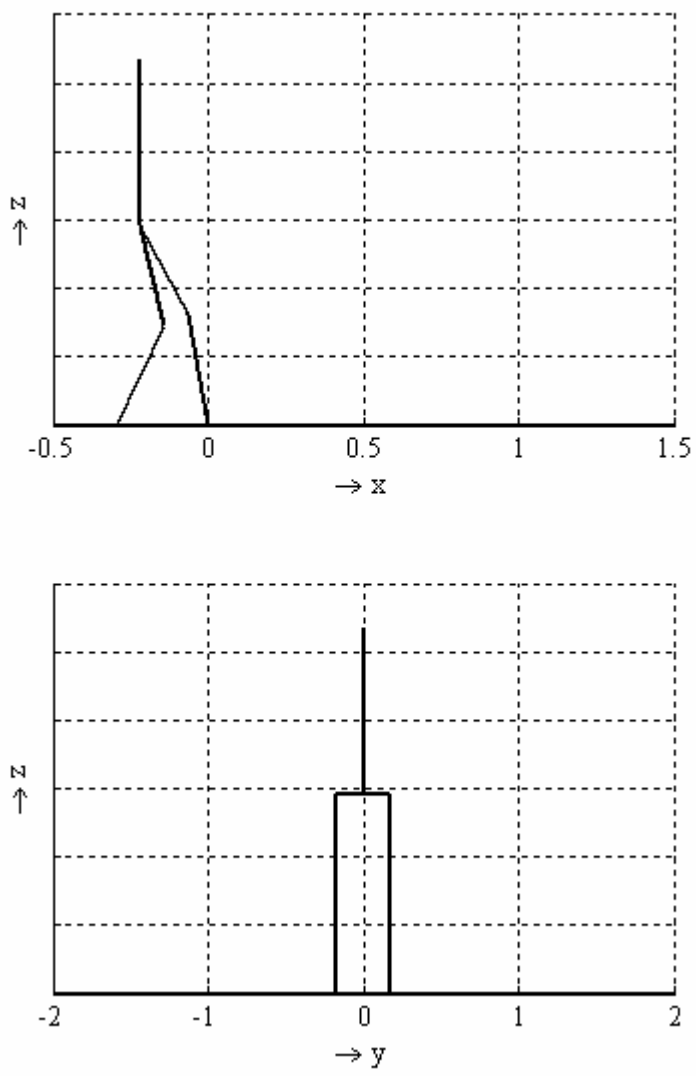

Figure 6.2 Biped simulator sagittal (top) and frontal (bottom) plane views

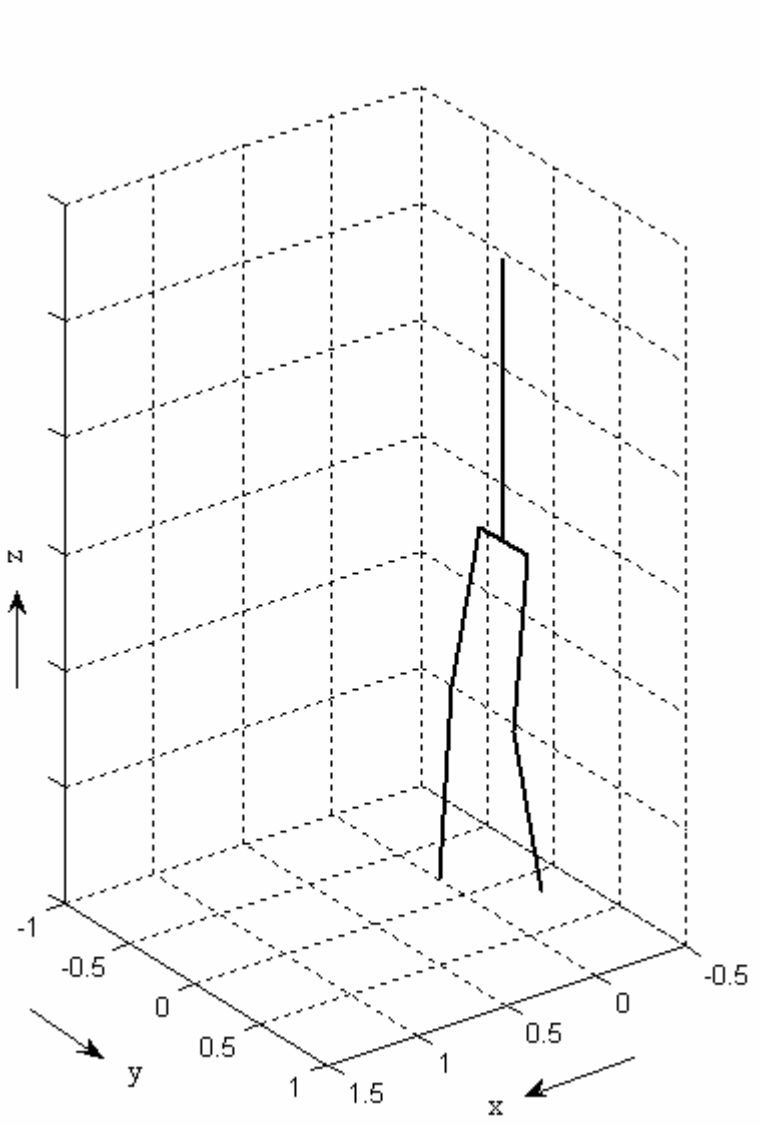

Figure 6.3 Biped simulator 3D view

6.4 Simulation Results

6.4.1 Preliminary Work Simulation Results

6.4.1.1 Ground Reaction Force Analysis

SL is used to realize the dynamic simulation of biped locomotion in the Ground Reaction Force Analysis, which is realized as a preliminary work prior to the development of the BipedWalker3D. The robot model used in this simulator is 7-link 10 DOF robot. The link

structure of the robot is given in Figure 6.4. The simulation is done under the assumption that the movement of the robot is independent in frontal and sagittal planes. In frontal plane, the total DOF is 4 and in sagittal plane, the total DOF is 6. Total height of the robot is 1.325 m. The walking cycle of the robot is 2 seconds and the reference input data frequency is 100 datas/second.

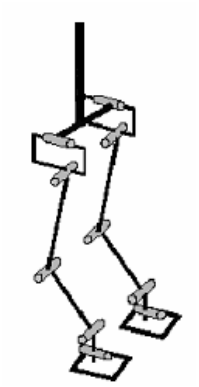

Figure 6.4 Link structe of the biped robot as used in the SL simulation

After collecting data from simulation results, the analysis of smooth transition and landing impact is done and MATLAB is used as a graphical tool to plot the results of the simulation. The snapshots of walking simulation in frontal and sagittal planes are given in Figure 6.5.

The analysis of parametric change is divided into two parts. In the first part, the effects of controller gain parameters on GRF and ZMP is discussed and the simulation results corresponding to different gain values (high gain-low gain) is presented. In the second part, the effects of frontal gait Inverted Pendulum Model parameters such as change in the lean angle and change in the double-support & single-support time ratio on GRF and ZMP is compared and the simulation results are given.

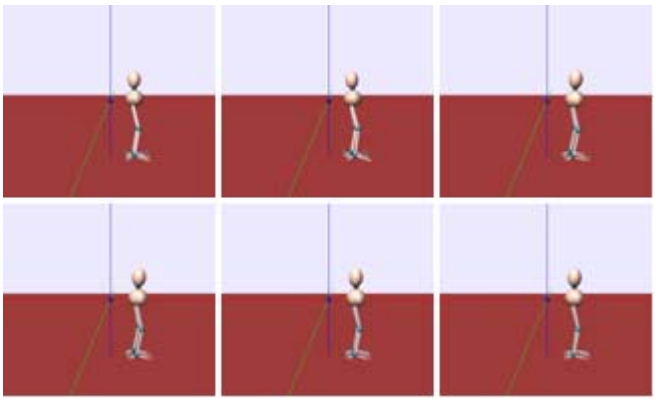

a) Sagittal Plane

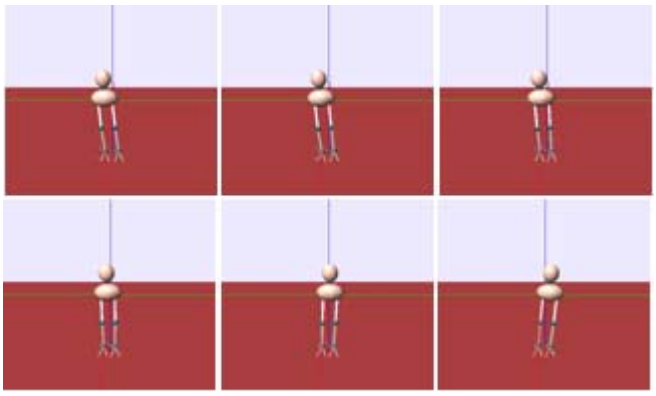

b) Frontal Plane

Figure 6.5 Experimental results using SL simulation

The simulation results showing GRF and ZMP for default values used for controller gain parameters and Inverted Pendulum Model are given in Figure 6.6 and Figure 6.7, respectively.

Default values of the PID proportional gain parameters are 500 for hip and knee joints and 200 for ankle joints. The effects of changing gain in sagittal and frontal planes are considered separately. In SL Simulation, the contact ground has an elastic structure. So the result obtained from the simulation is processed using a thresholding filter and then the results are given. In the sagittal plane, when the PID proportional controller parameter is changed, the performance of the robot so the smoothness of the transition is also changed. When the gain is increased, the robot can walk faster but the stability is worse and when

the gain is decreased, the robot performance is slower but the stability is higher. The simulation results for different values of controller parameter is given in Figure 6.8.

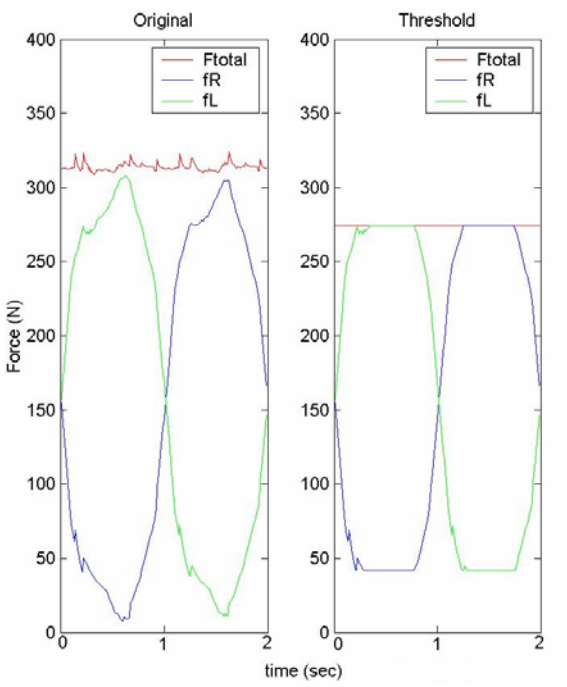

Figure 6.6 GRF simulation results for the default values of controller gain and inverted pendulum model parameters

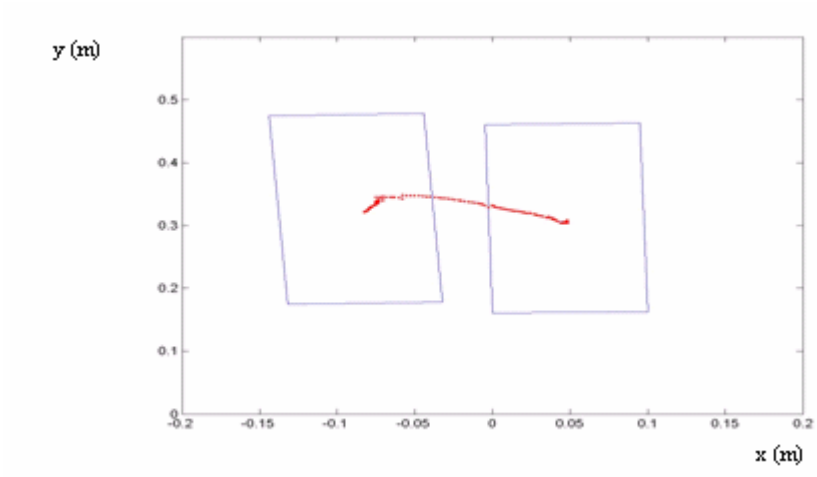

Figure 6.7 ZMP simulation results for the default values of controller gain and inverted pendulum model parameters

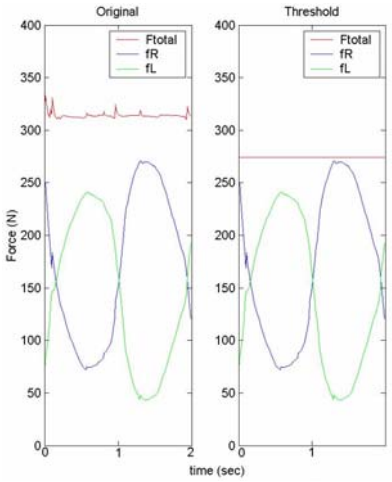

a) High Gain

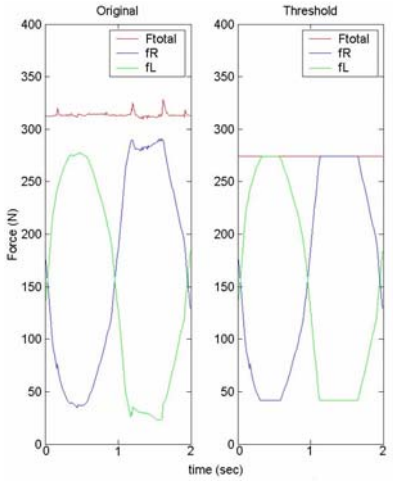

b) Low Gain

Figure 6.8 Simulation results for sagittal plane controller gain parameters

In frontal plane, when the PID proportional controller parameter is increased, the performance of the robot increased in terms of fast response, but the stability margin is decreased. The simulation results for different values of controller parameter is given in Figure 6.9.

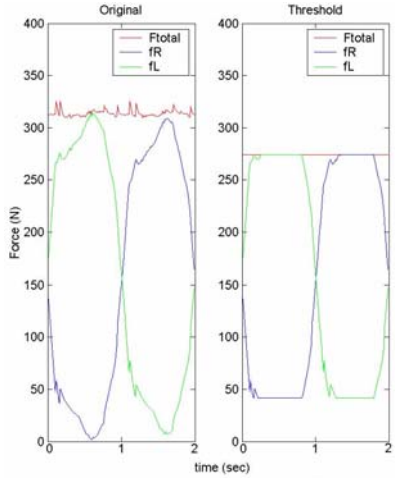

a) High Gain

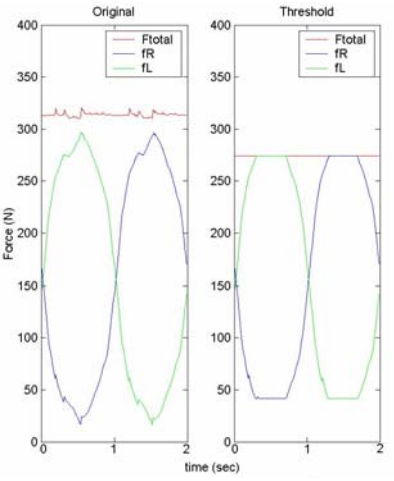

b) Low Gain

Figure 6.9 Simulationesults for frontal plane controller gain parameters

Decreasing the lean angle in frontal plane Inverted Pendulum model results in a decrease of ZMP stability margin. On the other hand, increase of lean angle causes a faster walking but also results difficulty in locomotion initialization process. Another parameter that is used for analysis in frontal gait model is double-support/single-support (ds/ss) time ratio that is affecting the GRF and ZMP trajectory. Increase in the ds/ss time ratio results in better stability margin and good walking performance. The simulation results show that the desired GRF trajectory is realistic. The GRF results obtained from the simulation for different parametric constraints also show that in single support phase, total external force is under the foot touching ground and almost constant, and in double support phase, the transition of force from one foot to the other is smooth. In order to control the GRF and ZMP trajectories, high-level intelligent control techniques, such as neural network algorithms, fuzzy logic and reinforcement learning can be applied.

6.4.1.2 Hybrid Fuzzy Control Using 3D Inverted Pendulum Model

The PD controller parameters that are used in the simulation are the boundary values of fuzzy controller for changing the controller from one to another. The simulation results for different fuzzy controller parameters are presented in Figure 6.10.

The best result from the simulation is obtained for the following values of the fuzzy controller:

a=4 and b=8

When we a and b parameters are increased further, the stability of the system gets worse. The application of this controller to a biped system results in a stable walking in the simulation. The IPM model of the biped system is used in order to have a periodic stable biped walking. The fuzzy controller is used to control the stabilization process. When the pendulum is near to and away from the vertical position, different PD controllers with different PD parameters are used in order to respond different conditions of walking.

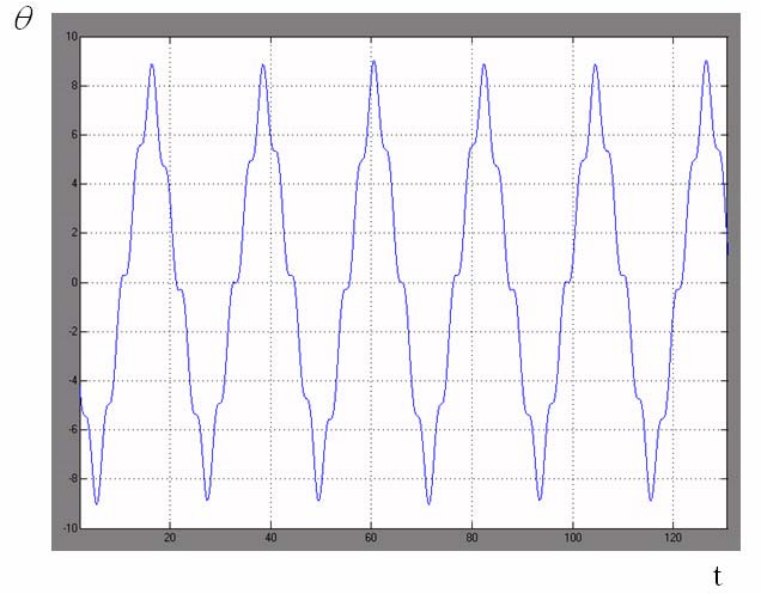

a) a=4, b=8

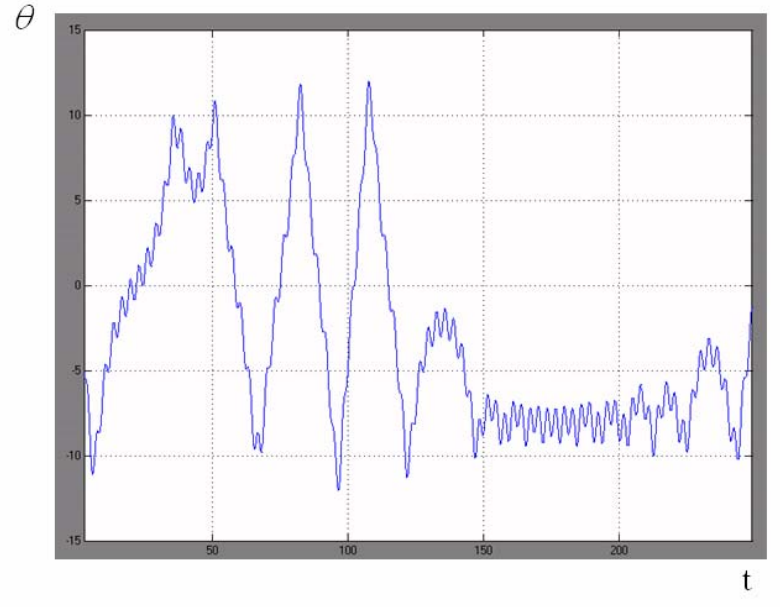

b) a=8, b=10

Figure 6.10 Simulation results for various values of fuzzy controller parameters

6.4.2 Reference and Simulator Trajectories

The biped always starts walking by its left foot, which means right leg is the stance and left leg is the swing feet during the first step. Afterwards, sequentially, the order changes as shown in Figure 6.11.

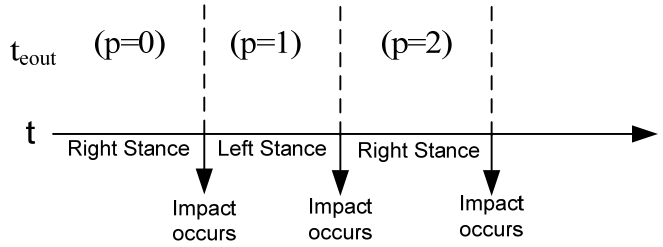

Figure 6.11 Biped robot walking sequence

A very important purpose in biped locomotion is to achieve a dynamic walking that follows the desired trajectory as much as possible. The reference trajectory vs. simulator trajectory results are given in Figure 6.12 and Figure 6.13.

Furthermore, the corresponding reference and simulator angle and angular velocity trajectories are given in Figure 6.14 to Figure 6.17.

The tracking error between the reference and simulated angle and velocity trajectories for the system controlled by PID controller is also depicted in Figure 6.18 and Figure 6.19.

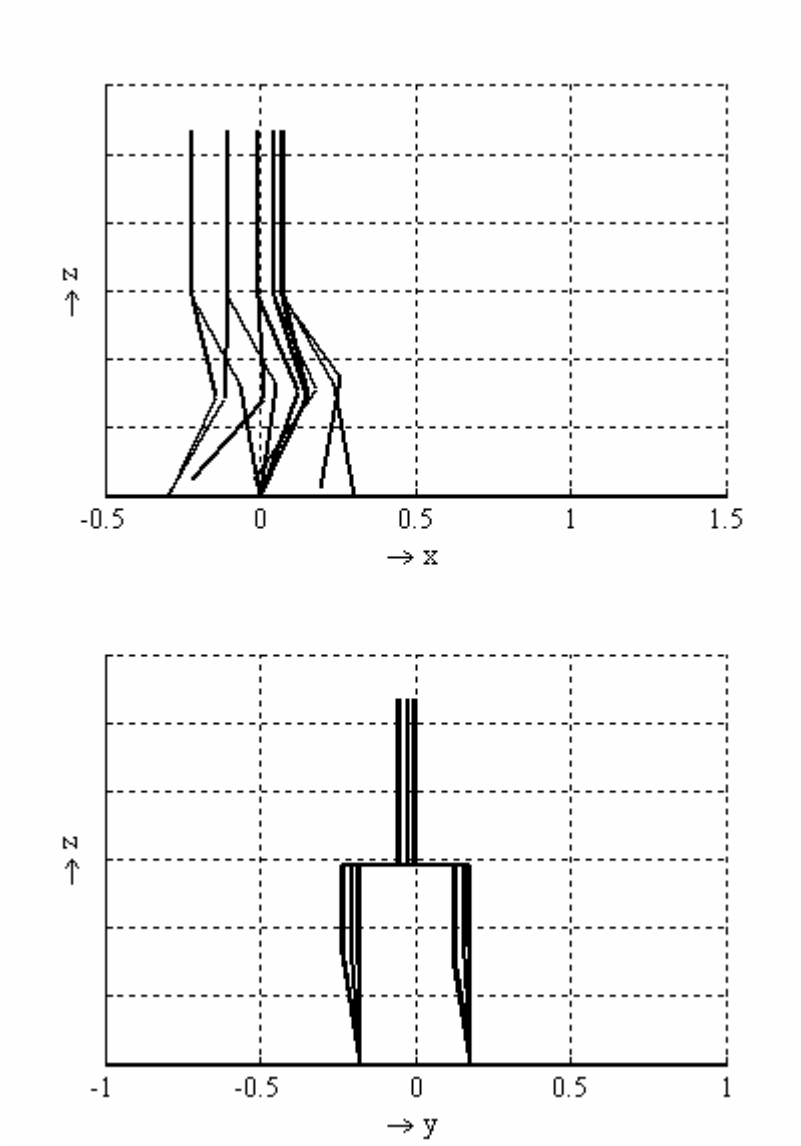

Figure 6.12 Reference trajectory walking snapshot - sagittal (top) and frontal (bottom) plane views

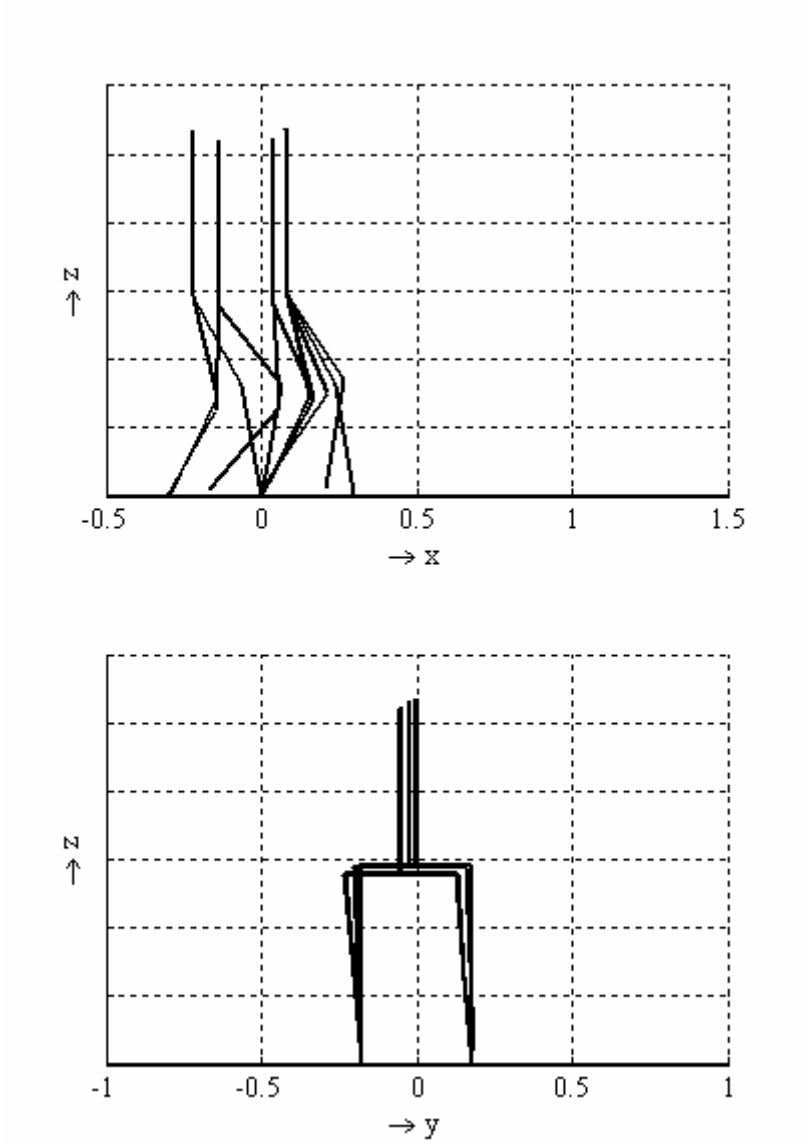

Figure 6.13 Simulator trajectory walking snapshots

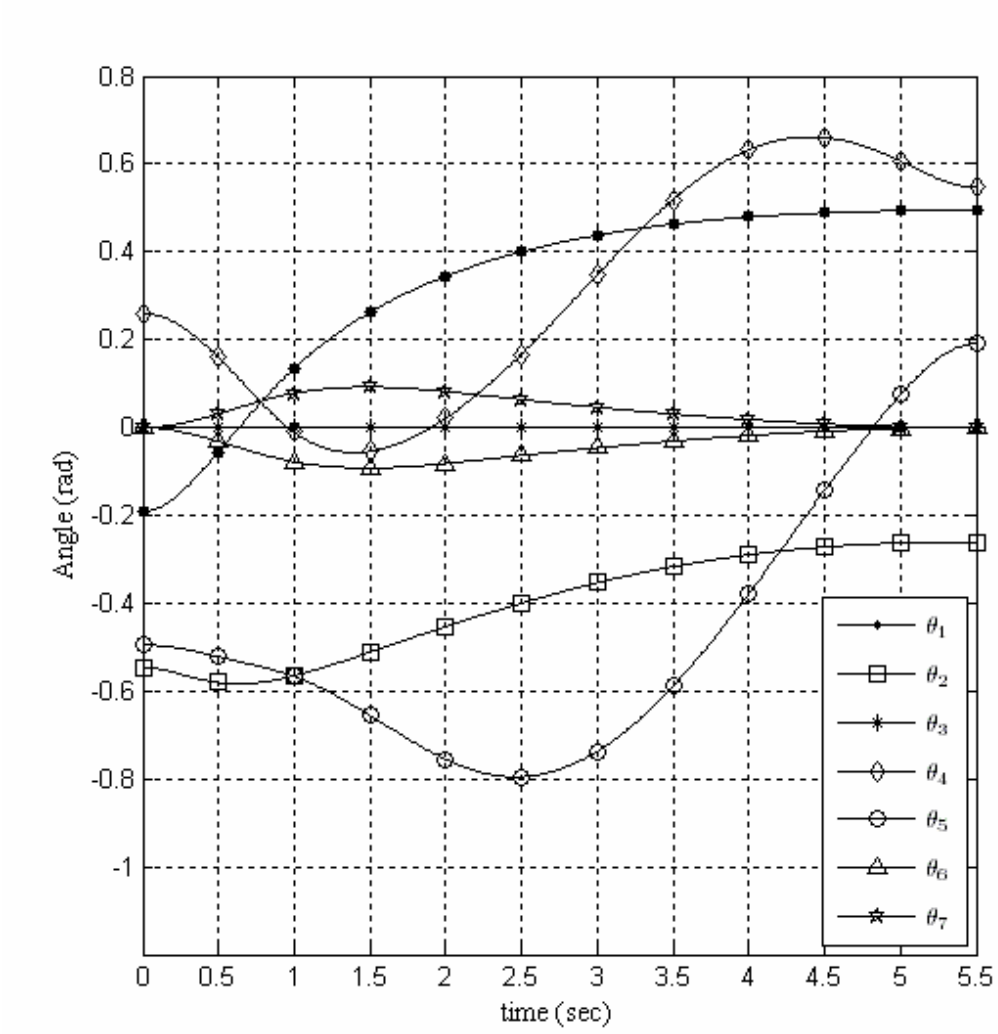

Figure 6.14 Reference trajectory joint angle profile

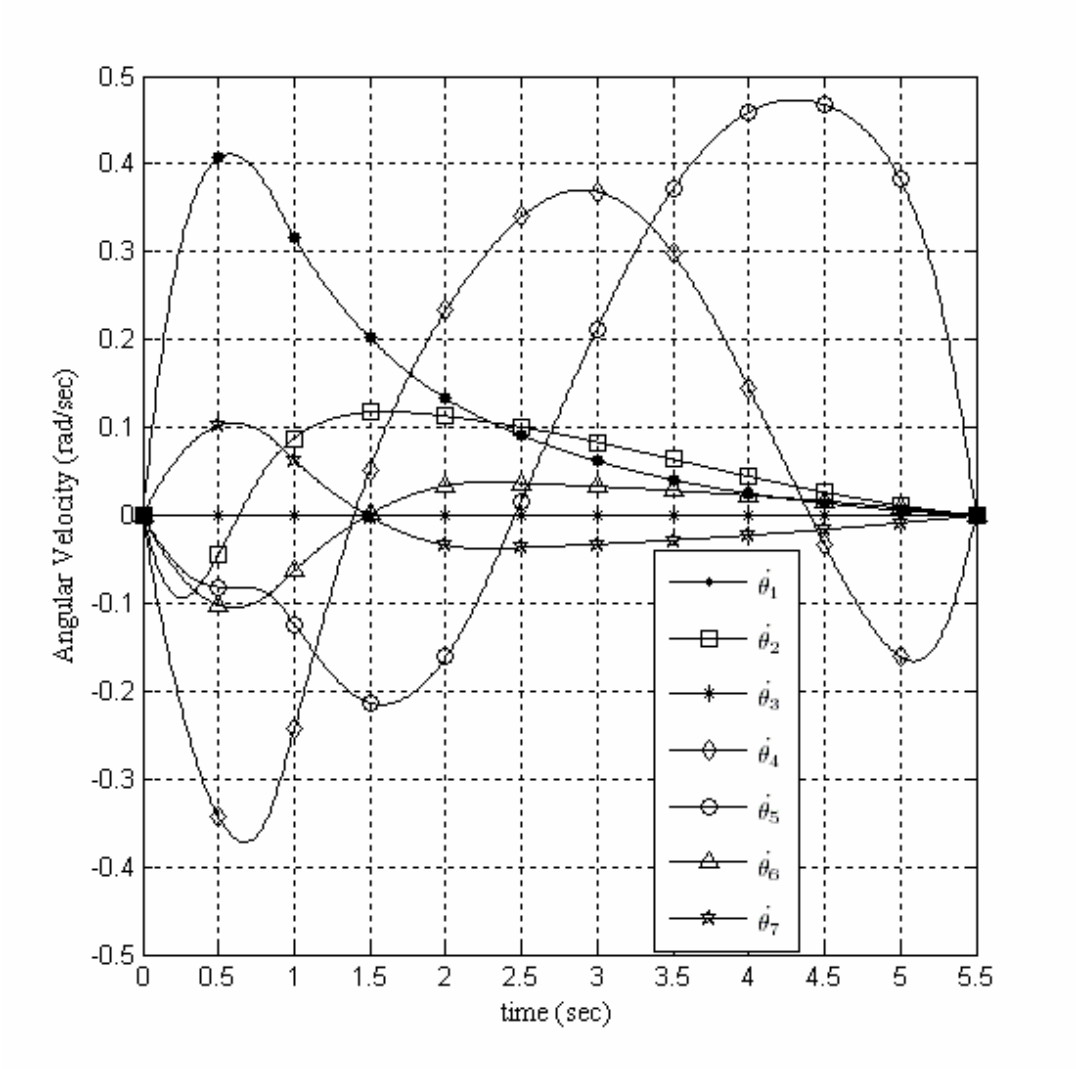

Figure 6.15 Reference trajectory joint angular velocity profile

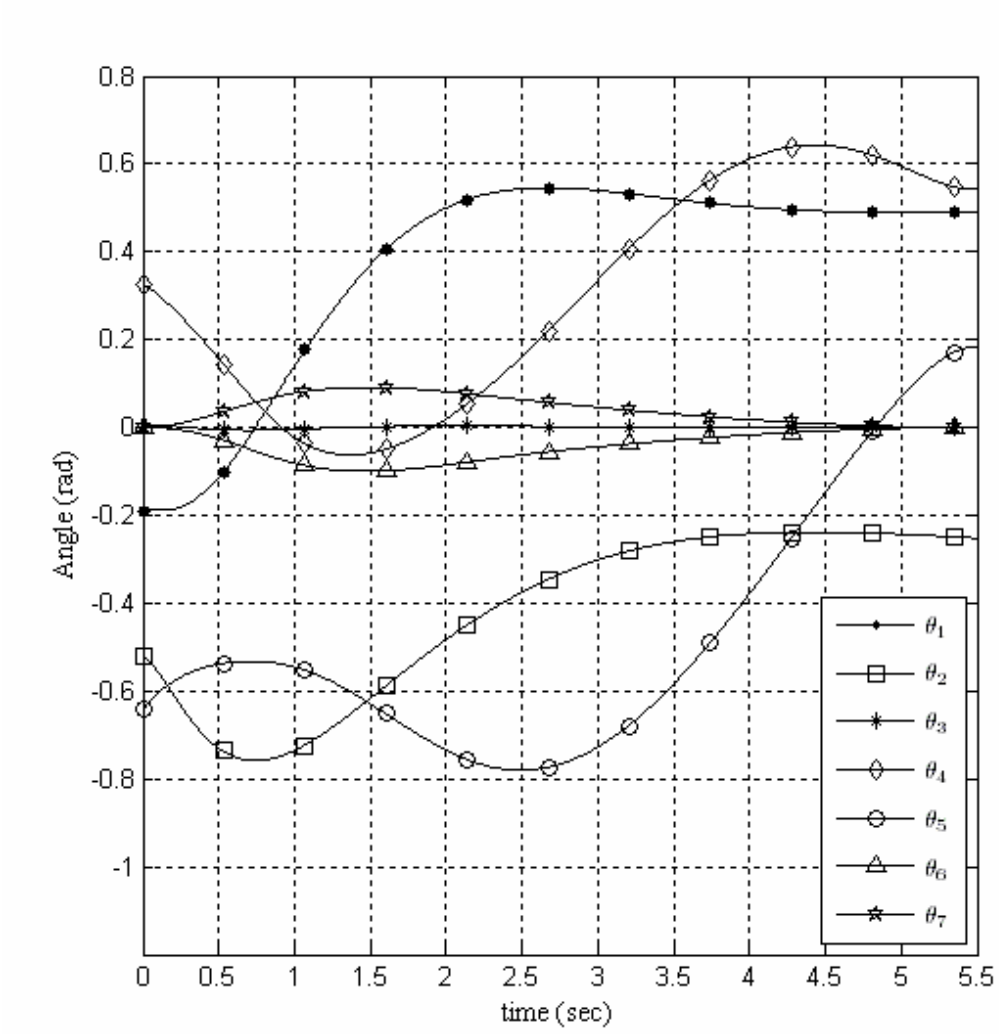

Figure 6.16 Simulated trajectory joint angle profile

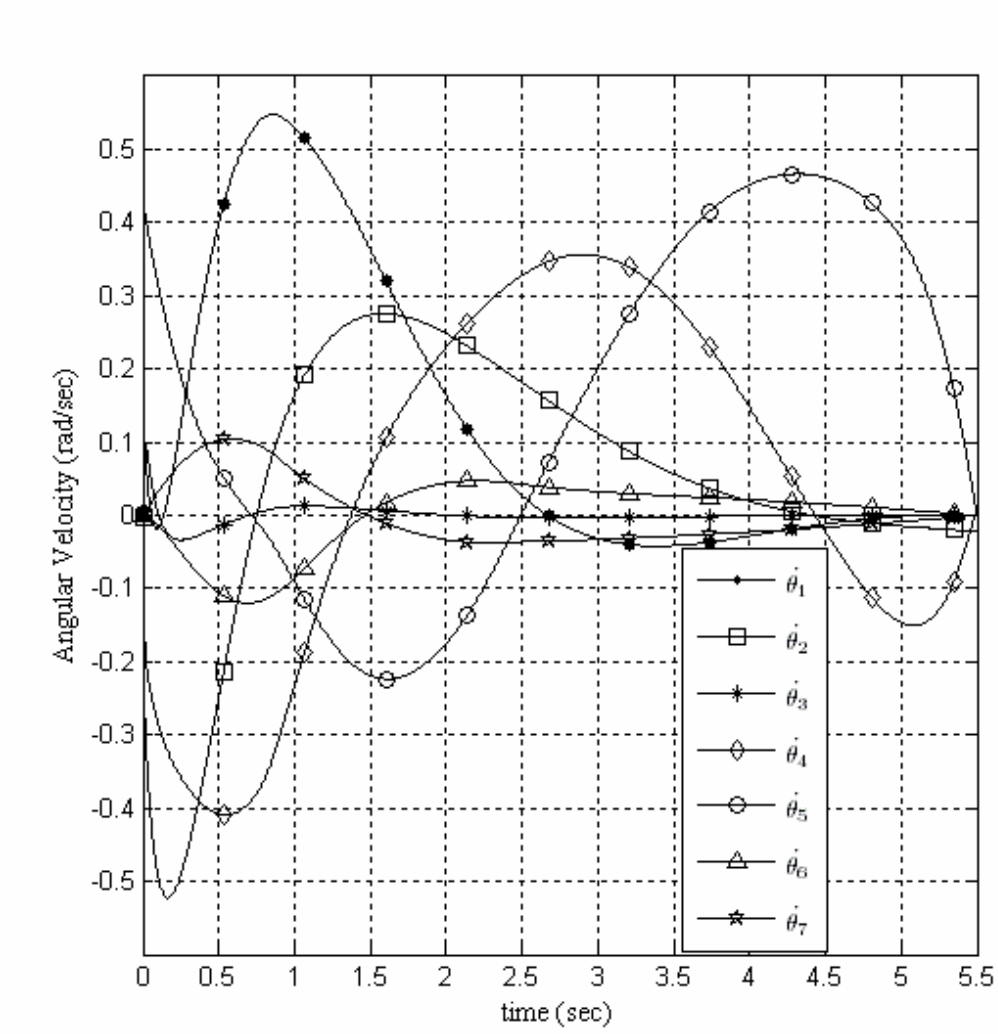

Figure 6.17 Simulated trajectory joint angular velocity profile

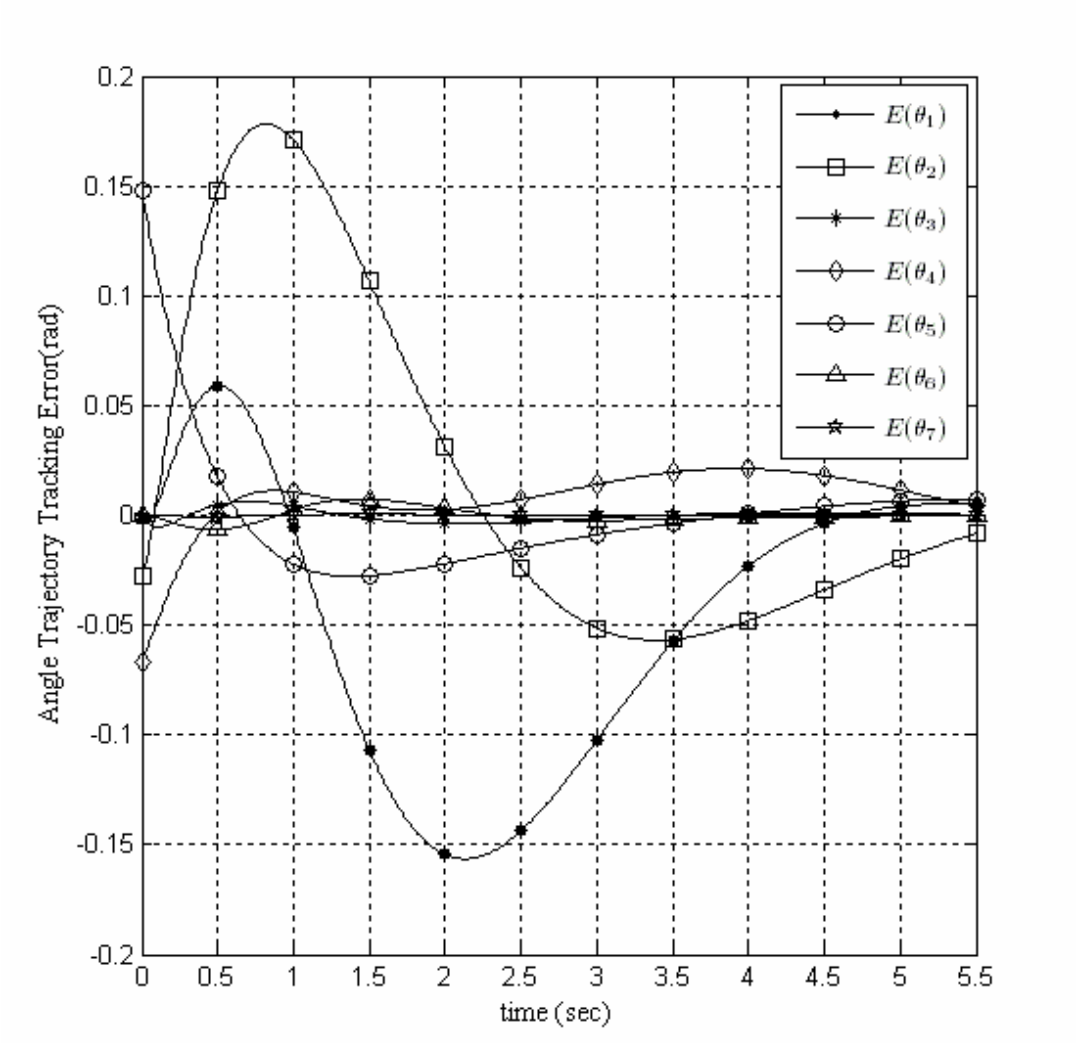

Figure 6.18 Angle trajectory tracking error obtained with PID controller

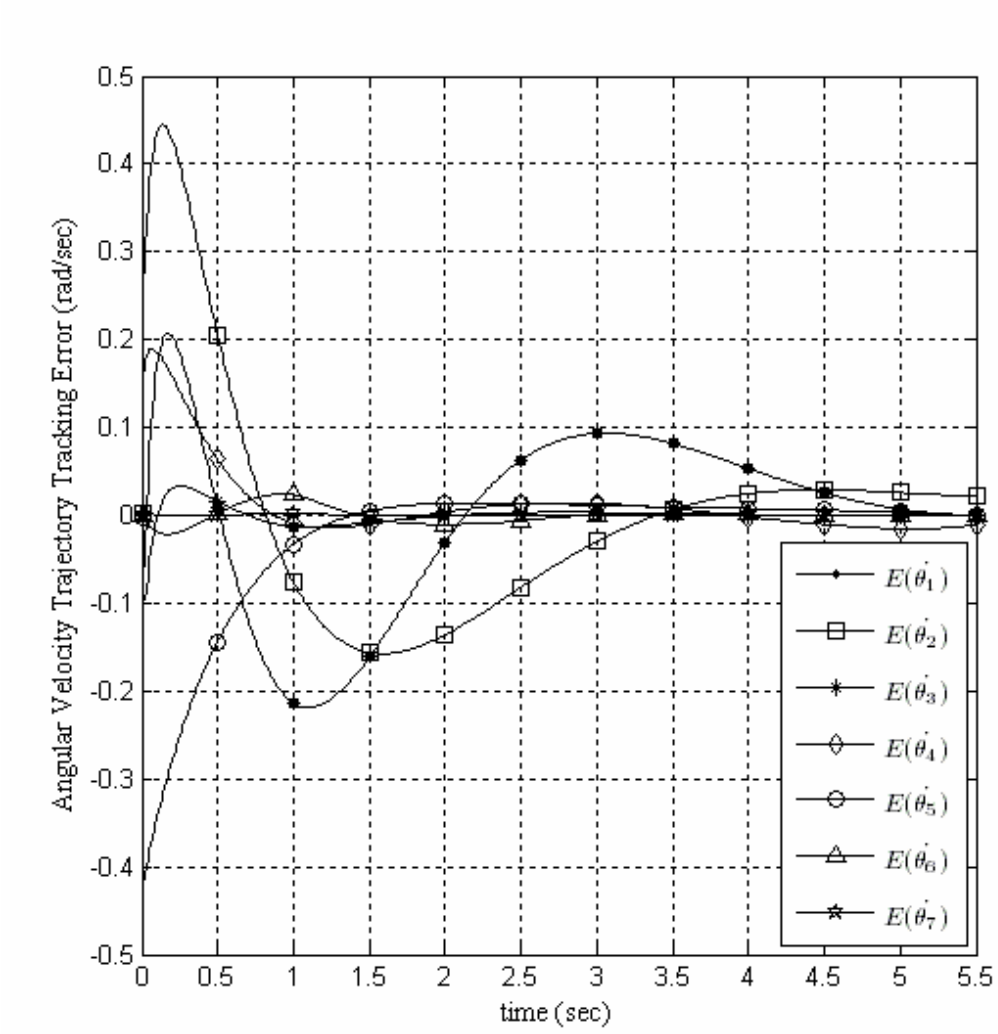

Figure 6.19 Angular velocity trajectory tracking error obtained with PID controller

6.4.3 Walking at Different Locomotion Parameters

Biped walking implies many different locomotion parameters, such as walking speed, step length, swing leg ankle point maximum height, etc. For different parameters, the results of the walking trajectory, the measure of stability, controller inputs, etc., generally, change.

In this context, when the walking speed is doubled from 5.4545 cm/sec to 10.9091 cm/sec by decreasing the step time from 5.5 sec to 2.75 sec while keeping the step length constant, the resulting angle and angular velocity trajectories and the snapshots of the walking are given in Figure 6.20 to Figure 6.22. For the initial speed motion, the corresponding angle and angular velocity trajectories and the snapshots of the walking were given before in Figure 6.14 to Figure 6.17.

When the speed of the walking is doubled by decreasing the step time, the walking of the biped is still stable and looks like natural human walking. On the other hand, the overshoot in the angular velocity profiles is increased.

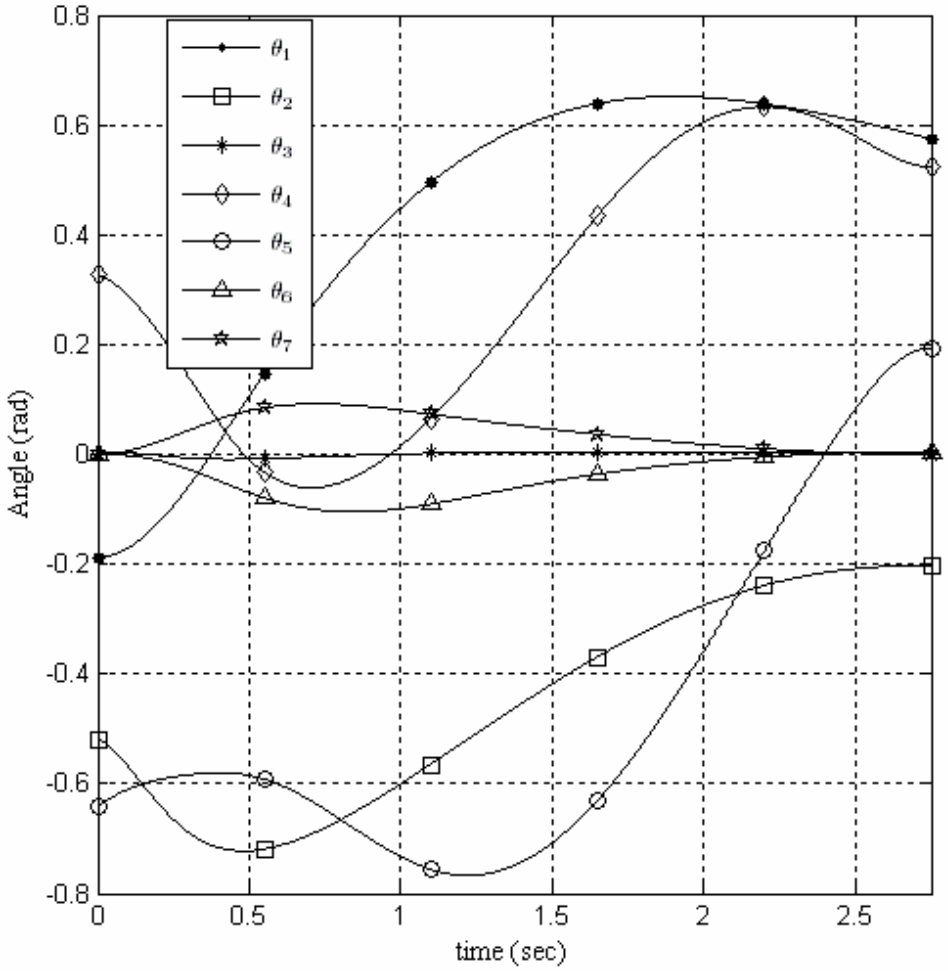

Figure 6.20 Simulated trajectory joint angle profile for doubled speed motion

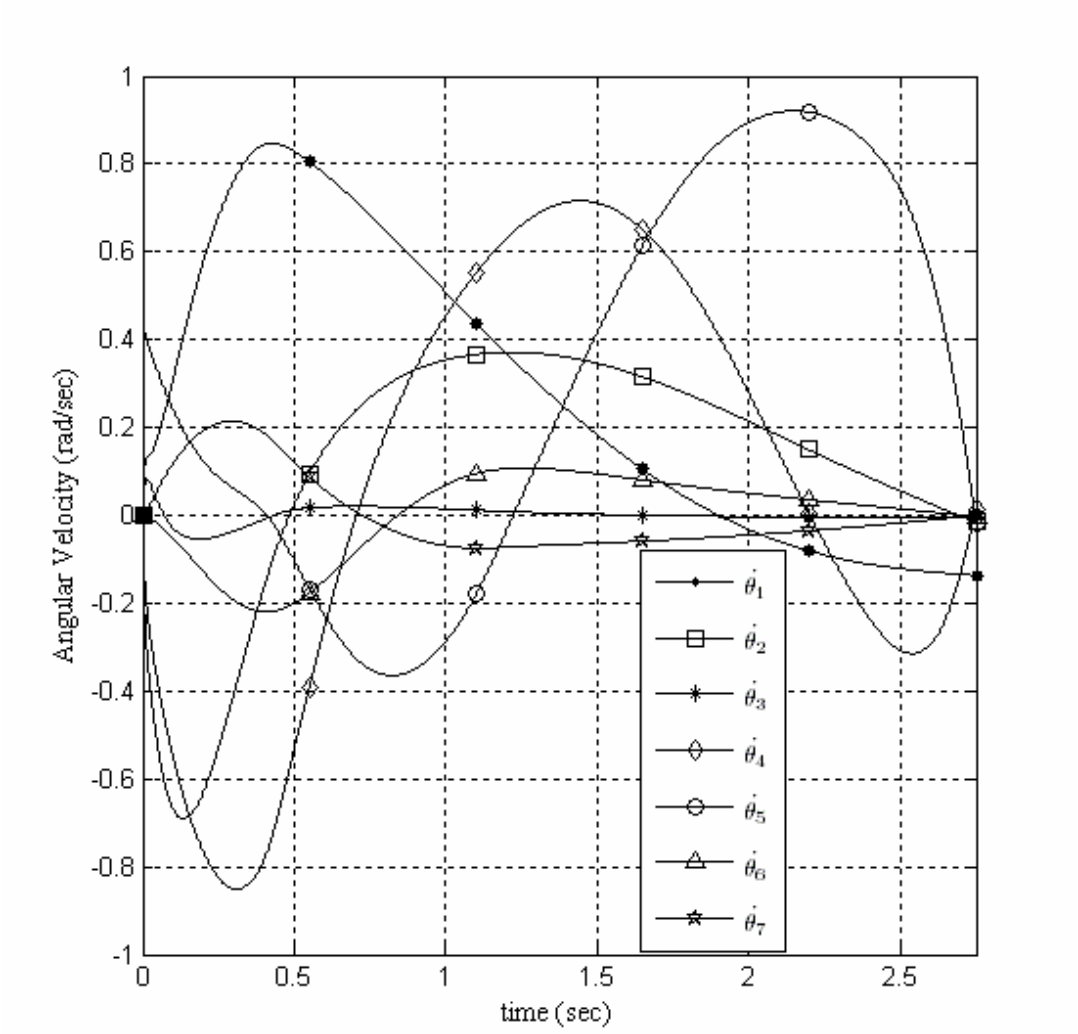

Figure 6.21 Simulated trajectory joint angular velocity profile for doubled speed motion

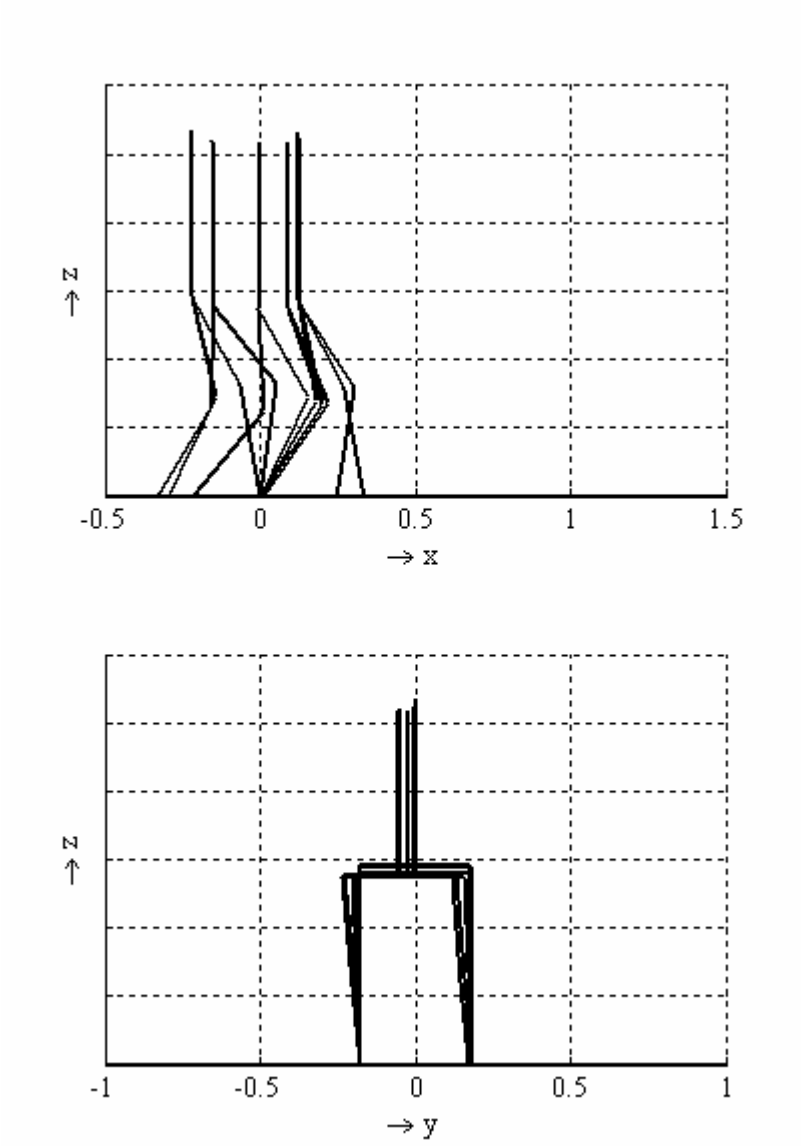

Figure 6.22 Simulated trajectory walking snapshot - sagittal (top) and frontal (bottom) plane views – for doubled speed motion

When the walking speed is decreased from 5.4545 cm/sec to 4.5455 cm/sec by decreasing the step length from 0.3 m to 0.25 m while keeping the step time constant, the resulting angle and angular velocity trajectories and the snapshots of the walking are given in Figure 6.23 to Figure 6.25. For the initial step length motion, the corresponding angle and angular velocity trajectories and the snapshots of the walking were given before in Figure 6.14 to Figure 6.17.

When the speed of the walking is decreased by decreasing the step length, the walking of the biped is stable and looks like the natural human walking. Also, the overshoot in the angular velocity profiles is decreased.

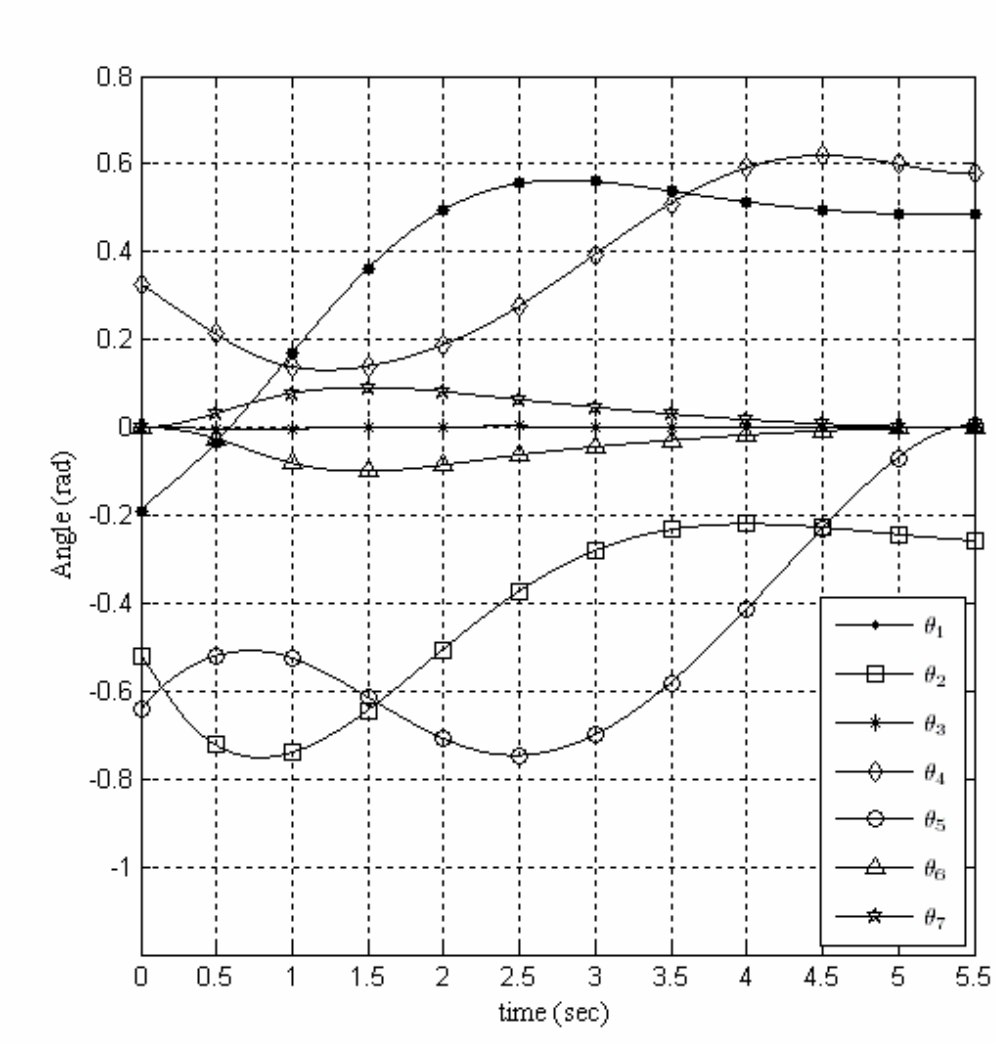

Figure 6.23 Simulated trajectory joint angle profile for slow speed motion

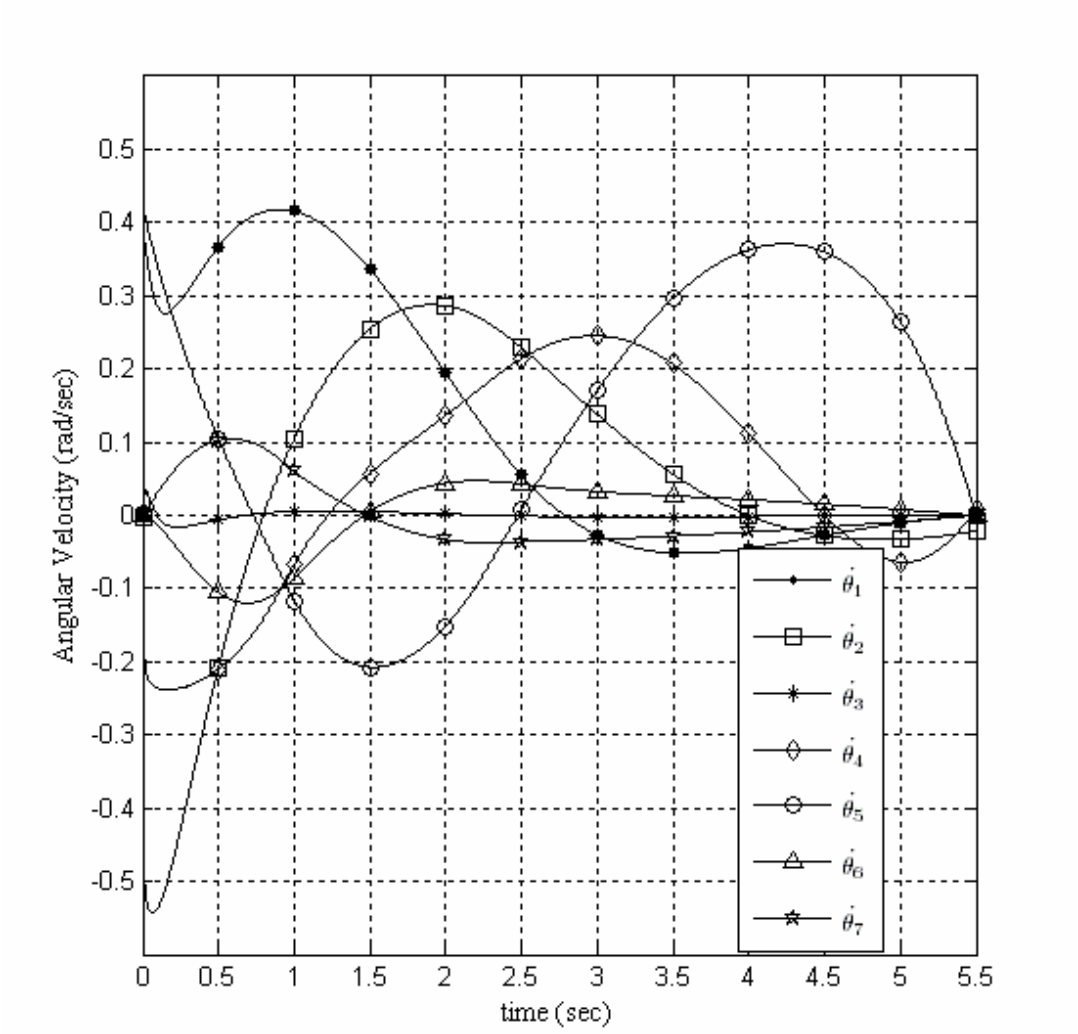

Figure 6.24 Simulated trajectory joint angular velocity profile for slow speed motion

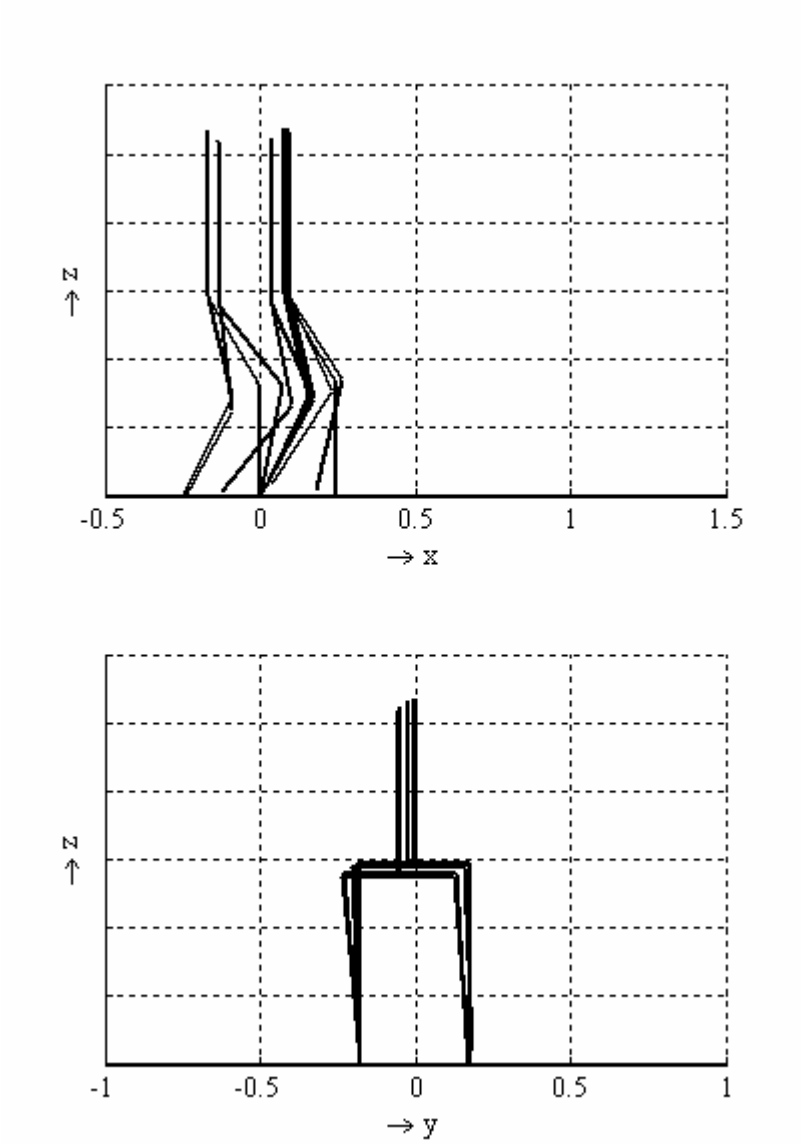

Figure 6.25 Simulated Trajectory Walking Snapshot - sagittal (top) and frontal (bottom) plane views - for slow speed motion

When the swing leg ankle point maximum height is doubled from 0.05 m to 0.1 m while keeping other walking parameters constant, the resulting angle and angular velocity trajectories and the snapshots of the walking are given in Figure 6.26 to Figure 6.28. For the initial step length motion, the corresponding angle and angular velocity trajectories and the snapshots of the walking were given before in Figure 6.14 to Figure 6.17. When the swing leg ankle point maximum height is doubled, the walking of the biped is still stable and this pattern of walking with a higher swing leg ankle point also corresponds to the walking of the biped by stepping over obstacles as illustrated in Figure 6.29.

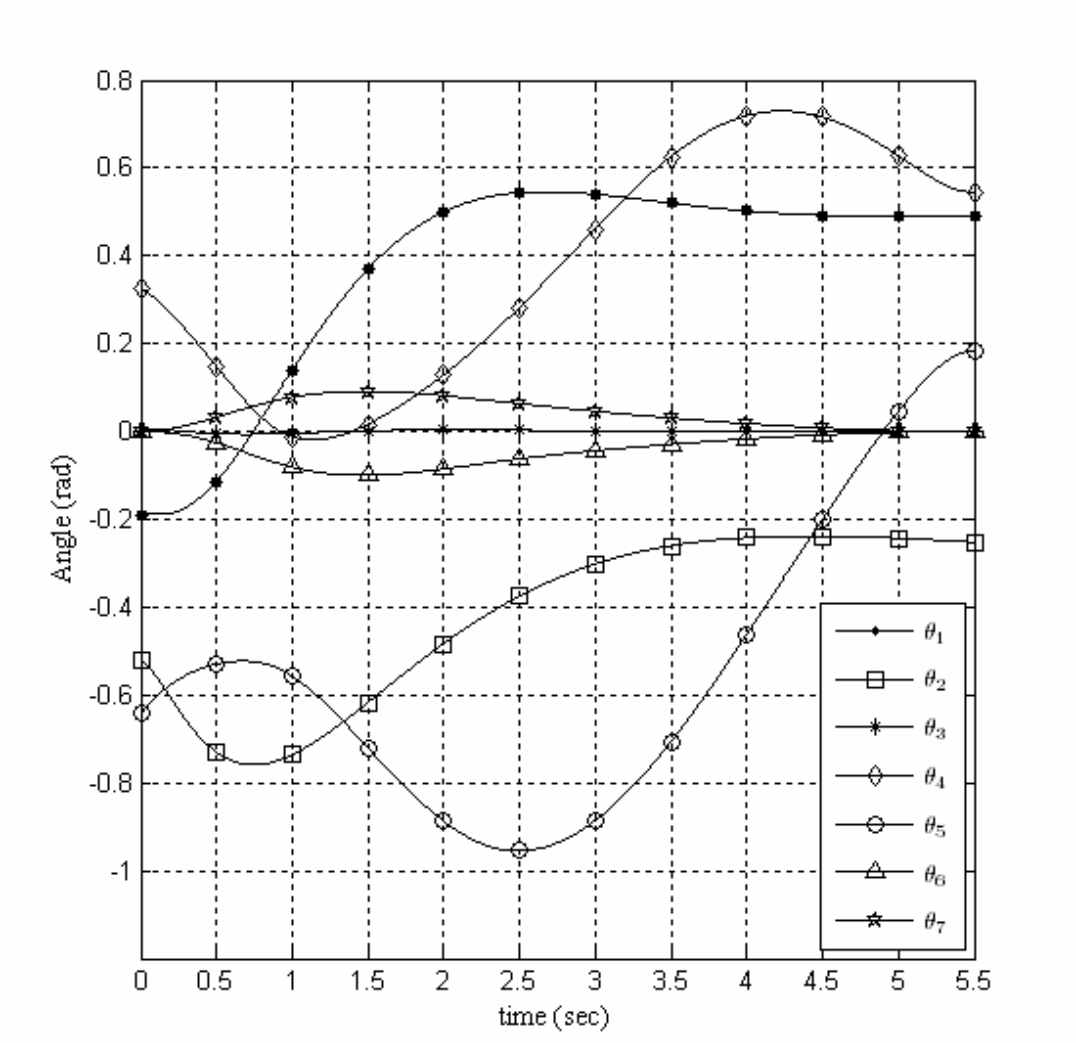

Figure 6.26 Simulated trajectory joint angle profile for doubled swing leg ankle point maximum height

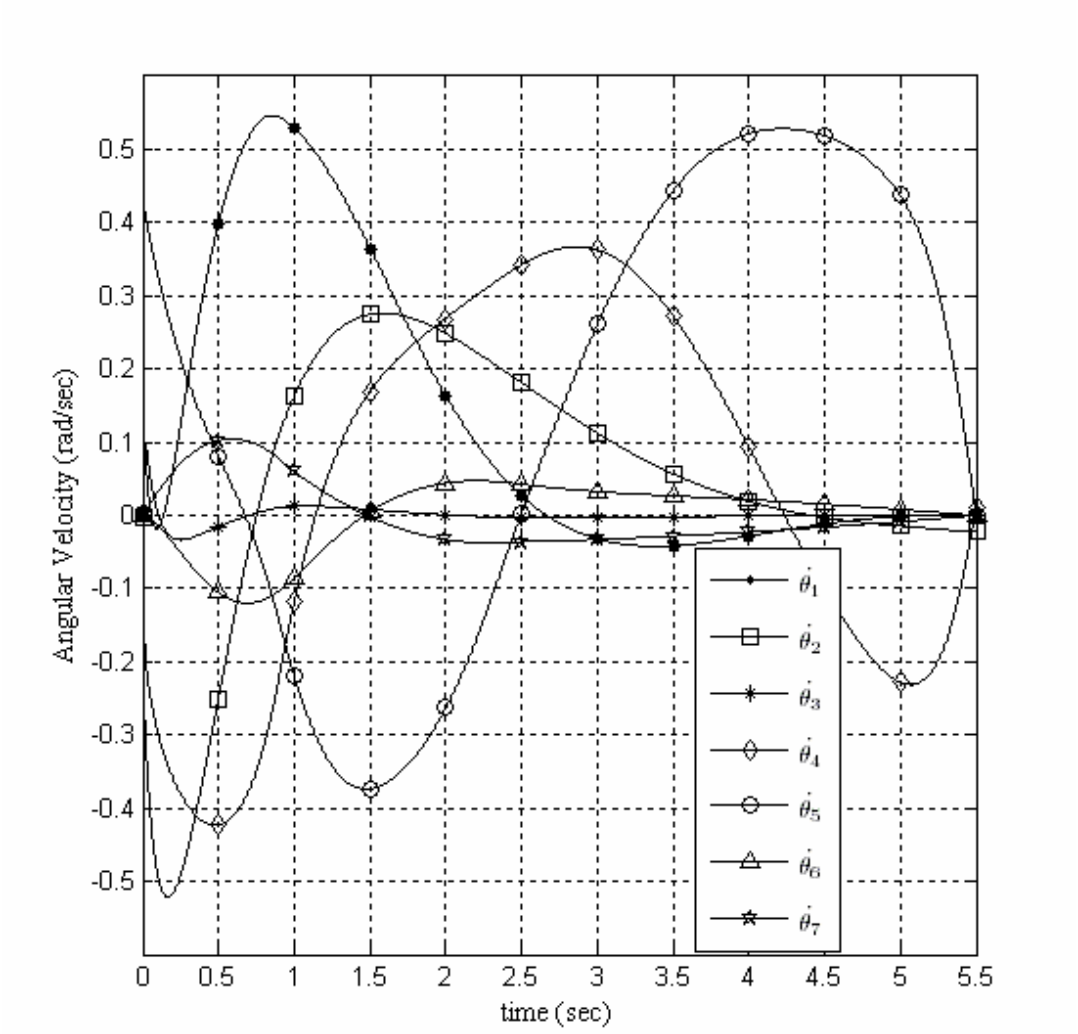

Figure 6.27 Simulated trajectory joint angular velocity profile for doubled swing leg ankle point maximum height

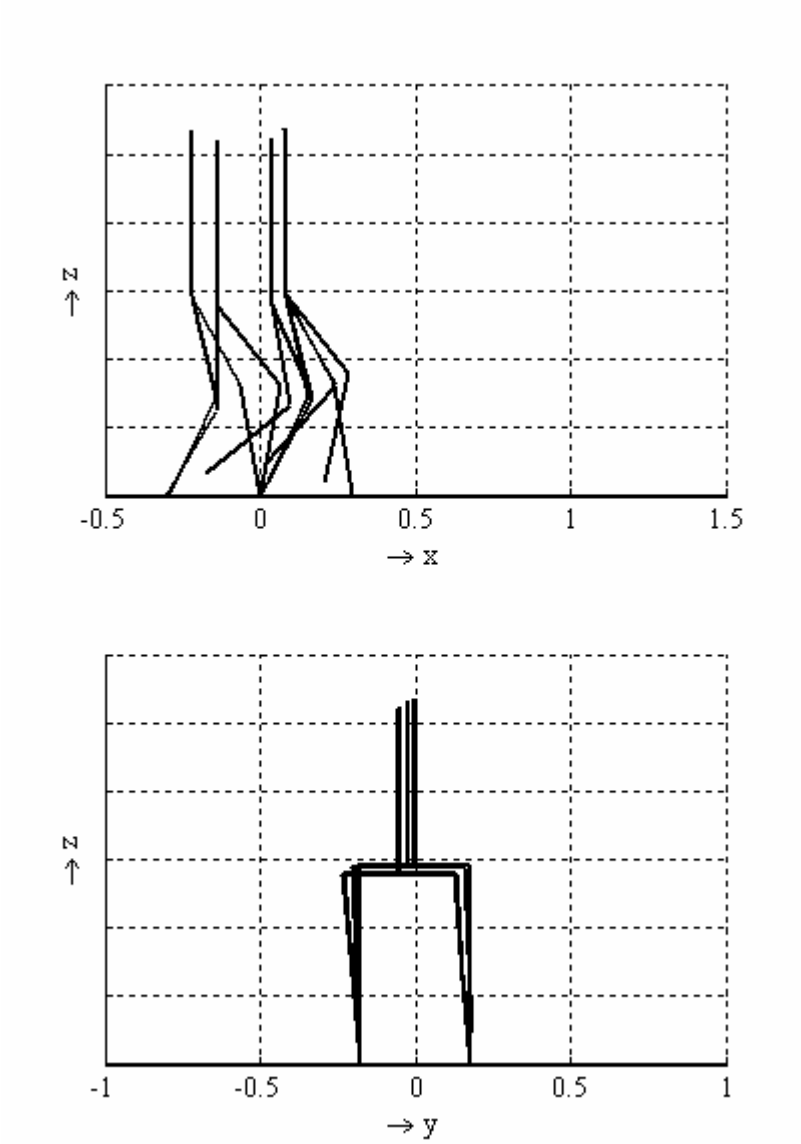

Figure 6.28 Simulated trajectory walking snapshot - sagittal (top) and frontal (bottom) plane views - for doubled swing leg ankle point maximum height

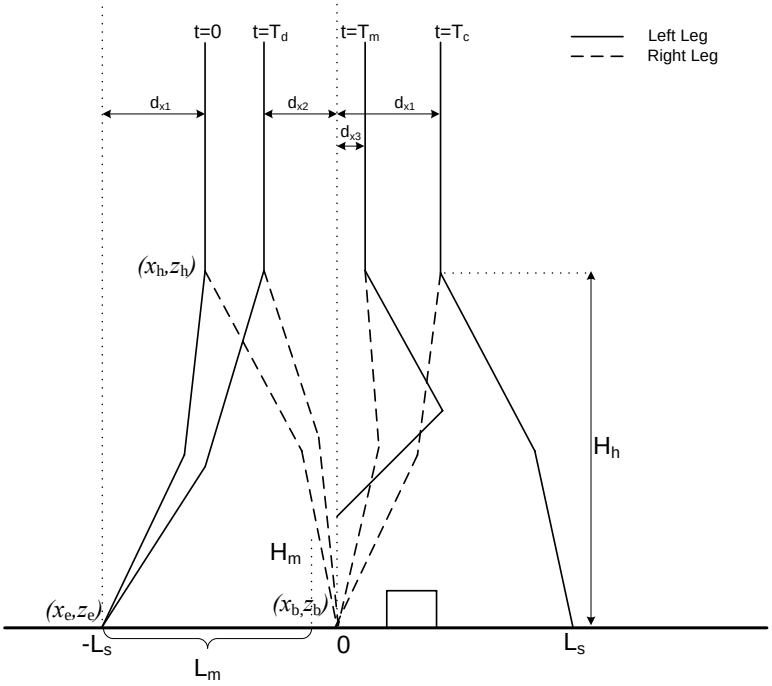

Figure 6.29 Illustration of biped robot stepping over an obstacle

6.4.4 Comparison of Low Level Controllers

In the biped locomotion model generated, there are 5 links and in this 5 links there are total of 7 DOF. In each knee joint of the biped, there is 1 DOF that causes sagittal plane motion and in each hip, there are 2 DOF that causes both sagittal and frontal plane motions. These joints are provided by independent control inputs for each DOF. The unit providing these inputs to the joints is called the low level controller. In this thesis, many different low level controllers are designed and tested. Namely, PID controller, Computed Torque Controller, Modified Computed Torque Controller (added an integral term) and Optimal Controller (Steepest Descent, LQR and Hooke & Jeeves methods) are implemented.

The low level control output, namely, “control input”, is provided to the biped system aiming to result in the desired natural look-like stable walking. Below, the results of the low level controllers are given for each type of the controller.

Unless otherwise stated, PID controller is used as the default low level controller of the system. The controller parameters used by the default PID controller is as given below:

$$K_P = 40 * I(7,7)$$

$$K_I = 170 * I(7,7)$$

$$K_D = 80 * I(7,7)$$

Note that, in this formulation $I(7,7)$ si the 7x7 identity matrix and for example, “40” is the multiplier coefficient for K_P case. This point forward, the PID and Computed Torque Control parameters will only be stated with the multiplier coefficient, for notification simplicity, as shown in Table 6-2.

For the default parameters of the PID controller, the resulting control input trajectory is given in Figure 6.30. The corresponding simulator system response in the form of angle and angular velocity trajectories and the snapshots of the walking were given before in Figure 6.13, Figure 6.16 and Figure 6.17. When the PID controller parameters are decreased, as decreased values are listed in Table 6-2, the resulting angle and angular velocity trajectories, control input trajectory and the snapshots of the walking are given in Figure 6.31 to Figure 6.34. In this case, the overshoot of the control input is increased. When the PID controller parameters are increased, as increased values are listed in Table 6-2, the resulting angle and angular velocity trajectories, control input trajectory and the snapshots of the walking are given in Figure 6.35 to Figure 6.38. In this case, the overshoot of the control input is decreased.

Table 6-2 The PID and Computed Torque controller parameters

	PID Contoller			Computed Torque Controller	
	K_P	K_I	K_D	K_D	K_P
Default	40	170	80	50	625
Decreased	20	85	40	30	225
Increased	60	200	120	60	900

Similarly, the Computed Torque Controller (CTC) is tested against its controller parameters and the results are given. For the default parameters of the CTC, the resulting

angle and angular velocity trajectories, control input trajectory and the snapshots of the walking are given in Figure 6.39 to Figure 6.42. When the CTC parameters are decreased, as decreased values are listed in Table 6-2, the resulting angle and angular velocity trajectories, control input trajectory and the snapshots of the walking are given in Figure 6.43 to Figure 6.46. When the CTC parameters are increased, as increased values are listed in Table 6-2, the resulting angle and angular velocity trajectories, control input trajectory and the snapshots of the walking are given in Figure 6.47 to Figure 6.50.

Also, the Optimal Controller is designed and tested to control the biped system. Three different methods, namely, Steepest Descent, LQR, Hooke & Jeeves Methods are implemented. For each method, an initial control input trajectory is fed into the controller algorithm aiming to generate a new control input trajectory that optimizes the energy during walking while satisfying the system dynamics and physical constraints. The output of the controller, namley, the control input trajectory is then fed to the biped system. Even if each of these three methods worked in other simple systems (tested in Stirred-Tank Chemical Reactor Problem) successfully, they result in an unstable locomotion and so fail to achieve stable biped walking in 5-link 7 DOF biped system. The main reason behind is that, the open loop type control (providing the control input trajectory as “read-only” data without a feedback) results in unstable motion and so fails the system to achieve walking, since the biped system is highly complex and nonlinear; has unstability tendency and interacts with the environment that causes unexpected disturbance to the system. The resulting angle and angular velocity and control input trajectories of the Optimal Control Steepest Descent method are given in Figure 6.51 to Figure 6.53.

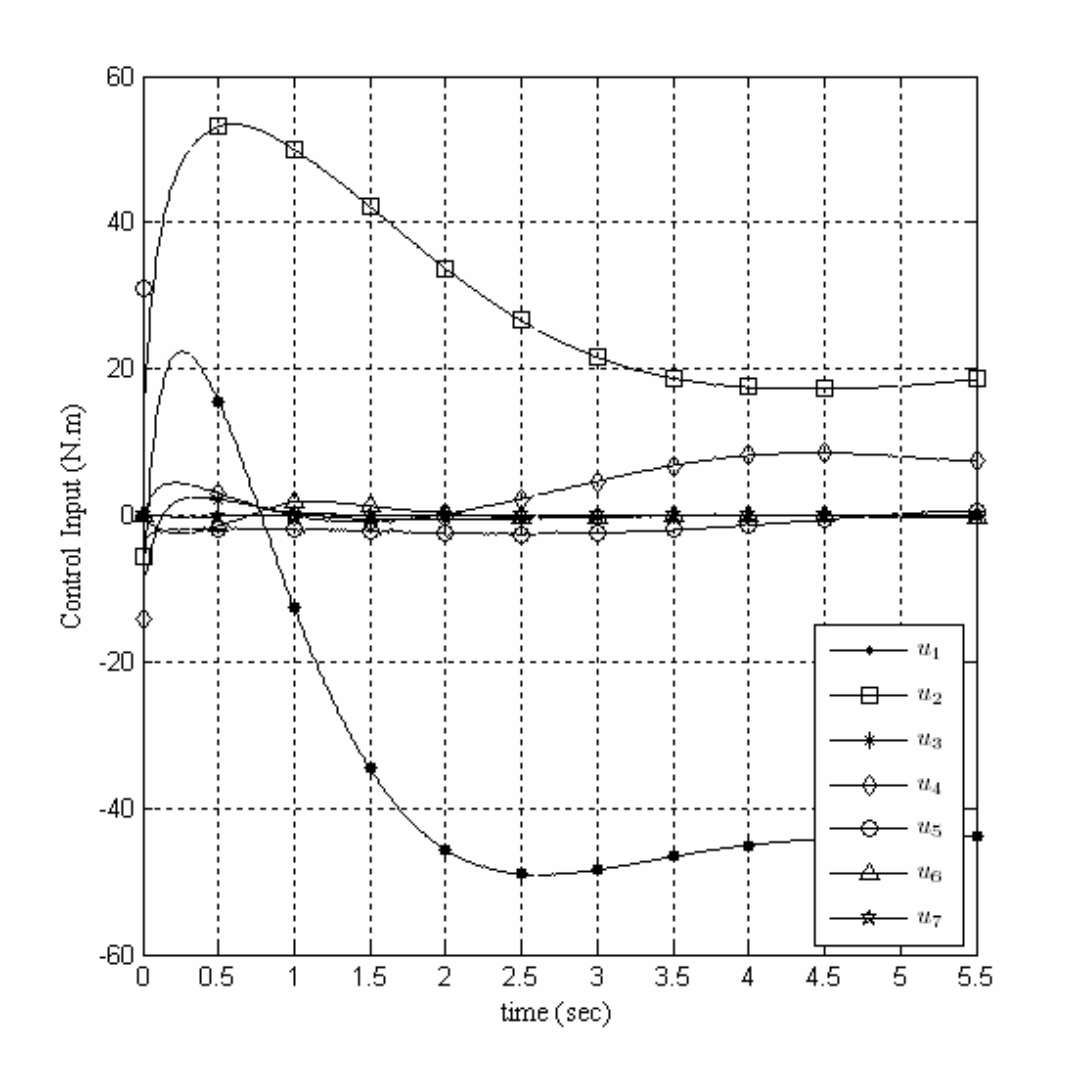

Figure 6.30 Simulated trajectory control input profile

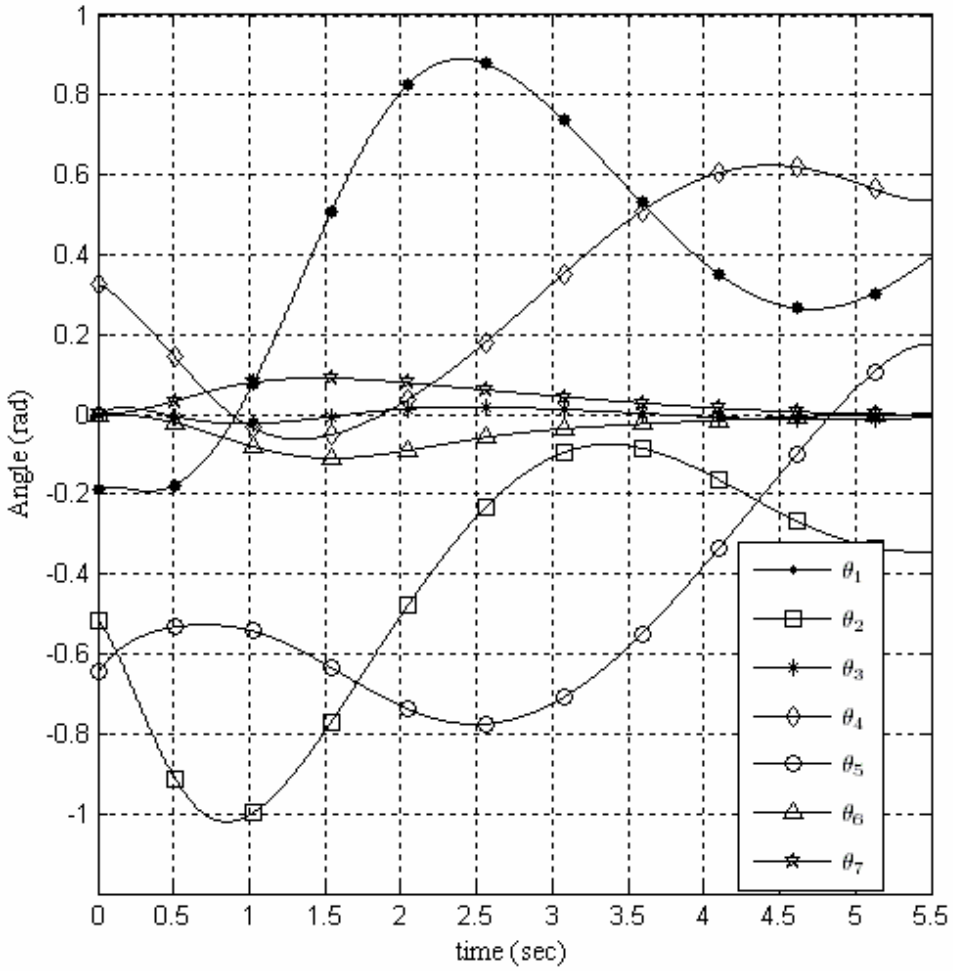

Figure 6.31 Simulated trajectory joint angle profile for decreased PID controller parameters

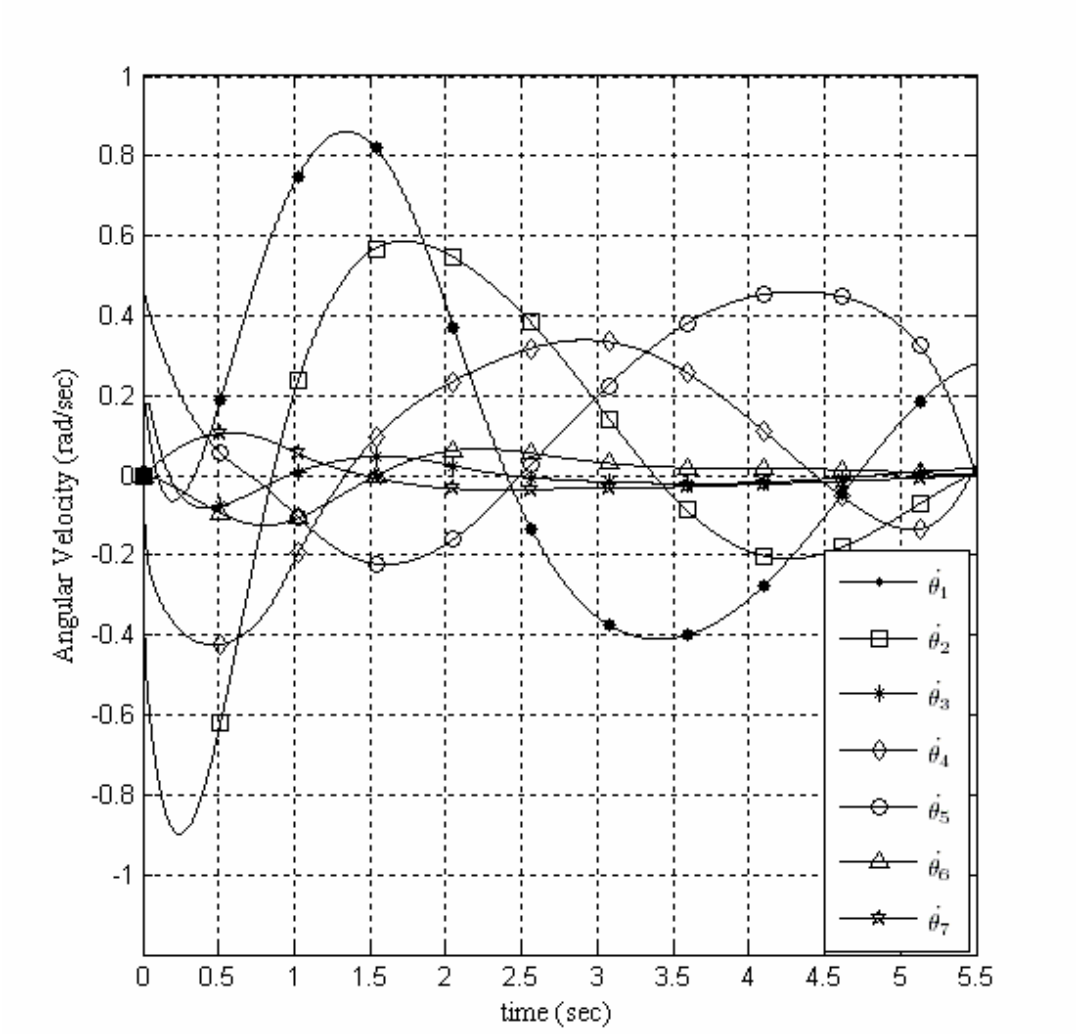

Figure 6.32 Simulated trajectory joint angular velocity profile for decreased PID controller parameters

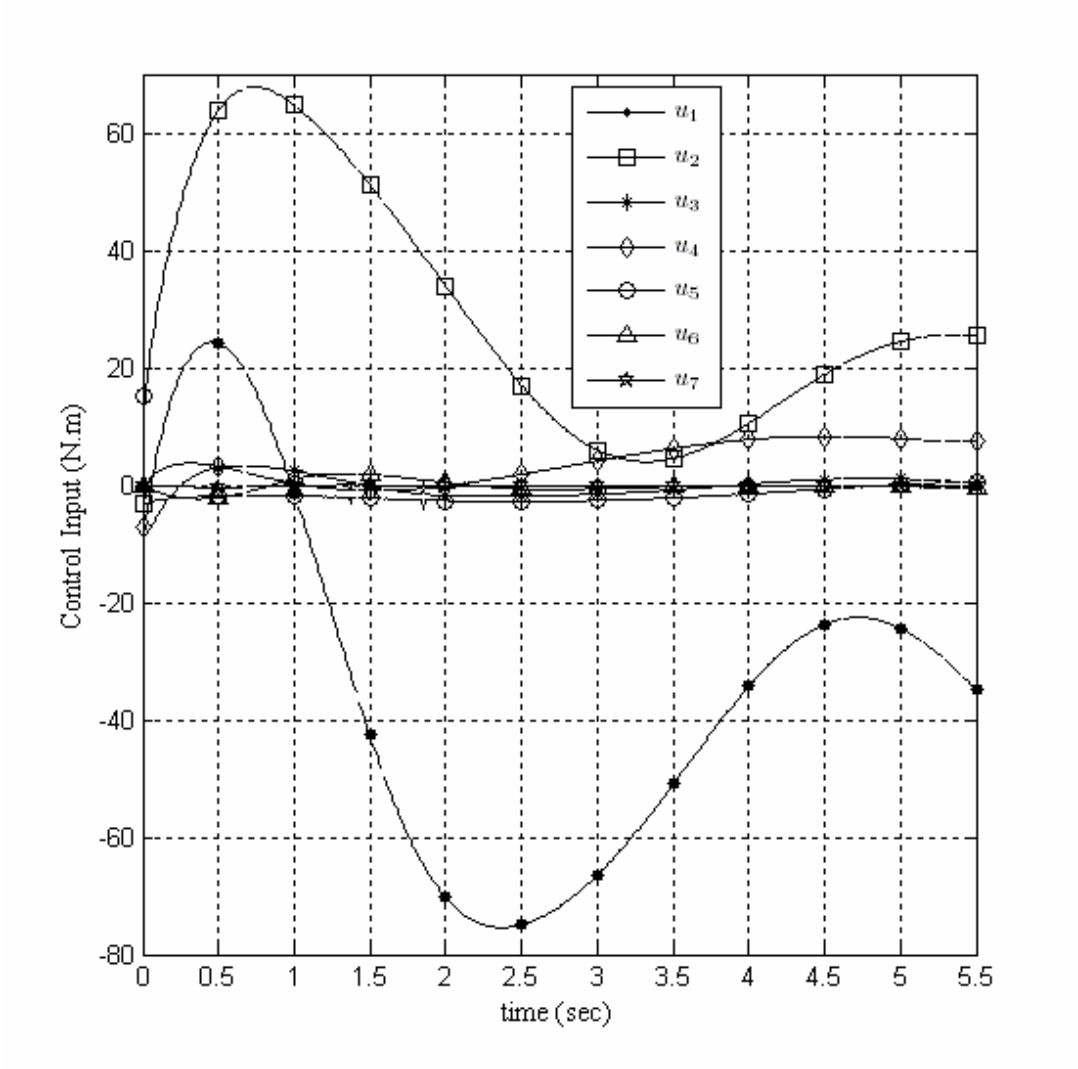

Figure 6.33 Simulated trajectory control input profile for decreased PID controller parameters

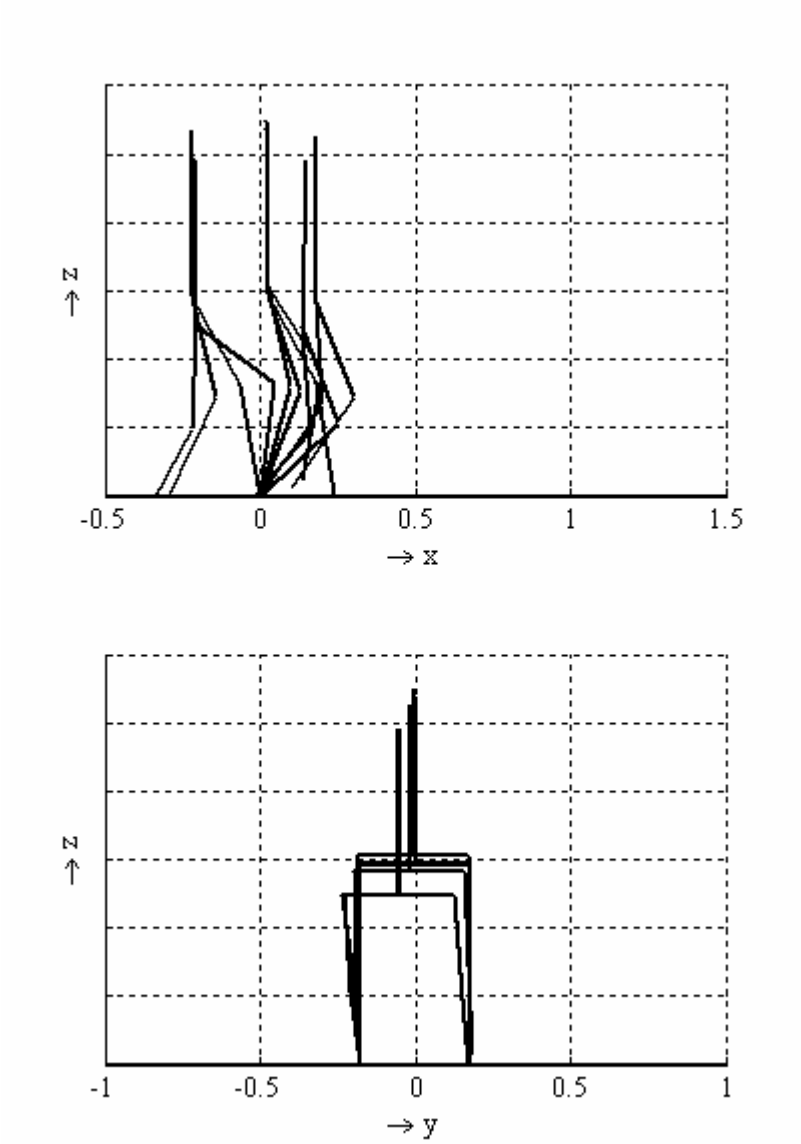

Figure 6.34 Simulated trajectory walking snapshot - sagittal (top) and frontal (bottom) plane views - for decreased PID controller parameters

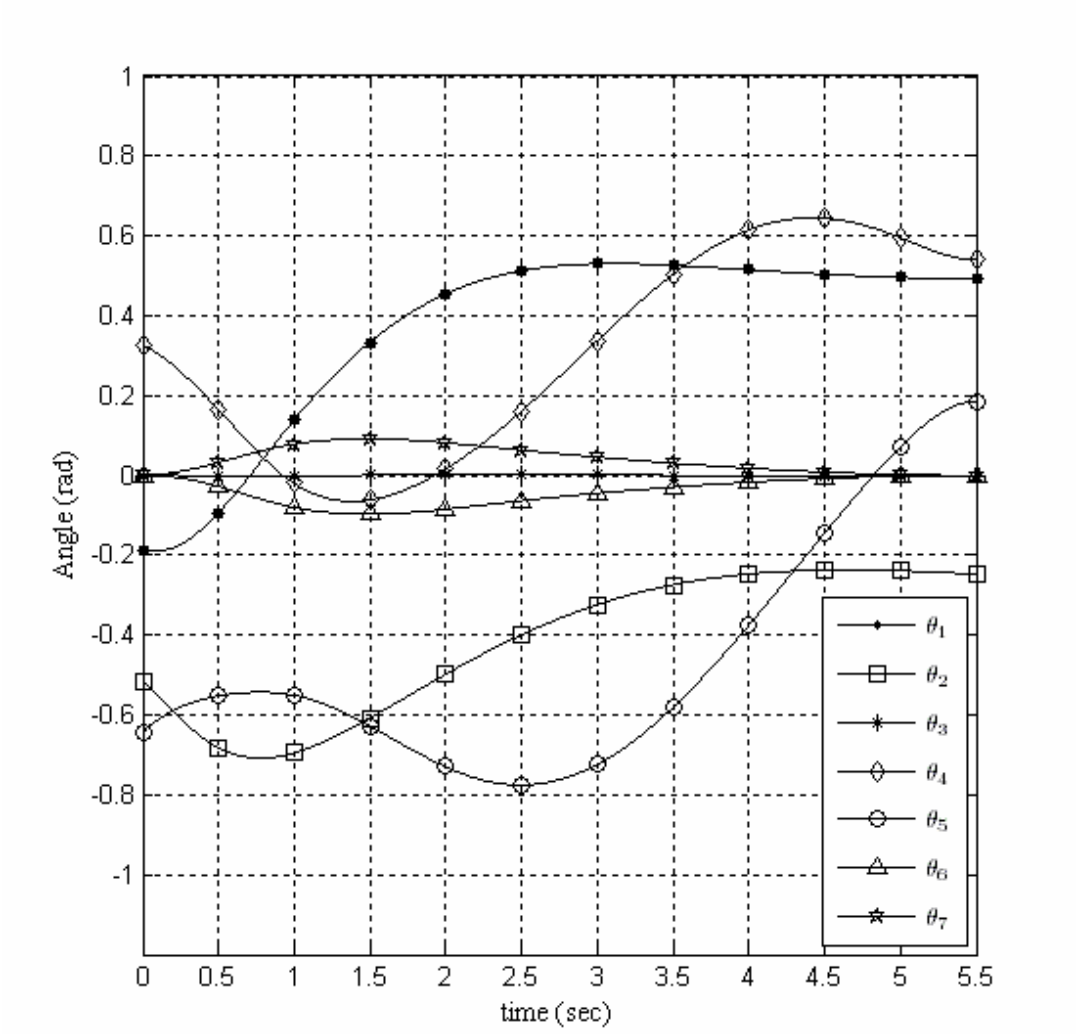

Figure 6.35 Simulated trajectory joint angle profile for increased PID controller parameters

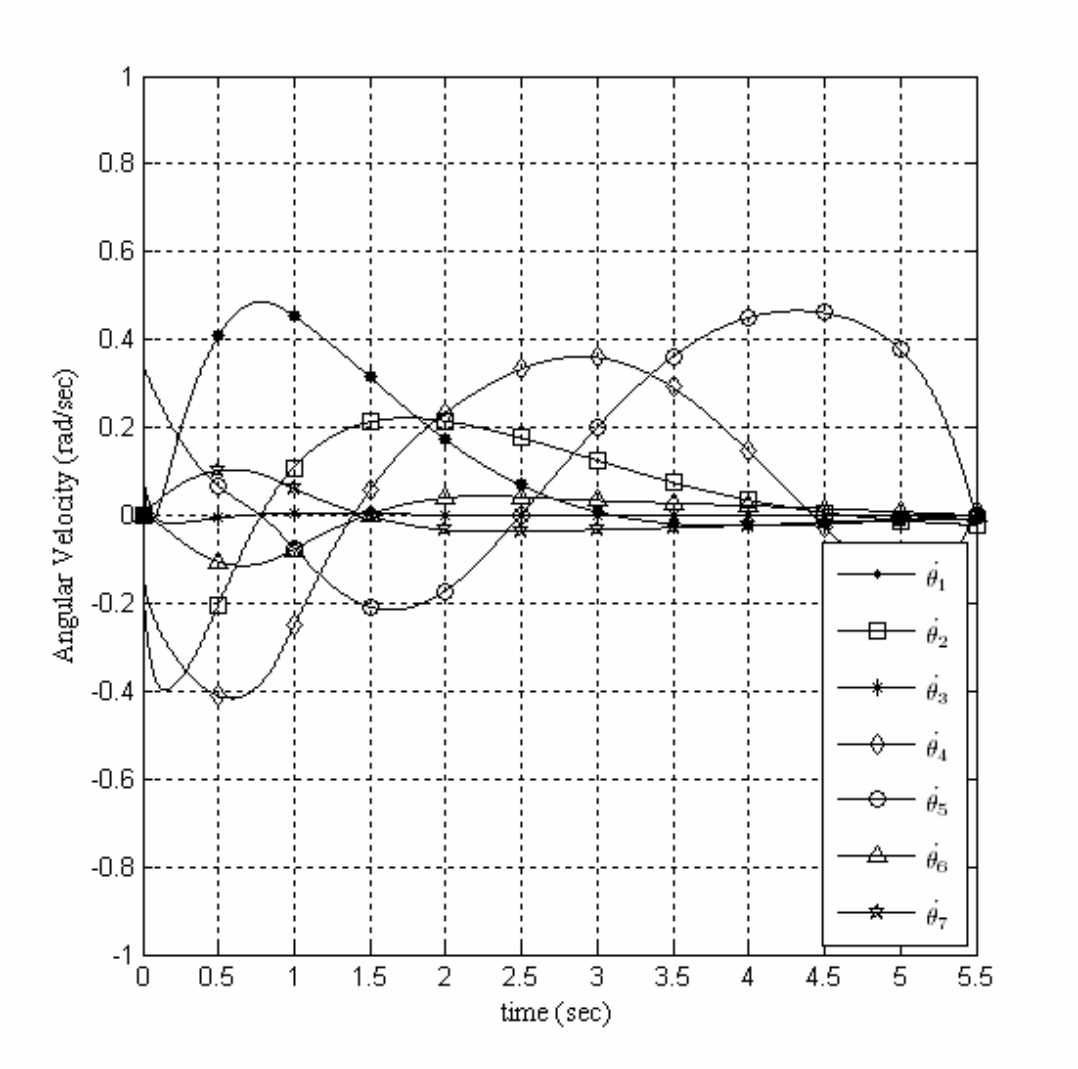

Figure 6.36 Simulated trajectory joint angular velocity profile for increased PID controller parameters

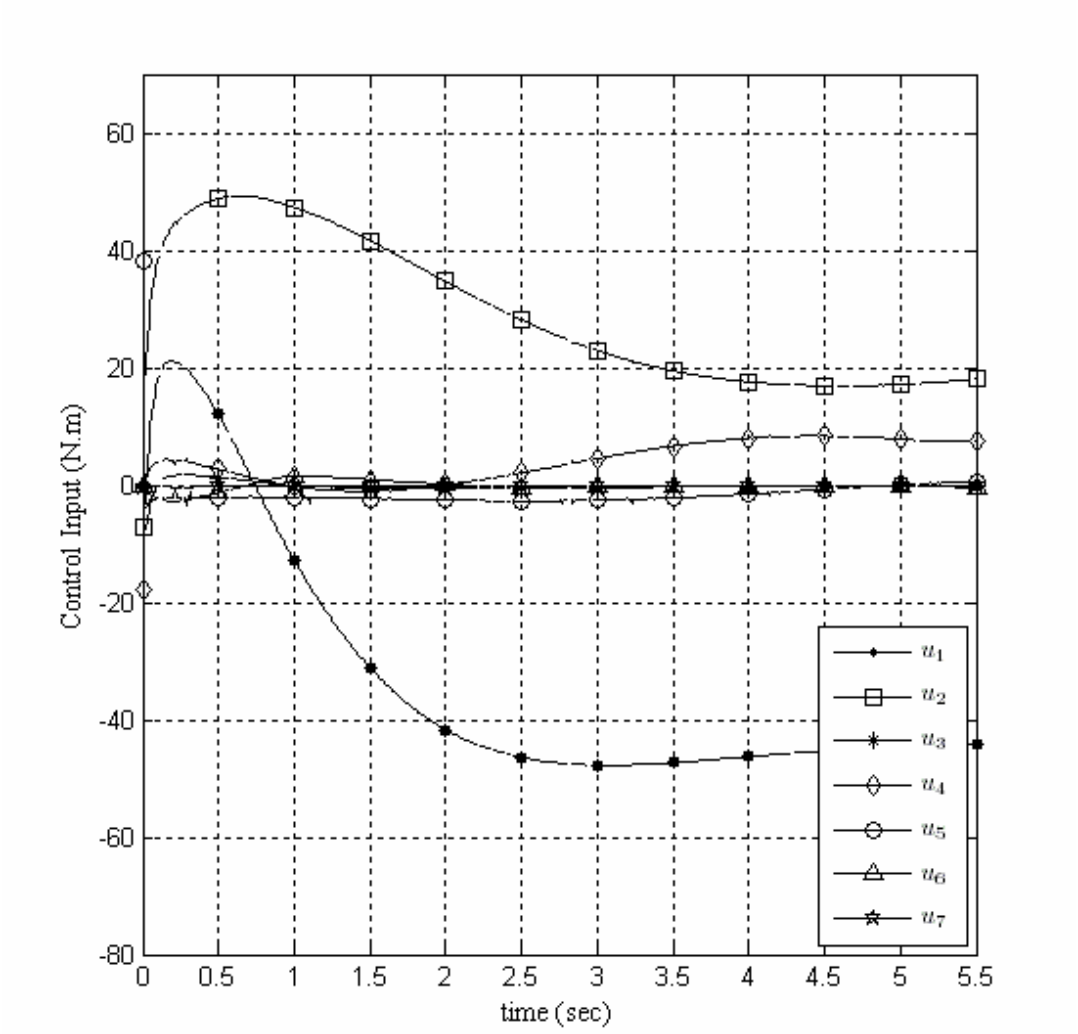

Figure 6.37 Simulated trajectory control input profile for increased PID controller parameters

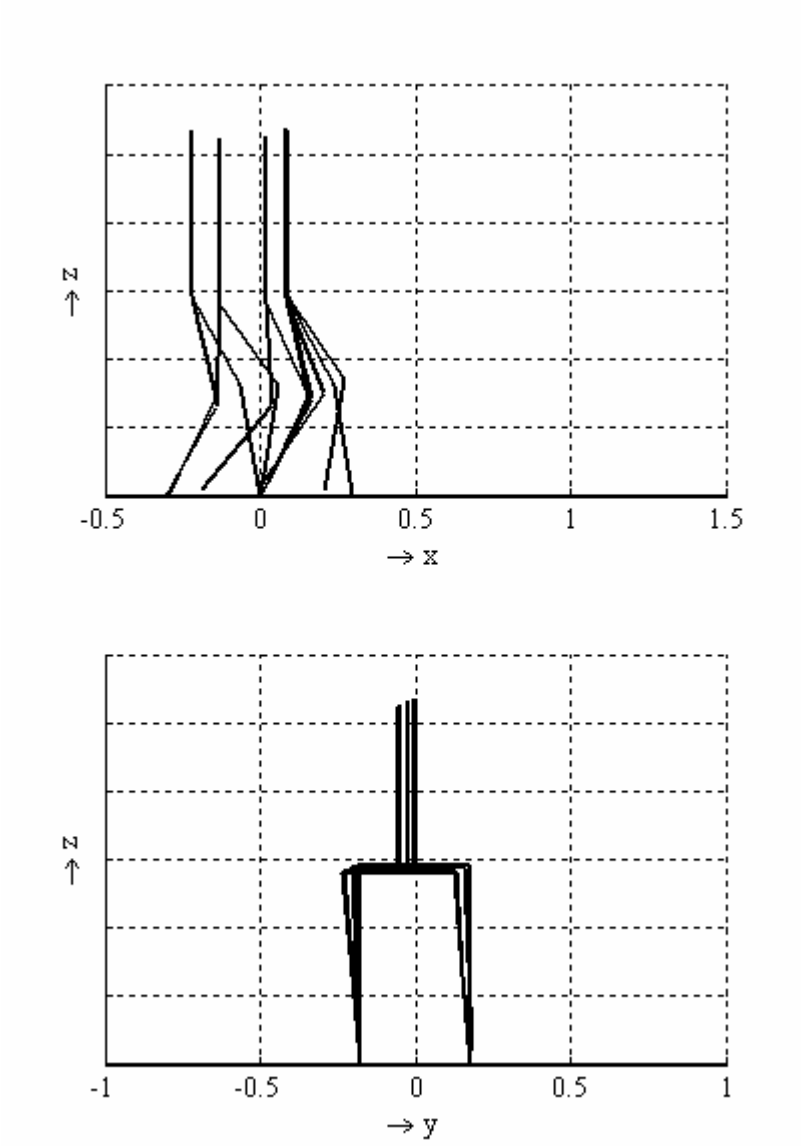

Figure 6.38 Simulated trajectory walking snapshot - sagittal (top) and frontal (bottom) plane views - for increased PID controller parameters

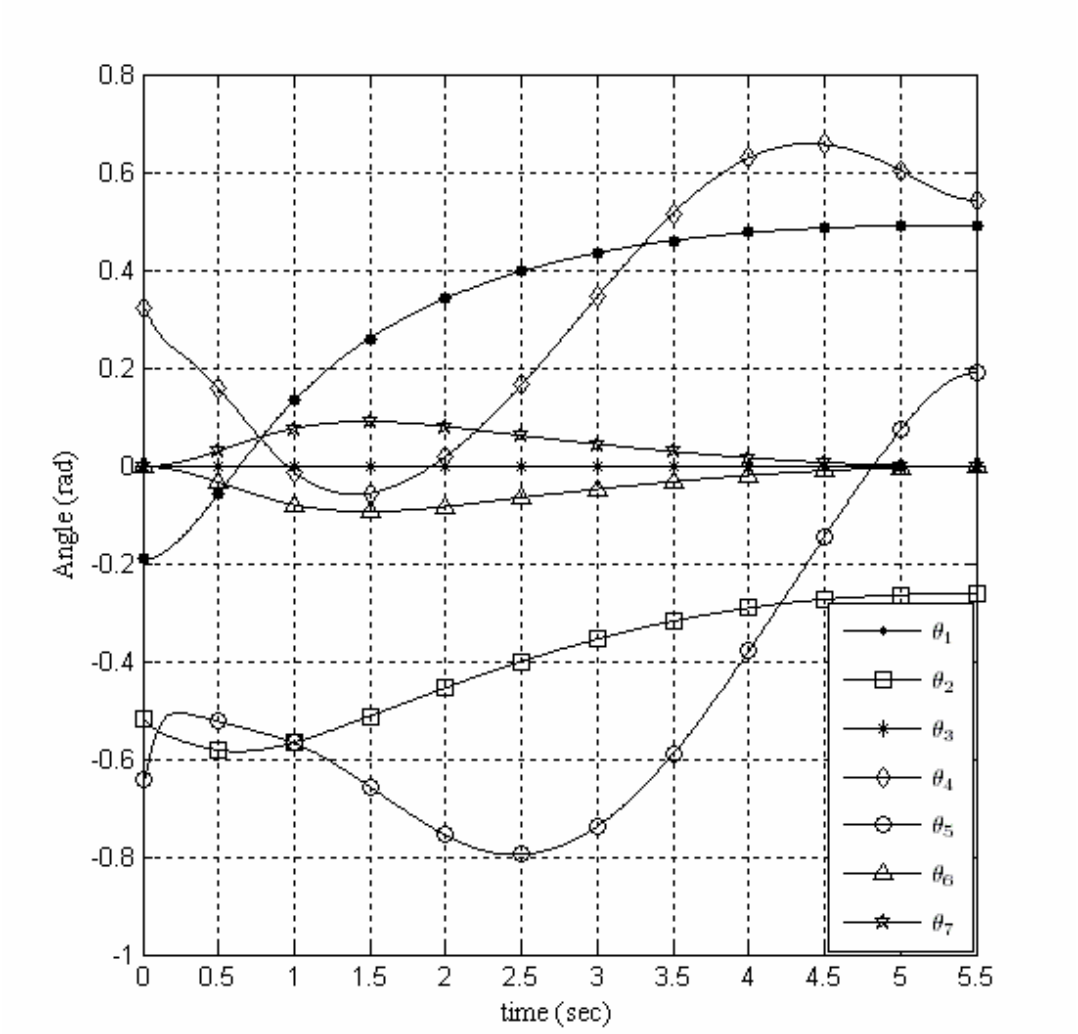

Figure 6.39 Simulated trajectory joint angle profile for Computed Torque Controller default parameters

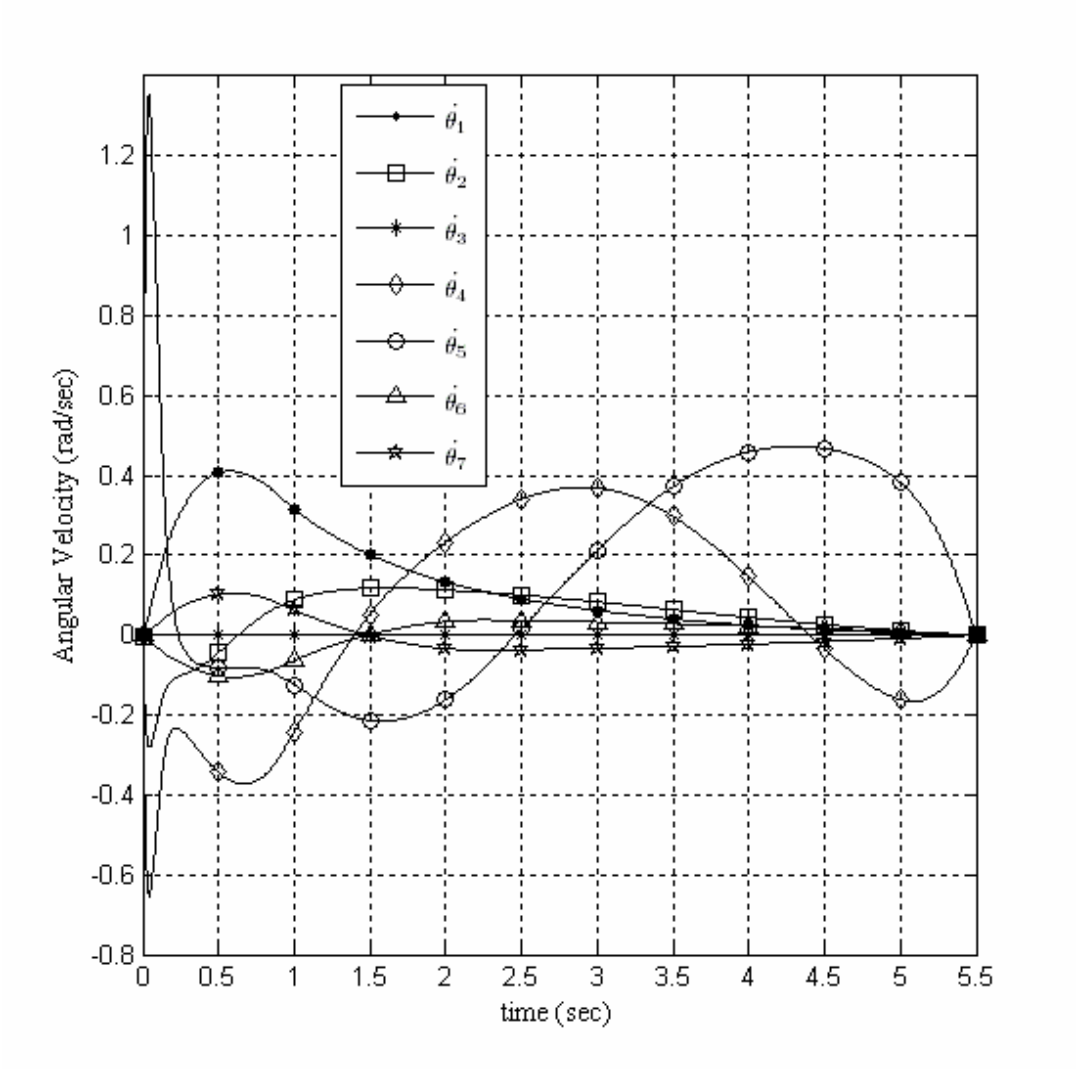

Figure 6.40 Simulated trajectory joint angular velocity profile for Computed Torque Controller default parameters

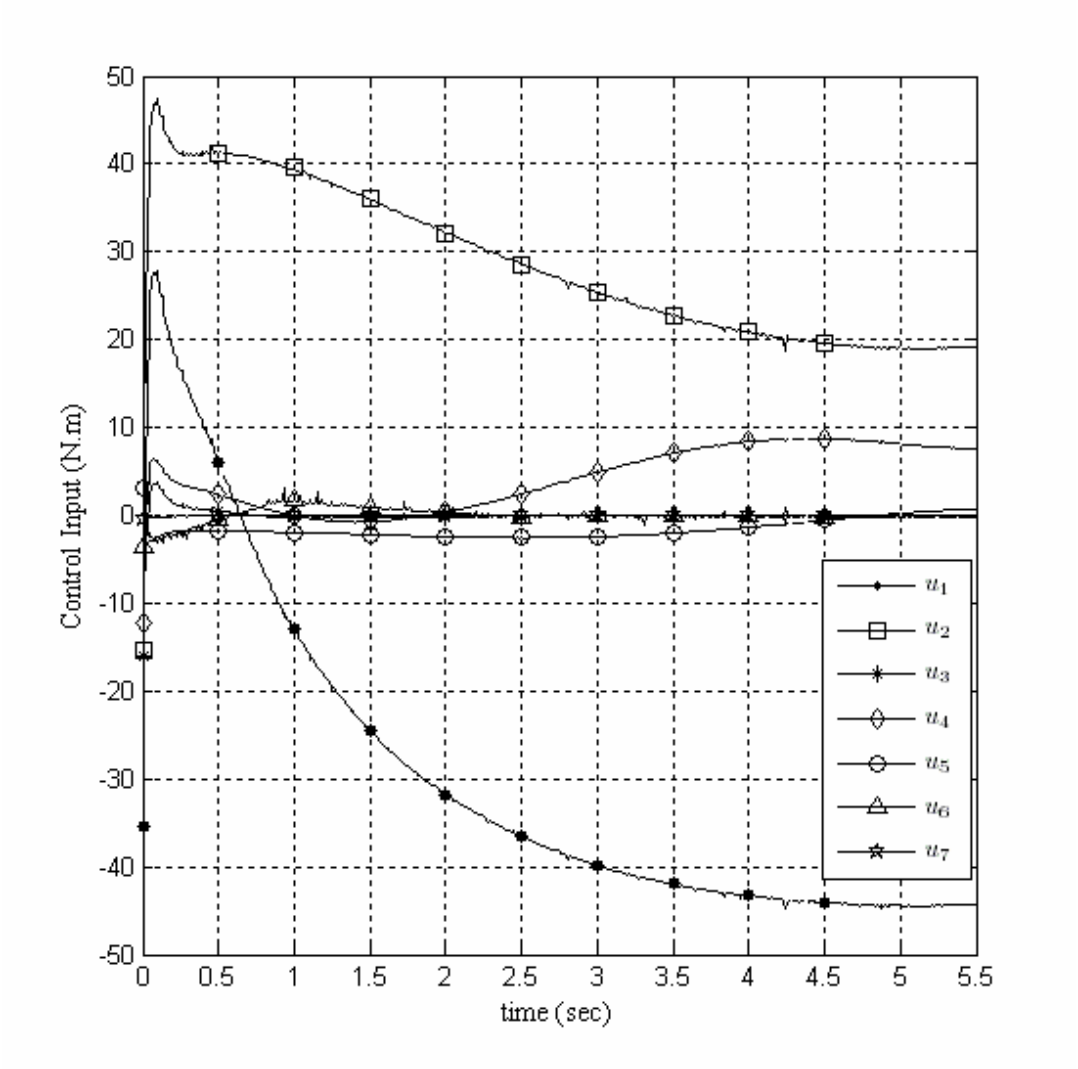

Figure 6.41 Simulated trajectory control input profile for Computed Torque Controller default parameters

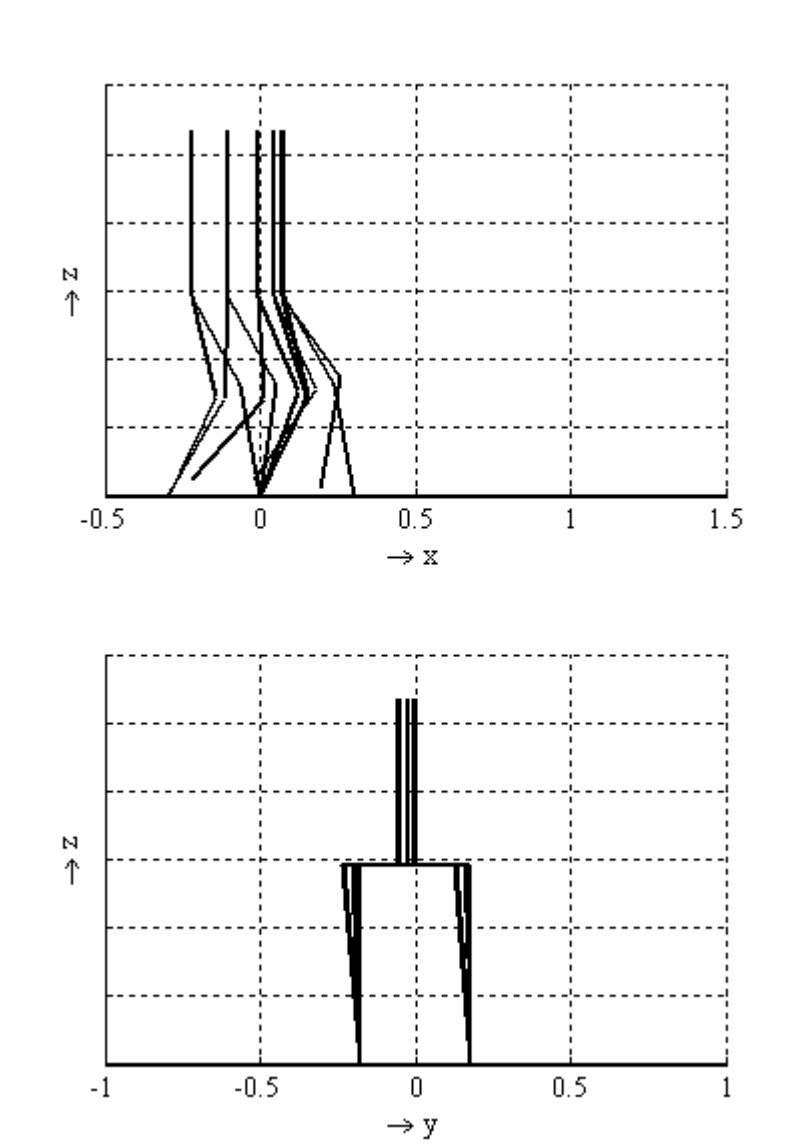

Figure 6.42 Simulated trajectory walking snapshot - sagittal (top) and frontal (bottom) plane views - for Computed Torque Controller default parameters

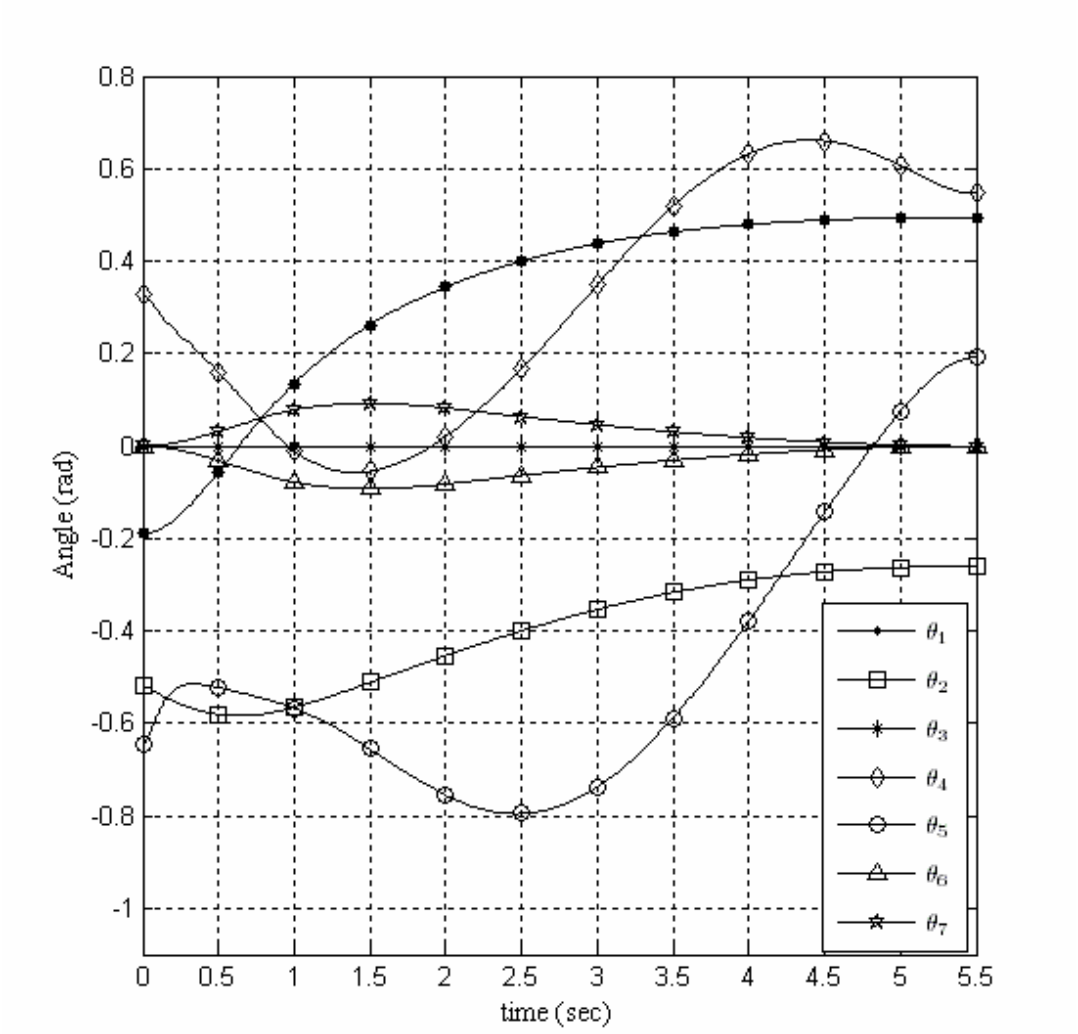

Figure 6.43 Simulated trajectory joint angle profile for decreased Computed Torque Controller parameters

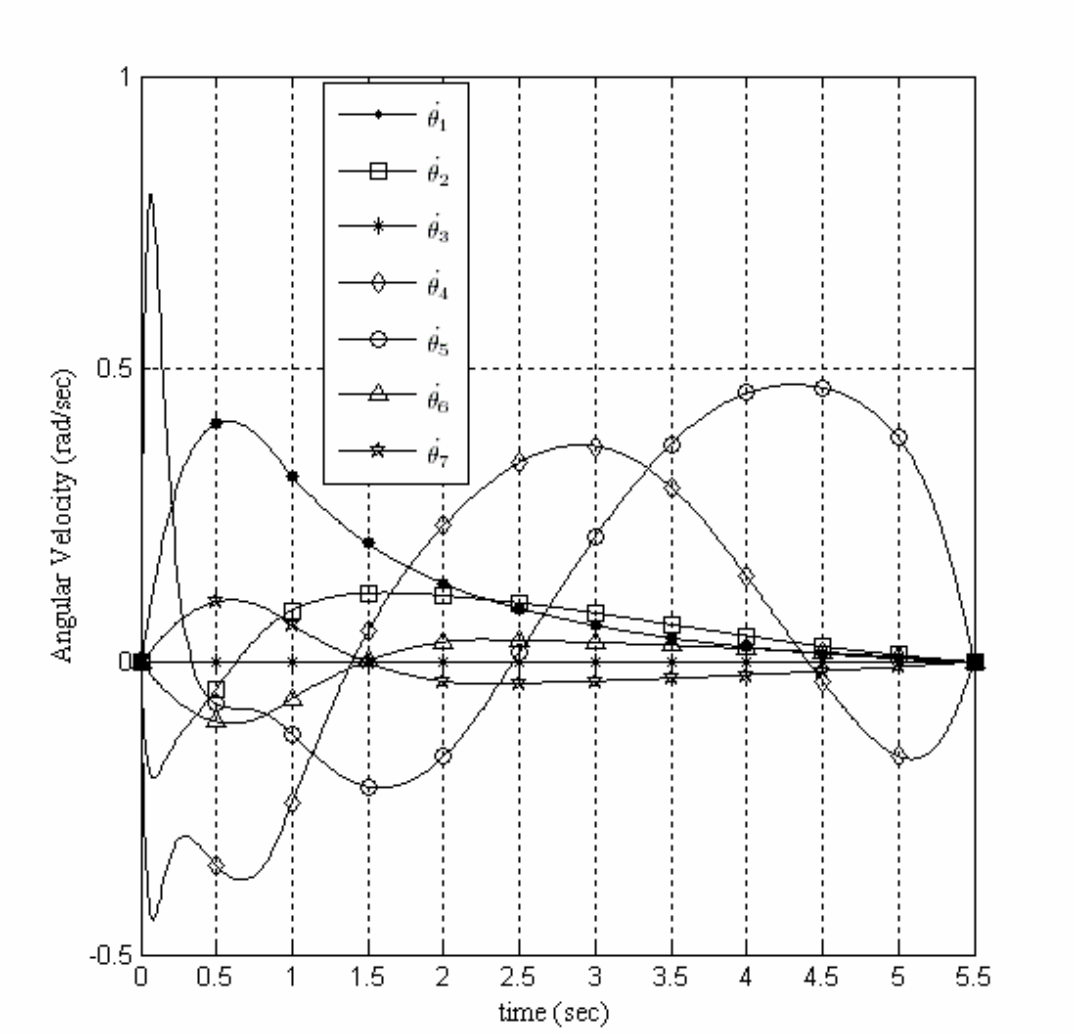

Figure 6.44 Simulated trajectory joint angular velocity profile for decreased Computed Torque Controller parameters

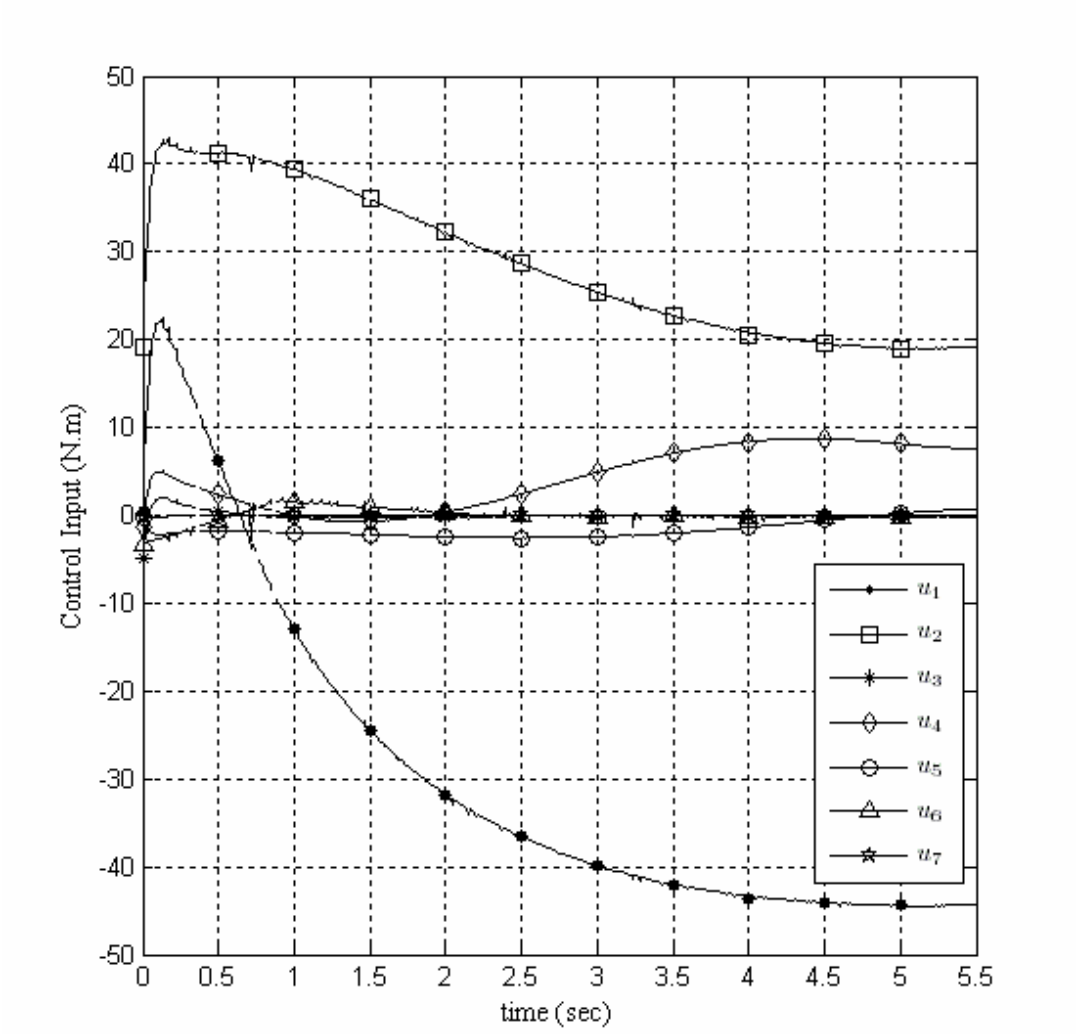

Figure 6.45 Simulated trajectory control input profile for decreased Computed Torque Controller parameters

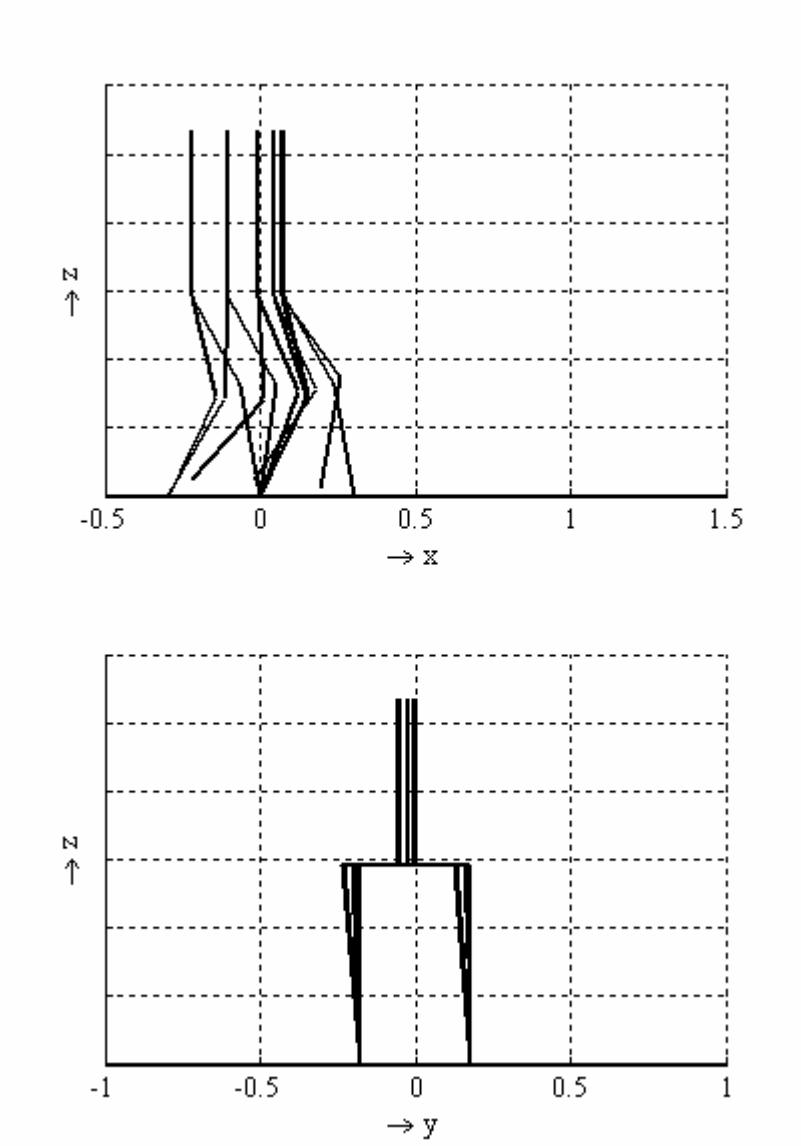

Figure 6.46 Simulated trajectory walking snapshot - sagittal (top) and frontal (bottom) plane views - for decreased Computed Torque Controller parameters

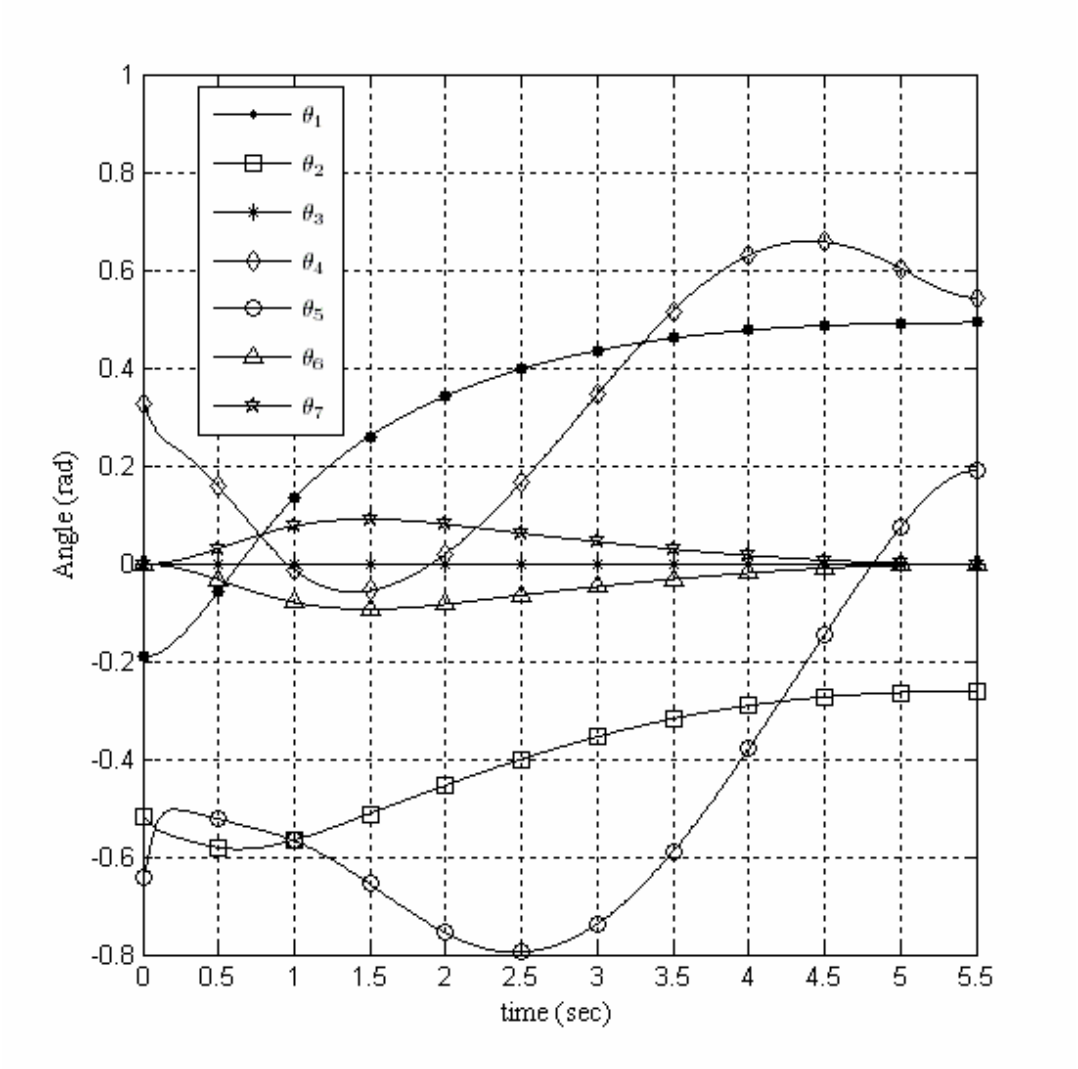

Figure 6.47 Simulated trajectory joint angle profile for increased Computed Torque Controller parameters

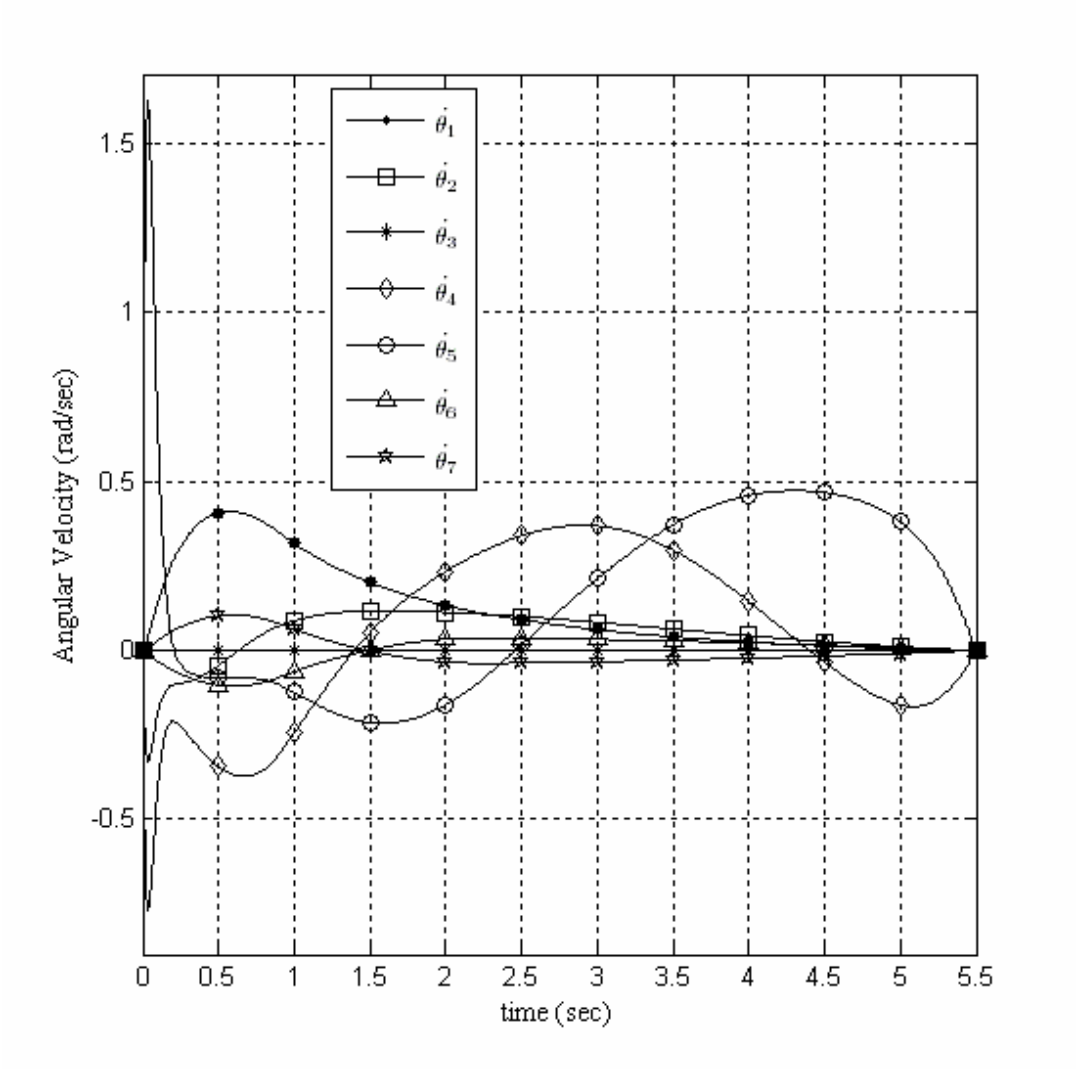

Figure 6.48 Simulated trajectory joint angular velocity profile for increased Computed Torque Controller parameters

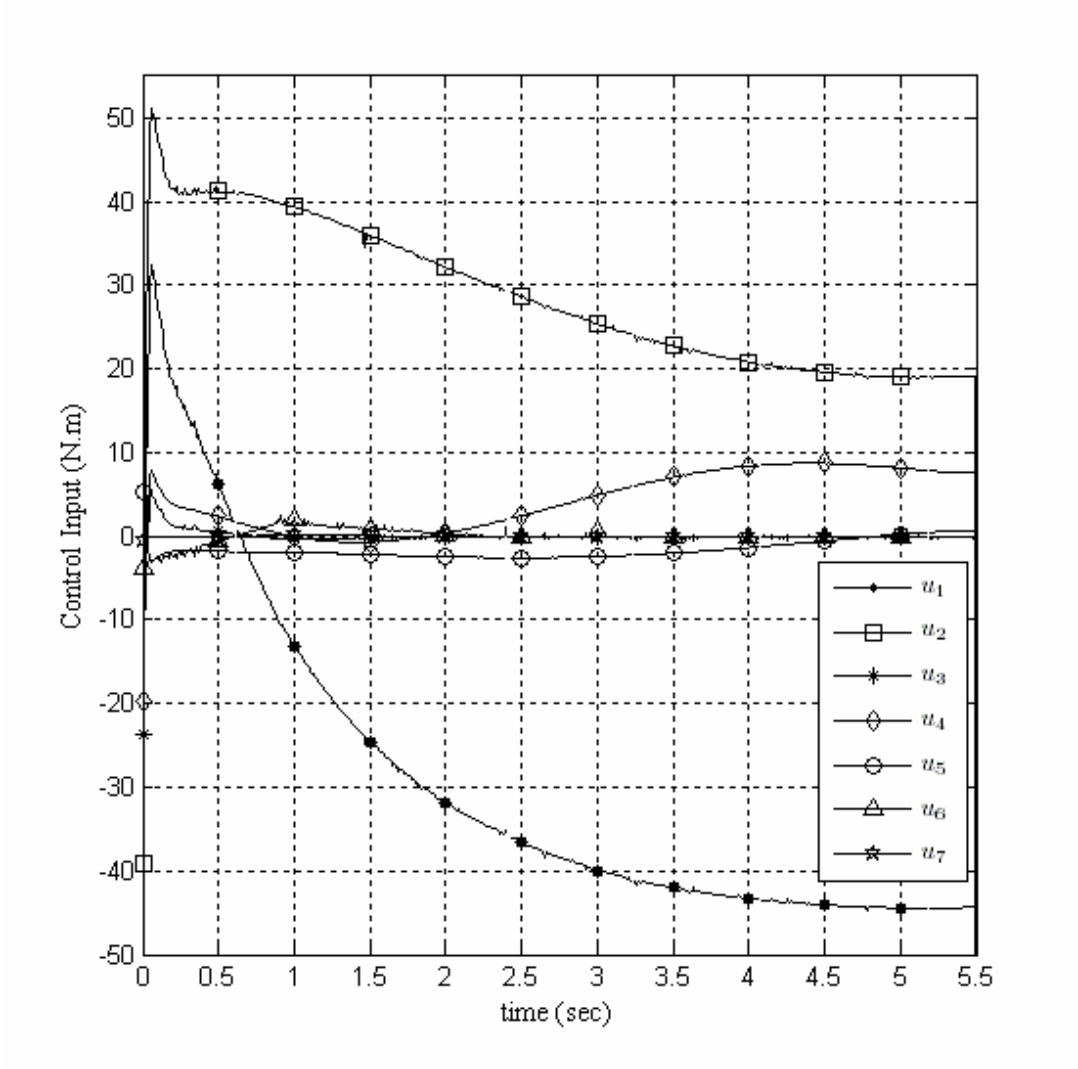

Figure 6.49 Simulated trajectory control input profile for increased Computed Torque Controller parameters

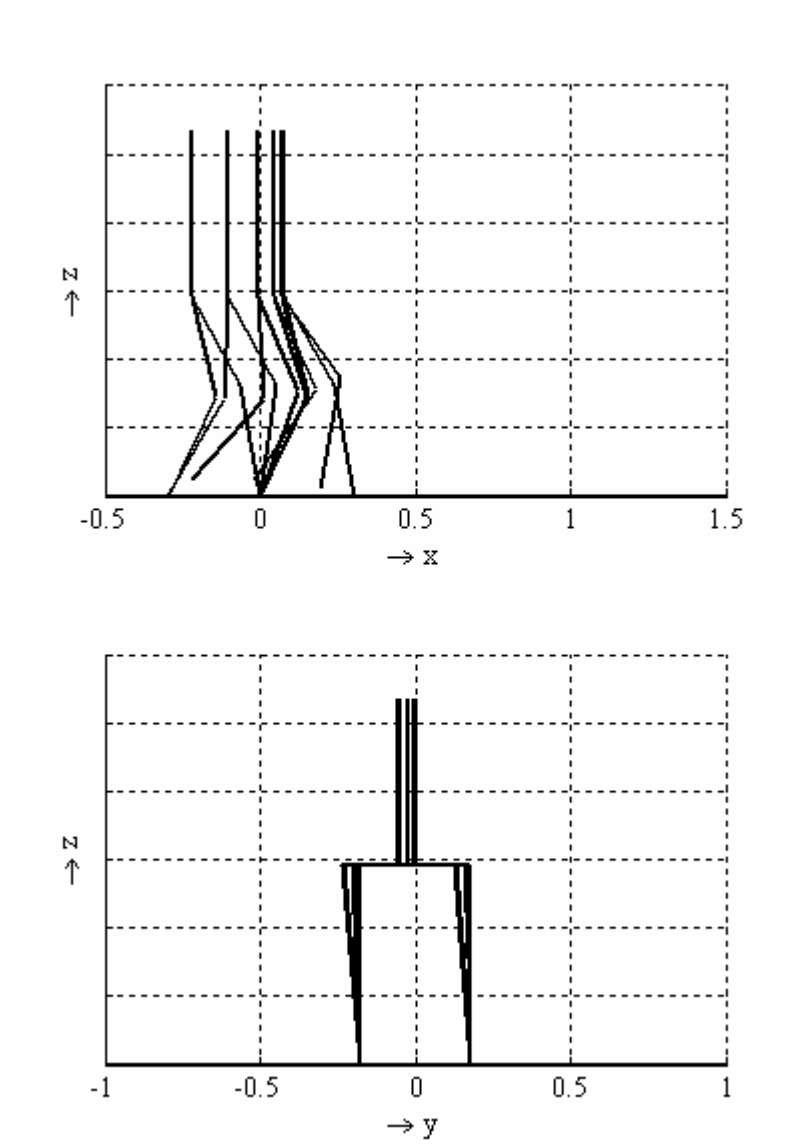

Figure 6.50 Simulated trajectory walking snapshot - sagittal (top) and frontal (bottom) plane views - for increased Computed Torque Controller parameters

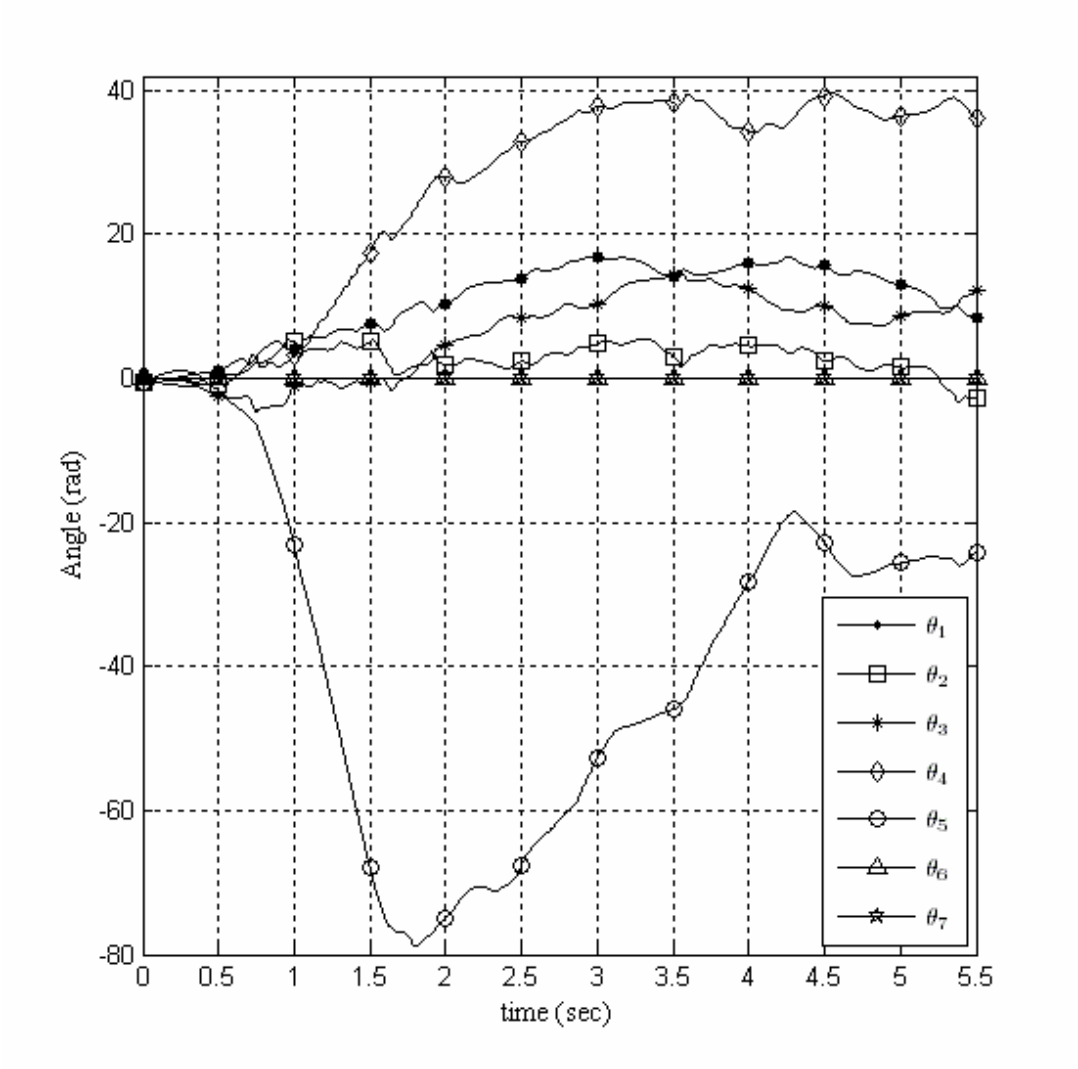

Figure 6.51 Simulated trajectory joint angle profile for Optimal Controller SD parameters

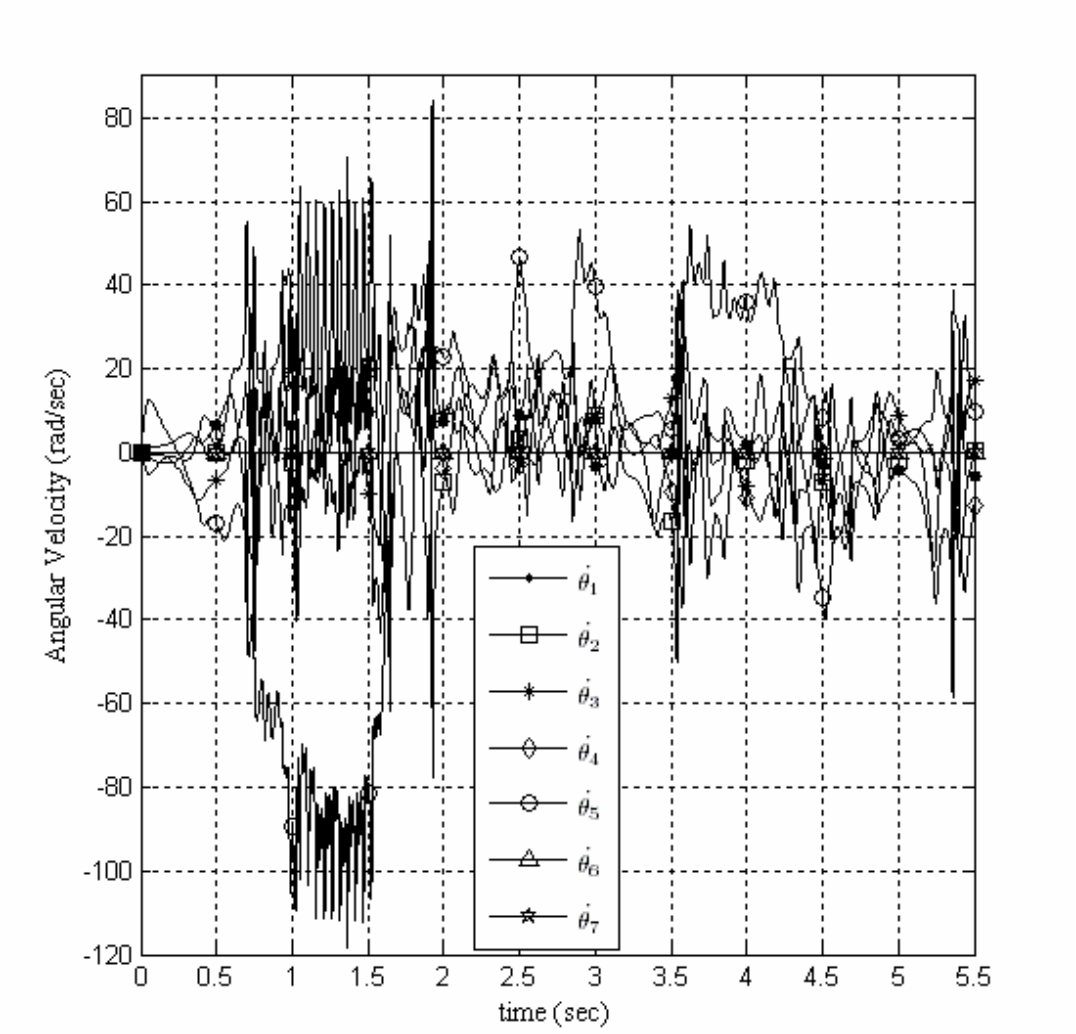

Figure 6.52 Simulated trajectory joint angular velocity profile for Optimal Controller SD parameters

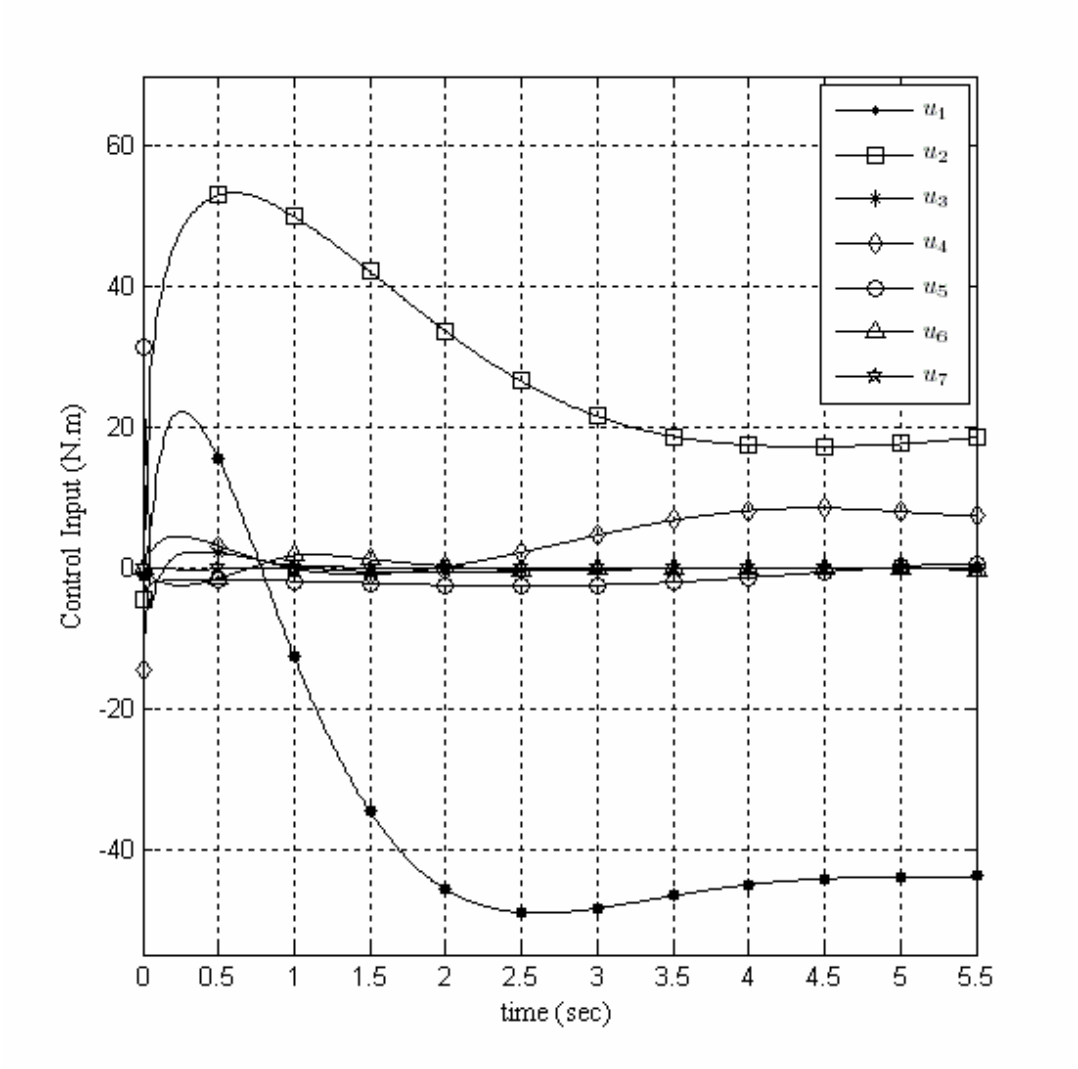

Figure 6.53 Simulated trajectory control input profile for Optimal Controller SD parameters

6.4.5 Differential Equation Solvers

In the biped simulator, three different differential equation solvers are used. The default solver used is the MATLAB ODE45 solver. Unless otherwise specified, the results given are obtained by using MATLAB ODE45 solver. Furthermore, two other solvers, namely, Runge-Kutta (4,5) and Forward Integrator, as the details are given in Appendix D, are also used in the simulation. The simulation results by using Runge-Kutta (4,5) and Forward Integrator solvers are given in Figure 6.54 to Figure 6.59.

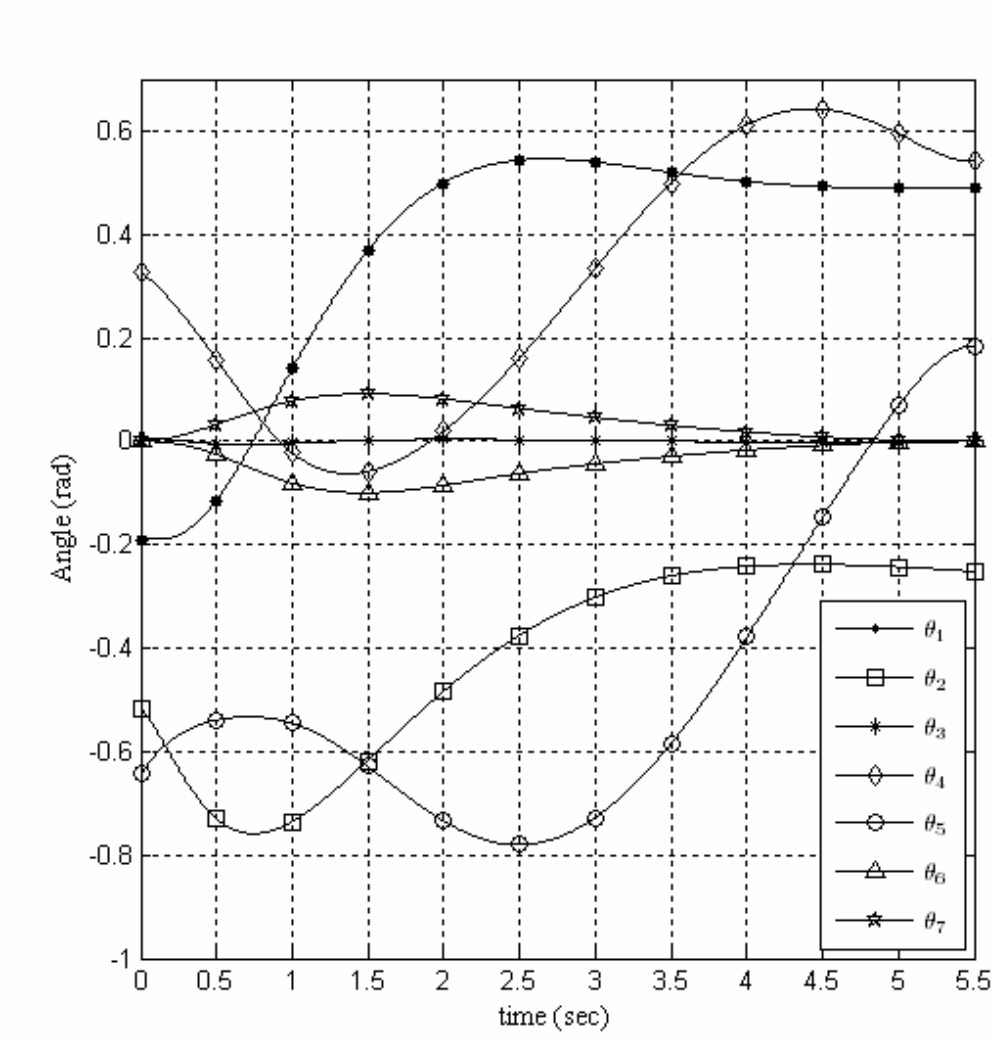

Figure 6.54 Simulated trajectory joint angle profile by using Runge-Kutta 45 method

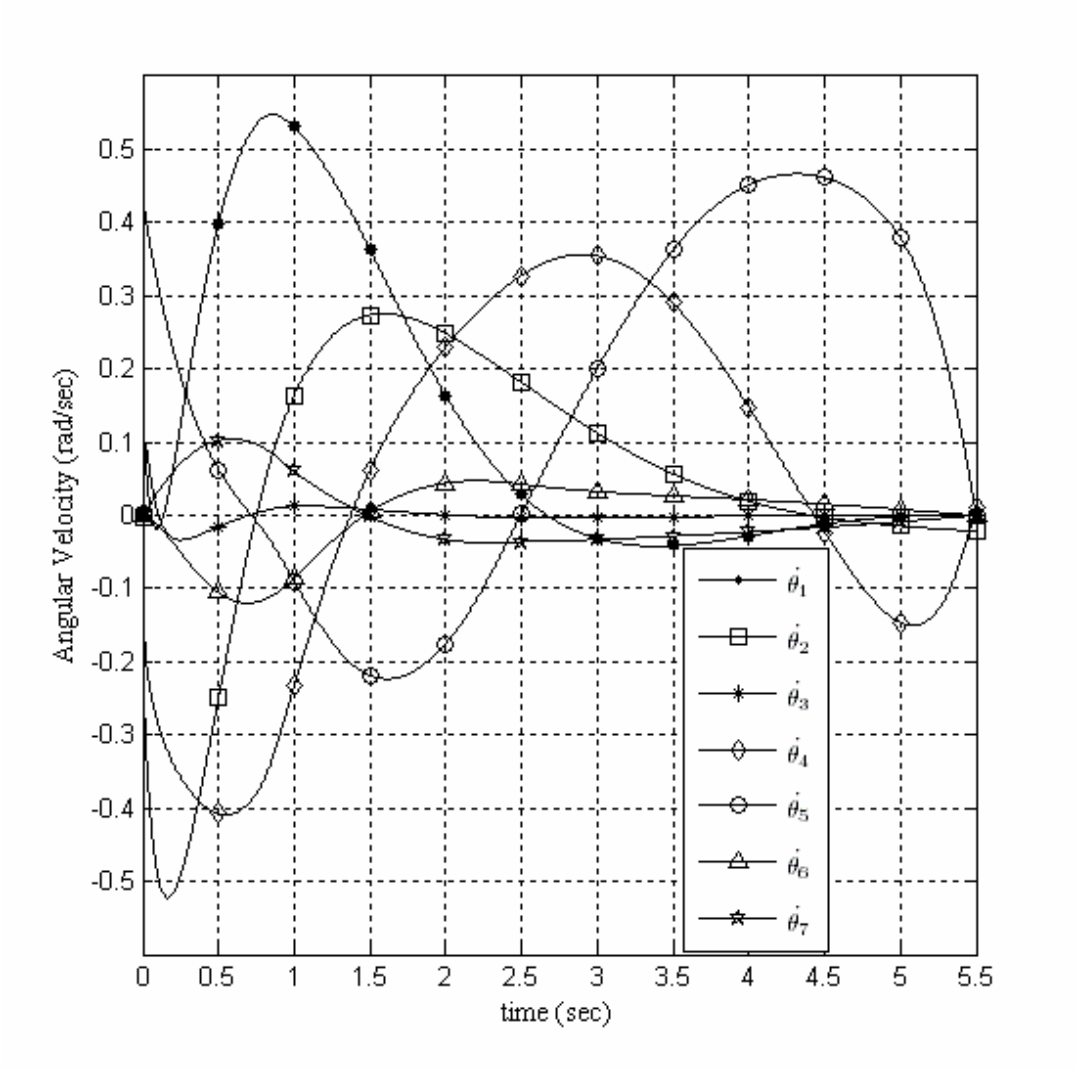

Figure 6.55 Simulated trajectory joint angular velocity profile by using Runge-Kutta 45 method

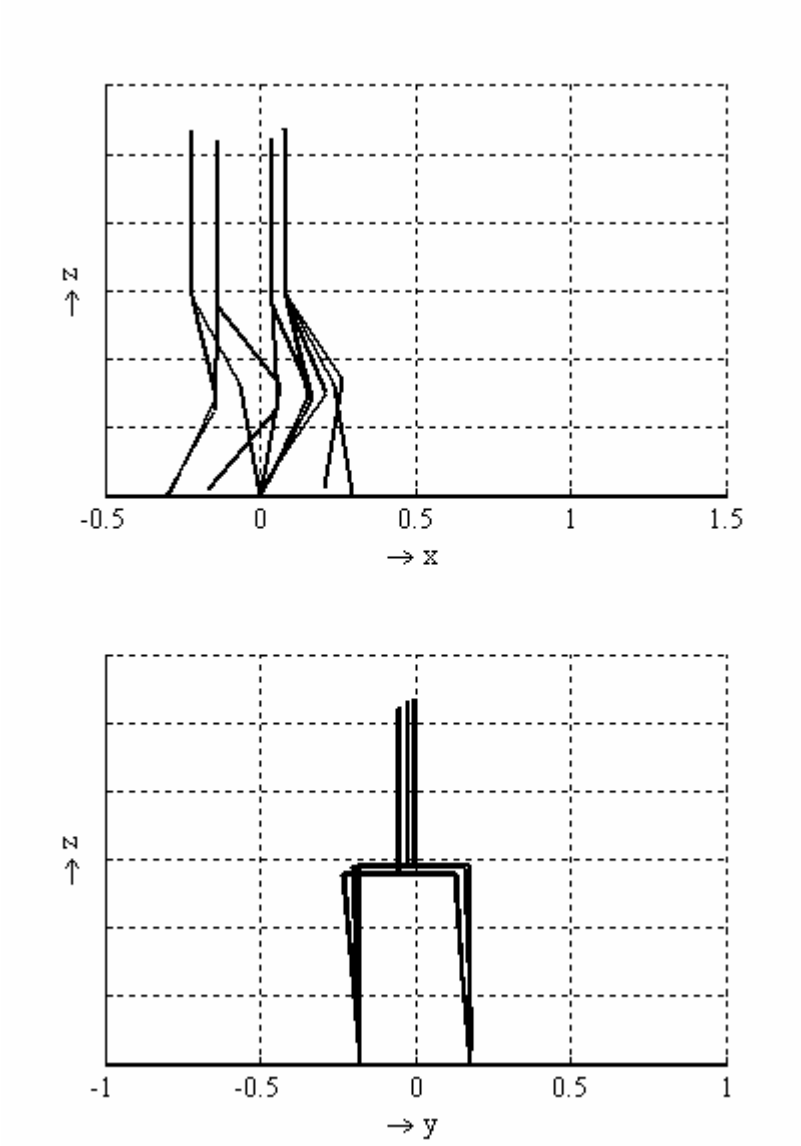

Figure 6.56 Simulated trajectory walking snapshot - sagittal (top) and frontal (bottom) plane views - by using Runge-Kutta 45 method

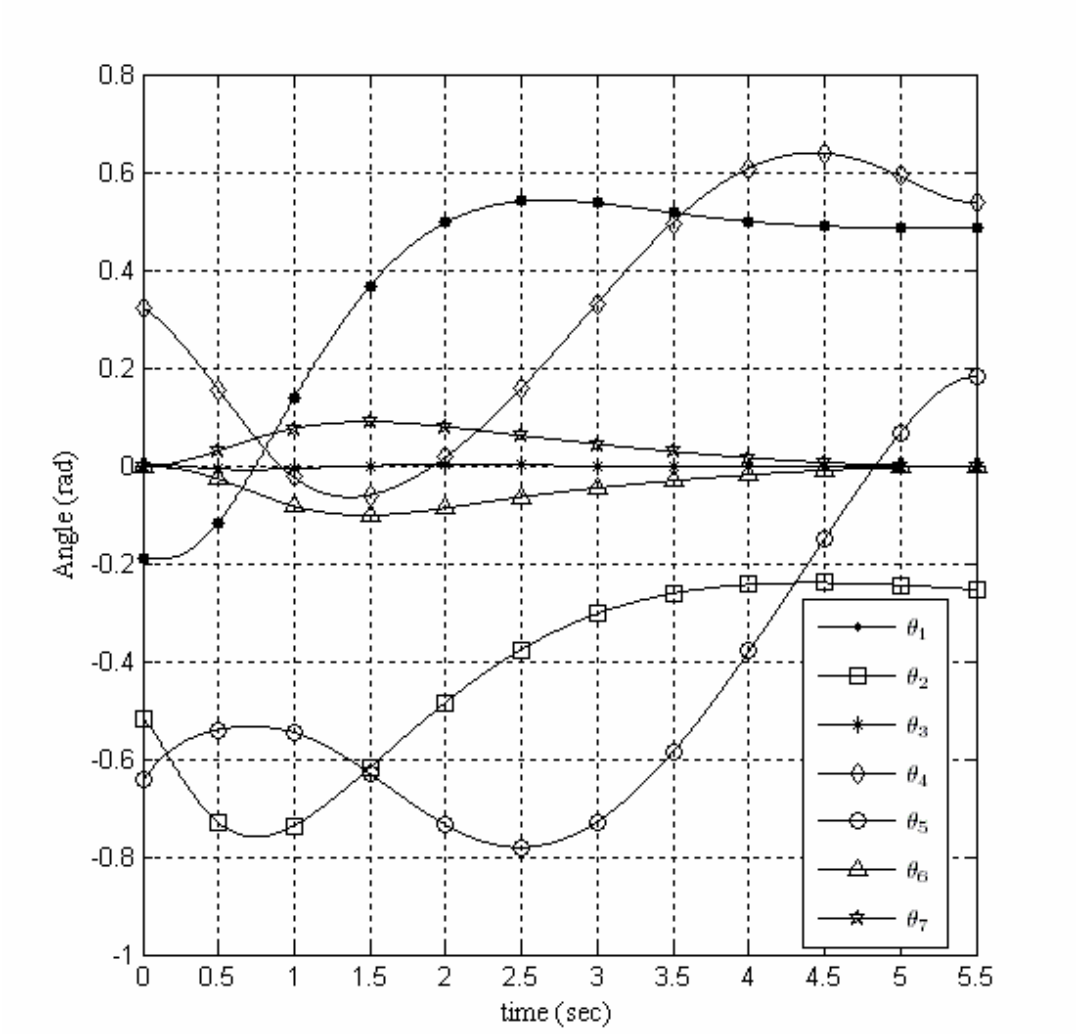

Figure 6.57 Simulated trajectory joint angle profile by using Forward Integrator method

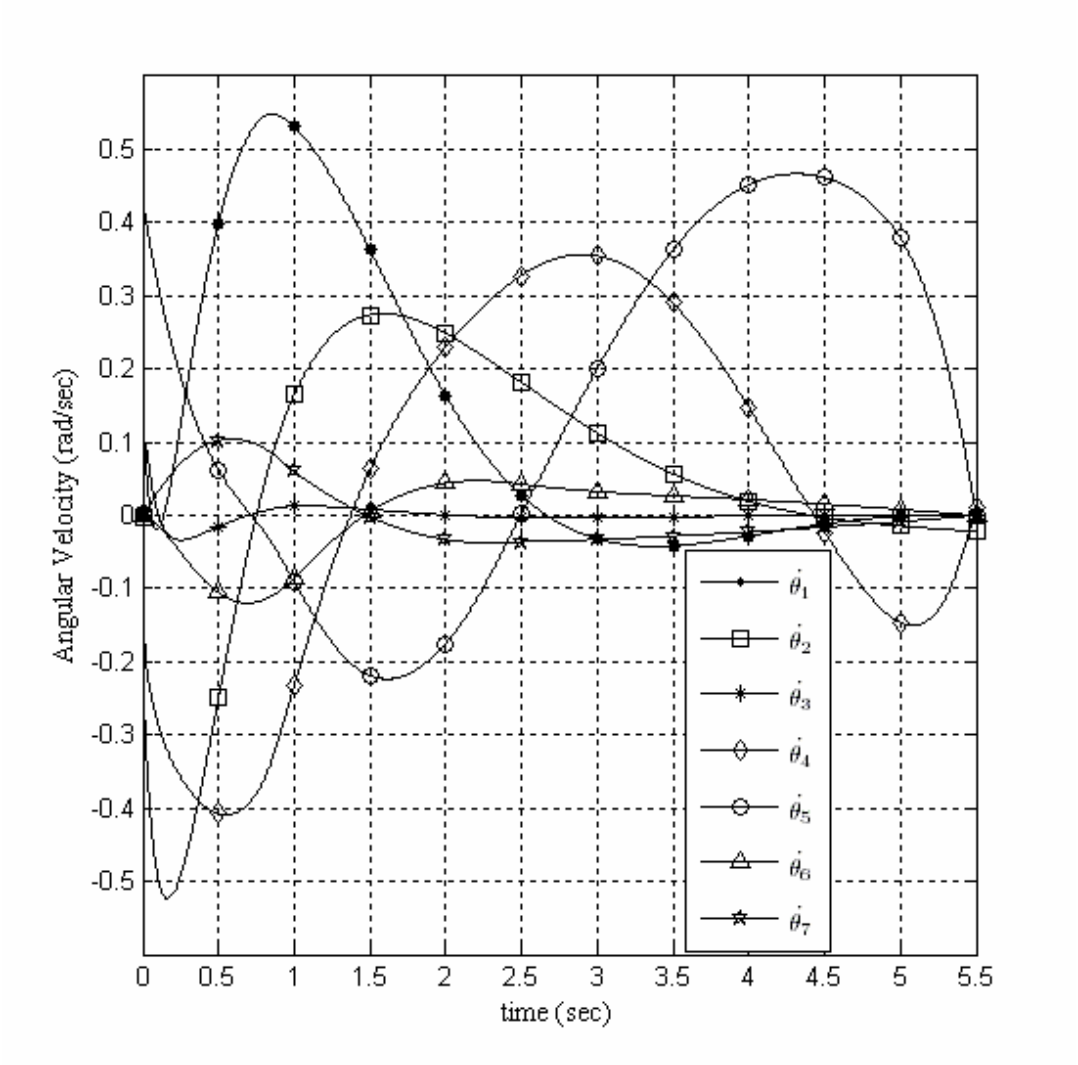

Figure 6.58 Simulated trajectory joint angular velocity profile by using Forward Integrator method

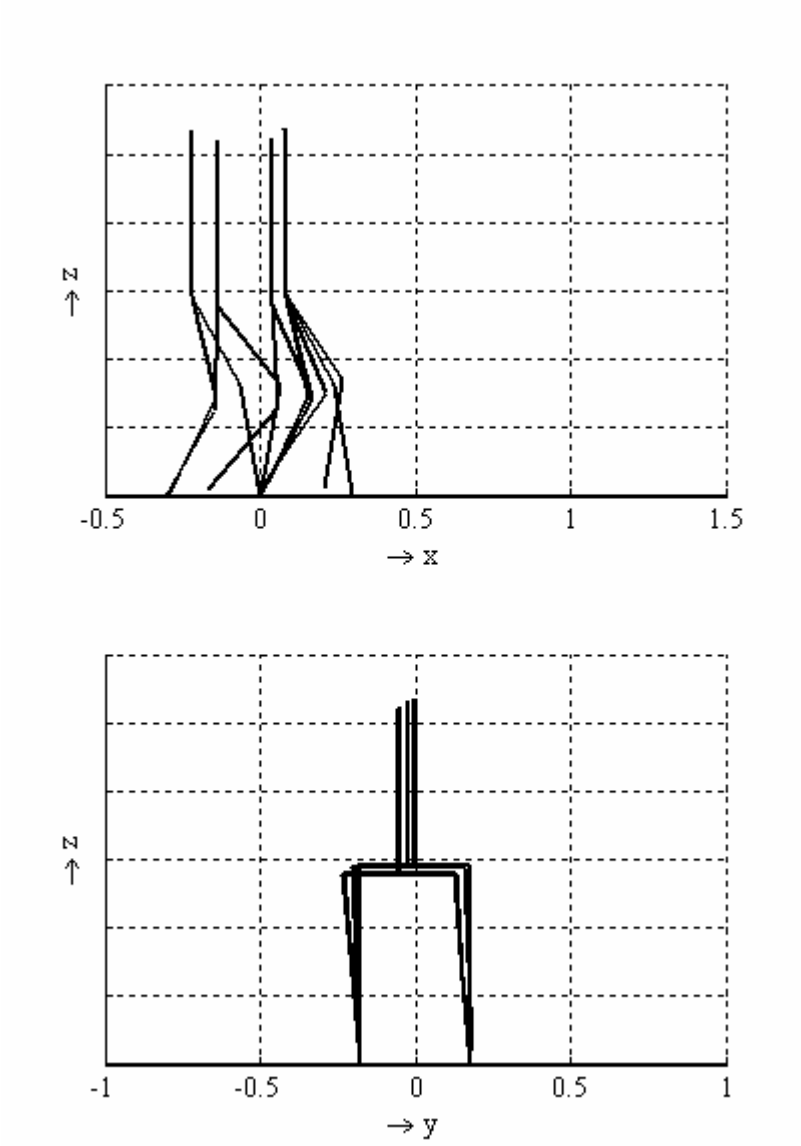

Figure 6.59 Simulated trajectory walking snapshot - sagittal (top) and frontal (bottom) plane views - by using Forward Integrator method

6.4.6 Periodic Walking Trajectories for Different Floor Conditions

The walking is classified into 9 patterns, as per the environmental conditions that robot interacts taken into account. The simulation results for even floor walking (Pattern 1) for different walking and controller parameters are presented up to this point. For illustrating the other pattern results, the angle and angular velocity trajectories and the snapshots of the walking are given in Figure 6.60 to Figure 6.62 for Pattern 2 and Figure 6.63 to Figure 6.65 for Pattern 5. To further elaborate the walking patterns, the periodic motion is investigated and the results are given in detail. The simulator results of the periodic even floor walking are given in Figure 6.66 to Figure 6.68. The simulator results of the periodic stair up walking are given in Figure 6.69 to Figure 6.71. Similarly, the simulator results of the periodic stair down walking are given in Figure 6.72 to Figure 6.74.

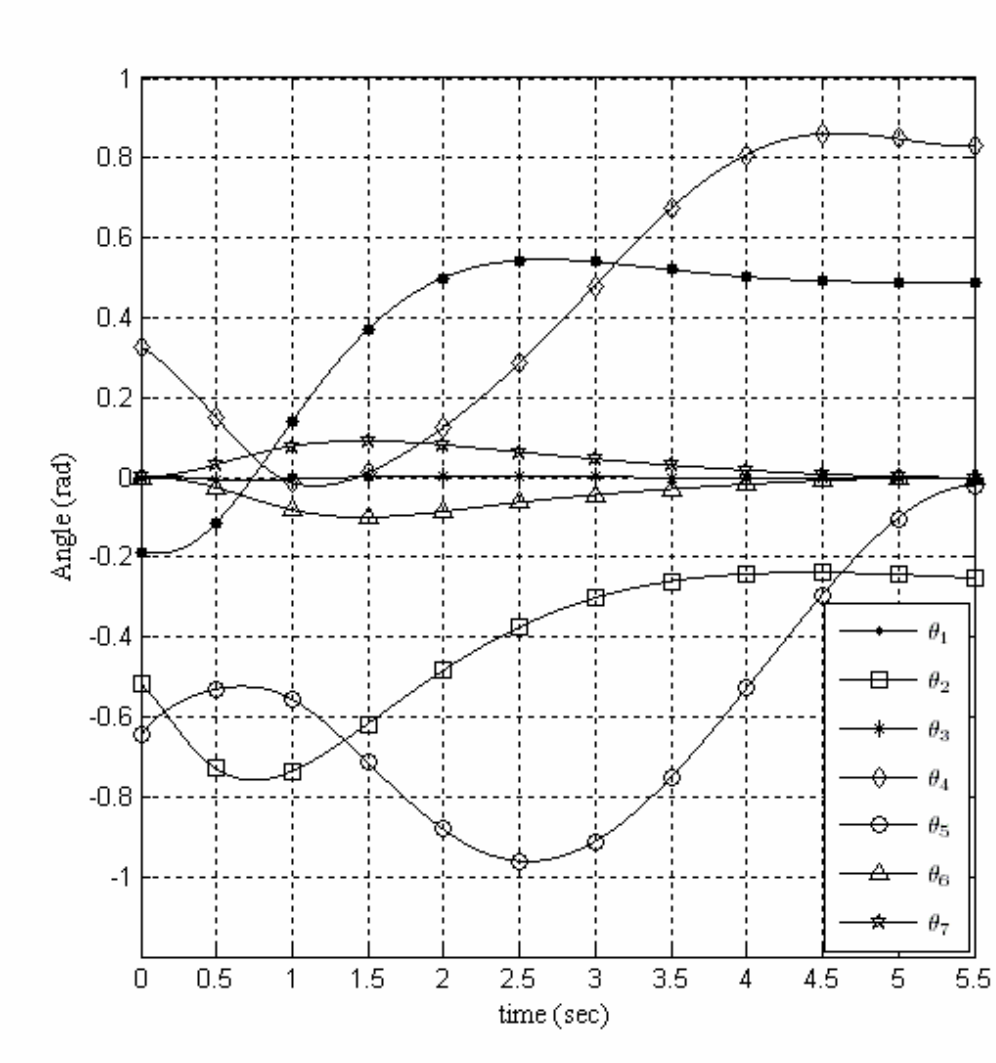

Figure 6.60 Simulated trajectory joint angle profile for Pattern 2

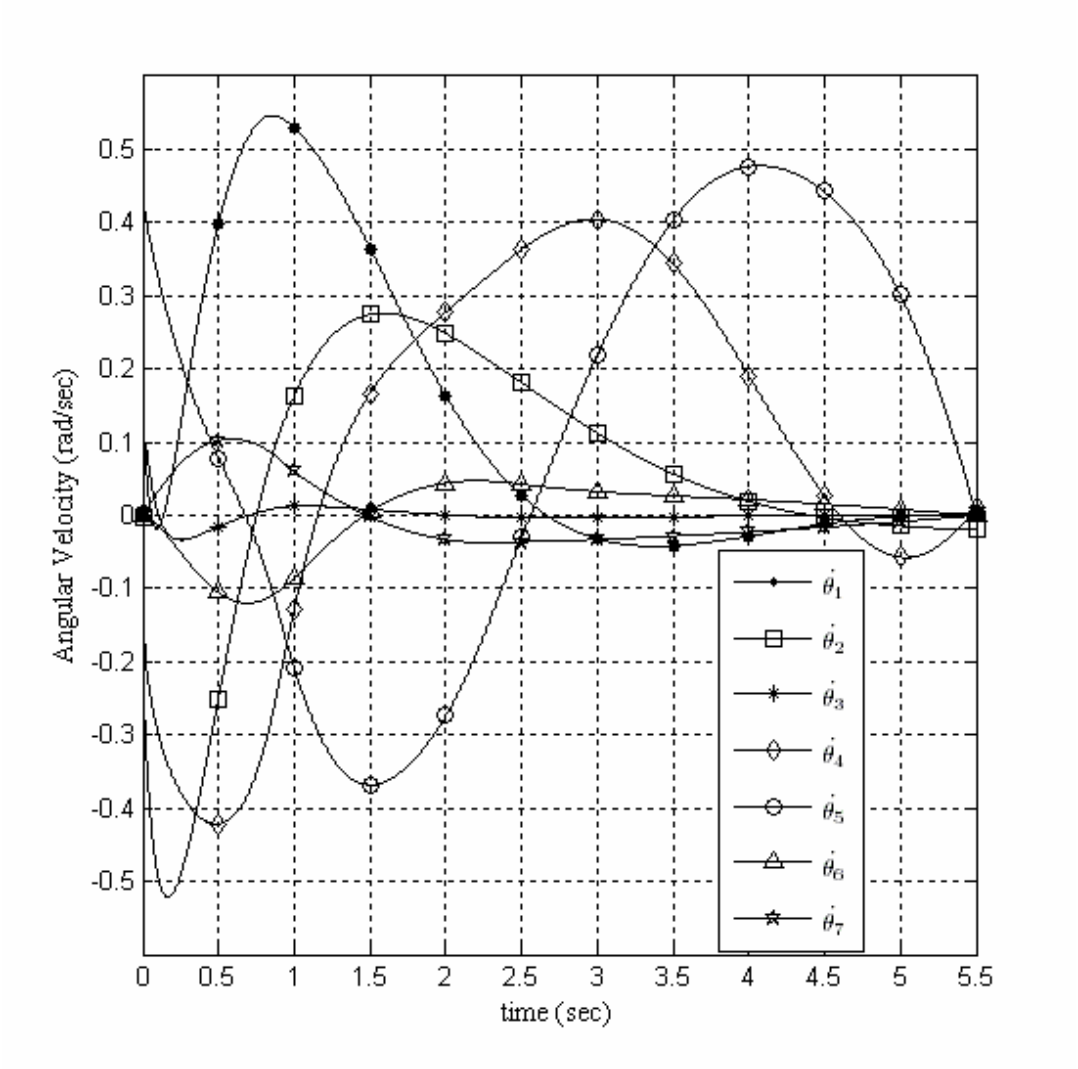

Figure 6.61 Simulated trajectory joint angular velocity profile for Pattern 2

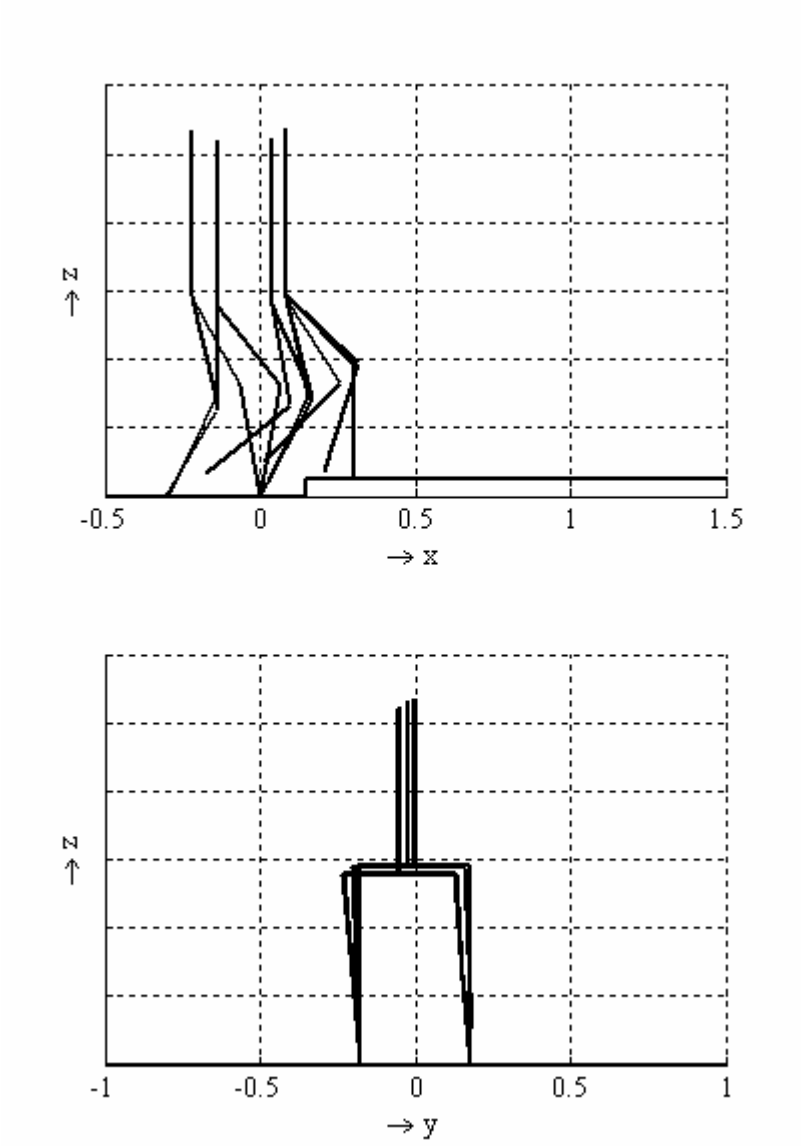

Figure 6.62 Simulated trajectory walking snapshot - sagittal (top) and frontal (bottom) plane views - for Pattern 2

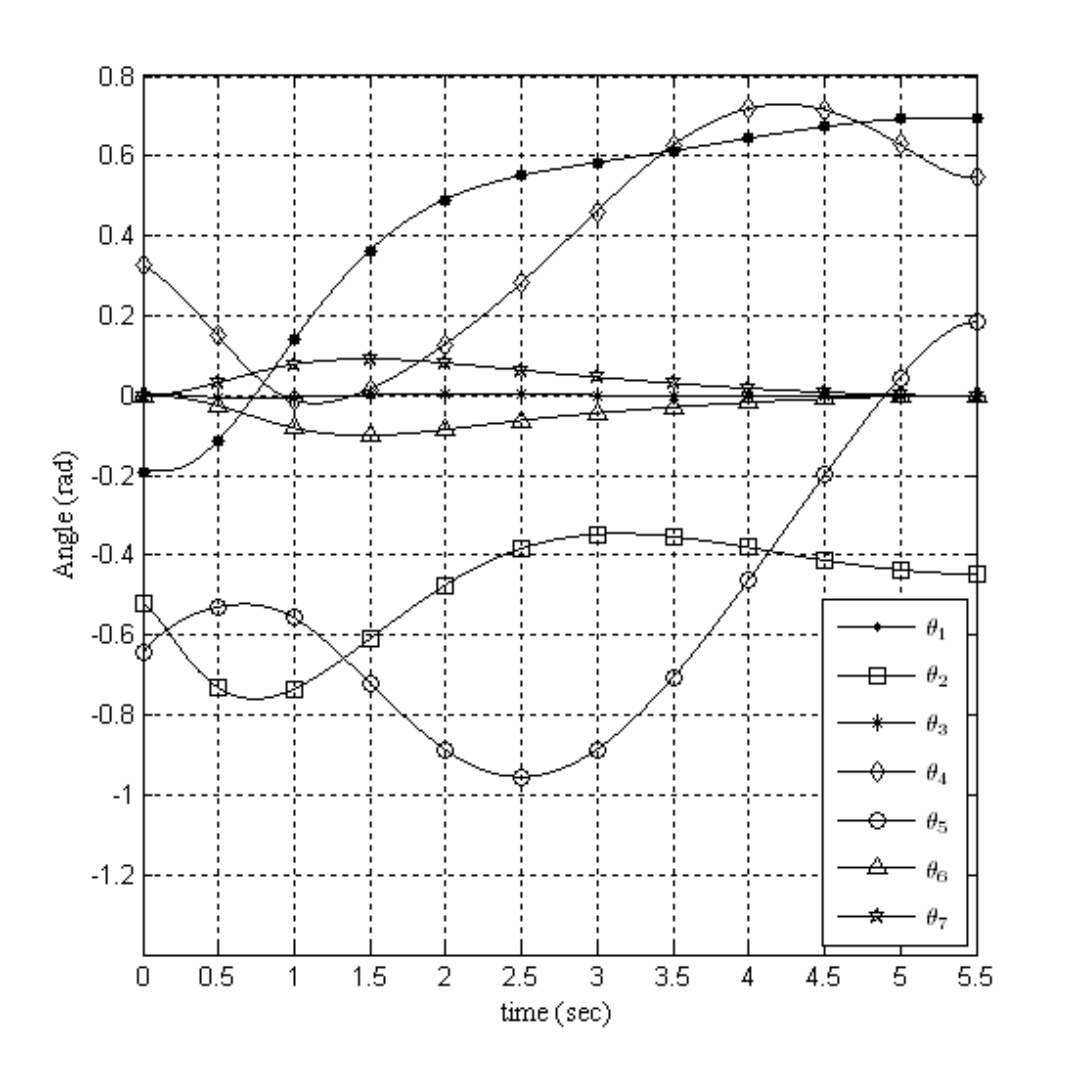

Figure 6.63 Simulated trajectory joint angle profile for Pattern 5

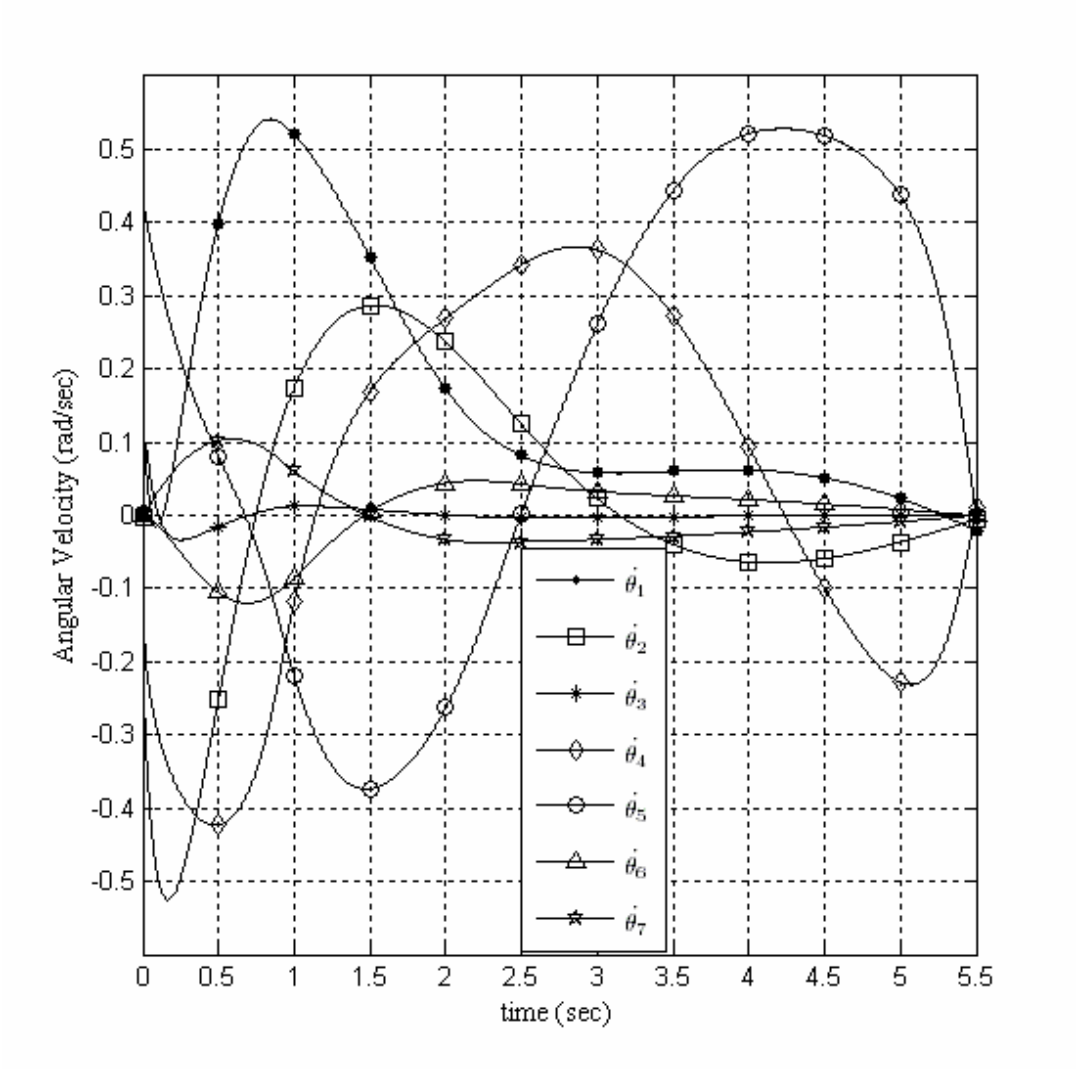

Figure 6.64 Simulated trajectory joint angular velocity profile for Pattern 5

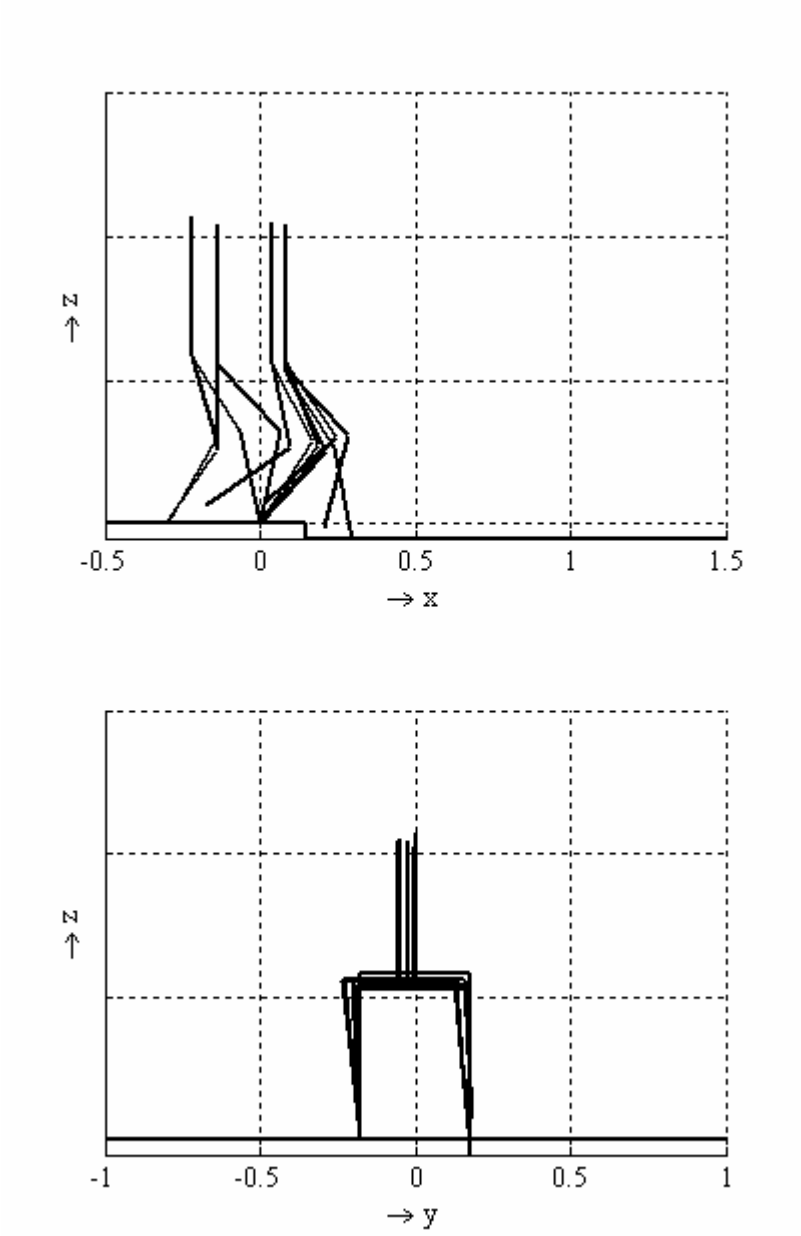

Figure 6.65 Simulated trajectory walking snapshot - sagittal (top) and frontal (bottom) plane views - for Pattern 5

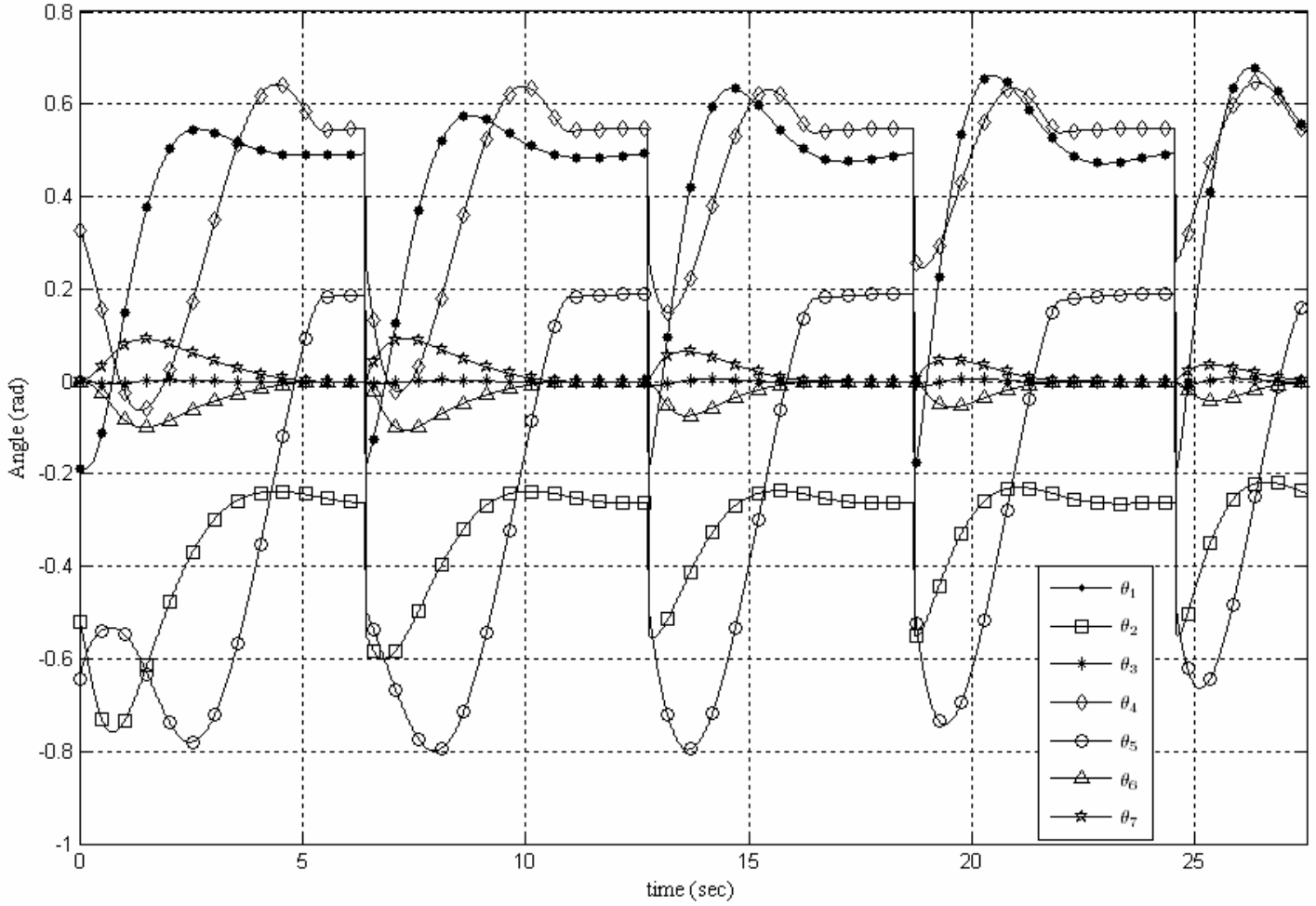

Figure 6.66 Simulated trajectory joint angle profile for periodic even floor walking

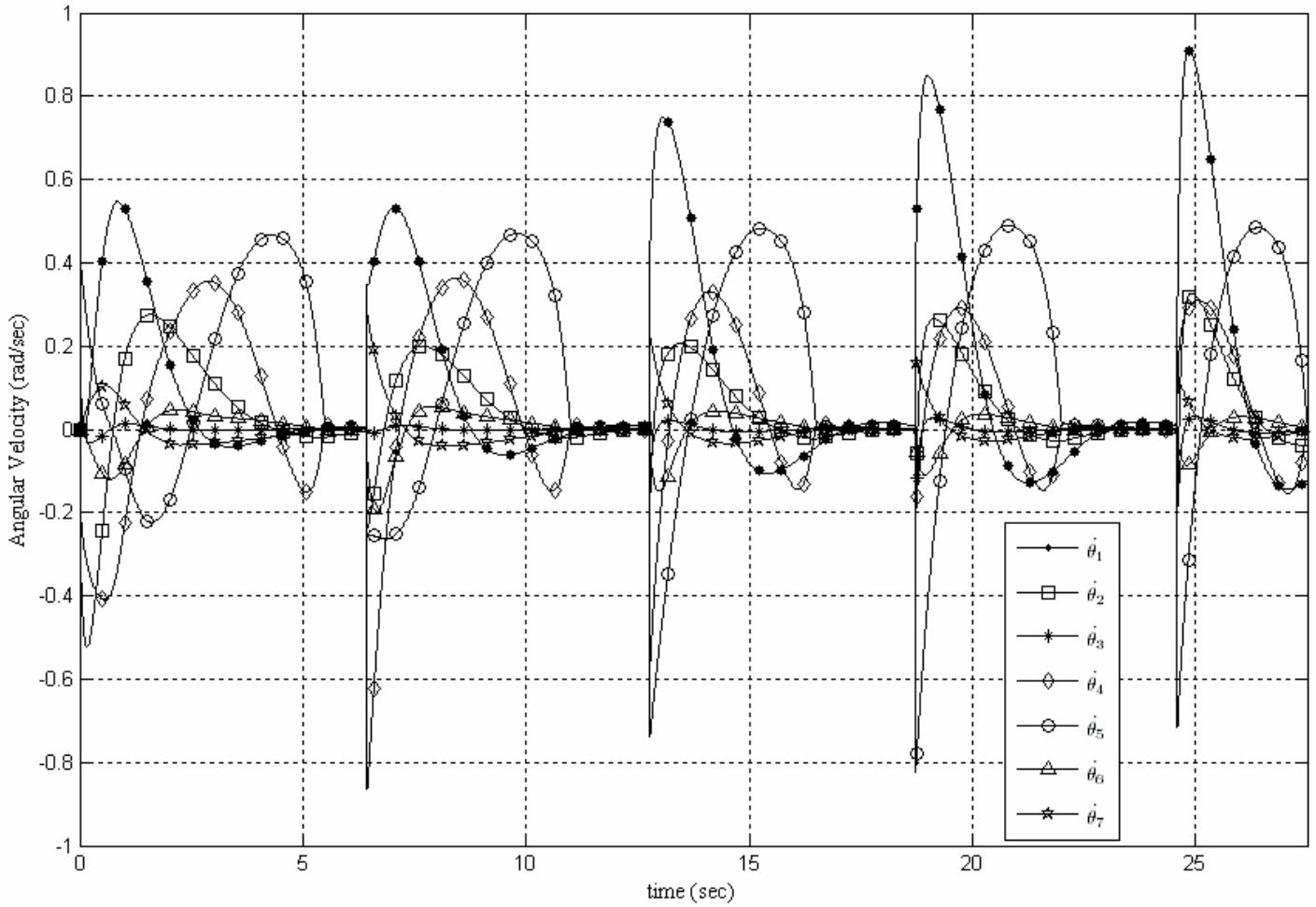

Figure 6.67 Simulated trajectory joint angular velocity profile for periodic even floor walking

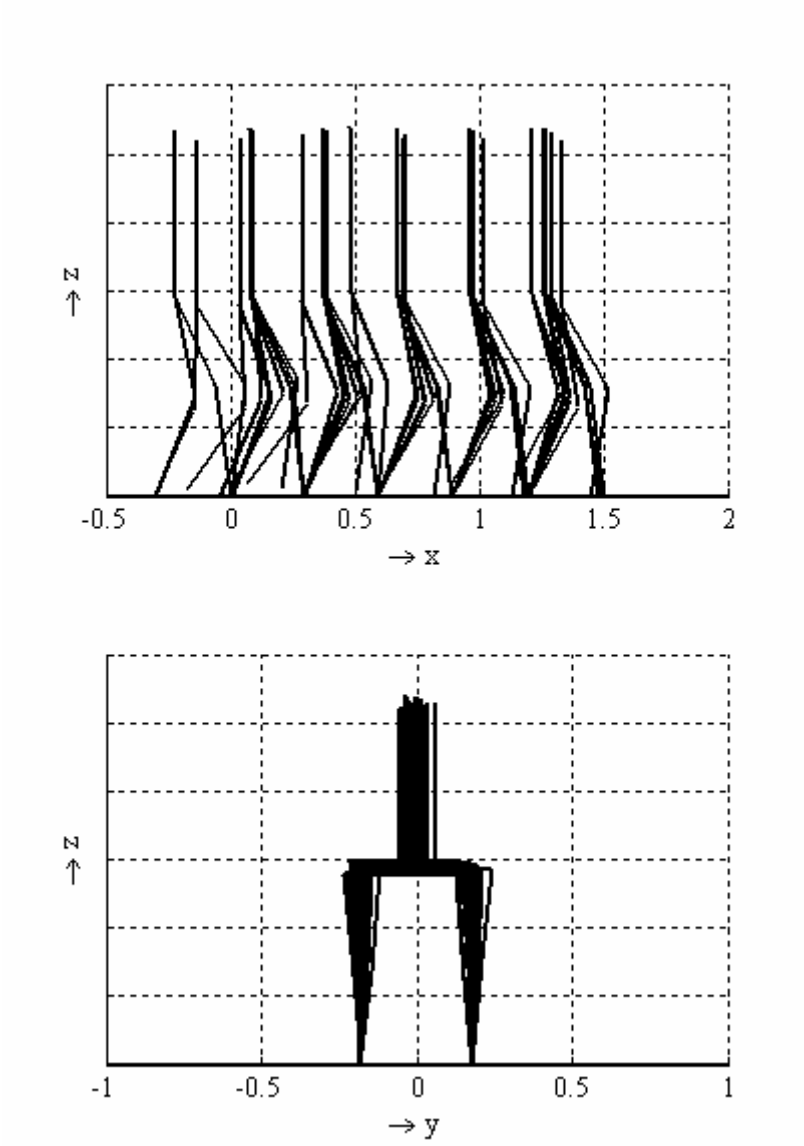

Figure 6.68 Simulated trajectory walking snapshot - sagittal (top) and frontal (bottom) plane views - for periodic even floor walking

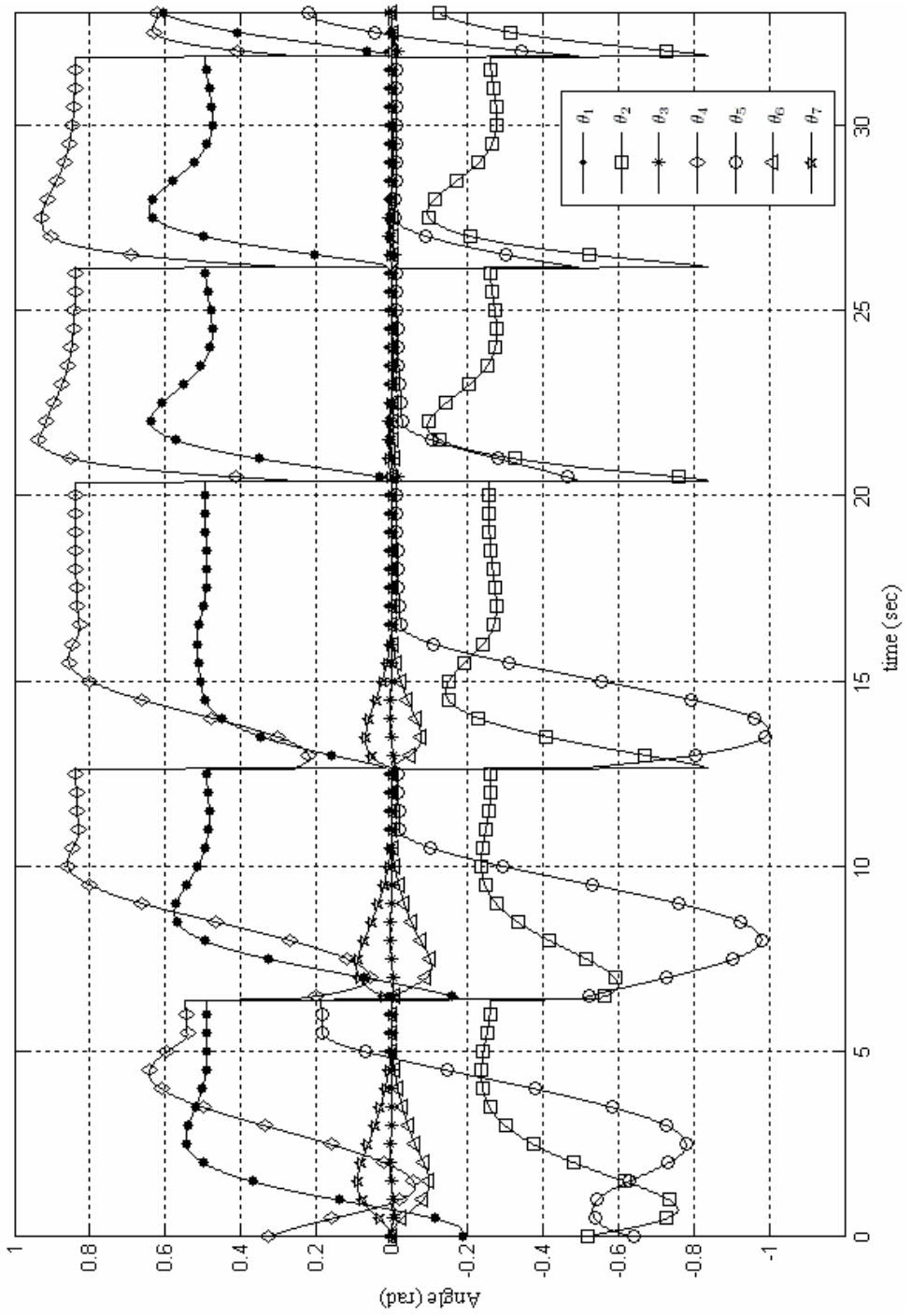

Figure 6.69 Simulated trajectory joint angle profile for periodic stair up walking

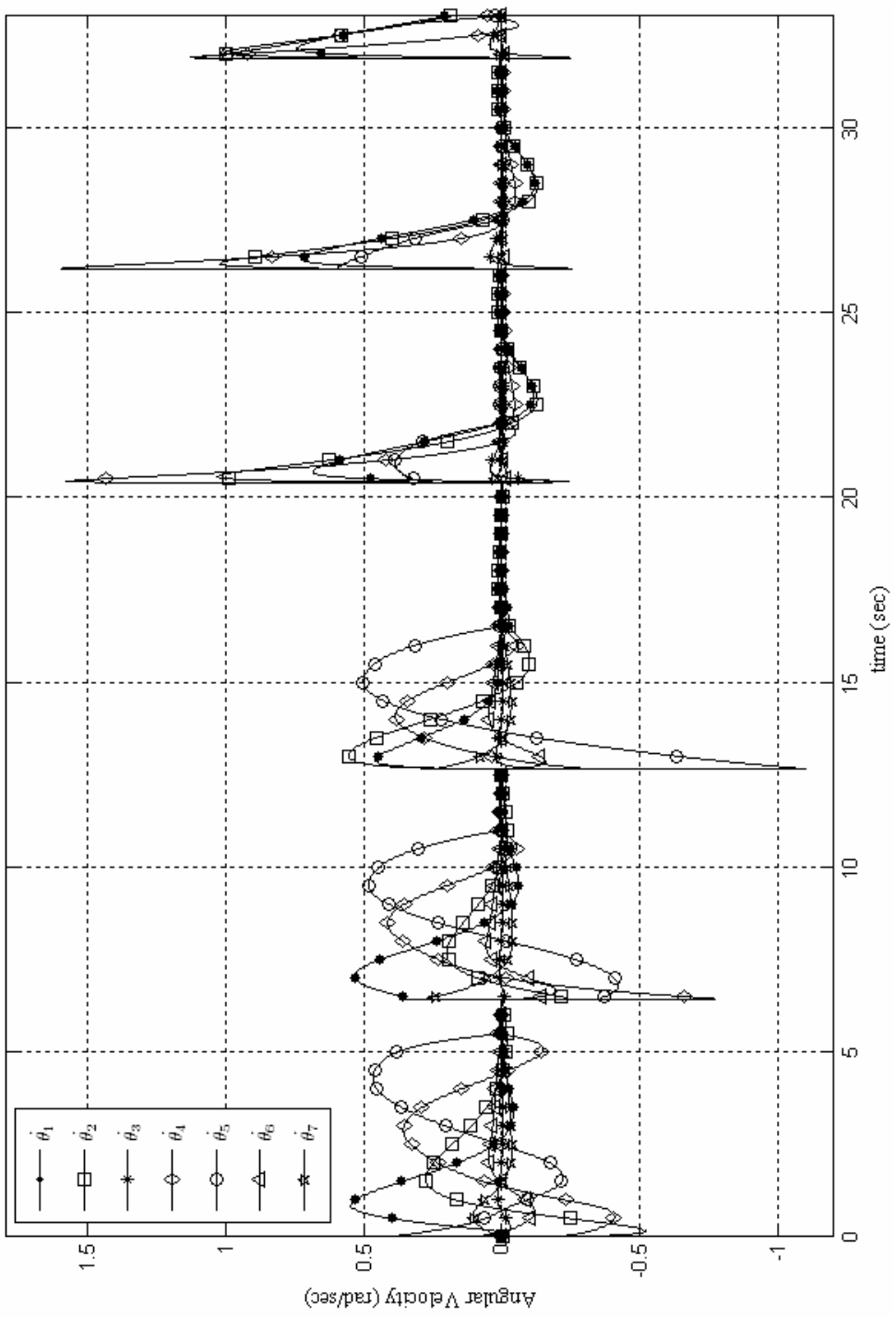

Figure 6.70 Simulated trajectory joint angular velocity profile for periodic stair up walking

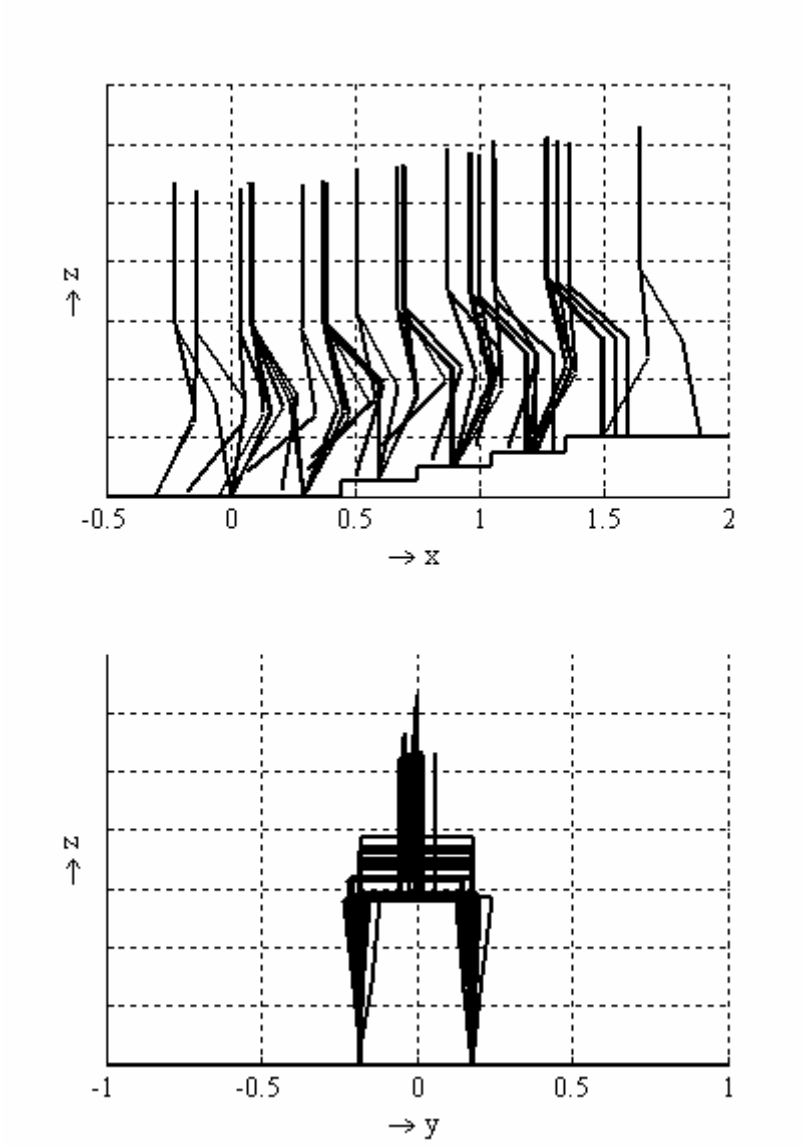

Figure 6.71 Simulated trajectory walking snapshot - sagittal (top) and frontal (bottom) plane views - for periodic stair up walking

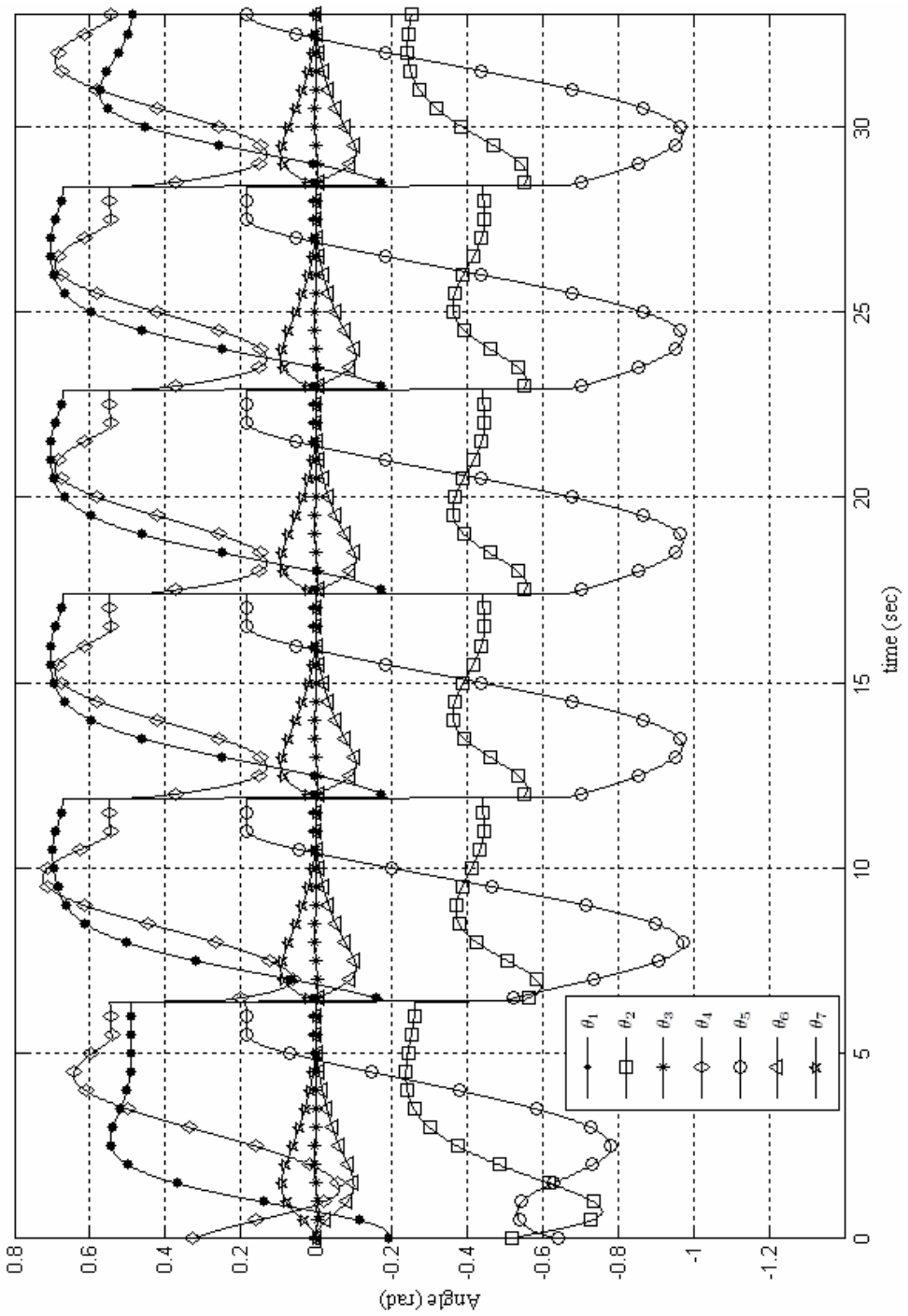

Figure 6.72 Simulated trajectory joint angle profile for periodic stair down walking

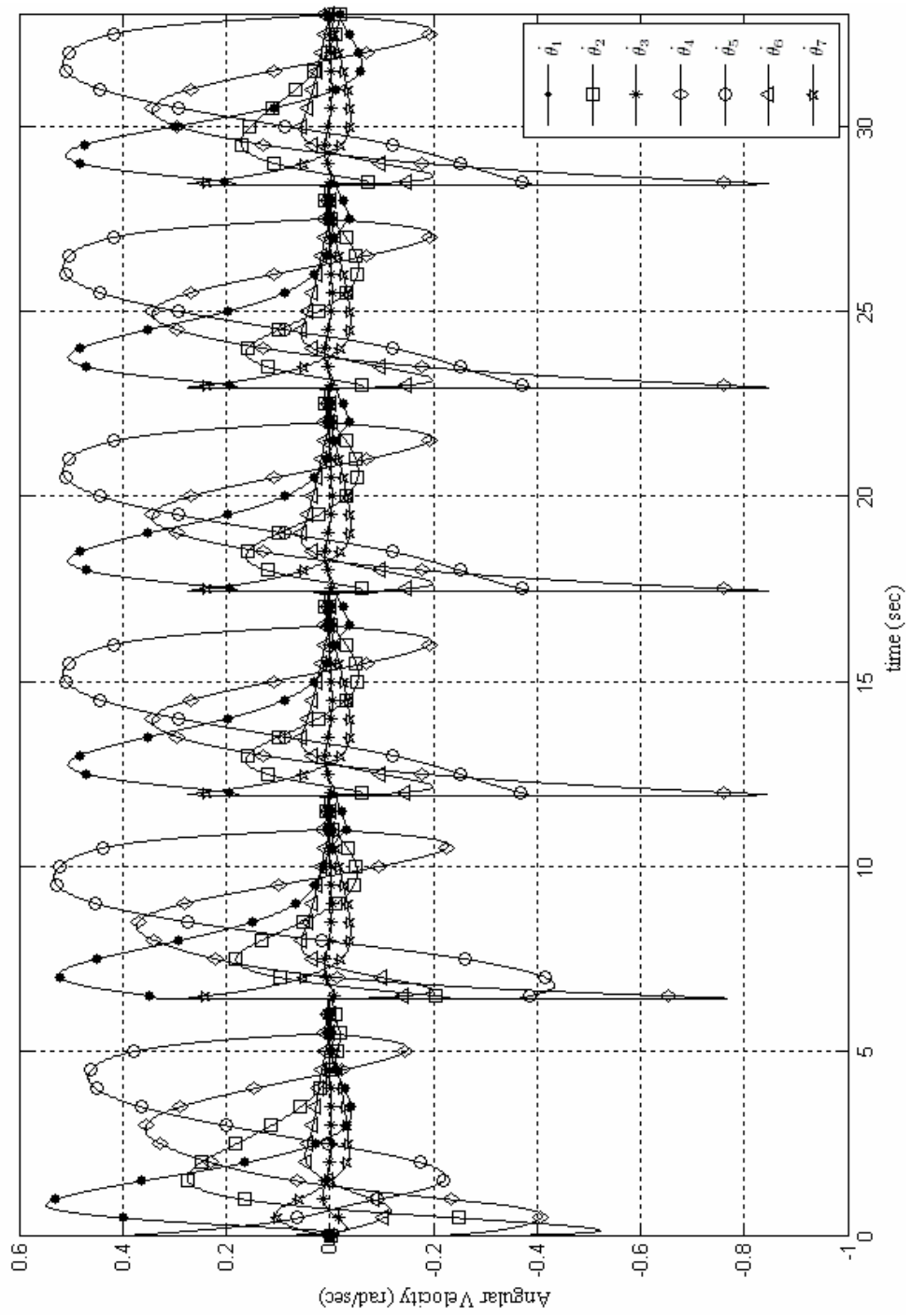

Figure 6.73 Simulated trajectory joint angular velocity profile for periodic stair down walking

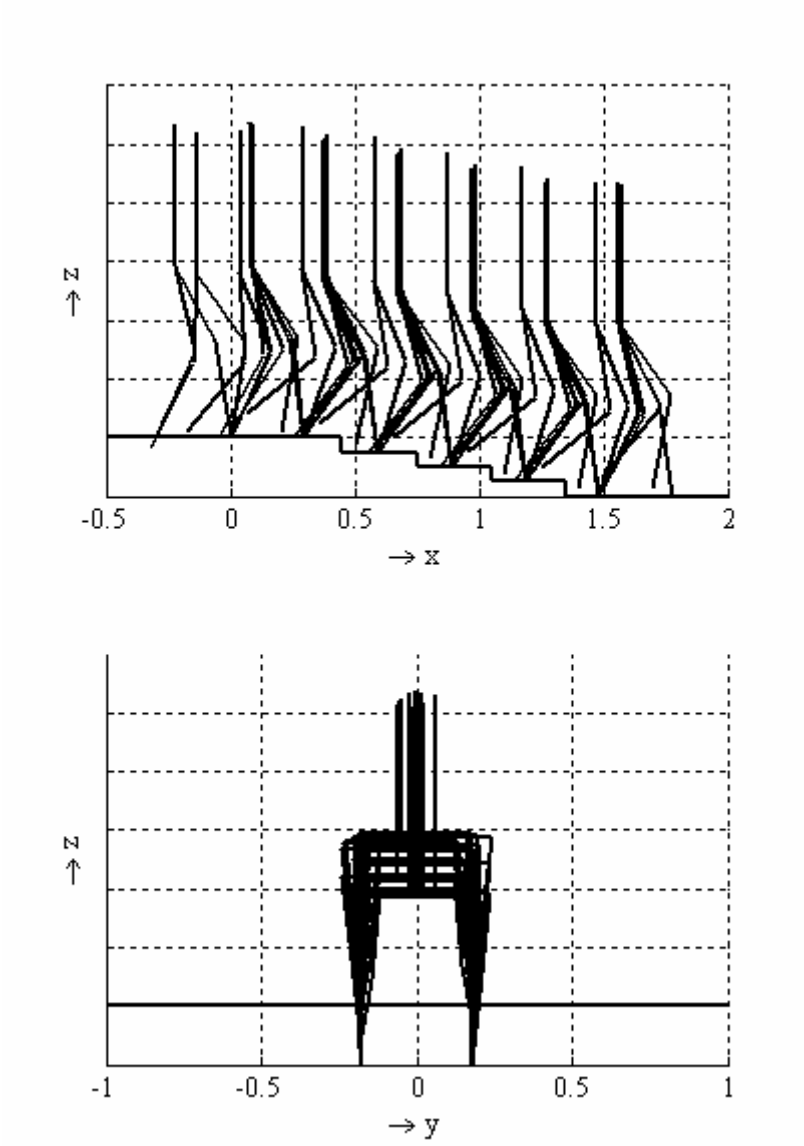

Figure 6.74 Simulated trajectory walking snapshot - sagittal (top) and frontal (bottom) plane views - for periodic stair down walking

6.4.7 Desired Path and Reference Trajectory for Performance Evaluation

The overall system performance is evaluated by using the environment of global desired path as depicted in Figure 6.75. For this global path given, the Guidance Controller, designed as a Genetic Algorithm based HLC, determines the biped system's reference footstep walking trajectory from a given global path data while minimizing the performance measure (a measure of energy consumed during walking) by ensuring the stability of biped. For this given global path, the GA based method is used to solve the problem and to determine the sequence of pattern classes to be followed by the biped robot by using optimality principle and stability of biped for this given global path. As a result a step trajectory in terms of step pattern sequence is generated. The resulting reference and simulated angle, angular velocity trajectories and the snapshots of walking for reference and simulated cases are given in Figure 6.76 to Figure 6.78 and in Figure 6.79 to Figure 6.81, respectively.

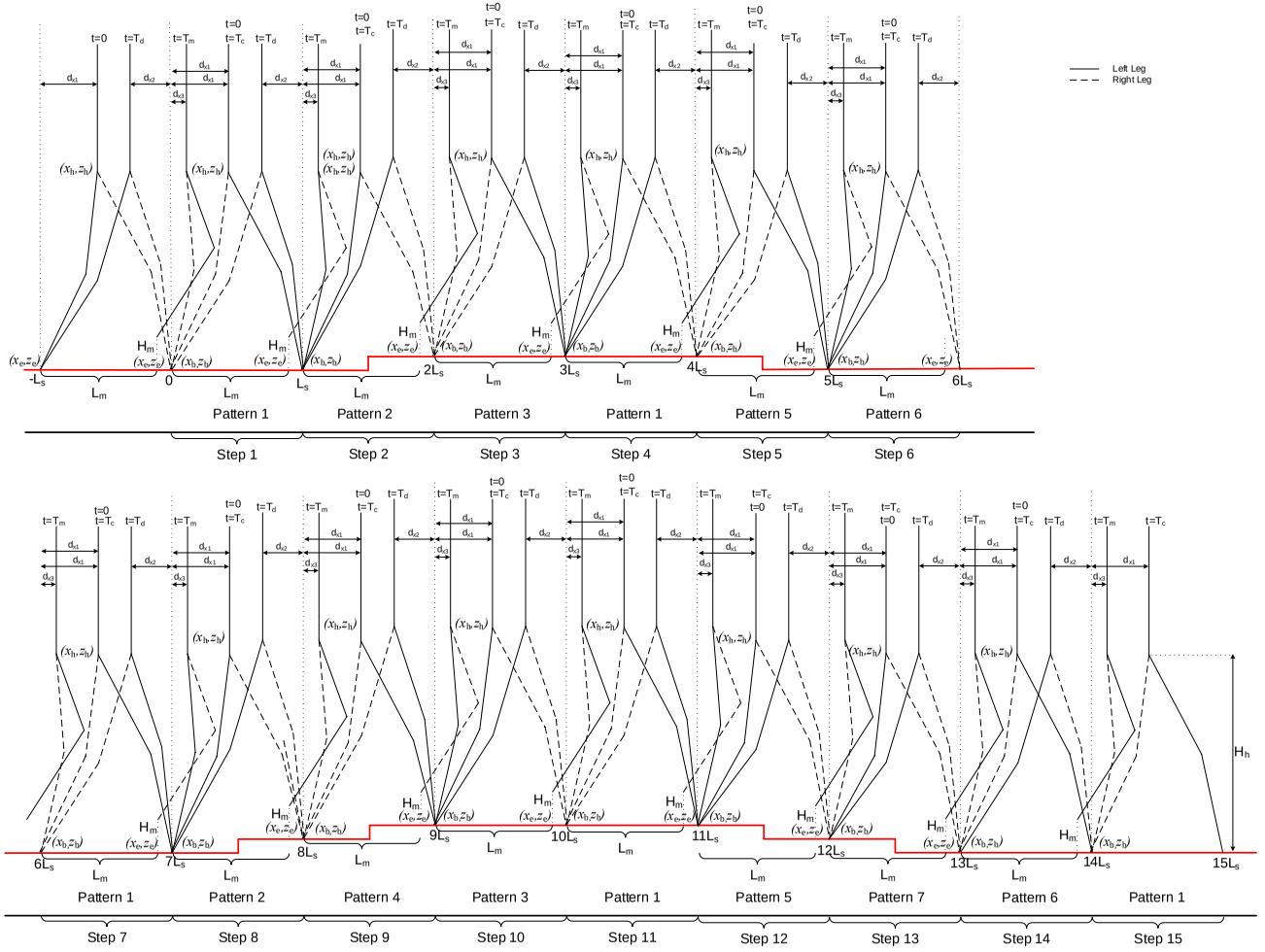

Figure 6.75 Desired Biped Path

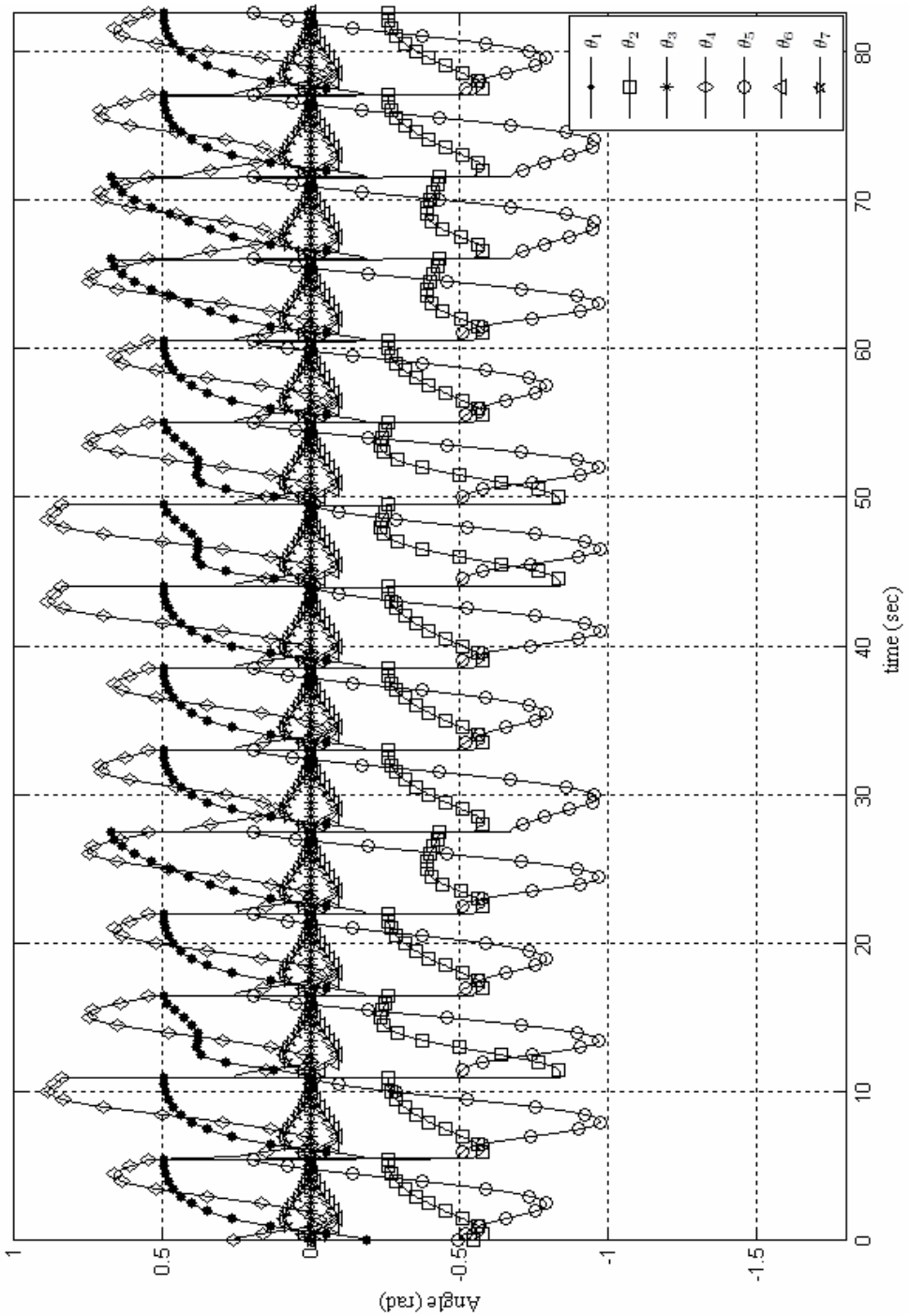

Figure 6.76 Reference trajectory joint angle profile for given path

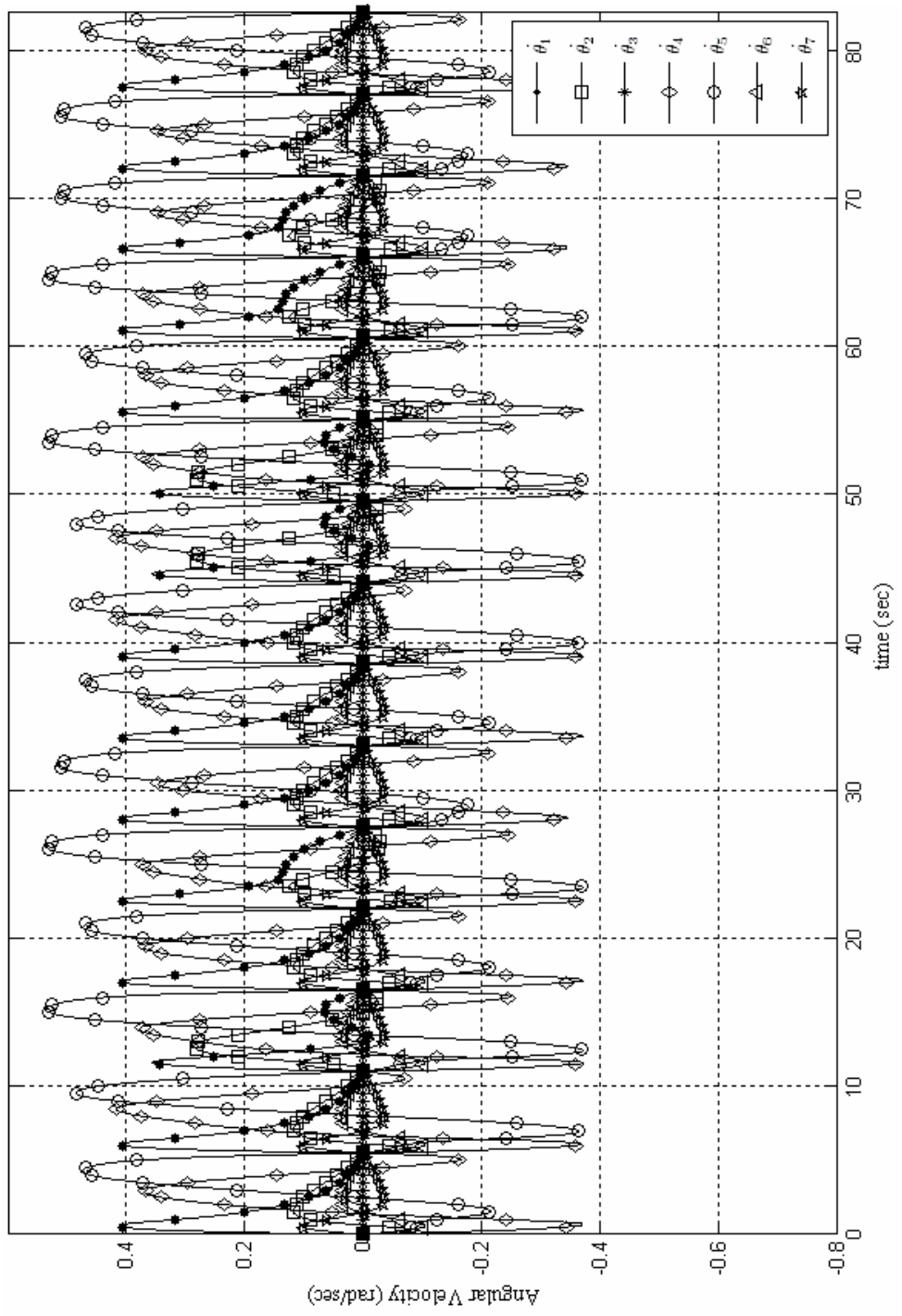

Figure 6.77 Reference trajectory joint angular velocity profile for given path

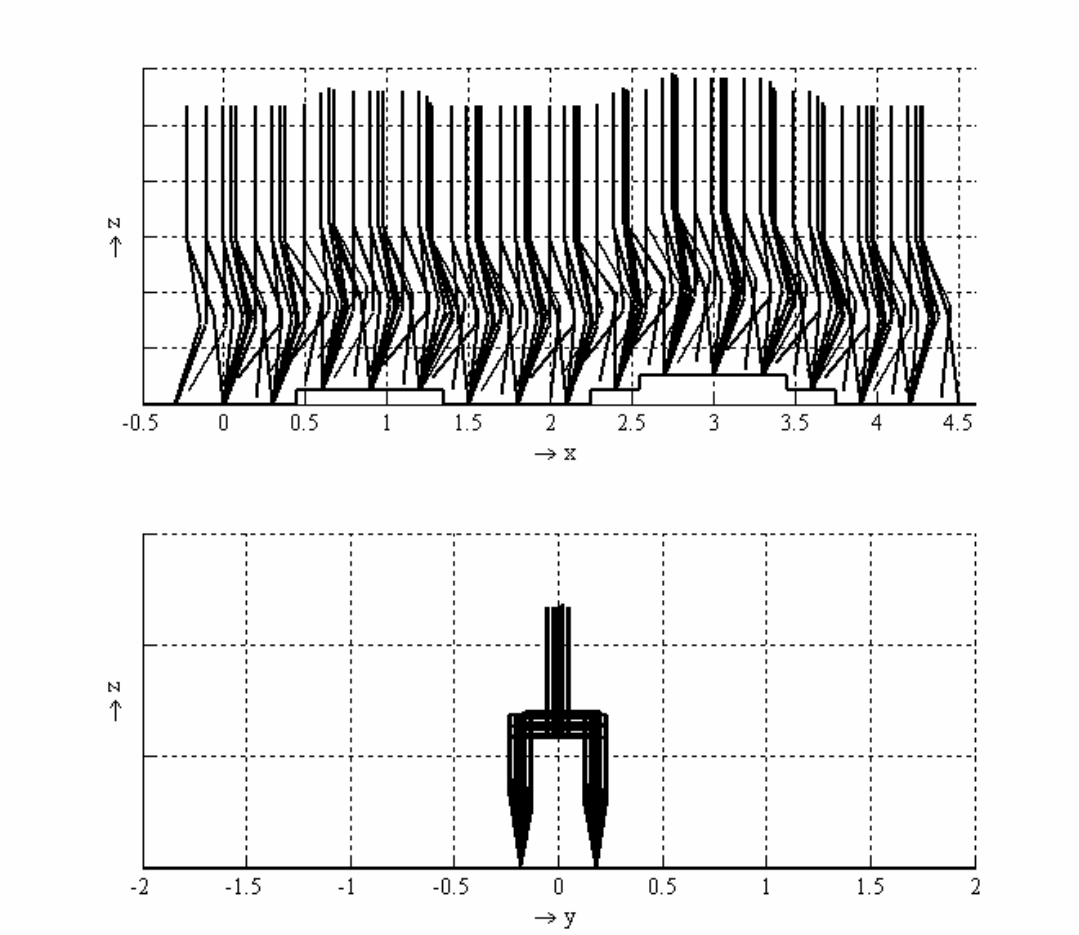

Figure 6.78 Reference trajectory walking snapshot - sagittal (top) and frontal (bottom) plane views - for given path

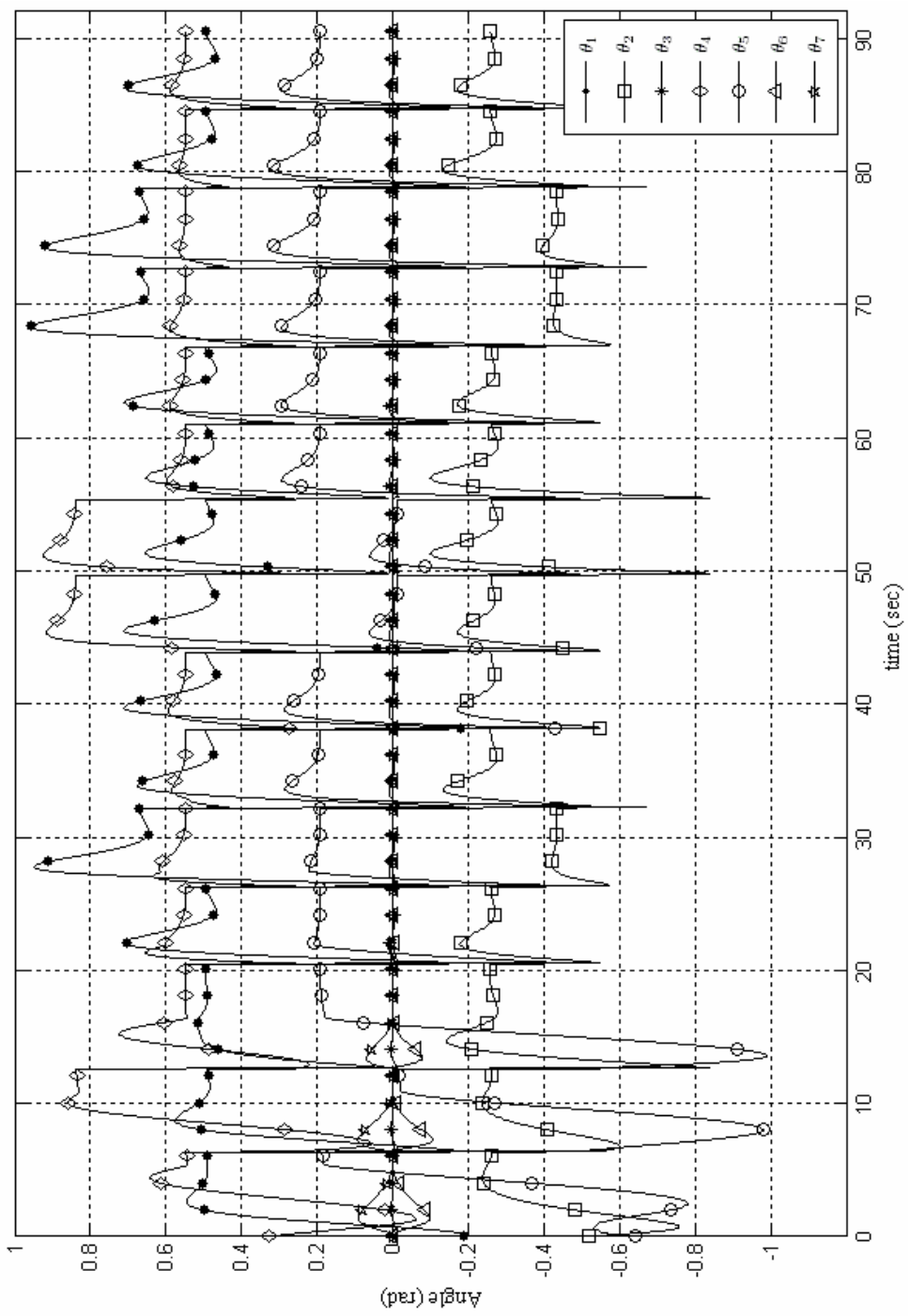

Figure 6.79 Simulated trajectory joint angle profile for given path

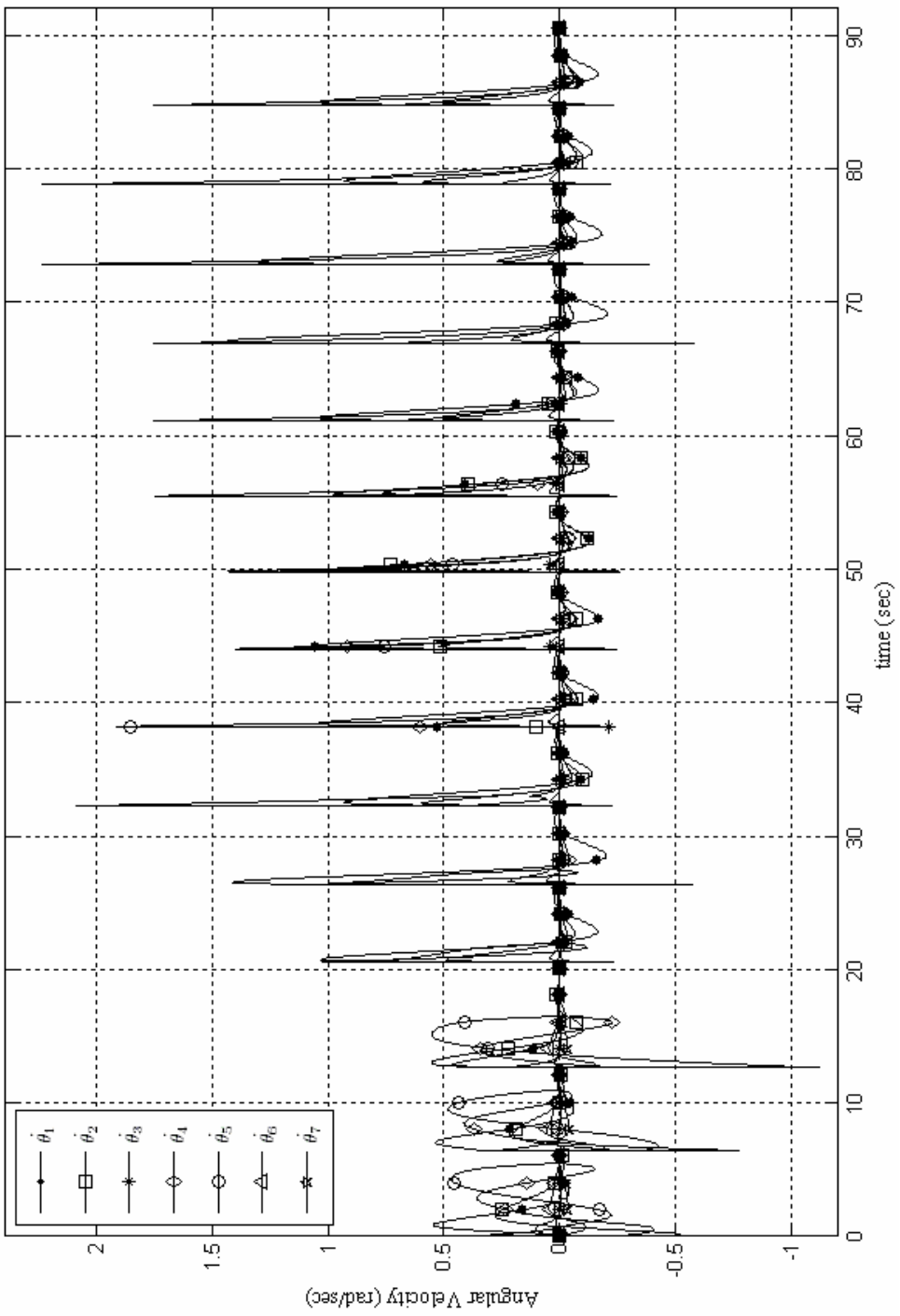

Figure 6.80 Simulated trajectory joint angular velocity profile for given path

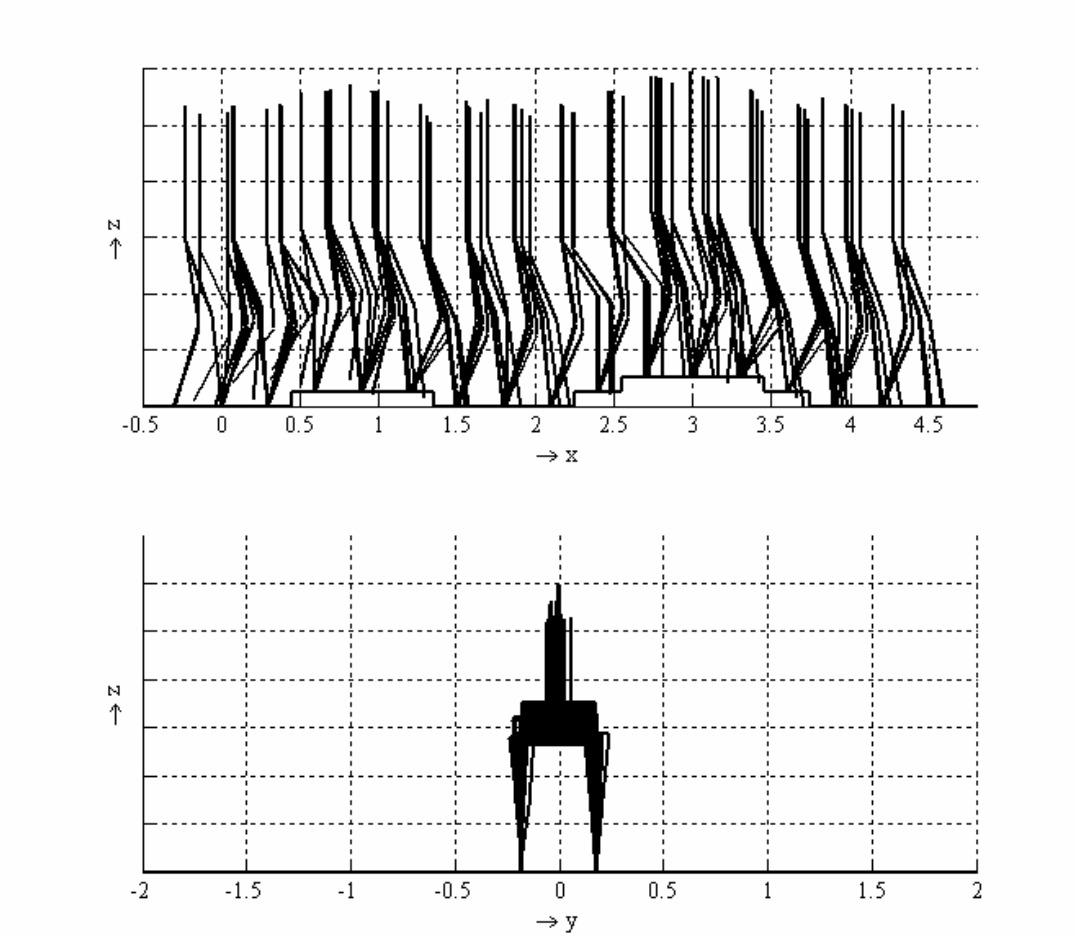

Figure 6.81 Simulated trajectory walking snapshot - sagittal (top) and frontal (bottom) plane views - for given path

CHAPTER 7

CONCLUSION

It was the aim of this thesis to pose and answer many unsolved questions and enhance the techniques relating to the improvement of biped locomotion and control. As being very natural imitation of the universe, biped robots are realizing the dreams and necessities in improving the human life, and are direct choice for locomotion in environments designed for humans. The main purpose in the biped robot studies is to enhance the technology in this area to achieve efficient, safe and reliable bipeds behaving very likely to human beings and also being capable of performing at least the human performance. What should be done to enhance the biped robot technology to achieve this aim? The answer to this question varies depending on the aspect of work since this subject is highly interdisciplinary. Hence, a lot of work needs to be done to improve many aspects of biped robot technology, such as actuators, sensors, materials, energy accumulator, controller, hardware and software that can be utilized to realize user-friendly biped robots.

In this thesis, the background information of locomotion in nature, specifically human locomotion, and the reasons and methods of studying biped robot locomotion have been introduced. The robotics history and the previous work done in different aspects of biped robot development are also examined.

In its basic sense, the complete biped locomotion system is composed of Biped System's dynamic (mathematical) model, High Level Controller (Guidence Unit), Low Level Controller (Supervisory Unit), and Reference Trajectory Generator. In realizing these components, different methods are implemented and the results are compared, especially for the control techniques. To simplify analysis and understanding, investigations first concentrated on the mathematical modeling of the biped robot in Chapter 2. A 3D 5-link 7 DOF biped model is developed by keeping the purpose of human-like natural locomotion and the fact of model complexity in mind. This model represents the minimal biped configuration that can achieve the desired tasks, meets the needs of the analysis aimed to be realized and supports the development of new methods. Kinematic and dynamic

equations of motion derived in detail for the two phases of motion, namely, Single Support and Double Support Phases. The kinematics equations are derived analytically and the dynamic equations are derived by using Lagrangian Method.

In Chapter 3, the dynamic balance and stability definitions are extended and the stability criterion for biped locomotion is defined to be used in High Level Controller design. Furthermore, Chapter 4 deals with the reference trajectory generation problem. There are many methods to realize this. At this point, an analytical method, namely, 3rd order (cubic) spline interpolation method is used to generate the desired walking trajectory in this study. This method was chosen since one of the most suitable ways to develop a trajectory is to imitate the nature of bipedal locomotion. It can clearly be seen from the simulation results that using this technique gives an outcome resembling natural human locomotion. In other words, this algorithm results in a joint angle profile coherent with the human-like motion as desired. The locomotion studied in this study also extends from even floor walking to stepping over obstacles and stair up/down walking. A systematical method that classifies the walking patterns of a 5-link 7 DOF biped robot during walking on even surface, stepping over obstacles, stepping up and stepping down motions which result in a natural human-like walking is developed. In short, as per the classified patterns, the biped hip and ankle trajectories are generated by spline interpolation and afterwards, the inverse kinematics is used to obtain the joint angle profiles.

The work was then extended to the control in Chapter 5. In due course it became apparent that enough problems were unsolved for controlling bipeds, some of which are exposed and solved in this thesis. This chapter gives a detailed survey on the previous control methods used in the past. Some of these methods are also implemented and compared to each other in order to identify the successful methods for biped locomotion control problem. The aim of control, in the context of this thesis, is to sustain the response of the system in accordance with the reference walking trajectory of the biped robot by ensuring the stability and natural look like motion. The control of biped robot is a challenge since the biped system is complex and preserving its balance is difficult. As a preliminary work, the ground reaction force in terms of smooth transition and landing impact under the parametric change of frontal gait trajectory, which is realized by inverted pendulum model, and the parametric change of the proportional gain of PID feedback controller is analyzed. Another preliminary work done is the implementation of a hybrid fuzzy controller by using 3D inverted pendulum model to achieve a stable biped locomotion.

The main focus of Chapter 5 is the design and implementation of controllers for biped system. Be it the case in human walking, the control of the biped system is divided into two levels of control: Low Level Control and High Level Control. The Low Level Control serves as the supervisory unit for the system and many different controllers are designed in this level. The implementation details and comparison of the designed controllers, namely, PID Controller, Computed Torque Controller and Optimal Controller are also given. High Level Controller serves as the guidance unit for the system. This unit aims to define certain walking parameters and footstep trajectory. To achieve this; for the given predefined desired global path, the High Level Controller aims to form a footstep trajectory (sequence of walking patterns with pattern properties, such as step length and speed) that optimizes the consumed energy of the robot while ensuring the stability criterion. High Level Controller is constructed as a genetic algorithm problem with stability and natural-like walking constraints.

The implementation of the overall system is realized by developing a biped dynamic simulator program in MATLAB. Chapter 6 presented the details of biped dynamic simulator and gave the corresponding simulation results. It also gave the physical parameters used by the simulator, the algorithms developed, and the comparison and the evaluation of the methods used. A wide range of scenarios is covered by the analysis and the results are also presented graphically.

The biped robot technology in any sense is improving very fast day by day. In due course the ideal biped that can at least be capable as of human and realize any human tasks is to be improved. Future trends in the development of robots implies that perhaps about the year 2020, the process will have produced the first broadly competent “universal robots” with lizardlike minds that can be programmed for almost any routine chore [41]. With anticipated increases in computing power, by 2030, second-generation robots with trainable mouselike minds may become possible. Besides application programs, these robots may host a suite of software “conditioning modules” that generate positive – and negative – reinforcement signals in predefined circumstances. By 2040, computing power should make third-generation robots with monkeylike minds possible. Such robots would learn from mental rehearsals in simulations that would model physical, cultural, and psychological factors. Physical properties would include shape, weight, strength, texture, and appearance of things and knowledge of how to handle them. Cultural aspects would include a thing's name, value, proper location, and purpose. Psychological factors, applied

to humans and other robots, would include goals, beliefs, feelings, and preferences. The simulation would track external events and would tune its models to keep them faithful to reality. This should let a robot learn by imitation and afford it a kind of consciousness. By the middle of the 21st century, fourth-generation robots may exist with humanlike mental power able to abstract and generalize. Researchers hope that such machines will result from melding powerful reasoning programs to third-generation machines. Properly educated, fourth-generation robots are likely to become intellectually formidable.

From the summary of the current technology and expectations for future technology of biped robots, it is clear that research on this area is far from complete. This is mainly due to the fact that the ideal biped system is complex, unstable, nonlinear and subject to restrictions caused by the environment. In other words, in order to implement the development of such biped robots, there are still many functionalities needed to be accomplished in the future. The stability and control needed to be extended to allow walking stably and easily in the difficult, uneven and unknown environments even if any kind of disturbance exists, and to provide versatile walking with high mobility.

In conclusion, the ultimate purpose of this thesis was to positively contribute to scientific knowledge, clarify several aspects relating to the biped locomotion and control techniques, and hopefully, to pose many questions that may catch the imagination of future researchers. With hindsight to previous works done on this subject, this thesis can be seen as a bridge to enhance the biped locomotion and control techniques.

REFERENCES

[1] *The American Heritage, Dictionary of the English Language*, 4th Ed., 2000.

[2] J. Devine, "The Versatility of Human Locomotion," *American Anthropologist, New Series*, vol. 87, no. 3, pp. 550-570, Sep. 1985.

[3] Human evolution, *http://www.britannica.com/eb/article-250595/human-evolution*, August 2008.

[4] Terrestrial locomotion, *http://en.wikipedia.org/wiki/Terrestrial_locomotion*, August 2008.

[5] K. Čapek, *R.U.R (Rossum's Universal Robots): A Fantastic Melodrama*, Doubleday, Page & Co., Garden City, NY, 1923.

[6] Robot, *http://www.britannica.com/eb/article-9063935/robot*, August 2008.

[7] K.S. Fu, R.C. Gonzales, C.S.G. Lee, *Robotics Control, Sensing, Vision, and Intelligence*, Mc.Graw-Hill International Ed. Singapore, 1988.

[8] Automaton, *http://www.britannica.com/eb/article-9011374/automaton*, August 2008.

[9] M.W. Thring, *Robots and Telechirs: Manipulators with Memory; Remote Manipulators; Machine Limbs for the Handicapped*, Ellis Horwood Ltd. John Wiley & Sons, New York, 1983.

[10] *World ROBOTICS 2007-Statistics, Market Analysis, Forecasts, Case Studies and Profitability of Robot Investment*, United Nations Economic Commission for Europe (UNECE) and International Federation of Robotics (IFR), 2007.

[11] F. Operto, “Roboethics: an Interdisciplinary Approach to the Social Implications of Robotics,” *http://www.ciaorobot.org/public/OpertoAvignon07%20Roboethics.pdf*, August 2008.

[12] M. H. Raibert, *Legged Robots that Balance*, MIT Press, Cambridge, Mass., 1986.

[13] M. Wisse, *Essentials of dynamic walking analysis and design of two-legged robots*, Ph.D. dissertation, Technische Universiteit Delft, 2004.

[14] M. E. Rosheim, *Leonardo’s Lost Robots*, Springer, Berlin, 2006.

[15] “A mechanical man: Some new features of an invention many will remember,” *The New York Times*, 15 April 1893.

[16] Humanoid Robotics Institute, *http://www.humanoid.waseda.ac.jp/history.html*, August 2008.

[17] H. Miura, I. Shimoyama, “Dynamic Walk of a Biped,” *the International Journal of Robotics Research*, vol. 3, no. 2, pp. 60-74, 1984.

[18] J. Furusho, M. Masubuchi, “Control of a Dynamical Biped Locomotion System for Steady Walking,” *Journal of Dynamic Systems, Measurement, and Control*, vol. 108, pp. 111–118, 1986.

[19] J. Furusho, A. Sano, “Sensor-Based Control of a Nine-Link Biped,” *the International Journal of Robotics Research*, vol. 9, no. 2, pp. 83-98, 1990.

[20] Furusho Laboratory, *http://www-dyna.mech.eng.osaka-u.ac.jp/welcome-e.html*, August 2008.

[21] Y.F. Zheng, F.R. Sias, Jr., “Design and Motion Control of Practical Biped Robots,” *International Journal of Robotics and Automation*, vol. 3, no.2, pp. 70-77, 1988.

[22] Y.F. Zheng, J. Shen, "Gait Synthesis for the SD-2 Biped Robot to Climb Sloping Surface," *IEEE Transactions on Robotics and Automation*, vol. 6, iss. 1, pp. 86-96, Feb. 1990.

[23] T. McGeer, "Passive Walking with Knees," *Proc.of IEEE Robotics & Automation Conference*, pp. 1640-1645, 1990.

[24] A. Goswami, B. Espiau, A. Keramane, "Limit Cycles and Their Stability in a Passive Bipedal Gait," *Proceedings of the IEEE International Conference on Robotics and Automation*, vol. 1 , pp. 246-251, April 1996.

[25] S.H. Collins, M. Wisse, A. Ruina, "A Three-Dimensional Passive-Dynamic Walking Robot with Two Legs and Knees," *International Journal of Robotics Research*, vol. 20, no. 7, pp. 607-615, 2001.

[26] S. Kajita, K. Tani, A. Kobayashi, "Dynamic Walk Control of a Biped Robot along the Potential Energy Conserving Orbit," *Proceedings of IEEE International Workshop on Intelligent Robots and Systems (IROS): Towards a New Frontier of Applications*, vol. 2, pp. 789-794, 1990.

[27] S. Kajita, T. Yamaura, A. Kobayashi, "Dynamic Walking Control of a Biped Robot Along a Potential Energy Conserving Orbit," *IEEE Trans. on Robotics and Automation*, vol 8, no 4, 1992.

[28] S. Kajita, K. Tani, "Experimental Study of Biped Dynamic Walking," *IEEE Control Systems Magazine*, vol. 16, pp. 13-19, Feb. 1996.

[29] W. T. Miller, "Real-Time Control of a Biped Walking Robot," *Proc. of International Congress on Neural Networks*, July 1993.

[30] W.T. Miller, "Real-Time Neural Network Control of a Biped Walking Robot," *IEEE Control Systems Magazine*, vol. 14, iss. 1, pp. 41 -48, 1994.

[31] A. L. Kun, *A Sensory-Based Adaptive Walking Control Algorithm for Variable Speed Biped Robot Gaits*, Ph.D. dissertation, Dept. of Electrical and Computer Engineering, University of New Hampshire, May 1997.

[32] A.A. Grishin, IA.M. Formal'sky, A.V. Lensky, S.V. Zhitomirsky, "Dynamic Walking of a Vehicle With Two Telescopic Legs Controlled by Two Drives," *the International Journal of Robotics Research*, vol. 13, no. 2, pp. 137-147, 1994.

[33] E.R. Dunn, R.D. Howe, "Towards Smooth Bipedal Walking," *Proc. of the IEEE International Conference on Robotics and Automation*, vol. 3, pp. 2489-2494, 1994.

[34] E.R. Dunn, R.D. Howe, "Foot Placement and Velocity Control in Smooth Bipedal Walking," *Proceedings of the IEEE International Conference on Robotics and Automation*, vol. 1, pp. 578-583, 1996.

[35] J.E. Pratt, *Exploiting Inherent Robustness and Natural Dynamics in the Control of Bipedal Walking Robots*, Ph.D. dissertation, Dept. of Electrical Engineering and Computer Science, MIT, June 2000.

[36] ASIMO Humanoid Robot, *http://asimo.honda.com*, August 2008.

[37] QRIO – Wikipedia, *http://en.wikipedia.org/wiki/QRIO*, August 2008.

[38] Kawada, *http://www.kawada.co.jp/global/ams/hrp_2.html*, August 2008.

[39] ZMP, *http://zmp.co.jp/*, August 2008.

[40] Hubo Lab, *http://hubolab.kaist.ac.kr/index.php*, August 2008.

[41] Robot, *http://www.britannica.com/eb/article-248211/robot*, August 2008.

[42] J. Perry, *Gait Analysis: Normal and Pathological Function*, SLACK Incorporated, 1992.

[43] M.W. Whittle, *Gait Analysis: An Introduction*, Butterworth-Heinemann, 2002.

[44] M.P. Murray, A.B. Drought, R.C. Kory, "Walking Patterns of Normal Men," *Journal of Bone and Joint Surgery*, vol. 46, pp. 335-360, 1964.

[45] R.K. Jensen, "Human morphology: its role in the mechanics of movement," *Journal of Biomechanics*, vol. 26, suppl. 1, pp. 81-94, 1993.

[46] E. Muybridge, *The Human Figure in Motion*, Dover, New York, 1887.

[47] M. Vukobratovic, D. Juricic, "Contribution to the Synthesis of Biped Gait," *IEEE Transactions on Biomedical Engineering*, vol. 16, pp. 1-6, 1969.

[48] M. Vukobratovic, A. Frank, D. Juricic, "On the Stability of Biped Locomotion," *IEEE Trans. Biomedical Engineering*, vol. BME-17, no. 1, 1970.

[49] A.A. Frank, "An Approach to the Dynamic Analysis and Synthesis of Biped Locomotion Machines," *Medical and Biological Engineering and Computing*, vol. 8, no. 5, Sept. 1970.

[50] R.B. McGhee, M.B. Kuhner, "On the Dynamic Stability of Legged Locomotion Systems," *Proceedings of the Third International Symposium on External Control of Human Extremities*, pp. 431-442, August 1969.

[51] R.B. McGhee, "A Mathematical Theory for Legged Locomotion Systems," *Proceedings of the Thirteenth Midwest Symposium on Circuit Theory*, pp. I.3.1-I.3.14, May 1970.

[52] H. Hemami, F. Weimer, S. Koozekanani, "Some Aspects of the Inverted Pendulum Problem for Modeling of Locomotion Systems, *IEEE Trans. on Automatic Control*, vol. 18, pp.658-661, 1973.

[53] H. Hemami, A. Katbab, "Constrained Inverted Pendulum Model for Evaluating Upright Postural Stability," *ASME J. Dyn. Syst. Meas. Contr.*, vol. 104, pp. 343-349, 1982.

[54] F. Gubina, H. Hemami, R.B. McGhee,, "On the Dynamic Stability of Biped Locomotion," *IEEE Transactions on Biomedical Engineering*, vol. BME-21, iss. 2, pp. 102-108, March 1974.

[55] C.L. Golliday, H. Hemami, "An Approach to Analyzing Biped Locomotion Dynamics and Designing Robot Locomotion Controls," *IEEE Trans. on Automatic Control*, vol. 22, no. 6, pp. 963-972, 1977.

[56] H. Hemami, Y.F. Zheng, "Dynamics and Control of Motion on the Ground and in the Air with Application to Biped Robots," *Journal of Robotic Systems*, vol. 1, no. 1, pp.101-116, 1984.

[57] J. Furusho, M. Masubuchi, "A Theoretically Motivated Reduced Order Model for the Control of Dynamic Biped Locomotion," *ASME Journal of Dynamic Systems, Measurement, and Control*, vol.109, pp. 155-163, 1987.

[58] Y. Hurmuzlu, "Dynamics of Bipedal Gait Part I: Objective Functions and the Contact Event of a Planar Five-Link Biped," 24 Feb. 1998.

[59] F. Gravez, O. Bruneau and F. B. Ouezdou, "Analytical and Automatic Modeling of Digital Humanoids," *International Journal of Humanoid Robotics*, vol. 2; no. 3, pp. 337-360, 2005.

[60] S. Tzafestas, M. Raibert, C. Tzafestas, "Robust Sliding-Mode Control Applied to a 5-Link Biped Robot," *Journal of Intelligent and Robotic Systems*, vol. 15, pp.67-133, 1996.

[61] Balance, *http://moon.ouhsc.edu/dthompso/balance/*, August 2008

[62] E. Nicholls, *Bipedal Dynamic Walking in Robotics*, M.S. Thesis, Dept. of Electrical and Electronics Engineering, the University of Western Australia, October 1998.

[63] H. Benbrahim, *Biped Dynamic Walking Using Reinforcement Learning*, Ph.D. dissertation, Electrical and Computer Engineering, University of New Hampshire, December 1996.

[64] H. Hemami, R. L. Farnsworth, "Postural and Gait Stability of a Planar Five Link Biped by Simulation," *IEEE Transactions on Automatic Control*, , vol. 22, no. 6, pp. 452-458, June 1977.

[65] Y.F. Zheng, J. Shen, "Gait Synthesis for the SD-2 Biped Robot to Climb Sloping Surface," *IEEE Transactions on Robotics and Automation*, vol. 6, no. 1, pp. 53-59, Feb. 1990.

[66] A.W. Salatian, Y.F. Zheng, "Gait Synthesis for a Biped Robot Climbing Sloping Surfaces Using Neural Networks, Part I: Static Learning," *Proceedings of the International Conference on Robotics and Automation*, pp. 2601-2606, May 1992.

[67] H. Hemami, B.R. Chen, "Stability Analysis and Input Design of a Two-Link Planar Biped," *the International Journal of Robotics Research*, vol.3, no.2, pp. 93-100, 1984.

[68] Y.F. Zheng, H. Hemami, "Impact Effects of Biped Contact with the Environment," *IEEE Trans. Syst. Man Cyber.*, vol. SMC-14, no.3, pp.437-443, 1984.

[69] R. Katoh, M. Mori, "Control Method of Biped Locomotion Giving Asymptotic Stability of Trajectory," *Automatica*, vol. 20, no. 4, pp. 405-414, 1984.

[70] Y. Hurmuzlu, "Dynamics of Bipedal Gait Part II: Stability Analysis of a Planar Five-Link Biped," 24 Feb. 1998.

[71] Y. Hurmuzlu, G. Moskowitz, "The Role of Impact in the Stability of Biped Locomotion," *Dynamics and Stability of Systems*, vol. 1, pp. 217-234, 1986.

[72] M. Vukobratovic, B. Borovac, D. Surdilovic, "Zero-Moment Point - Thirty Five Years of Its Life," *Int. Journal of Humanoid Robotics*, vol.1, no.1, pp. 157-173, 2004.

[73] K. Sorao, T. Murakami, K. Ohnishi, “A Unified Approach to ZMP and Gravity Center Control in Biped Dynamic Stable Walking,” *Proc. IEEE/ASME Int. Conf. on Advanced Intelligent Mechatronicsm*, 1997.

[74] A. Takanishi, Y. Egusa, M. Tochizawa, T. Takeya, I. Kato, “Realization of Dynamic Biped Walking Stabilized with Trunk Motion,” *Proceedings of the Seventh CISMIFTOMM Symposium on Theory and Practice of Robots and Manipulators*, pp. 68–79, 1988.

[75] A. Takanishi, H.O. Lim, M. Tsuda, I. Kato, “Realisation of Dynamic Biped Walking Stabilised by Trunk Motion on a Sagitally Uneven Surface,” *Proceedings of the 1990 IEEE Int. Workshop on Intelligent Robots and Systems*, pp. 323–330, 1990.

[76] T. Kato, A. Takanishi, H. Jishikawa, I. Kato, “The Realization of the Quasi-Dynamic Walking by the Biped Walking Machine, *Fourth Symposium on Theory and Practice of Robots and Manipulators*, pp. 341–351, 1983.

[77] A. Takanishi, M. Ishida, Y. Yamazaki, I. Kato, “The Realization of Dynamic Walking by the Biped Walking Robot WL-10RD,” *ICAR*, pp. 459–466, 1985.

[78] J. Hodgins, J. Koechling, M. H. Raibert, “Running Experiments with a Planar Biped,” *3rd Int. Symp. Robotics Research*, pp. 349–355, 1986.

[79] W.T. Miller, A.L. Kun, “Dynamic Balance of a Biped Walking Robot,” *Neural Systems for Robotics*, pp.17-35, 1997.

[80] A. Kun, W. T. Miller, “Adaptive Dynamic Balance of a Biped Robot Using Neural Networks,” *Proc. IEEE Int. Conf. on Robotics and Automation*, pp.240-245, 1996.

[81] M. J. Coleman, *A Stability Study of a Three-Dimensional Passive-Dynamic Model of Human Gait*, Ph.D. dissertation, Cornell University, 1998.

[82] J.V. Fowble, A. D. Kuo, “Stability and Control of Passive Locomotion in 3D,” *Proceedings of the Conference on Biomechanics and Neural Control Movement*, pp. 28-29, 1996.

[83] M. Garcia, A. Chatterjee, A. Ruina, “Speed, Efficiency and Stability of Small-Slope 2D Passive Dynamic Bipedal Walking,” *IEEE International Conference on Robotics and Automation*, vol. 3, pp. 2351-2356, 1998.

[84] A.D. Kuo, “Stabilization of Lateral Motion in Passive Dynamic Walking,” *the International Journal of Robotics Research*, vol. 18, no. 9, pp. 917-930, 1999.

[85] T. McGeer, “Passive Dynamic Walking,” *the International Journal of Robotics Research*, vol. 9, no. 2, pp.62-82, 1990.

[86] M. Vukobratovic, B. Brovac, D. Surla, D. Stokic, *Biped Locomotion: Dynamics, Stability, Control and Application*, Scientific Fundamentals of Robotics, Springer-Verlag, 1990.

[87] D.A. Winter, *Biomechanics and Motor Control of Human Movement*, John Wiley and Sons, Inc., New York, 1990

[88] S.G. Tzafestas, T.E. Kricochoritis, C.S. Tzafestas, “Robust Sliding-Mode Control of Nine-Link Biped Robot Walking,” *Journal of Intelligent and Robotics Systems*, pp. 375-402, 1997.

[89] Y. Kurematsu, S. Kitamura, Y. Kondo, “Trajectory Planning and Control of a Biped Locomotive Robot - Simulation and Experiment,” *Robotics & Manufacturing, Recent Trends in Research, Education & Applications*, pp. 65-72, 1988.

[90] J.G. Juang, C.S. Lin, “Gait Synthesis of a Biped Robot Using Backpropagation through Time Algorithm,” *IEEE International Conference on Neural Networks*, vol. 3 , pp. 1710 -1715, June 1996.

[91] J.S. Bay, H. Hemami, "Modeling of a Neural Pattern Generator with Coupled Nonlinear Oscillators," *IEEE Transactions on Biomedical Engineering*, vol. BME-34, iss. 4, pp. 297-306, April 1987.

[92] T. Zielinska, "Coupled Oscillators Utilised as Gait Rhythm Generators of Two Legged Walking Machine," *Biological Cybernetics*, vol. 4, no. 3, pp. 263-273, 1996.

[93] L. Jalics, H. Hemami, Y.F. Zheng, "Pattern Generation Using Coupled Oscillators for Robotic and Biorobotic Adaptive Periodic Movement," *Proceedings of the IEEE International Conference on Robotics and Automation*, vol. 1 , pp. 179-184, 1997.

[94] H. Benbrahim and J.A. Franklin, "Biped Dynamic Walking Using Reinforcement Learning," *Robotics and Autonomous Systems*, vol. 22, iss. 3-4, pp. 283-302, 1997.

[95] Y. Kurematsu, T. Maeda and S. Kitamura, "Autonomous Trajectory Generation of a Biped Locomotive Robot Using Neuro Oscillator," IEEE 1993.

[96] L.S. Brotman, A.N. Netravali, "Motion Interpolation by Optimal Control," *ACM SIGGRAPH Computer Graphics*, vol. 22 , iss. 4 , pp. 309-315, 1988.

[97] F.M. Silva, J.A.T. Machado, "Kinematic Aspects of Robotic Biped Locomotion Systems," *Proceedings of the 1997 IEEE/RSJ International Conference on Intelligent Robots and Systems*, vol. 1, pp. 266-272, Sept. 1997.

[98] C.L. Shih, "Gait Synthesis for a Biped Robot," *Robotica,* vol. 15, pp. 599-607, 1997.

[99] C.L. Shih, "Ascending and Descending Stairs for a Biped Robot," *IEEE Transactions on Systems, Man and Cybernetics-Part A: Systems and Humans*, vol. 29, no. 3, May 1999.

[100] Q. Huang; S. Kajita, N. Koyachi, K. Kaneko, K. Yokoi, H. Arai, K. Komoriya, K. Tanie, "A High Stability, Smooth Walking Pattern for a Biped Robot," *Proceedings of the IEEE International Conference on Robotics and Automation*, vol. 1, pp. 65-71, 1999.

[101] Q. Huang, K. Yokoi, S. Kajita, K. Kaneko, H. Arai, N. Koyachi, K. Tanie, "Planning Walking Patterns for a Biped Robot," *IEEE Transactions on Robotics and Automation*, vol. 17, no. 3, pp.280-289, June 2001.

[102] Z. Tang, C. Zhou, Z. Sun, "Gait Planning for Soccer-Playing Humanoid Robots," *Lecture Notes in Control & Information Sciences*, vol. 299, pp. 241-262, 2004.

[103] T.T. Lee, P.L. Jeng, W.A. Gruver, "Control of a 5-Link Biped Robot for Steady Walking," *Proceedings of the IEEE International Symposium on Intelligent Control*, pp. 484-489, 1988.

[104] S. Kitamura, Y. Kurematsu, M. Iwata, "Motion Generation of a Biped Locomotive Robot Using an Inverted Pendulum Model and Neural Networks," *Proceedings of the 29th IEEE Conference on Decision and Control*, pp. 3308-3312, 1990.

[105] Y. Kurematsu, O. Katayama, M. Iwata, S. Kitamura, "Autonomous Trajectory Generation of a Biped Locomotive Robot," *IEEE International Joint Conference on Neural Networks*, vol.3, pp. 1983-1988, Nov. 1991.

[106] S. Kajita, K. Tani, "Study of Dynamic Biped Locomotion on Rugged Terrain-Derivation and Application of the Linear Inverted Pendulum Mode," *Proceedings of the IEEE International Conference on Robotics and Automation*, vol. 2, pp. 1405-1411, 1991.

[107] S. Kajita, K. Tani, "Study of Dynamic Biped Locomotion on Rugged Terrain-Theory and Basic Experiment," *Fifth International Conference on Advanced Robotics: Robots in Unstructured Environments*, vol. 1, pp. 741 -746, 1991.

[108] A. Dasgupta, Y. Nakamura, "Making Feasible Walking Motion of Humanoid Robots from Human Motion Capture Data," *Proceedings of the IEEE International Conference on Robotics and Automation*, vol. 2, pp. 1044 -1049, 1999.

[109] K. Hirai, M. Hirose, T. Takenaka, "The Development of Honda Humanoid Robot," *Proc. of the 1998 IEEE Int. Conf. on Robotics & Automtion*, May 1998.

[110] C.L. Shih, Y.Z. Li, S. Churng, T.T. Lee, W.A. Gruver, "Trajectory Synthesis and Physical Admissibility for a Biped Robot During the Single-Support Phase," *Proceedings of the IEEE International Conference on Robotics and Automation*, vol.3, pp. 1646-1652, 1990.

[111] C. Zhou, "Neuro-Fuzzy Gait Synthesis with Reinforcement Learning for a Biped Walking Robot," *Soft Computing, Springer – Verlag*, vol. 4, iss. 4, pp. 0238-0250, 2000.

[112] C. Zhou, "Robot Learning with GA-based Fuzzy Reinforcement Learning Agents," *Information Sciences*, vol. 145, pp. 45-68, 2002.

[113] C. Zhou and Q. Meng, "Dynamic Balance of a Biped Robot Using Fuzzy Reinforcement Learning Agents," *Fuzzy Sets and Systems, Elsevier*, vol. 134, pp. 169-187, 2003.

[114] A.L. Kun, W.T. Miller, "Control of Variable-Speed Gaits for a Biped Robot," *IEEE Robotics & Automation Magazine*, Sept. 1999.

[115] C. Chevallereau, A. Formal'sky, B. Perrin, "Low Energy Cost Reference Trajectories for a Biped Robot," *Proceedings of the IEEE International Conference on Robotics and Automation*, vol. 2 , pp. 1398 -1404, 1998.

[116] C. Chevallereau, Y. Aoustin, A. Formal'sky, "Optimal Walking Trajectories for a Biped," *Proceedings of the First Workshop on Robot Motion and Control*, pp. 171 -176, 1999.

[117] C. Chevallereau and Y. Aoustin, "Optimal Reference Trajectories for Walking and Running of a Biped Robot," *Robotica*, vol. 19, pp.557-569, 2001.

[118] P.H. Channon, S.H. Hopkins, D.T. Pham, "Derivation of Optimal Walking Motions for a Bipedal Walking Robot," *Robotica,* vol. 10, part 2, pp. 165-172, 1992.

[119] P.H. Channon, S.H. Hopkins, D.T. Pham, "A Variational Approach to the Optimization of Gait for a Bipedal Robot," *Proceedings of the Institution of Mechanical Engineers, Part C-Journal of Mechanical Engineering Science*, vol. 210, no. 2, pp. 177-186, 1996.

[120] M.L. Nagurka, V. Yen, "Fourier-based optimal control of nonlinear dynamic systems," *Journal of Dynamics, Measurement and Control*, vol. 112, pp. 17-26, March 1990.

[121] G. Cabodevila, G. Abba, "Quasi Optimal Gait for a Biped Robot Using Genetic Algorithm," *IEEE International Conference on Systems, Man, and Cybernetics: Computational Cybernetics and Simulation*, vol. 4 , pp. 3960 -3965, 1997.

[122] L. Roussel, C. Canuds-de-Wit, A. Goswami, "Comparative Study of Method for Energy-Optimal Gait Generation for Biped Robots," *International Conference on Informatics and Control*, 1997.

[123] L. Roussel, C. Canudas-De-Wit, A. Goswami, "Generation of Energy Optimal Complete Gait Cycles for Biped Robots," *Proceedings of the IEEE International Conference on Robotics and Automation*, vol. 3 , pp. 2036 -2041, 1998.

[124] F. Anderson, J. Ziegler, M. Pandy, R. Whalen, "Application of High-Performance Computing to Numerical-Simulation of Human Movement," *Journal of Biomechanical Engineering-Transactions of the ASME*, vol. 117, no. 1, pp. 155-157, Feb. 1995.

[125] Q. Wu, C.Y.A. Chan, “Design of Energy Efficient Joint Profiles for a Planar Five-Link Biped Robot," *Proceedings of the IEEE International Symposium on Computational Intelligence in Robotics and Automation*, pp. 35-40, 2001.

[126] F.M. Silva, J.A.T. Machado, “Towards Efficient Biped Robots,” *Proc. of the IEEE/RSJ International Conference on Intelligent Robots and Systems*, pp. 394-399, 1998.

[127] C.L. Shih, “Analysis of the Dynamics of a Biped Robot with Seven Degrees of Freedom,” *Proceedings of the IEEE International Conference on Robotics and Automation*, vol. 4 , pp. 3008 -3013, 1996.

[128] C.L. Shih, Y. Zhu, W.A. Gruver, “Optimization of the Biped Robot Trajectory,” *Proceedings of the IEEE International Conference on Systems, Man, and Cybernetics: Decision Aiding for Complex Systems*, vol. 2, pp. 899 – 903, 1991.

[129] C.L. Shih, “Inverted Pendulum-Like Walking Pattern of a 5-Link Biped Robot,” *Proceedings of the 8th International Conference on Advanced Robotics,* pp. 83 - 88, 1997.

[130] M.Y. Cheng, C.S. Lin, “Genetic Algorithm for Control Design of Biped Locomotion,” *Journal of Robotic Systems*, vol. 14, iss. 5 , pp. 365-373, 1998.

[131] G. Capi, S. Kaneko, K. Mitobe, L. Barolli, Y. Nasu, “Optimal Trajectory Generation for a Prismatic Joint Biped Robot Using Genetic Algorithms,” *Robotics and Autonomous Systems*, vol. 38, iss. 2, pp. 119-128, 2002.

[132] M. Rostami, G. Bessonnet, “Impactless Sagittal Gait of a Biped Robot During the Single Support Phase,” *Proceedings of the IEEE International Conference on Robotics and Automation*, vol. 2 , pp. 1385 -1391, 1998.

[133] K. Ono, R.Q. Liu, “Optimal Biped Walking Locomotion Solved by Trajectory Planning Method,” *Journal of Dyn. Syst., ASME*, vol. 124, no. 4, pp. 554-565, Dec 2002.

[134] J.Y. Lee, J.J. Lee, "Optimal Walking Trajectory Generation for a Biped Robot Using Multi-Objective Evolutionary Algorithm," *5th Asian Control Conference*, vol. 1, pp. 357-364, 2004.

[135] J.Y. Lee, M.S. Kim, J.J. Lee, "Multi-Objective Walking Trajectories Generation for a Biped Robot," *Proceedings of the IEEE/RSJ International Conference on Intelligent Robots and Systems*, vol. 4, pp. 3853-3858, 2004.

[136] A. Chemori, A. Loria, "Walking Control Strategy for a Planar Under-Actuated Biped Robot Based on Optimal Reference Trajectories and Partial Feedback Linearization," *Proceedings of the Fourth International Workshop on Robot Motion and Control*, pp. 61-66, 2004.

[137] D. Djoudi, C. Chevallereau, Y. Aoustin, "Optimal Reference Motions for Walking of a Biped Robot," *Proceedings of the IEEE International Conference on Robotics and Automation,* pp. 2002-2007, 2005.

[138] J.H. Yoon, O. Kwon, J.S. Yeon, J.H. Park, "Optimal Trajectory Generation of Serially-Linked Parallel Biped Robots," *Proceedings of the IEEE International Conference on Robotics and Automation*, pp. 1610 - 1615, 2006.

[139] T. Hase, Q. Huang, "Energy-Efficient Trajectory Planning Using Inequality State Constraint for Biped Walking Robot with Upper Body Mass," *IEEE/RSJ International Conference on Intelligent Robots and Systems*, pp. 5913 – 5918, 2006.

[140] Y.F. Zheng, A Neural Gait Synthesizer for Autonomous Biped Robots," *Proceedings of the IEEE International Workshop on Intelligent Robots and Systems: Towards a New Frontier of Applications*, vol. 2, pp. 601-608, July 1990.

[141] T. Arakawa, T. Fukuda, "Natural Motion Trajectory Generation of Biped Locomotion Robot Using Genetic Algorithm through Energy Optimization," *IEEE International Conference on Systems, Man, and Cybernetics*, , vol. 2, pp. 1495-1500, 1996.

[142] M. Vukobratovic, Y. Stepanenko, “On the Stability of Anthropomorphic Systems,” *Math. Biosci.*, vol. 15, pp. 1-37, 1972.

[143] A. Sano, J. Furusho, “Realization of Natural Dynamic Walking Using the Angular Momentum Information,” *Proceedings of the IEEE International Conference on Robotics and Automation*, vol. 3, pp. 1476-1481, 1990.

[144] A. Takanishi, T. Takeya, H. Karaki, I. Kato, “A Control Method for Dynamic Biped Walking under Unknown External Force,” Proceedings of the IEEE International Workshop on Intelligent Robots and Systems: Towards a New Frontier of Applications, vol. 2, pp. 795 -801, 1990.

[145] C.L. Shih, W.A. Gruver, “Control of a Biped Robot in the Double-Support Phase,” IEEE Transactions on Systems, Man and Cybernetics, vol. 22, iss. 4, pp. 729 -735, 1992.

[146] Y. Fujimoto, A. Kawamura, “Three Dimensional Digital Simulation and Autonomous Walking Control for Eight-Axis Biped Robot,” *Proceedings of the IEEE International Conference on Robotics and Automation*,. vol. 3 , pp. 2877-2884, 1995.

[147] Y. Fujimoto, A. Kawamura, “Proposal of Biped Walking Control Based on Robust Hybrid Position/Force Control,” *Proceedings of the IEEE International Conference on Robotics and Automation*, vol. 3 , pp. 2724 -2730, 1996.

[148] Y. Fujimoto, S. Obata, A. Kawamura, “Robust Biped Walking with Active Interaction Control between Foot and Ground,” *Proc. Of the IEEE Int. Conf. on Robotics & Automtion*, May 1998.

[149] H. Wang, T.T. Lee, W.A. Gruver, “A Neuromorphic Controller for a Three-Link Biped Robot,” *IEEE Transactions on Systems, Man and Cybernetics*, vol. 22, no. 1, pp. 164-169, 1992.

[150] H. Hemami, B.F. Wyman, "Modeling and Control of Constrained Dynamic Systems with Application to Biped Locomation in the Frontal Plane," *IEEE Trans. on Automatic Control*, vol. 24, no. 4, pp. 526-535, 1979.

[151] Y.F. Zheng, *Modeling, Control and Simulation of Three-Dimensional Robotic Systems with Applications to Biped Locomotion*, Ph.D. dissertation, Ohio State University, 1984.

[152] M. Raibert, S. Tzafestas, C. Tzafestas, "Comparative Simulation Study of Three Control Techniques Applied to a Biped Robot," *Proceedings of the International Conference on Systems, Man and Cybernetics: Systems Engineering in the Service of Humans*, vol. 1, pp. 494-502, 1993.

[153] J.E. Pratt, G.A. Pratt, "Exploiting Natural Dynamics in the Control of a Planar Bipedal Walking Robot," *Proceedings of the Thirty-Sixth Annual Allerton Conference on Communication, Control, and Computing*, pp. 739-748, 1998.

[154] J.E. Pratt, G.A. Pratt, "Exploiting Natural Dynamics in the Control of a 3D Bipedal Walking Simulation," *International Conference on Climbing and Walking Robots*, Sept. 1999.

[155] J.E. Pratt, G.A. Pratt, "Intuitive Control of a Planar Bipedal Walking Robot," *Proceedings of the IEEE International Conference on Robotics & Automation*, May 1998.

[156] B. Yuksel, B., C. Zhou, K. Leblebicioglu, "Ground Reaction Force Analysis in Biped Locomotion," *IEEE Conference on Cybernetics and Intelligent Systems and IEEE Conference on Robotics, Automation and Mechatronics*, 2004.

[157] K. Mitobe, N. Mori, K. Aida, Y. Nasu, "Nonlinear Feedback Control of a Biped Walking Robot," *Proc. of the IEEE International Conference on Robotics and Automation*, pp. 2865–2870, May 1995.

[158] J.H. Park, K.D. Kim, “Biped Robot Walking Using Gravity-Compensated Inverted Pendulum Mode and Computed Torque Control,” *Proc. of the 1998 IEEE Int. Conf. on Robotics & Automtion*, May 1998.

[159] T.H. Chang, Y. Hurmuzlu, “Sliding Control without Reaching Phase and its Application to Bipedal Locomotion,” *ASME Journal of Dynamic Systems, Measurement and Control*, vol. 115, pp. 447-455, Sept. 1993.

[160] S. Kajita, K. Tani, “Adaptive Gait Control of a Biped Robot Based on Realtime Sensing of the Ground Profile,” *Proceedings of the IEEE International Conference on Robotics and Automation*, vol. 1, pp. 570 -577, 1996.

[161] S. Murakami, E. Yamamoto, K. Fujimoto, “Fuzzy Control of Dynamic Biped Walking Robot,” *Proceedings of the International Joint Conference of the Fourth IEEE International Conference on Fuzzy Systems and The Second International Fuzzy Engineering Symposium*, vol. 1, pp. 77-82, 1995.

[162] C.L. Shih, W.A. Gruver, Y. Zhu, “Fuzzy Logic Force Control for a Biped Robot,” Proceedings of the IEEE International Symposium on Intelligent Control, pp. 269 - 274, 1991.

[163] L. Magdalena, F. Monasterio, “Fuzzy Controlled Gait Synthesis for a Biped Walking Machine,” *Second IEEE International Conference on Fuzzy Systems*, vol. 2, pp. 1334 -1339, 1993.

[164] C. Zhou, K. Jagannathan, “Adaptive Network Based Fuzzy Control of a Dynamic Biped Walking Robot,” *IEEE International Joint Symposia on Intelligence and Systems*, pp. 109 -116, 1996.

[165] P.I. Doerschuk, V.D. Nguyen, A.L. Li, “Neural Network Control of a Three-Link Leg,” *Proceedings of the Seventh International Conference on Tools with Artificial Intelligence*, pp. 278-281, 1995.

[166] P.I. Doerschuk, V.D. Nguyen, W. Simon, F. Kwong, “Intelligent Ballistic Control of a Jointed Leg,” *IEEE International Joint Symposia on Intelligence and Systems*, pp. 117-124, 1996.

[167] A.L. Kun, W.T. Miller, “Unified Walking Control for a Biped Robot Using Neural Networks,” *Proceedings of the 1998 IEEE International Symposium on Intelligent Control*, pp. 283 -288, 1998.

[168] G. Taga, “Self-Organized Control of Bipedal Locomotion by Neural Oscillators in Unpredictable Environment,” *Biological Cybernetics*, vol. 65, pp. 147-159, 1991.

[169] J. Juang, “Fuzzy Modeling Control for Robotic Gait Synthesis,” *Proceedings of the 36th IEEE Conference on Decision and Control*, vol. 4, pp. 3670-3675, 1997.

[170] J. Juang, “Bipedal Trajectory Control Based on Neurofuzzy Networks,” *Proc. of the IEEE International Conference on Control Applications*, vol. 2, pp. 802-806, 1998.

[171] N. Wagner, M.C. Mulder, M.S. Hsu, “A Knowledge Based Control Strategy for a Biped,” *Proceedings of the IEEE International Conference on Robotics and Automation*, vol. 3, pp. 1520-1524, 1988.

[172] J. Yamaguchi, N. Kinoshita, A. Takanishi, I. Kato, “Development of a Dynamic Biped Walking System for Humanoid Development of a Biped Walking Robot Adapting to the Humans' Living Floor,” *Proceedings of the IEEE International Conference on Robotics and Automation*, vol. 1 , pp. 232 -239, 1996.

[173] J. Yamaguchi, D. Nishino, A. Takanishi, “Realization of Dynamic Biped Walking Varying Joint Stiffness Using Antagonistic Driven Joints,” *Proceedings of the IEEE International Conference on Robotics and Automation*, vol. 3, pp. 2022-2029, 1998.

[174] J. Yamaguchi, E. Soga, S. Inoue, A. Takanishi, "Development of a Bipedal Humanoid Robot Control Method of Whole Body Cooperative Dynamic Biped Walking," *Proceedings of the IEEE International Conference on Robotics and Automation*, vol. 1, pp. 368-374, 1999.

[175] Q. Li, A. Takanishi, I. Kato, "Learning Control of Compensative Trunk Motion for Biped Walking Robot Based on ZMP Stability Criterion," *Proceedings of the lEEE/RSJ International Conference on Intelligent Robots and Systems*, vol. 1, pp. 597-603, 1992.

[176] Q. Li, A. Takanishi, I. Kato, "Learning Control for a Biped Walking Robot with a Trunk," *Proceedings of the IEEE/RSJ International Conference on Intelligent Robots and Systems*, vol. 3, pp. 1771-1777, 1993.

[177] J. Pratt, P. Dilworth, G. Pratt, "Virtual Model Control of a Bipedal Walking Robot," *Proc. IEEE Int. Conf. on Robotics and Automation*, pp. 193-198, 1997.

[178] J. Pratt, C.M. Chew, A. Torres, P. Dilworth, G. Pratt, "Virtual Model Control: An Intuitive Approach for Bipedal Locomotion," *the International Journal of Robotics Research*, vol. 20, no. 2, pp. 129-143, Feb. 2001.

[179] T. Saidouni, G. Bessonnet, "Generating Globally Optimised Sagittal Gait Cycles of a Biped Robot," *Robotica*, vol. 21, part 2, pp. 199-210, 2003.

[180] M. Rostami, G. Bessonnet, "Sagittal Gait of a Biped Robot During the Single Support Phase, Part 2: Optimal Motion," *Robotica*, vol. 19, part 3, pp. 241-253, 2001.

[181] W. Schiehlen, "Energy-Optimal Design of Walking Machines," *Multibody Syst. Dyn.*, vol. 13, no. 1, pp. 129-141, Feb. 2005.

[182] G. Capi, Y. Nasu, K. Mitobe, "Autonomous Humanoid Robot Locomotion Based on Neural Networks, *Industrial Robot.*, vol. 29, no. 3, pp. 252-258, 2002.

[183] M. Hardt, K. Kreutz-Delgado, J.W. Helton, "Minimal Energy Control of a Biped Robot with Numerical Methods and a Recursive Symbolic Dynamic Model," *Proceedings of the 37th IEEE Conference on Decision and Control*, vol. 1, pp. 413-416, 1998.

[184] E.R. Westervelt, J.W. Grizzle, "Design of Asymptotically Stable Walking for a 5-Link Planar Biped Walker via Optimization," *ICRA*, 2002.

[185] M. Vukobratovic, O. Timcenko, "Experiments with Nontraditional Hybrid Control Technique of Biped Locomotion Robots," *Journal of Intelligent and Robotic System*, vol. 16, no. 1, pp. 25-43, 1996.

[186] J.H. Park, H. Chung, "Hybrid Control for Biped Robots Using Impedance Control and Computed-Torque Control," *Proceedings of the IEEE International Conference on Robotics and Automation*, vol. 2 , pp. 1365 -1370,s 1999.

[187] B. Yuksel, C. Zhou, K. Leblebicioglu, "Hybrid Fuzzy Control of Biped Locomotion Using 3D Inverted Pendulum Model," *Computational Intelligence, Robotics and Autonomous Systems*, 2005.

[188] M. Coleman, M. Garcia, A. Ruina, J. Camp, "Stability and Chaos in Passive-Dynamic Locomotion," *IUTAM Conference on New Applications of Nonlinear Dynamics and Chaos in Mechanics*, 1997.

[189] J. Adolfsson, H. Dankowicz, A. Nordmark, "3-D Stable Gait in Passive Bipedal Mechanisms," *Proceedings of 357 Euromech*, 1998.

[190] E.R. Westervelt, J.W. Grizzle, D.E. Koditschek, "Zero Dynamics of Underactuated Planar Biped Walkers," *IFAC 15th Triennial World Congress*, 2002.

[191] The SL Simulation and Real-Time Control Software Package, Stefan Schaal, *http://www-clmc.usc.edu/~sschaal/*, August 2008.

[192] S. Kudoh, T. Komura, "C2 Continuous Gait-Pattern Generation for Biped Robots," *International Conference on Intelligent Robots and Systems*, 2003.

[193] D. Maravall, “Control and Stabilization of the Inverted Pendulum via Vertical Forces,” *Robotic Welding, Intelligence and Automation, Springer-Verlag*, pp. 190-211, 2003.

[194] D. Maravall, C. Zhou, J. Alonso, “Hybrid Fuzzy Control of the Inverted Pendulum via Vertical Forces,” *International Journal of Intelligent Systems*, vol. 20, pp. 195-211, 2005.

[195] N.F. Ünver, S.T. Tümer, M.K. Özgören, “Simulation of Human Gait Using Computed Torque Control,” *Technology and Health Care, IOS Press*, vol. 8, pp. 53-66, 2000.

[196] D.E. Kirk, *Optimal Control Theory: An Introduction*, Prentice-Hall, 1970.

[197] F.L. Lewis, V.L. Syrmos, *Optimal Control*, John Wiley & Sons, 2nd ed.

[198] M.S. Bazaraa, H.D. Sherali, C.M. Shetty, *Nonlinear Programming: Theory and Algorithms*, John Wiley & Sons, 2nd ed.

APPENDIX A

THIRD ORDER SPLINE INTERPOLATION

Given $f_1,...,f_n$ finite values defined at points $t_1,...,t_n$, respectively as below;

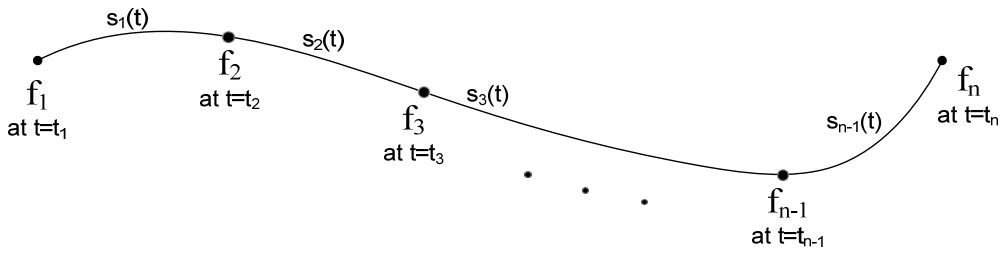

the (n-1)[th] order spline is calculated by the function $s(t)$, satisfying the below conditions:

$$s(t_j) = f_j \text{ for } j = 1,...,n$$

Third order spline interpolation, also known as "cubic spline interpolation", is a special case of above formulation for $n = 4$.

Spline function $s(t)$ can be formulated as

$$s(t) = \begin{Bmatrix} s_1(t) & if\ t_1 \le t < t_2 \\ s_2(t) & if\ t_2 \le t < t_3 \\ . & \\ . & \\ s_{n-1}(t) & if\ t_{n-1} \le t < t_n \end{Bmatrix} \quad \text{(A.1)}$$

where

$$s_j(t) = a_j(t-t_j)^3 + b_j(t-t_j)^2 + c_j(t-t_j) + d_j \tag{A.2}$$

Let us calculate the unknown parameters in these equations:

$$\dot{s}_j(t) = 3a_j(t-t_j)^2 + 2b_j(t-t_j) + c_j \quad for\ j = 1,...,n-1$$

$$\ddot{s}_j(t) = 6a_j(t-t_j)^2 + 2b_j \quad for\ j = 1,...,n-1 \tag{A.3}$$

Note that;

$$f_j = \mathrm{s}_j(t_j) \ \ for\ j = 1,...,n-1 \tag{A.4}$$

$$=> a_j(t_j - t_j)^3 + b_j(t_j - t_j)^2 + c_j(t_j - t_j) + d_j = f_j$$

$$=> d_j = f_j \quad for\ j = 1,...,n-1 \tag{A.5}$$

and

$$f_n = \mathrm{s}_{n-1}(t_n) \tag{A.6}$$

Let us define $h_j = t_{j+1} - t_j$ for $j = 1,...,n-1$

$$f_n = \mathrm{s}_{n-1}(t_n)$$

$$=> a_{n-1}(t_n - t_{n-1})^3 + b_{n-1}(t_n - t_{n-1})^2 + c_{n-1}(t_n - t_{n-1}) + d_{n-1} = f_n$$

$$=> a_{n-1}{h_{n-1}}^3 + b_{n-1}{h_{n-1}}^2 + c_{n-1}h_{n-1} + d_{n-1} = f_n$$

$$=> a_{n-1} = \frac{f_n}{{h_{n-1}}^3} - \frac{b_{n-1}}{h_{n-1}} - \frac{c_{n-1}}{{h_{n-1}}^2} - \frac{d_{n-1}}{{h_{n-1}}^3} \tag{A.7}$$

Also,

$$s_j(t_{j+1}) = \mathrm{s}_{j+1}(t_{j+1}) \text{ for } j = 1,...,n-2 \tag{A.8}$$

$$=> a_j h_j^{\,3} + b_j h_j^{\,2} + c_j h_j + d_j = d_{j+1}$$

$$=> c_j = (-a_j h_j^{\,2} - b_j h_j) + \frac{d_{j+1} - d_j}{h_j} \quad for\ j = 1,...,n-2 \tag{A.9}$$

$$\dot{s}_j(t_{j+1}) = \dot{\mathrm{s}}_{j+1}(t_{j+1}) \text{ for } j = 1,...,n-2 \tag{A.10}$$

$$=> 3a_j h_j^{\,2} + 2b_j h_j + c_j = c_{j+1}$$

$$=> c_{j+1} = 3a_j h_j^{\,2} + 2b_j h_j + c_j \quad for\ j = 1,...,n-2 \tag{A.11}$$

$$\ddot{s}_j(t_{j+1}) = \ddot{\mathrm{s}}_{j+1}(t_{j+1}) \text{ for } j = 1,...,n-2 \tag{A.12}$$

$$=> 6a_j h_j + 2b_j = 2b_{j+1}$$

$$=> a_j = \frac{2b_{j+1} - 2b_j}{6h_j} \quad for\ j = 1,...,n-2 \tag{A.13}$$

After defining $M_j = \ddot{s}_j(t_j)$ for $j = 1,...,n-1$, it can be written as

$$M_j = 2b_j \quad and\ so \quad b_j = \frac{M_j}{2} \quad for\ j = 1,...,n-1 \tag{A.14}$$

Then, let us insert this finding to equations A.13, A.9 and A.11 equations:

$$=> a_j = \frac{2b_{j+1} - 2b_j}{6h_j} \tag{A.15}$$

$$=> a_j = \frac{M_{j+1} - M_j}{6h_j} \quad for\ j = 1,...,n-2 \tag{A.16}$$

Also,

$$=> c_j = (-a_j h_j^{\,2} - b_j h_j) + \frac{d_{j+1} - d_j}{h_j}$$

$$=> c_j = (-\frac{M_{j+1} - M_j}{6h_j} h_j^{\,2} - \frac{M_j}{2} h_j) + \frac{d_{j+1} - d_j}{h_j}$$

$$=> c_j = (-a_j h_j^{\,2} - b_j h_j) + \frac{d_{j+1} - d_j}{h_j}$$

$$=> c_j = (-\frac{M_{j+1} - M_j}{6h_j} h_j^{\,2} - \frac{M_j}{2} h_j) + \frac{d_{j+1} - d_j}{h_j}$$

$$=> c_j = -\frac{h_j}{6}(M_{j+1} - M_j) - \frac{h_j}{2} M_j + \frac{d_{j+1} - d_j}{h_j}$$

$$=> c_j = -\frac{h_j}{6} M_{j+1} - \frac{h_j}{3} M_j + \frac{f_{j+1} - f_j}{h_j}$$

$$=> c_j = \frac{f_{j+1} - f_j}{h_j} - (\frac{M_{j+1} + 2M_j}{6})h_j \quad for\ j = 1,...,n-2 \tag{A.17}$$

So now, in summary, we obtain the following relations:

$$a_j = \frac{M_{j+1} - M_j}{6h_j} \quad for\ j = 1,...,n-2 \tag{A.18}$$

$$b_j = \frac{M_j}{2} \quad for\ j = 1,...,n-1 \tag{A.19}$$

$$c_j = \frac{f_{j+1} - f_j}{h_j} - \frac{M_{j+1} + 2M_j}{6} h_j \quad for\ j = 1, ..., n-2 \tag{A.20}$$

$$d_j = f_j \quad for\ j = 1, ..., n-1 \tag{A.21}$$

And finally,

$$c_{j+1} = 3a_j h_j^{\ 2} + 2b_j h_j + c_j \tag{A.22}$$

$$=> 3\frac{M_{j+1} - M_j}{6h_j} h_j^{\ 2} + 2\frac{M_j}{2} h_j + \frac{f_{j+1} - f_j}{h_j} - (\frac{M_{j+1} + 2M_j}{6}) h_j = c_{j+1} \tag{A.23}$$

$$\begin{aligned} => & \frac{M_{j+1} - M_j}{2h_j} h_j^{\ 2} + M_j h_j \\ & + \frac{f_{j+1} - f_j}{h_j} - (\frac{M_{j+1} + 2M_j}{6}) h_j = \frac{f_{j+2} - f_{j+1}}{h_{j+1}} - (\frac{M_{j+2} + 2M_{j+1}}{6}) h_{j+1} \end{aligned} \tag{A.24}$$

$$for\ j = 1, ..., n-3$$

$$\frac{M_{n-1} - M_{n-2}}{2} h_{n-2} + M_{n-2} h_{n-2} + \frac{f_{n-1} - f_{n-2}}{h_{n-2}} - \frac{M_{n-1} + 2M_{n-2}}{6} h_{n-2} = c_{n-1} \tag{A.25}$$

$$for\ j = n-2$$

The above equations can be simplified into the following form:

$$\begin{aligned} => & \frac{h_j}{6} M_j + (\frac{h_j}{3} + \frac{h_{j+1}}{3}) M_{j+1} + \frac{h_{j+1}}{6} M_{j+2} \\ & = \frac{1}{h_j} f_j - (\frac{1}{h_j} + \frac{1}{h_{j+1}}) f_{j+1} + \frac{1}{h_{j+1}} f_{j+2} \quad for\ j = 1, ..., n-3 \end{aligned} \tag{A.26}$$

$$\frac{h_{n-2}}{2} M_{n-2} + \frac{h_{n-2}}{3} M_{n-1} - c_{n-1} = -\frac{1}{h_{n-2}} f_{n-1} + \frac{1}{h_{n-2}} f_{n-2} \tag{A.27}$$

$$for\ j = n-2$$

Note that, in the above equation, we have n unknowns ($M_1, M_2, ..., M_{n-1}$ & c_{n-1}) but ($n-2$) equations. So 2 equations are missing in order to have a unique solution.

Let us assume that, the below assumptions take place in order to have a unique solution;

1) The initial constraint: $\dot{s}(t_1) = 0$
2) The end constraint: $\dot{s}(t_n) = 0$

$$\dot{s}(t_1) = 0 \quad => \quad \dot{s}_1(t_1) = 0$$

$$=> \quad 3a_1(t_1 - t_1)^2 + 2b_1(t_1 - t_1) + c_1 = 0$$

$$=> \quad c_1 = 0 \tag{A.28}$$

where

$$c_1 = \frac{f_2 - f_1}{h_1} - (\frac{M_2 + 2M_1}{6})h_1 \tag{A.29}$$

So,

$$\frac{f_2 - f_1}{h_1} - (\frac{M_2 + 2M_1}{6})h_1 = 0 \tag{A.30}$$

$$=> \frac{h_1}{3}M_1 + \frac{h_1}{6}M_2 = \frac{-1}{h_1}f_1 + \frac{1}{h_1}f_2 \tag{A.31}$$

$$\dot{s}(t_n) = 0 \quad => \quad \dot{s}_{n-1}(t_n) = 0$$

$$=> \quad 3a_{n-1}{h_{n-1}}^2 + 2b_{n-1}h_{n-1} + c_{n-1} = 0$$

$$=> \quad 3(\frac{f_n}{{h_{n-1}}^3} - \frac{b_{n-1}}{h_{n-1}} - \frac{c_{n-1}}{{h_{n-1}}^2} - \frac{d_{n-1}}{{h_{n-1}}^3}){h_{n-1}}^2 + 2b_{n-1}h_{n-1} + c_{n-1} = 0$$

$$=> \quad 3\frac{f_n}{h_{n-1}} - 3b_{n-1}h_{n-1} - 3c_{n-1} - 3\frac{d_{n-1}}{h_{n-1}} + 2b_{n-1}h_{n-1} + c_{n-1} = 0$$

$$=> \quad 3\frac{f_n}{h_{n-1}} - b_{n-1}h_{n-1} - 2c_{n-1} - 3\frac{d_{n-1}}{h_{n-1}} = 0$$

$$=> \quad 3\frac{f_n}{h_{n-1}} - \frac{M_{n-1}}{2}h_{n-1} - 2c_{n-1} - 3\frac{f_{n-1}}{h_{n-1}} = 0$$

$$=> \quad h_{n-1}M_{n-1} + 4c_{n-1} = \frac{6}{h_{n-1}}f_n - \frac{6}{h_{n-1}}f_{n-1} \qquad \text{(A.32)}$$

So, let us write these n equations into matrix form:

$$\begin{bmatrix}
\frac{h_1}{6} & \frac{h_1+h_2}{3} & \frac{h_2}{6} & 0 & 0 & \dots & & & & 0 \\
0 & \frac{h_2}{6} & \frac{h_2+h_3}{3} & \frac{h_3}{6} & 0 & \dots & & \ddots & & 0 \\
\vdots & & & & & \dots & & & & \vdots \\
0 & & \ddots & & & \dots & 0 & \frac{h_{n-3}}{6} & \frac{h_{n-3}+h_{n-2}}{3} & \frac{h_{n-2}}{6} & 0 \\
0 & 0 & 0 & & & \dots & 0 & 0 & \frac{h_{n-2}}{6} & \frac{h_{n-2}}{3} & -1 \\
\frac{h_1}{3} & \frac{h_1}{6} & 0 & & & \dots & 0 & 0 & 0 & 0 & 0 \\
0 & 0 & 0 & & & \dots & 0 & 0 & 0 & h_{n-1} & 4
\end{bmatrix}_{n\times n}
\begin{bmatrix} M_1 \\ M_2 \\ \\ \\ \\ \vdots \\ \\ \\ \\ M_{n-1} \\ c_{n-1} \end{bmatrix}_{n\times 1} =$$

$$
= \begin{bmatrix}
\frac{1}{h_1} f_1 - (\frac{1}{h_1} + \frac{1}{h_2}) f_2 + \frac{1}{h_2} f_3 \\
\frac{1}{h_1} f_2 - (\frac{1}{h_2} + \frac{1}{h_3}) f_3 + \frac{1}{h_3} f_4 \\
\\
\vdots \\
\\
\frac{1}{h_{n-3}} f_{n-3} - (\frac{1}{h_{n-3}} + \frac{1}{h_{n-2}}) f_{n-2} + \frac{1}{h_{n-2}} f_{n-1} \\
-\frac{1}{h_{n-2}} f_{n-1} + \frac{1}{h_{n-2}} f_{n-2} \\
-\frac{1}{h_1} f_1 + \frac{1}{h_1} f_2 \\
\frac{6}{h_{n-1}} f_n - \frac{6}{h_{n-1}} f_{n-1}
\end{bmatrix}_{n \times 1} \tag{A.33}
$$

APPENDIX B

INVERSE KINEMATICS CALCULATION

B.1 In Sagittal Plane

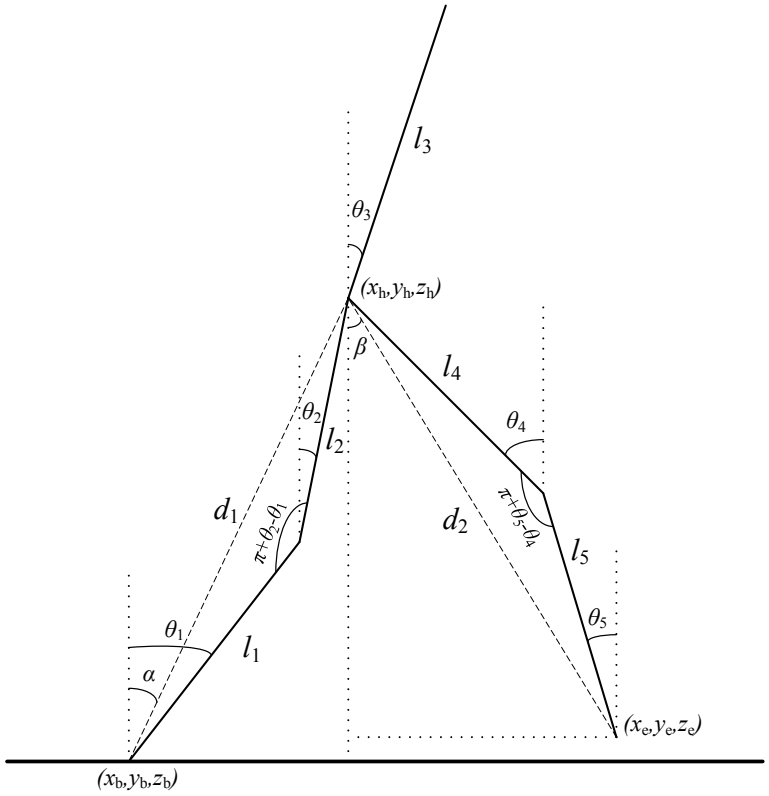

$$d_1 = \sqrt{(x_h - x_b)^2 + (z_h - z_b)^2} \tag{B.1}$$

$$d_2 = \sqrt{(x_e - x_h)^2 + (z_h - z_e)^2} \tag{B.2}$$

Note that; $\theta = \sin^{-1} x$ is well-defined and unique in $-\pi/2 \le \theta \le \pi/2$ and $\theta = \cos^{-1} x$ is well-defined and unique in $0 \le \theta \le \pi$

Also note that,

$$\sin\alpha = \frac{x_h - x_b}{d_1} \tag{B.3}$$

$$\cos\alpha = \frac{z_h - z_b}{d_1} \tag{B.4}$$

$$\sin\beta = \frac{x_e - x_h}{d_2} \tag{B.5}$$

$$\cos\beta = \frac{z_h - z_e}{d_2} \tag{B.6}$$

Also, for any given triangle

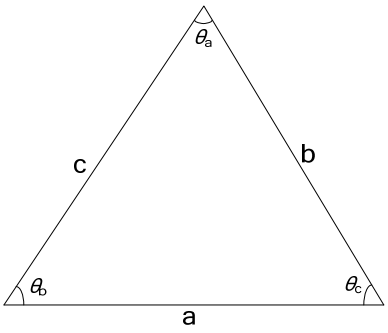

1) $a^2 = b^2 + c^2 - 2bc\cos\theta_a$ (B.7)

2) $\frac{a}{sin\theta_a} = \frac{b}{sin\theta_b} = \frac{c}{sin\theta_c}$ (B.8)

And also, if $\sin\theta$ and $\cos\theta$ are known, then θ can be calculated uniquely as below:

$$\theta = a\tan(\sin\theta, \cos\theta) \tag{B.9}$$

So, in this case; assuming that $\theta_1 = \text{constant}$, let us first derive θ_1 & θ_2 and then θ_4 & θ_5, from the given posture (hip point, stance foot and swing foot coordinates) and the model parameters of the biped robot:

$$d_1^2 = l_1^2 + l_2^2 - 2l_1 l_2 \cos(\pi + \theta_2 - \theta_1) \text{ where } 0 \le \pi + \theta_2 - \theta_1 \le \pi \tag{B.10}$$

$$\Rightarrow \cos(\pi + \theta_2 - \theta_1) = \frac{-d_1^2 + l_1^2 + l_2^2}{2l_1 l_2} \tag{B.11}$$

Since $0 \le \pi + \theta_2 - \theta_1 \le \pi$, $\pi + \theta_2 - \theta_1$ can be uniquely written as below:

$$\pi + \theta_2 - \theta_1 = \arccos\left(\frac{-d_1^2 + l_1^2 + l_2^2}{2l_1 l_2}\right) \tag{B.12}$$

In order to find θ_1 (where $-\pi/2 \le \theta_1 \le \pi/2$); let us first find α (where $-\pi/2 \le \alpha \le \pi/2$):

$$\tan\alpha = \frac{x_h - x_b}{z_h - z_b} \tag{B.13}$$

On the other hands;

$$\frac{l_2}{sin(\theta_1 - \alpha)} = \frac{d_1}{sin(\pi + \theta_2 - \theta_1)} \tag{B.14}$$

$$\Rightarrow sin(\theta_1 - \alpha) = \frac{l_2}{d_1} sin(\pi + \theta_2 - \theta_1) \tag{B.15}$$

Also, $l_2^2 = l_1^2 + d_1^2 - 2l_1 d_1 \cos(\theta_1 - \alpha)$

$$\Rightarrow \cos(\theta_1 - \alpha) = \frac{l_1^2 + d_1^2 - l_2^2}{2l_1 d_1} \tag{B.16}$$

$$\theta_1 = (\theta_1 - \alpha) + \alpha \tag{B.17}$$

$$\Rightarrow \cos(\theta_1) = \cos((\theta_1 - \alpha) + \alpha) \tag{B.18}$$

$$\Rightarrow \cos(\theta_1) = \cos(\theta_1 - \alpha)\cos\alpha - \sin(\theta_1 - \alpha)\sin\alpha \tag{B.19}$$

$$\Rightarrow \cos(\theta_1) = \frac{l_1^2 + d_1^2 - l_2^2}{2 l_1 d_1} \cdot \frac{z_h - z_b}{d_1} - \frac{x_h - x_b}{d_1} \cdot \frac{l_2}{d_1} \sin(\pi + \theta_2 - \theta_1) \tag{B.20}$$

where $(\pi + \theta_2 - \theta_1)$ has already been computed

$$\Rightarrow \cos(\theta_1) = \frac{(l_1^2 + d_1^2 - l_2^2)}{2 l_1 d_1} \frac{(z_h - z_b)}{d_1} - \frac{(x_h - x_b)}{d_1} \frac{l_2}{d_1} \sin(\arccos(\frac{-d_1^2 + l_1^2 + l_2^2}{2 l_1 l_2})) \tag{B.21}$$

Now, let us find $\sin(\theta_1)$:

$$\sin(\theta_1) = \sin((\theta_1 - \alpha) + \alpha) \tag{B.22}$$

$$\Rightarrow \sin(\theta_1) = \sin(\theta_1 - \alpha)\cos\alpha + \cos(\theta_1 - \alpha)\sin\alpha \tag{B.23}$$

$$\Rightarrow \sin(\theta_1) = \frac{l_2}{d_1} \sin(\pi + \theta_2 - \theta_1) \frac{z_h - z_b}{d_1} + \frac{x_h - x_b}{d_1} \cdot \frac{l_1^2 + d_1^2 - l_2^2}{2 l_1 d_1} \tag{B.24}$$

$$\Rightarrow \sin\theta_1 = \frac{l_2}{d_1} \sin(\arccos(\frac{-d_1^2 + l_1^2 + l_2^2}{2 l_1 l_2})) \frac{z_h - z_b}{d_1} + \frac{(x_h - x_b)}{d_1} \frac{(l_1^2 + d_1^2 - l_2^2)}{2 l_1 d_1} \tag{B.25}$$

Since $\cos(\theta_1)$ & $\sin(\theta_1)$ are obtained so that θ_1 (where $-\pi/2 \le \theta_1 \le \pi/2$) can be derived uniquely as

$$=> \theta_1 = a\tan(\sin\theta_1, \cos\theta_1) \tag{B.26}$$

Afterwards, θ_2 can also be uniquely obtained as below:

$$\theta_2 = (\pi + \theta_2 - \theta_1) + \theta_1 - \pi \text{ (where } -\pi/2 \le \theta_2 \le \pi/2\text{)} \tag{B.27}$$

$$=> \theta_2 = \arccos(\frac{-d_1^{\,2} + l_1^{\,2} + l_2^{\,2}}{2l_1 l_2}) + \theta_1 - \pi \tag{B.28}$$

Similarly, let us calculate θ_4 & θ_5:

$$d_2^{\,2} = l_4^{\,2} + l_5^{\,2} - 2l_4 l_5 \cos(\pi + \theta_5 - \theta_4) \text{ where } 0 \le \pi + \theta_5 - \theta_4 \le \pi \tag{B.29}$$

$$=> \cos(\pi + \theta_5 - \theta_4) = \frac{-d_2^{\,2} + l_4^{\,2} + l_5^{\,2}}{2l_4 l_5} \tag{B.30}$$

Since $0 \le \pi + \theta_5 - \theta_4 \le \pi$, $\pi + \theta_5 - \theta_4$ can be uniquely written as below:

$$\pi + \theta_5 - \theta_4 = \arccos(\frac{-d_2^{\,2} + l_4^{\,2} + l_5^{\,2}}{2l_4 l_5}) \tag{B.31}$$

In order to find θ_4 (where $-\pi/2 \le \theta_4 \le \pi/2$); let us first find β (where $-\pi/2 \le \beta \le \pi/2$):

$$\tan\beta = \frac{x_e - x_h}{z_h - z_e} \tag{B.32}$$

$$\frac{l_4}{sin(\theta_4 - \beta)} = \frac{d_2}{sin(\pi + \theta_5 - \theta_4)} \tag{B.33}$$

$$=> sin(\theta_4 - \beta) = \frac{l_4}{d_2} sin(\pi + \theta_5 - \theta_4) \tag{B.34}$$

Also,

$$l_4^{\,2} = l_5^{\,2} + d_2^{\,2} - 2l_5 d_2 \cos(\theta_4 - \beta) \tag{B.35}$$

$$\Rightarrow \cos(\theta_4 - \beta) = \frac{l_5^{\,2} + d_2^{\,2} - l_4^{\,2}}{2l_5 d_2} \tag{B.36}$$

$$\theta_4 = (\theta_4 - \beta) + \beta \tag{B.37}$$

$$\Rightarrow \cos(\theta_4) = \cos((\theta_4 - \beta) + \beta) \tag{B.38}$$

$$\Rightarrow \cos(\theta_4) = \cos(\theta_4 - \beta)\cos\beta - \sin(\theta_4 - \beta)\sin\beta \tag{B.39}$$

$$\Rightarrow \cos(\theta_4) = \frac{l_5^{\,2} + d_2^{\,2} - l_4^{\,2}}{2l_5 d_2} \cdot \frac{z_h - z_e}{d_2} - \frac{x_e - x_h}{d_2} \cdot \frac{l_4}{d_2} \sin(\pi + \theta_5 - \theta_4) \tag{B.40}$$

where $(\pi + \theta_5 - \theta_4)$ has already been computed as

$$\begin{aligned} \Rightarrow \cos(\theta_4) = {} & \frac{(l_5^{\,2} + d_2^{\,2} - l_4^{\,2})}{2l_5 d_2} \frac{(z_h - z_e)}{d_2} \\ & - \frac{(x_e - x_h)}{d_2} \frac{l_4}{d_2} \sin\left(\arccos\left(\frac{-d_2^{\,2} + l_4^{\,2} + l_5^{\,2}}{2l_4 l_5}\right)\right) \end{aligned} \tag{B.41}$$

Now, let us find $\sin(\theta_4)$:

$$\sin(\theta_4) = \sin((\theta_4 - \beta) + \beta) \tag{B.42}$$

$$\Rightarrow \sin(\theta_4) = \sin(\theta_4 - \beta)\cos\beta + \cos(\theta_4 - \beta)\sin\beta \tag{B.43}$$

$$\Rightarrow \sin(\theta_4) = \frac{l_4}{d_2} \sin(\pi + \theta_5 - \theta_4) \frac{z_h - z_e}{d_2} + \frac{x_e - x_h}{d_2} \cdot \frac{l_5^{\,2} + d_2^{\,2} - l_4^{\,2}}{2l_5 d_2} \tag{B.44}$$

$$\Rightarrow \sin(\theta_4) = \frac{l_4}{d_2}\sin(\arccos(\frac{-{d_2}^2 + {l_4}^2 + {l_5}^2}{2l_4 l_5}))\frac{z_h - z_e}{d_2} + \frac{(x_e - x_h)}{d_2}\frac{({l_5}^2 + {d_2}^2 - {l_4}^2)}{2l_5 d_2} \quad \text{(B.45)}$$

$$\Rightarrow \theta_4 = a\tan(\sin\theta_4, \cos\theta_4) \quad \text{(B.46)}$$

Since $\cos(\theta_4)$ & $\sin(\theta_4)$ are obtained, θ_4 (where $-\pi/2 \le \theta_4 \le \pi/2$) can be derived uniquely as

$$\Rightarrow \theta_4 = a\tan(\sin\theta_4, \cos\theta_4) \quad \text{(B.47)}$$

Afterwards, θ_5 can be obtained uniquely as below:

$$\theta_5 = (\pi + \theta_5 - \theta_4) + \theta_4 - \pi \text{ (where } -\pi/2 \le \theta_5 \le \pi/2) \quad \text{(B.48)}$$

$$\Rightarrow \theta_5 = \arccos(\frac{-{d_2}^2 + {l_4}^2 + {l_5}^2}{2l_4 l_5}) + \theta_4 - \pi \quad \text{(B.49)}$$

B.2 In Frontal Plane

Note that; $\theta = \cos^{-1} a$ is well-defined and unique for $0 \le \theta \le \pi$.

In frontal plane, $-\pi/2 \le \theta_6 \le \pi/2$ and as a result, $0 \le (\pi/2 + \theta_6) \le \pi$. Also,

$$\cos(\pi/2 + \theta_6) = \frac{y_b - y_h + L_h}{l_1 + l_2} \quad \text{(B.50)}$$

$$\Rightarrow \pi/2 + \theta_6 = arc\cos(\frac{y_b - y_h + L_h}{l_1 + l_2}) \quad \text{(B.51)}$$

$$\Rightarrow \theta_6 = -\pi/2 + arc\cos(\frac{y_b - y_h + L_h}{l_1 + l_2}) \text{ where } -\pi/2 \le \theta_6 \le \pi/2 \quad \text{(B.52)}$$

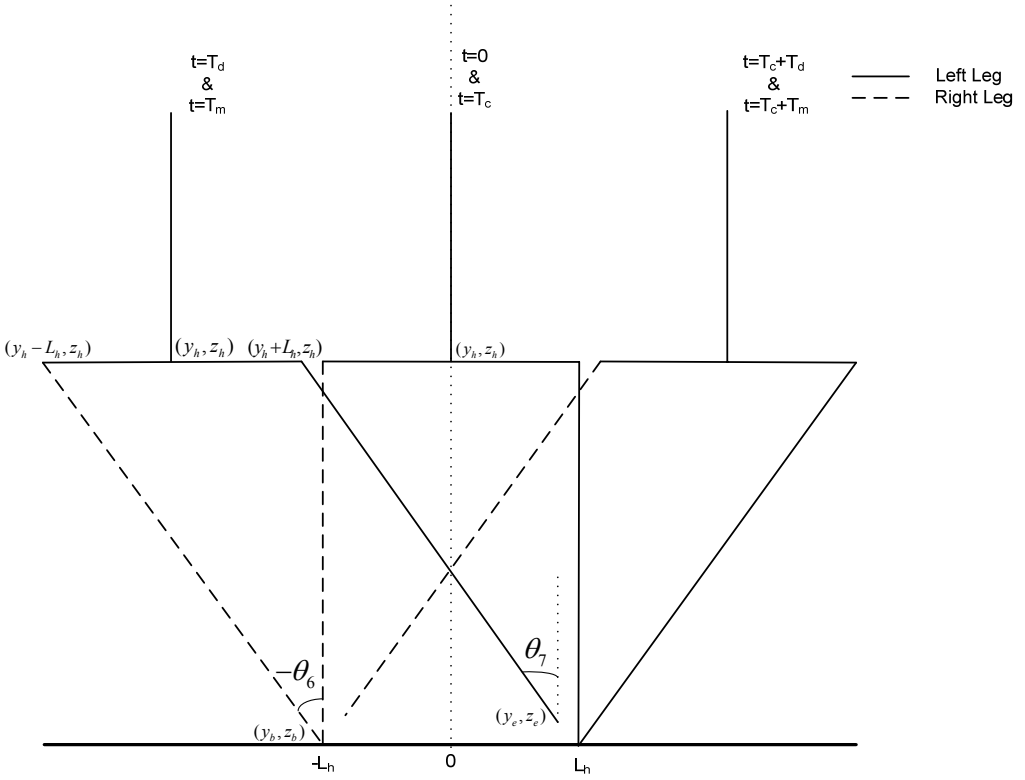

Similarly, since $0 \le (\pi/2 - \theta_7) \le \pi$, θ_7 can be found as

$$\cos(\pi/2 - \theta_7) = \frac{y_e - y_h - L_h}{l_4 + l_5} \quad \text{(B.53)}$$

$$\Rightarrow \pi/2 - \theta_7 = arc\cos(\frac{y_e - y_h - L_h}{l_4 + l_5}) \quad \text{(B.54)}$$

$$\Rightarrow \theta_7 = \pi/2 - arc\cos(\frac{y_e - y_h - L_h}{l_4 + l_5}) \text{ where } -\pi/2 \le \theta_7 \le \pi/2 \quad \text{(B.55)}$$

APPENDIX C

EULER-LAGRANGE EQUATION CALCULATIONS

C.1 Calculation of $\frac{\partial H}{\partial \underline{u}}$

$$\frac{\partial H}{\partial \underline{u}} = \frac{\partial g}{\partial \underline{u}} + \frac{\partial a}{\partial \underline{u}}^{T} \; p \tag{C.1}$$

where

$$\frac{\partial g}{\partial \underline{u}} = \alpha R \underline{u} \tag{C.2}$$

and

$$\frac{\partial a}{\partial \underline{u}} = \begin{bmatrix} \frac{\partial a_1}{\partial u_1} & \frac{\partial a_1}{\partial u_2} & \cdots & \frac{\partial a_1}{\partial u_7} \\ \frac{\partial a_2}{\partial u_1} & \frac{\partial a_2}{\partial u_2} & \cdots & \frac{\partial a_2}{\partial u_7} \\ \vdots & \vdots & \ddots & \vdots \\ \frac{\partial a_{14}}{\partial u_1} & \frac{\partial a_{14}}{\partial u_2} & \cdots & \frac{\partial a_{14}}{\partial u_7} \end{bmatrix} \Rightarrow \frac{\partial a}{\partial \underline{u}} = \begin{bmatrix} \begin{pmatrix} 0 & \cdots & 0 \\ \vdots & \ddots & \vdots \\ 0 & \cdots & 0 \end{pmatrix}_{7x7} \\ \hline D^{-1}(\underline{x}_1) \end{bmatrix}_{14x7} \tag{C.3}$$

$$\Rightarrow \frac{\partial H}{\partial \underline{u}} = \alpha R \underline{u} + \begin{bmatrix} \begin{pmatrix} 0 & \cdots & 0 \\ \vdots & \ddots & \vdots \\ 0 & \cdots & 0 \end{pmatrix}_{7x7} \\ \hline D^{-1}(\underline{x}_1) \end{bmatrix}^{T}_{14x7} \; p \tag{C.4}$$

C.2 Calculation of $\frac{\partial H}{\partial \underline{x}}$

$$\frac{\partial H}{\partial \underline{x}} = \frac{\partial g}{\partial \underline{x}} + \left(\frac{\partial a}{\partial \underline{x}}\right)^T p \tag{C.5}$$

and

$$\frac{\partial g}{\partial \underline{x}} = Q(\underline{x} - \underline{x}_d) \tag{C.6}$$

and

$$\frac{\partial \underline{a}}{\partial \underline{x}} = \begin{bmatrix} \frac{\partial a_1}{\partial x_1} & \frac{\partial a_1}{\partial x_2} & \cdots & \frac{\partial a_1}{\partial x_{14}} \\ \frac{\partial a_2}{\partial x_1} & \frac{\partial a_2}{\partial x_2} & \cdots & \frac{\partial a_2}{\partial x_{14}} \\ \vdots & \vdots & \ddots & \vdots \\ \frac{\partial a_{14}}{\partial x_1} & \frac{\partial a_{14}}{\partial x_2} & \cdots & \frac{\partial a_{14}}{\partial x_{14}} \end{bmatrix} \tag{C.7}$$

$$\Rightarrow \frac{\partial \underline{a}}{\partial \underline{x}} = \left[\begin{array}{c|c} \begin{pmatrix} 0 & \cdots & 0 \\ \vdots & \ddots & \vdots \\ 0 & \cdots & 0 \end{pmatrix}_{7x7} & \begin{pmatrix} 1 & 0 & \cdots & 0 \\ 0 & \ddots & \ddots & \vdots \\ \vdots & \ddots & \ddots & 0 \\ 0 & \cdots & 0 & 1 \end{pmatrix}_{7x7} \\ \hline \frac{\partial}{\partial \underline{\theta}}(D^{-1}u - D^{-1}h\dot{\theta} - D^{-1}G) & \frac{\partial}{\partial \underline{\dot{\theta}}}(-D^{-1}h\dot{\theta}) \end{array}\right]_{14x14} \tag{C.8}$$

$$\Rightarrow \frac{\partial H}{\partial \underline{x}} = Q(\underline{x} - \underline{x}_d)$$

$$+ \left[\begin{array}{c|c} \begin{pmatrix} 0 & \cdots & 0 \\ \vdots & \ddots & \vdots \\ 0 & \cdots & 0 \end{pmatrix}_{7x7} & \begin{pmatrix} 1 & 0 & \cdots & 0 \\ 0 & \ddots & \ddots & \vdots \\ \vdots & \ddots & \ddots & 0 \\ 0 & \cdots & 0 & 1 \end{pmatrix}_{7x7} \\ \hline \frac{\partial}{\partial \underline{\theta}}(D^{-1}u - D^{-1}h\dot{\theta} - D^{-1}G) & \frac{\partial}{\partial \underline{\dot{\theta}}}(-D^{-1}h\dot{\theta}) \end{array} \right]^T_{14x14} p \tag{C.9}$$

C.3 Calculation of $\frac{\partial h}{\partial \underline{x}}$

$$\frac{\partial h}{\partial \underline{x}} = F(\underline{x}(t_f) - \underline{x}_d(t_f)) \tag{C.10}$$

$$\Rightarrow p_f = F(\underline{x}(t_f) - \underline{x}_d(t_f)) \tag{C.11}$$

APPENDIX D

NUMERICAL METHODS

D.1 Numerical Integration Methods

For solving first order ordinary differential equations (ODEs), numerical integration methods are commonly used.

Given the initial value problem (IVP),

$$\dot{y} = f(t, y) \text{ where } y(t_0) = y_0 \tag{D.1}$$

there are several methods to solve this problem numerically:

- Forward integration by difference approximation
- Trapezoidal integration by difference approximation
- Backward integration by difference approximation
- Runge Kutta 45

The solution to the given IVP is $y(t)$ for $\forall t$. The time t can be discretized with Δt that is the time interval between two consequent points of time, i.e. $t_{n+1} = t_n + \Delta t$ where $t = t_0, t_1, ..., t_n, ...$ Also, y_n is defined as the solution of the IVP at $t = t_n$.

D.1.1 Forward Integration by Difference Approximation

In order to solve the given IVP $\dot{y} = f(t, y)$ with $y(t_0) = y_0$, the forward difference approximation can be applied by using a recursive numerical integration algorithm.

Let us approximate

$$\dot{y} = (y_{n+1} - y_n) / \Delta t \text{ and by using } \dot{y} = f(t, y) \tag{D.2}$$

$$\Rightarrow y_{n+1} = y_n + \Delta t\, f(t_n, y_n) \tag{D.3}$$

The recursive calculation of the solution to the IVP can be found as below:

$$y_1 = y_0 + \Delta t\, f(t_0, y_0) \tag{D.4}$$

$$y_2 = y_1 + \Delta t\, f(t_1, y_1) \tag{D.5}$$

$$\vdots$$

$$y_{n+1} = y_n + \Delta t\, f(t_n, y_n) \tag{D.6}$$

D.1.2 Trapezoidal integration by difference approximation

In order to solve the given IVP $\dot{y} = f(t, y)$ with $y(t_0) = y_0$, the trapezoidal rule of difference approximation can be applied by using a recursive numerical integration algorithm and by approximating:

$$y_{n+1} = y_n + \frac{\Delta t}{2}\left[f(y_{n+1}, t_{n+1}) + f(y_n, t_n)\right] \tag{D.7}$$

D.1.3 Backward integration by difference approximation

In order to solve the given IVP $\dot{y} = f(t, y)$ with $y(t_0) = y_0$, the backward difference approximation can be applied by using a recursive numerical integration algorithm and by approximating:

$$y_{n+1} = y_n + \Delta t\, f(y_{n+1}, t_{n+1}) \tag{D.8}$$

$$\Rightarrow y_n = y_{n+1} - \Delta t\, f(y_{n+1}, t_{n+1}) \tag{D.9}$$

D.1.4 Runge Kutta 45

In order to solve the given IVP $\dot{y} = f(t, y)$ with $y(t_0) = y_0$, the Runge Kutta 45 method can be applied by using a forth order recursive numerical integration algorithm, which is described below:

$$k_1 = \Delta t \; f(t_n, y_n) \tag{D.10}$$

$$k_2 = \Delta t \; f(t_n + \frac{1}{2}\Delta t, y_n + \frac{1}{2}k_1) \tag{D.11}$$

$$k_3 = \Delta t \; f(t_n + \frac{1}{2}\Delta t, y_n + \frac{1}{2}k_2) \tag{D.12}$$

$$k_4 = \Delta t \; f(t_n + \frac{1}{2}\Delta t, y_n + \frac{1}{2}k_3) \tag{D.13}$$

$$y_{n+1} = y_n + \frac{k_1}{6} + \frac{k_2}{3} + \frac{k_3}{3} + \frac{k_4}{6} + O(\Delta t^5) \tag{D.14}$$

D.2 Numerical Differentiation Methods

For a given function $f(t, y)$, the derivative of it can be approximated by the methods listed below:

- Forward difference approximation
- Backward difference approximation
- Central difference approximation

D.2.1 Forward Difference Approximation

$$\dot{f}(x) = \frac{f(x+h) - f(x)}{h} \tag{D.15}$$

where h is the interval of difference approximation

D.2.2 Backward Difference Approximation

$$\dot{f}(x) = \frac{f(x) - f(x-h)}{h} \tag{D.16}$$

where h is the interval of difference approximation

D.2.3 Central Difference Approximation

$$\dot{f}(x) = \frac{f(x+h) - f(x-h)}{2h} \tag{D.17}$$

where h is the interval of difference approximation

D.2.4 Five-Point Stencil Difference Approximation

$$\dot{f}(x) = \frac{-f(x+2h) + 8f(x+h) - 8f(x-h) + f(x-2h)}{12h} \tag{D.18}$$

Proof:

Using the Taylor series approximation for $f(x \pm h)$ and $f(x \pm 2h)$, the following equations are obtained:

$$f(x+h) = f(x) + h\dot{f}(x) + \frac{h^2}{2}\ddot{f}(x) + \frac{h^3}{6}\dddot{f}(x) + O(h.o.t) \tag{D.19}$$

$$f(x-h) = f(x) - h\dot{f}(x) + \frac{h^2}{2}\ddot{f}(x) - \frac{h^3}{6}\dddot{f}(x) + O(h.o.t) \tag{D.20}$$

By combining D.20 and D.21, the following equation will be obtained:

$$f(x+h) - f(x-h) = 2h\dot{f}(x) + \frac{h^3}{3}\dddot{f}(x) + O(h.o.t) \tag{D.21}$$

Similarly,

$$f(x+2h) = f(x) + 2h\dot{f}(x) + 2h^2\ddot{f}(x) + \frac{4h^3}{3}\dddot{f}(x) + O(h.o.t) \quad \text{(D.22)}$$

$$f(x-2h) = f(x) - 2h\dot{f}(x) + 2h^2\ddot{f}(x) - \frac{4h^3}{3}\dddot{f}(x) + O(h.o.t) \quad \text{(D.23)}$$

By combining D.23 and D.24, the following equation will be obtained:

$$f(x+2h) - f(x-2h) = 4h\dot{f}(x) + \frac{8h^3}{3}\dddot{f}(x) + O(h.o.t) \quad \text{(D.24)}$$

By eliminating the 3rd order derivetive terms using (D.22) and (D.25), the following equation is obtained:

$$8f(x+h) - 8f(x-h) - f(x+2h) + f(x-2h) = 12h\dot{f}(x) + O(h.o.t) \quad \text{(D.25)}$$

By rearranging the D.26, the five-point stencil difference approximation is obtained.

CURRICULUM VITAE

PERSONAL INFORMATION

Surname, Name: Yüksel, Başak

Nationality: Turkish (TC)

Date and Place of Birth: 13 September 1979, Gaziantep/Turkey

Marital Status: Single

Phone: +90 535 598 00 89

e-mail: basak@ieee.org

EDUCATION

Degree	Institution	Year of Graduation
MS	METU Electrical and Electronics Engineering	2003
BS	METU Mathematics	2002
BS	METU Electrical and Electronics Engineering	2001
High School	İçel Anadolu Lisesi, Mersin	1997

WORK EXPERIENCE

Year	Place	Enrollment
2005-Present	Havelsan	Senior Systems Engineer
2002-2005	METU Electrical and Electronics Engineering Department	Teaching/Research Assistant
2001	Aselsan	Design Engineer
1999-2001	Aselsan	Part-Time Researcher
2000 Summer	Alcatel	Intern
1999 Summer	Aselsan	Intern

PUBLICATIONS

1. B. Yuksel, B., C. Zhou, K. Leblebicioglu, "Ground Reaction Force Analysis in Biped Locomotion," *IEEE Conference on Cybernetics and Intelligent Systems and IEEE Conference on Robotics, Automation and Mechatronics*, Singapore, 1-3 Dec. 2004

2. B. Yuksel, C. Zhou, K. Leblebicioglu, “Hybrid Fuzzy Control of Biped Locomotion Using 3D Inverted Pendulum Model,” *Computational Intelligence, Robotics and Autonomous Systems*, Singapore, 14-16 Dec. 2005.

FOREIGN LANGUAGES

Advanced English, Intermediate German, Intermediate Japanese, Beginner French

HOBBIES

Athletism, scuba diving, squash, photography, books, origami and classical music.

MEMBERSHIPS

IEEE